

**Structural and biochemical  
characterization of  
3-hydroxybenzoate 6-hydroxylase**

**Stefania Montersino**

## **Thesis committee**

### **Thesis supervisor**

Prof. dr. W. J. H. van Berkel  
Personal chair at the Laboratory of Biochemistry  
Wageningen University

### **Thesis co-supervisor**

Prof. A. Mattevi  
Professor of Molecular Biology  
Universita' degli Studi di Pavia, Italy

### **Other members**

Prof. dr. J. van der Oost, Wageningen University  
Prof. dr. L. Dijkhuizen, University of Groningen  
Prof. dr. A. J. R. Heck, Utrecht University  
Prof. dr. ir. M. W. Fraaije, University of Groningen

This research was conducted under the auspices of the Graduate School VLAG (Advanced studies in Food Technology, Agrobiotechnology, Nutrition and Health Sciences).

**Structural and biochemical  
characterization of  
3-hydroxybenzoate 6-hydroxylase**

**Stefania Montersino**

**Thesis**

submitted in fulfilment of the requirements for the degree of doctor  
at Wageningen University  
by the authority of the Rector Magnificus  
Prof. dr. M.J. Kropff,  
in the presence of the  
Thesis Committee appointed by the Academic Board  
to be defended in public  
on Thursday 14 June 2012  
at 11 a.m. in the Aula.

Stefania Montersino  
Structural and biochemical characterization of  
3-hydroxybenzoate 6-hydroxylase  
158 pages

Thesis, Wageningen University, Wageningen, NL (2012)  
With references and summaries in Dutch and English

ISBN 978-94-6173-278-1



## Table of Contents

<i>Chapter 1</i>	
General Introduction	7
<i>Chapter 2</i>	
Catalytic and structural features of flavoprotein hydroxylases and epoxidases	19
<i>Chapter 3</i>	
Functional annotation and characterization of 3-hydroxybenzoate 6-hydroxylase from <i>Rhodococcus jostii</i> RHA1	51
<i>Chapter 4</i>	
Crystal structure of the flavoprotein monooxygenase 3-hydroxybenzoate 6-hydroxylase: identification of a mysterious guest	71
<i>Chapter 5</i>	
Phosphatidylinositol is the natural phospholipid ligand of <i>Rhodococcus jostii</i> 3-hydroxybenzoate 6-hydroxylase	89
<i>Chapter 6</i>	
Exploring natural diversity of 3-hydroxybenzoate 6-hydroxylases: revisiting the properties of the enzyme from <i>Pseudomonas alcaligenes</i> NCIMB 9867	103
<i>Chapter 7</i>	
Mirror-image substrate binding directs regioselectivity of flavoprotein-dependent 3-hydroxybenzoate hydroxylation	115
Summary and General Discussion	133
Dutch Summary	
Acknowledgements	
<i>Curriculum vitae</i>	
List of publications	
Overview of completed training activities	



# General Introduction

Stefania Montersino<sup>1</sup> and Willem J. H. van Berkel<sup>1</sup>

<sup>1</sup> Laboratory of Biochemistry, Wageningen University,  
Dreijenlaan 3, 6703 HA Wageningen, The Netherlands



## Flavoenzymes

Flavoenzymes play an essential role in biological processes ranging from biosynthesis, energy production, light emission, protein folding, and axon guidance to detoxification, apoptosis, chromatin remodeling, and DNA repair (Joosten and van Berkel, 2007). They are widespread in every kingdom of life, and constitute between 0.1 to 3.5 % of proteins in a proteome (Macheroux *et al.*, 2011). Flavoenzymes are of great interest in biotechnology due to their natural ability to perform complex enantio- and regioselective chemical transformations, often with no counterpart in organic chemistry.

Flavoenzymes contain a flavin mononucleotide (FMN) or flavin adenine dinucleotide (FAD) as redox-active prosthetic group. Both these cofactors originate from the precursor riboflavin (vitamin B<sub>2</sub>) (Fig.1). The flavin cofactor confers a characteristic yellow appearance to the protein and is generally non-covalently bound. Most flavoenzymes are oxidoreductases, but around 10% of them are transferases, isomerases, lyases and ligases (Macheroux *et al.*, 2011). The chemical versatility of flavin resides in the isoalloxazine moiety, which may oscillate between oxidized, one electron-reduced (semiquinone), and two electron-reduced (hydroquinone) states (Fig.1).

Oxidative flavoenzymes perform a variety of *oxygen-consuming* reactions (Ghisla and Massey, 1989; Massey, 1994; Baron, McCammon and Mattevi, 2009a). While

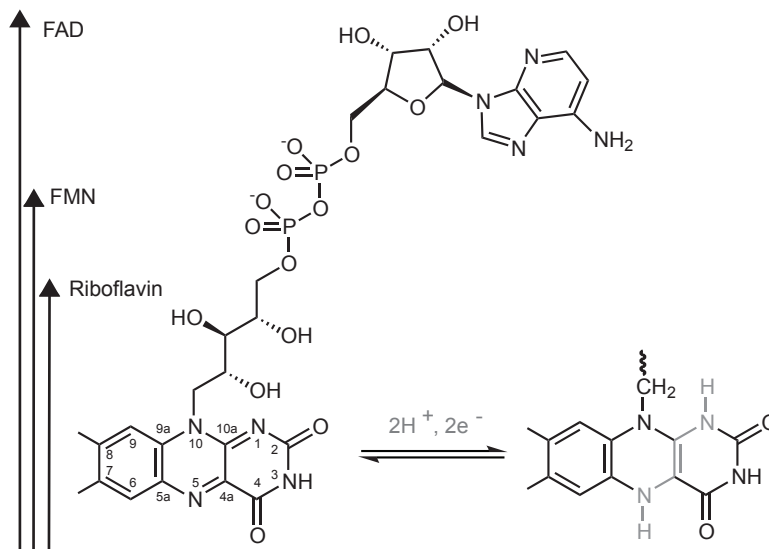


**Figure 1. Structure of riboflavin, FMN and FAD in the oxidized and reduced state.** The redox-active isoalloxazine ring is shown in its oxidized and two-electron reduced state (gray). The numbering scheme for the isoalloxazine ring is indicated in the oxidized structure on the left.

## 1

oxidases produce hydrogen peroxide as a result of flavin reoxidation, monooxygenases turn molecular oxygen into a true substrate by forming a rather stable flavin-oxygen adduct. Furthermore, embedment of flavin in the protein active site makes that the normally poor reactivity of flavin with oxygen becomes strongly increased (Massey, 1994; Entsch and van Berkel, 1995). The structural and chemical boundaries of oxygen reactivity of flavoenzymes are not fully understood. However, accessibility, charge distribution and distortions of the flavin are important factors involved (Baron, Riley, Chenprakhon, Thotsaporn, *et al.*, 2009b; Baron, McCammon and Mattevi, 2009a; Palfey and McDonald, 2010; McDonald *et al.*, 2011)

## Flavoprotein monooxygenases

Flavoprotein monooxygenases catalyze the insertion of a single atom of molecular oxygen into the substrate, while the other oxygen atom is reduced to water. Oxygen activation of flavoprotein monooxygenases involves the (transient) stabilization of flavin C4a-(hydro)peroxide. This species performs either a nucleophilic or electrophilic attack on the substrate. Oxygenation reactions catalyzed by flavoprotein monooxygenases include hydroxylations, epoxidations, Baeyer-Villiger oxidations, and sulfoxidations.

Based on fold and function, flavoprotein monooxygenases can be divided into six subfamilies (van Berkel *et al.*, 2006) (Table 1; Scheme 1). Class A and B enzymes rely on NAD(P)H as coenzyme, while flavin reduction and oxygenation take place in the same polypeptide chain. Two-component enzymes, on the other hand, are composed of a NAD(P)H-dependent flavin reductase and a flavin-specific monooxygenase.

Single-component flavoprotein hydroxylases (**class A**) typically act according to an electrophilic aromatic substitution mechanism. They are very regioselective and display a subtle mechanism of substrate, coenzyme and oxygen recognition.

**Table 1. Flavoprotein monooxygenase classification** (van Berkel *et al.*, 2006).

Subclass	Prototype	Reaction	Reference
A	<i>p</i> -Hydroxybenzoate hydroxylase	Hydroxylation	(Palfey and McDonald, 2010; Montersino <i>et al.</i> , 2011;
B	Cyclohexanon monooxygenase	Baeyer-Villiger oxidation	(Kamerbeek <i>et al.</i> , 2003; Olucha and Lamb, 2011)
		<i>S</i> -oxidation	
		<i>N</i> -hydroxylation	
C	Alkane sulfonate monooxygenase	Baeyer-Villiger oxidation	(Ellis, 2010)
	Luciferase	<i>S</i> -oxidation	
		Light emission	
D	4-Hydroxyphenylacetate 3-hydroxylase	Hydroxylation	(van Berkel <i>et al.</i> , 2006)
E	Styrene monooxygenase	Epoxidation	(Montersino <i>et al.</i> , 2011)
F	Tryptophan 7-halogenase	Halogenation	(van Pée and Patallo, 2006; Blasiak and Drennan, 2009)

Single-component flavin hydroxylases comprehend important enzymes in microbial degradation of aromatic compounds, antibiotic resistance and biosynthesis of polyketides (Montersino *et al.*, 2011). The exquisite regioselective hydroxylation in *ortho* or *para* position of the aromatic ring has no counterpart in other enzymatic systems.

Single-component **class B** enzymes perform Baeyer-Villiger oxidation, sulfoxidation and heteroatom hydroxylation reactions. Class B members are NADPH-specific, contain two Rossmann folds and keep the oxidized coenzyme bound during substrate oxygenation. Different from class A hydroxylases, the flavin-oxygen adduct is deprotonated and oxygen insertion goes via nucleophilic substitution (Ryerson *et al.*, 1982).

BVMOs convert ketones (or aldehydes) into esters or lactones and are widely used for the preparation of enantiopure compounds (Torres Pazmiño *et al.*, 2010). Initial milestone research was done on cyclohexanone monooxygenase (Ryerson *et al.*, 1982; Sheng *et al.*, 2001; Mirza *et al.*, 2009), 4-hydroxyacetophenone monooxygenase (Kamerbeek *et al.*, 2001; Fraaije *et al.*, 2002) and phenylacetone monooxygenase (Fraaije *et al.*, 2005; Malito *et al.*, 2004; Orru *et al.*, 2011). More recently, several new (thermostable) BVMOs were described (Torres Pazmiño *et al.*, 2010) and the stereopreference and substrate acceptance of selected BVMOs was improved by directed evolution (Reetz and Wu, 2009; Wu *et al.*, 2010) and extensive site directed mutagenesis (Dudek *et al.*, 2011). A new generation of self-sufficient BVMOs has also been reported (Torres Pazmiño *et al.*, 2009). In these systems the BVMO is fused to a thermostable phosphite dehydrogenase for cofactor regeneration. Among class B enzymes, siderophore *N*-hydroxylating enzymes gained emerging interest, since they uncover peculiar kinetics and structural features (Olucha and Lamb, 2011).

**Class C** comprehends two-component FMN binding monooxygenases with a TIM-barrel fold. Class C enzymes catalyze Baeyer-Villiger oxidations, the oxidation of long-chain alkanes (Li *et al.*, 2008), the desulfurization of sulfonates, and the oxidation of aldehydes coupled with generation of bioluminescence (Ellis, 2010). Clearly, the main interest for two-component monooxygenases lies in the mechanism of flavin transfer. At present, there is no clear consensus on whether this transfer occurs through diffusion or protein channeling (Ellis, 2010).

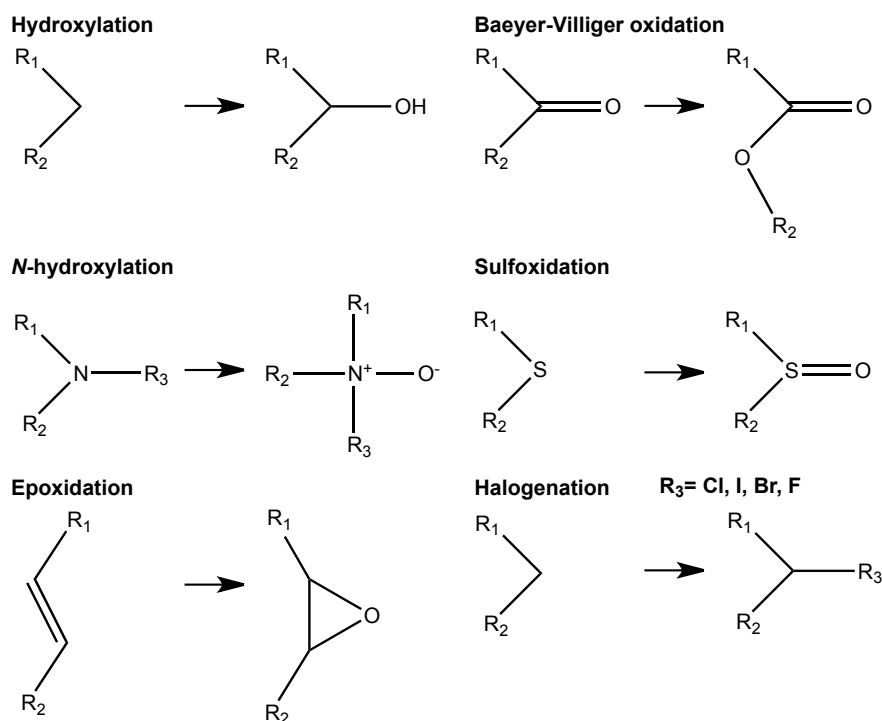
**Class D** two-component hydroxylases have an acyl-CoA dehydrogenase fold (Joosten and van Berkel, 2007). Most research on these enzymes has focused on 4-hydroxyphenylacetate 3-hydroxylase. This enzyme turned out to be a good model for studying flavin transfer (Sucharitakul *et al.*, 2007), oxygen diffusion (Baron, Riley, Chenprakhon, Thotsaporn, *et al.*, 2009b) and substrate regulation (Sucharitakul *et al.*, 2005; Tongsook *et al.*, 2011).

**Class E** flavoprotein monooxygenases are relatively rare (Mooney *et al.*, 2006; van Hellemond *et al.*, 2007; Lin *et al.*, 2010). These enzymes oxidize styrene derivatives to the corresponding epoxides and provide a highly enantioselective alternative to

## 1

chemical epoxidation catalysts (Schmid *et al.*, 2001). The monooxygenase component of the styrene converting system has many structural properties in common with class A aromatic hydroxylases (Ukaegbu *et al.*, 2010). Recently, the first self-sufficient single-component styrene monooxygenase/reductase system was discovered in a *Rhodococcus opacus* strain (Tischler *et al.*, 2009; Tischler *et al.*, 2010). This system is highly enantioselective but less efficient in substrate oxygenation.

**Class F** flavoprotein monooxygenases catalyze the regioselective chlorination and bromination of activated organic molecules (van Pée and Patallo, 2006; Blasiak and Drennan, 2009). These enzymes are of interest for the production of antibiotics,



Scheme 1. General overview of flavin-dependent monooxygenase reactions.

antitumor agents and other natural products (Butler and Sandy, 2009). The 3D structure of tryptophan 7-halogenase suggests a catalytic mechanism involving the formation of hypochlorous acid (HOCl), which is guided to the substrate binding site for the regioselective halogenation of the tryptophan (Dong *et al.*, 2005). More recent work suggests that the chloride addition reaction requires the critical involvement of a Lys and Glu residue (Flecks *et al.*, 2008) and provides interesting information about the structural determinants for regioselectivity control (Zhu *et al.*, 2009). Spectroscopic studies clearly showed a flavin-oxygen intermediate (C4a-hydroperoxyflavin), which could react with chloride anion to produce HOCl (Yeh *et al.*, 2007).



## ***Rhodococcus jostii* RHA1**

The genus *Rhodococcus* belongs to the *Actinomycetales* order of non-motile Gram-positive bacteria, characterized by a surprising catabolic diversity (Finnerty, 1992; Larkin *et al.*, 2005; Martínková *et al.*, 2009; van der Geize and Dijkhuizen, 2004). Important representatives of the same order are *Streptomyces*, producing most of the antibiotics in present use and *Mycobacterium*, first causing agent of bacterial infection human deaths.

*Rhodococcus* species are mostly non pathogenic with the exception of the horse and human pathogen *Rhodococcus equi* (Prescott, 1991) and the plant pathogen *Rhodococcus fascians* (Crespi *et al.*, 1992). Excluding antibiotic production, *Rhodococcus* is the most industrial relevant genus of *Actinomycetales*, especially for acrylamide production (Kobayashi and Shimizu, 1998), steroid production (Yam *et al.*, 2010; van der Geize and Dijkhuizen, 2004) and biosynthesis of natural surfactants (Lang and Philp, 1998).

*Rhodococcus jostii* RHA1, a potent degrader of polychlorinated biphenyls, was first isolated from contaminated soil (Seto *et al.*, 1995). It contains one of the largest bacterial genomes ever sequenced (9.7 Mb) (McLeod *et al.*, 2006), organized in a chromosome and three linear plasmids. From 16S analysis a close relationship emerges with *Rhodococcus opacus* (McLeod *et al.*, 2006). Whole proteome analysis highlights an interesting similarity with *Nocardia farcinica* IFM 10152 (43.3 %) and *Mycobacterium tuberculosis* H37Rv (35.5 %). The genetic and proteomic link between *R. jostii* RHA1 and *M. tuberculosis* has been used to study steroid degradation. It emerged that conserved steroid catabolism enzymes needed in *Mycobacterium* for macrophage survival (van der Geize *et al.*, 2007) can be an interesting target for vaccine development in *R. equi* (van der Geize *et al.*, 2011).

*R. jostii* RHA1 catabolic abilities are related to an extensive arsenal of oxygenases (203 putative genes), especially flavoprotein monooxygenases (80 putative sequences). This abundance makes the strain an interesting natural reservoir of novel oxidative flavoenzymes. Such metabolic flavin dependency is also present in *M. tuberculosis* and *Streptomyces coelicolor*, with yet no clear explanation (Macheroux *et al.*, 2011).

## 1

## Aim and outline

The work described in this thesis is the result of research performed in the BIOMOX cluster of the “Integrated Biosynthesis and Organic Synthesis (IBOS)” programme of the Netherlands Organization for Scientific Research (NWO). The goal was to develop new biocatalytic platforms to perform enantio- and regioselective oxidation reactions by using *R. jostii* RHA1 as biocatalysts source organism. The selected enzymatic reactions were hydroxylation, Baeyer-Villiger oxidations, epoxidation and sulfoxidations. Flavoprotein hydroxylases suited in the scope of the BIOMOX cluster in view of their unequalled ability to perform regioselective aromatic hydroxylations.

This thesis focuses on the molecular and structural characterization of 3-hydroxybenzoate 6-hydroxylase (3HB6H), one of the many flavoprotein monooxygenases present in *R. jostii* RHA1. 3HB6H catalyzes the *para*-hydroxylation of 3-hydroxybenzoate to 2,5-dihydroxybenzoate (gentisate), a compound used as matrix in MALDI-TOF mass spectrometry (Cvacka and Svatos, 2003) and as  $\alpha\beta$  oligomer assembly inhibitor (LeVine *et al.*, 2012).

The first part of this thesis (Chapters 3-5) describes the biochemical and structural characterization of 3HB6H from *R. jostii* RHA1. For this, the enzyme was produced in *Escherichia coli* and in a novel *R. jostii* RHA1#2 expression system. The second part of this thesis reports on the characterization of 3HB6H from *Pseudomonas alcaligenes* NCIMB 9867 (Chapter 6), exploring common features among 3HB6H enzymes. Finally, in Chapter 7, 3HB6H active site variants are studied regarding substrate binding and structural basis of regioselectivity.

**Chapter 2** presents an overview of the structural and catalytic properties of single-component flavoprotein hydroxylases. Within this subclass, some recurrent features are recognized and unanswered questions are discussed.

**Chapter 3** of the thesis describes a bioinformatics approach to mine the *R. jostii* RHA1 genome for flavoprotein hydroxylases. By using three specific protein fingerprints, a pool of flavoprotein hydroxylases was retrieved and several new functional assignments were made. 3HB6H, originally misannotated as salicylate hydroxylase, was selected for further biochemical characterization.

Until now, little is known about the structural properties of flavoprotein hydroxylases performing *para*-hydroxylations on monophenols. In **Chapter 4**, the crystallization and structural analysis of 3HB6H is presented. The three-dimensional structure of 3HB6H shows an overall fold typical for flavin-dependent aromatic hydroxylases. No substrate is found in the active site, but a phospholipid-like binds in a tunnel of the dimerization domain. Identification of the aliphatic ligand was

achieved by mass spectrometry and a role of the lipid in stabilizing the dimer has been proposed.

To further investigate the presence and role of the lipid guest, we overproduced 3HB6H in its original strain used as expression system under the induction of steroids. **Chapter 5** presents the first crystal structure of an enzyme produced in *R. jostii* RHA1#2. The Gram-positive expression host does not influence the structural and catalytic properties of 3HB6H, but a different type of membrane phospholipid is natively bound to the enzyme. Possible scenarios of sub-cellular localization and activity are discussed.

**Chapter 6** reports the characterization of 3HB6H from Gram-negative *P. alcaligenes* NCIMB 9867. Sequence comparison pointed to a less hydrophobic lipid binding site that might influence catalytic and oligomerization properties. 3HB6H from *P. alcaligenes* NCIMB 9867 has a similar coenzyme preference as *R. jostii* 3HB6H, but displays poor hydroxylation efficiency. In spite of significant sequence divergence, the enzyme retains the ability to bind phospholipids.

In **Chapter 7** we addressed the regioselectivity of hydroxylation of 3HB6H. From substrate docking and active site-directed mutagenesis, a Tyr-His pair, present in mirror-image fashion in 3-hydroxybenzoate 4-hydroxylase (3HB4H), seems to control the regioselectivity of 3-hydroxybenzoate hydroxylation.

## References

- Baron, R., McCammon, J.A. and Mattevi, A., (2009a) The oxygen-binding vs. oxygen-consuming paradigm in biocatalysis: structural biology and biomolecular simulation. *Current Opinion in Structural Biology*, 19(6), 672–679.
- Baron, R., Riley, C., Chenprakhon, P., Thotsaporn, K., et al., (2009b) Multiple pathways guide oxygen diffusion into flavoenzyme active sites. *Proceedings of the National Academy of Sciences of the United States of America*, 106(26), 10603–10608.
- Blasiak, L.C. and Drennan, C.L., (2009) Structural perspective on enzymatic halogenation. *Accounts of chemical research*, 42(1), 147–155.
- Butler, A. and Sandy, M., (2009) Mechanistic considerations of halogenating enzymes. *Nature*, 460(7257), 848–854.
- Chaiyen, P., (2010) Flavoenzymes catalyzing oxidative aromatic ring-cleavage reactions. *Archives of Biochemistry and Biophysics*, 493(1), 62–70.
- Crespi, M., Messens, E., Caplan, A.B., Van Montagu, M. and Desomer, J., (1992) Fasciation induction by the phytopathogen *Rhodococcus fascians* depends upon a linear plasmid encoding a cytokinin synthase gene. *EMBO Journal*, 11(3), 795–804.
- Cvacka, J. and Svatos, A., (2003) Matrix-assisted laser desorption/ionization analysis of lipids and high molecular weight hydrocarbons with lithium 2,5-dihydroxybenzoate matrix. *Rapid Communications in Mass Spectrometry*, 17(19), 2203–2207.
- Dong, C., Flecks, S., Unversucht, S., Haupt, C., van Pée, K.-H. and Naismith, J.H., (2005) Tryptophan 7-halogenase (PmA) structure suggests a mechanism for regioselective chlorination. *Science*, 309(5744), 2216–2219.
- Dudek, H.M., de Gonzalo, G., Pazmiño, D.E.T., Stepniak, P., Wyrwicz, L.S., Rychlewski, L. and Fraaije, M.W., (2011) Mapping the substrate binding site of phenylacetone monooxygenase from *Thermobifida fusca* by mutational analysis. *Applied and Environmental Microbiology*, 77(16), 5730–5738.
- Ellis, H.R., (2010) The FMN-dependent two-component monooxygenase systems. *Archives of Biochemistry and Biophysics*, 497(1-2), 1–12.
- Entsch, B. and van Berkel, W.J.H., (1995) Structure and mechanism of *para*-hydroxybenzoate hydroxylase. *FASEB Journal*, 9(7), 476–483.
- Finnerty, W.R., (1992) The biology and genetics of the genus *Rhodococcus*. *Annual Reviews in Microbiology*, 46(1), 193–218.
- Flecks, S., Patallo, E.P., Zhu, X., Ernyei, A.J., Seifert, G., Schneider, A., Dong, C., Naismith, J.H. and van Pée, K.-H., (2008) New insights into the mechanism of enzymatic chlorination of tryptophan. *Angewandte Chemie*, 47(49), 9533–9536.

- Fraaije, M.W., Kamerbeek, N.M., van Berkel, W.J.H. and Janssen, D.B., (2002) Identification of a Baeyer-Villiger monooxygenase sequence motif. *FEBS Letters*, 518(1-3), 43–47.
- Fraaije, M.W., Wu, J., Heuts, D.P.H.M., van Hellemond, E.W., Spelberg, J.H.L. and Janssen, D.B., (2005) Discovery of a thermostable Baeyer-Villiger monooxygenase by genome mining. *Applied Microbiology and Biotechnology*, 66(4), 393–400.
- Ghisla, S. and Massey, V., (1989) Mechanisms of flavoprotein-catalyzed reactions. *European journal of biochemistry*, 181(1), 1–17.
- Joosten, V. and van Berkel, W.J., (2007) Flavoenzymes. *Current Opinion in Chemical Biology*, 11(2), 195–202.
- Kamerbeek, N.M., Janssen, D.B., van Berkel, W.J.H. and Fraaije, M.W., (2003) Baeyer-Villiger monooxygenases, an emerging family of flavin-dependent biocatalysts. *Advanced Synthesis & Catalysis*, 345(6-7), 667–678.
- Kamerbeek, N.M., Moonen, M.J., van der Ven, J.G., van Berkel, W.J.H., Fraaije, M.W. and Janssen, D.B., (2001) 4-Hydroxyacetophenone monooxygenase from *Pseudomonas fluorescens* ACB. *European journal of biochemistry*, 268(9), 2547–2557.
- Kobayashi, M. and Shimizu, S., (1998) Metalloenzyme nitrile hydratase: structure, regulation, and application to biotechnology. *Nature Biotechnology*, 16(8), 733–736.
- Lang, S. and Philp, J.C., (1998) Surface-active lipids in rhodococci. *Antonie van Leeuwenhoek*, 74(1-3), 59–70.
- Larkin, M.J., Kulakov, L.A. and Allen, C.C.R., (2005) Biodegradation and *Rhodococcus*—masters of catabolic versatility. *Current Opinion in Biotechnology*, 16(3), 282–290.
- LeVine, H., Lampe, L., Abdelmoti, L. and Augelli-Szafran, C.E., (2012) Dihydroxybenzoic acid isomers differentially dissociate soluble biotinyl- $\text{A}\beta$ (1–42) oligomers. *Biochemistry*, 51(1), 307–315.
- Li, L., Liu, X., Yang, W., Xu, F., Wang, W., Feng, L., Bartlam, M., Wang, L. and Rao, Z., (2008) Crystal structure of long-chain alkane monooxygenase (LadA) in complex with coenzyme FMN: unveiling the long-chain alkane hydroxylase. *Journal of Molecular Biology*, 376(2), 453–465.
- Lin, H., Qiao, J., Liu, Y. and Wu, Z.L., (2010) Styrene monooxygenase from *Pseudomonas* sp. LQ26 catalyzes the asymmetric epoxidation of both conjugated and unconjugated alkenes. *Journal of Molecular Catalysis B: Enzymatic*, 67(3-4), 236–241.
- Macheroux, P., Kappes, B. and Ealick, S.E., (2011) Flavogenomics—a genomic and structural view of flavin-dependent proteins. *FEBS Journal*, 278(15), 2625–2634.
- Malito, E., Alfieri, A., Fraaije, M.W. and Mattevi, A., (2004) Crystal structure of a Baeyer-Villiger monooxygenase. *Proceedings of the National Academy of Sciences of the United States of America*, 101(36), 13157–13162.
- Martinková, L., Uhnáková, B., Pátek, M., Nešvera, J. and Křen, V., (2009) Biodegradation potential of the genus *Rhodococcus*. *Environment international*, 35(1), 162–177.
- Massey, V., (1994) Activation of molecular oxygen by flavins and flavoproteins. *Journal of Biological Chemistry*, 269(36), 22459–22462.
- McDonald, C.A., Fagan, R.L., Collard, F., Monnier, V.M. and Palfey, B.A., (2011) Oxygen reactivity in flavoenzymes: context matters. *Journal of the American Chemical Society*, 133(42), 16809–16811.
- McLeod, M.P., Warren, R.L., Hsiao, W.W.L., et al., (2006) The complete genome of *Rhodococcus* sp. RHA1 provides insights into a catabolic powerhouse. *Proceedings of the National Academy of Sciences of the United States of America*, 103(42), 15582–15587.
- Mirza, I.A., Yachnin, B.J., Wang, S., et al., (2009) Crystal structures of cyclohexanone monooxygenase reveal complex domain movements and a sliding cofactor. *Journal of the American Chemical Society*, 131(25), 8848–8854.
- Montersino, S., Tischler, D., Gassner, G.T. and van Berkel, W.J.H., (2011) Catalytic and structural features of flavoprotein hydroxylases and epoxidases. *Advanced Synthesis & Catalysis*, 353(13), 2301–2319.
- Mooney, A., Ward, P.G. and O'Connor, K.E., (2006) Microbial degradation of styrene: biochemistry, molecular genetics, and perspectives for biotechnological applications. *Applied Microbiology and Biotechnology*, 72(1), 1–10.
- Olucha, J. and Lamb, A.L., (2011) Mechanistic and structural studies of the *N*-hydroxylating flavoprotein monooxygenases. *Bioorganic Chemistry*, 39(5-6), 171–177.
- Orru, R., Dudek, H.M., Martinoli, C., Torres Pazmiño, D.E., Royant, A., Weik, M., Fraaije, M.W. and Mattevi, A., (2011) Snapshots of enzymatic Baeyer-Villiger catalysis. *Journal of Biological Chemistry*, 286(33), 29284–29291.
- Palfey, B.A. and McDonald, C.A., (2010) Control of catalysis in flavin-dependent monooxygenases. *Archives of Biochemistry and Biophysics*, 493(1), 26–36.
- Prescott, J.F., (1991) *Rhodococcus equi*: an animal and human pathogen. *Clinical microbiology reviews*, 4(1), 20–34.
- Reetz, M.T. and Wu, S., (2009) Laboratory evolution of robust and enantioselective Baeyer-Villiger monooxygenases for asymmetric catalysis. *Journal of the American Chemical Society*, 131(42), 15424–15432.
- Ryerson, C.C., Ballou, D.P. and Walsh, C., (1982) Mechanistic studies on cyclohexanone oxygenase. *Biochemistry*, 21(11), 2644–2655.
- Schmid, A., Hofstetter, K., Feiten, H.J., Hollmann, F. and Witholt, B., (2001) Integrated biocatalytic synthesis on gram scale: the highly enantioselective preparation of chiral oxiranes with styrene monooxygenase. *Advanced Synthesis & Catalysis*, 343(6-7), 732–737.
- Seto, M., Masai, E., Ida, M., Hatta, T., Kimbara, K., Fukuda, M. and Yano, K., (1995) Multiple polychlorinated biphenyl transformation systems in the Gram-Positive bacterium *Rhodococcus* sp. strain RHA1. *Applied and Environmental Microbiology*, 61(12), 4510–4513.
- Sheng, D., Ballou, D.P. and Massey, V., (2001) Mechanistic studies of cyclohexanone monooxygenase: chemical properties of intermediates involved in catalysis. *Biochemistry*, 40(37), 11156–11167.
- Sucharitakul, J., Chaiyen, P., Entsch, B. and Ballou, D.P., (2005) The reductase of *p*-hydroxyphenylacetate 3-hydroxylase from *Acinetobacter baumannii* requires *p*-hydroxyphenylacetate for effective catalysis. *Biochemistry*, 44(30), 10434–10442.
- Sucharitakul, J., Phongsak, T., Entsch, B., Svasti, J., Chaiyen, P. and Ballou, D.P., (2007) Kinetics of a two-component

*p*-hydroxyphenylacetate hydroxylase explain how reduced flavin is transferred from the reductase to the oxygenase. *Biochemistry*, 46(29), 8611–8623.

- Tischler, D., Eulberg, D., Lakner, S., Kaschabek, S.R., van Berkel, W.J.H. and Schlömann, M.**, (2009) Identification of a novel self-sufficient styrene monooxygenase from *Rhodococcus opacus* 1CP. *Journal of Bacteriology*, 191(15), 4996–5009.
- Tischler, D., Kermer, R., Gröning, J.A.D., Kaschabek, S.R., van Berkel, W.J.H. and Schlömann, M.**, (2010) StyA1 and StyA2B from *Rhodococcus opacus* 1CP: a multifunctional styrene monooxygenase system. *Journal of Bacteriology*, 192(19), 5220–5227.
- Tongsook, C., Sucharitakul, J., Thotsaporn, K. and Chaiyen, P.**, (2011) Interactions with the substrate phenolic group are essential for hydroxylation by the oxygenase component of *p*-hydroxyphenylacetate 3-hydroxylase. *Journal of Biological Chemistry*, 286(52), 44491–44502.
- Torres Pazmiño, D.E., Dudek, H.M. and Fraaije, M.W.**, (2010) Baeyer-Villiger monooxygenases: recent advances and future challenges. *Current Opinion in Chemical Biology*, 14(2), 138–144.
- Torres Pazmiño, D.E., Riebel, A., de Lange, J., Rudroff, F., Mihovilovic, M.D. and Fraaije, M.W.**, (2009) Efficient biooxidations catalyzed by a new generation of self-sufficient Baeyer-Villiger monooxygenases. *ChemBioChem*, 10(16), 2595–2598.
- Ukaegbu, U.E., Kantz, A., Beaton, M., Gassner, G.T. and Rosenzweig, A.C.**, (2010) Structure and ligand binding properties of the epoxidase component of styrene monooxygenase. *Biochemistry*, 49(8), 1678–1688.
- van Berkel, W.J.H., Kamerbeek, N.M. and Fraaije, M.W.**, (2006) Flavoprotein monooxygenases, a diverse class of oxidative biocatalysts. *Journal of Biotechnology*, 124(4), 670–689.
- van der Geize, R. and Dijkhuizen, L.**, (2004) Harnessing the catabolic diversity of rhodococci for environmental and biotechnological applications. *Current opinion in microbiology*, 7(3), 255–261.
- van der Geize, R., Grommen, A.W.F., Hessels, G.J., Jacobs, A.A.C. and Dijkhuizen, L.**, (2011) The steroid catabolic pathway of the intracellular pathogen *Rhodococcus equi* is important for pathogenesis and a target for vaccine development. *PLoS pathogens*, 7(8), e1002181.
- van der Geize, R., Yam, K., Heuser, T., et al.**, (2007) A gene cluster encoding cholesterol catabolism in a soil actinomycete provides insight into *Mycobacterium tuberculosis* survival in macrophages. *Proceedings of the National Academy of Sciences of the United States of America*, 104(6), 1947–1952.
- van Hellemond, E.W., Janssen, D.B. and Fraaije, M.W.**, (2007) Discovery of a novel styrene monooxygenase originating from the metagenome. *Applied and Environmental Microbiology*, 73(18), 5832–5839.
- van Pée, K.-H. and Patallo, E.P.**, (2006) Flavin-dependent halogenases involved in secondary metabolism in bacteria. *Applied Microbiology and Biotechnology*, 70(6), 631–641.
- Wu, S., Acevedo, J.P. and Reetz, M.T.**, (2010) Induced allostery in the directed evolution of an enantioselective Baeyer-Villiger monooxygenase. *Proceedings of the National Academy of Sciences of the United States of America*, 107(7), 2775–2780.
- Yam, K.C.Y.K.C., Okamoto, S.O.S., Roberts, J.N.R.J.N. and Eltis, L.D.E.L.D.**, (2010) Adventures in *Rhodococcus*-from steroids to explosives. *Canadian Journal of Microbiology*, 57(3), 155–168.
- Yeh, E., Blasiak, L.C., Koglin, A., Drennan, C.L. and Walsh, C.T.**, (2007) Chlorination by a long-lived intermediate in the mechanism of flavin-dependent halogenases. *Biochemistry*, 46(5), 1284–1292.
- Zhu, X., De Laurentis, W., Leang, K., Herrmann, J., Ihlefeld, K., van Pée, K.-H. and Naismith, J.H.**, (2009) Structural insights into regioselectivity in the enzymatic chlorination of tryptophan. *Journal of Molecular Biology*, 391(1), 74–85.



# Catalytic and structural features of flavoprotein hydroxylases and epoxidases

Stefania Montersino<sup>1\*</sup>, Dirk Tischler<sup>2,3\*</sup>, George T. Gassner<sup>3</sup> and  
Willem J. H. van Berkel<sup>1</sup>

<sup>1</sup> Laboratory of Biochemistry, Wageningen University,  
Dreijenlaan 3, 6703 HA Wageningen, The Netherlands

<sup>2</sup> Environmental Microbiology, TU Bergakademie Freiberg,  
Leipziger Str. 29, 09599 Freiberg, Germany

<sup>3</sup> Department of Chemistry and Biochemistry, San Francisco State University,  
1600 Holloway Avenue San Francisco, USA

\* These authors contributed equally

*Advanced Synthesis & Catalysis* (2011) 353: 2301-2319

## Abstract

2 Monooxygenases perform chemo-, regio- and/or enantioselective oxygenations of organic substrates under mild reaction conditions. These properties and the increasing number of representatives along with effective preparation methods, place monooxygenases in focus of industrial biocatalysis. Mechanistic and structural insights reveal reaction sequences and allow turning them into efficient tools for production of valuable products. Herein we describe two biocatalytically relevant subclasses of flavoprotein monooxygenases with a close evolutionary relation: subclass A represented by *p*-hydroxybenzoate hydroxylase (PHBH) and subclass E formed by styrene monooxygenases (SMOs). PHBH family members perform highly regioselective hydroxylations on a wide variety of aromatic compounds. The more recently discovered SMOs catalyze a number of stereoselective epoxidation and sulfoxidation reactions. Mechanistic and structural studies expose distinct characteristics, which provide a promising source for future biocatalyst development.



## Introduction

Biocatalytic oxygenation of aromatic compounds is a reaction performed mainly by heme, non-heme iron, copper, pterin and flavin-dependent enzymes (Torres Pazmino *et al.*, 2010). Especially flavoprotein monooxygenases are most abundant among prokaryotic as well as eukaryotic organisms. They cover a wide range of oxidation reactions and have been studied extensively and exploited for their ability to perform regio- and enantioselective hydroxylation, Baeyer-Villiger oxygenation, epoxidation, halogenation, and heteroatom oxidation (van Berkel *et al.*, 2006). The reaction between molecular oxygen and carbon in organic compounds is spin forbidden. However, embedded in the suitable protein environment, the flavin cofactor is able to activate the dioxygen molecule to transiently stable (hydro)peroxyflavin species that transfer one oxygen atom to the substrate. Such an important reaction is critical in many biological processes (Joosten and van Berkel, 2007) and therefore tightly regulated (Ballou *et al.*, 2005). Indeed, flavoprotein monooxygenases undergo different conformational changes to coordinate flavin adenine dinucleotide (FAD) reduction and oxygen insertion.

2

**Table 1. Flavoprotein hydroxylase and epoxidase structures.**

Subclass	PDB	Enzyme	Reference
A	1PBE	4-hydroxybenzoate 3-hydroxylase (PHBH)	(Schreuder <i>et al.</i> , 1989; Wierenga <i>et al.</i> , 1979)
A	1PN0 1FOH	phenol 2-hydroxylase (PHHY)	(Enroth, 2003; Enroth <i>et al.</i> , 1998)
A	2DKH SDKI	3-hydroxybenzoate 4-hydroxylase (MHBH)	(Hiromoto <i>et al.</i> , 2006)
A	2QA1 2QA2	UW16 12-hydroxylase (PgaE/CabE)	(Koskiniemi <i>et al.</i> , 2007)
A	2R0C 2R0G 2R0P	7-carboxy-K252c hydroxylase (RebC)	(Ryan <i>et al.</i> , 2007)
A	2VOU	2,6-dihydropyridine-3-hydroxylase (DHP)	(Treiber and Schulz, 2008)
A	2RGJ	phenazine-1-carboxylate hydroxylase (PhzS)	(Greenhagen <i>et al.</i> , 2008)
A	3IHG	aklavinone 11-hydroxylase (RdmE)	(Lindqvist <i>et al.</i> , 2009)
A	3GMB 3GMC	2-methyl-3-hydroxypyridine-5-carboxylic acid oxygenase (MHPCO)	(McCulloch <i>et al.</i> , 2009)
E	3IHM	styrene monooxygenase (StyA)	(Ukaegbu <i>et al.</i> , 2010)

Flavoprotein monooxygenases can be divided in six different subclasses according to structural features and oxygenation chemistry (van Berkel *et al.*, 2006). Single-component aromatic hydroxylases (subclass A) perform a wide range of strictly regioselective hydroxylation reactions. Most of the research on flavin-dependent aromatic hydroxylases has been done on 4-hydroxybenzoate 3-hydroxylase (PHBH) from *Pseudomonas* species. Moreover, for many years only crystal structures of PHBH and phenol hydroxylase (PHHY) were present in the PDB database. Since 2006, the number of available flavoprotein hydroxylase structures has increased (Table 1), and

more detailed studies on the catalytic mechanisms of such enzymes are opening a new season of research in the field.

Styrene monooxygenases (subclass E) are promising biocatalysts because of their ability to produce enantiopure epoxides and sulfoxides (Kuhn *et al.*, 2010; van Hellemond *et al.*, 2007; Mooney *et al.*, 2006; Schmid, Hofstetter, Feiten, Hollmann and Witholt, 2001b). Sequence analysis, mechanistic studies and recent structural investigations indicate that SMOs are evolutionary linked to the subclass A enzymes (Table 1) (van Berkel *et al.*, 2006; Ukaegbu *et al.*, 2010). Nearly all bacterial SMOs are two-component enzymes comprising a reductase and a monooxygenase. Remarkably, in a few cases, the reductase is fused to the monooxygenase, representing the first self-sufficient SMO (StyA2B) (Tischler *et al.*, 2009). StyA2B can also cooperate with a single monooxygenase (StyA1), resulting in a novel type of two-component SMO (Tischler *et al.*, 2010). We here give an overview of the latest findings regarding flavoprotein hydroxylases and epoxidases and correlate their three-dimensional structures with the performed catalysis. Conclusions and perspectives for future research are given and first pilot applications of flavoprotein monooxygenases in biotechnological processes are demonstrated.

## Flavoprotein Hydroxylases

**4-Hydroxybenzoate 3-Hydroxylase: The Root Of The Family.** The first flavin-dependent aromatic hydroxylase, salicylate 1-hydroxylase, was described more than 40 years ago (Yamamoto *et al.*, 1965). However, most knowledge about the structure-function relationship of these enzymes has been gained from studies on 4-hydroxybenzoate 3-hydroxylase (PHBH) (Palfey and McDonald, 2010; Entsch *et al.*, 2005; Entsch and van Berkel, 1995).

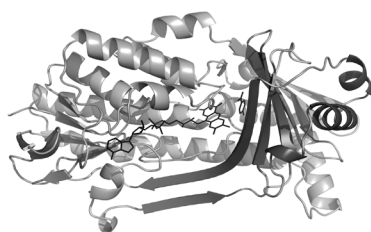
PHBH is a homodimer with each subunit containing a tightly non-covalently bound FAD. PHBH catalyzes the *ortho*-hydroxylation of 4-hydroxybenzoate to 3,4-dihydroxybenzoate, a key intermediate step in the microbial degradation of aromatic compounds, using NADPH and oxygen (Scheme 1A). PHBH has narrow substrate specificity. Besides the parent substrate, the enzyme is active with 2,4-dihydroxybenzoate, 4-mercaptobenzoate and a number of fluorinated and chlorinated substrate analogues (Spector and Massey, 1972; Husain *et al.*, 1980; Entsch, Ballou, Husain and Massey, 1976b; Jadan *et al.*, 2004). Potential substrates such as 4-aminobenzoate and 2-hydroxy-4-aminobenzoate bind perfectly in the active site but are not converted because they fail to stimulate the reduction of the flavin by NADPH (Entsch and van Berkel, 1995).

The protein topology of PHBH is shared by several flavoenzymes (Mattevi, 1998). It is organized in an FAD binding domain and a substrate binding domain (Fig. 1A) (Schreuder *et al.*, 1989). At the intersection between the two domains resides the active site. The first PHBH structure was solved in 1979 (Wierenga *et al.*, 1979)

and so far 35 structures of PHBH variants and complexes have been published.

PHBH catalysis follows a bi-uni-uni-ping-pong kinetic mechanism (Husain and Massey, 1979) and consists of two half-reactions according to the state of the flavin (Fig.2). In the reductive half-reaction, the oxidized flavin of the enzyme-substrate complex gets reduced by NADPH. The oxidative half-reaction involves the reaction of reduced FAD with oxygen, the hydroxylation of the substrate and the reoxidation of the flavin. Structural and rapid kinetics studies on wild-type and engineered enzyme

A)



B)

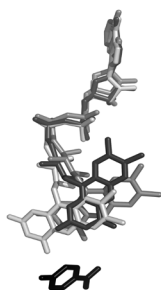


**Figure 1. PHBH structure and FAD mobility.**

**A)** Overall PHBH structure (PDB: 1PBE): light grey, FAD domain; dark grey, substrate domain. Black lines, FAD and 4-hydroxybenzoate. **B)** Stick representation of FAD conformation: light grey, *in* conformation; dark grey, *open* conformation; black, *out* conformation. 4-hydroxybenzoate is also represented in black sticks.

variants elucidated many details of the catalytic cycle of PHBH. Moreover, these investigations revealed that the isoalloxazine ring of the FAD cofactor is mobile and can swing *in* and *out* of the active site to ensure proper binding and catalysis (Gatti *et al.*, 1994; Schreuder *et al.*, 1994; van Berkel *et al.*, 1994).

Binding of 4-hydroxybenzoate to the oxidized enzyme happens via the FAD cleft (Fig. 1A). In the absence of substrate, the FAD exchanges between the *open* and *in* conformation with a negligible consumption of NADPH (Fig. 1B). With substrate bound, the FAD occupies the *in* conformation. Different PHBH variants carrying mutations affecting the *open-in* exchange were studied by rapid kinetics and crystallography (Entsch *et al.*, 2005). Binding studies indicated that 4-hydroxybenzoate is bound in the dianionic form (Shoun *et al.*, 1979; van Berkel and Muller, 1989). From mutagenesis studies it became apparent that the hydrogen-bond network formed by Tyr201, Tyr385 and His72 subtracts a proton from the 4-hydroxy group of the substrate thereby shifting its  $pK_a$  from 9.3

to 7.3 (Entsch and van Berkel, 1995; Palfey *et al.*, 1999). Binding and deprotonation of the substrate is coupled with flavin movement *out* of the active site, inducing cofactor reduction (Eppink and van Berkel, 1999; Entsch *et al.*, 2005). Strikingly, the reaction between enzyme and NADPH is stimulated  $\sim 10^5$  fold in the presence of the substrate (Husain and Massey, 1979; Eppink *et al.*, 1998). Compounds able to elicit flavin reduction are called effectors. Only few of them are substrate analogues (Table 2) and,

therefore, become hydroxylated. Non-substrate effectors (Table 2), on the other hand, stimulate the production of  $H_2O_2$  by uncoupling NADPH oxidation from substrate hydroxylation. Remarkable is the case of the folate intermediate 4-aminobenzoate: perfect binding but poor effector ability (Schreuder *et al.*, 1994; Entsch and van Berkel, 1995). Because 4-aminobenzoate fails to stimulate flavin movement, this potential substrate acts as a competitive inhibitor. Thus, by discriminating between substrates at the stage of FAD reduction, PHBH avoids a possible side reaction with an important growth factor.

NADPH cannot reduce the flavin in its *in* and *open* orientation, because there is no space for the nicotinamide moiety to enter the active site. A movement of  $30^\circ$  of the ribityl chain drives the flavin in the proper position for reduction (*out* position (Fig.1B)). PHBH structures in complex with 2,4-dihydroxybenzoate, 2-hydroxy-4-aminobenzoate and with arabino-FAD mimic the FAD orientation for proper reduction (Schreuder *et al.*, 1994; van Berkel *et al.*, 1994).

Flavin reduction by NADPH occurs by a hydride transfer mechanism and is followed by  $NADP^+$  release (Husain and Massey, 1979; Entsch *et al.*, 1991; Entsch *et*

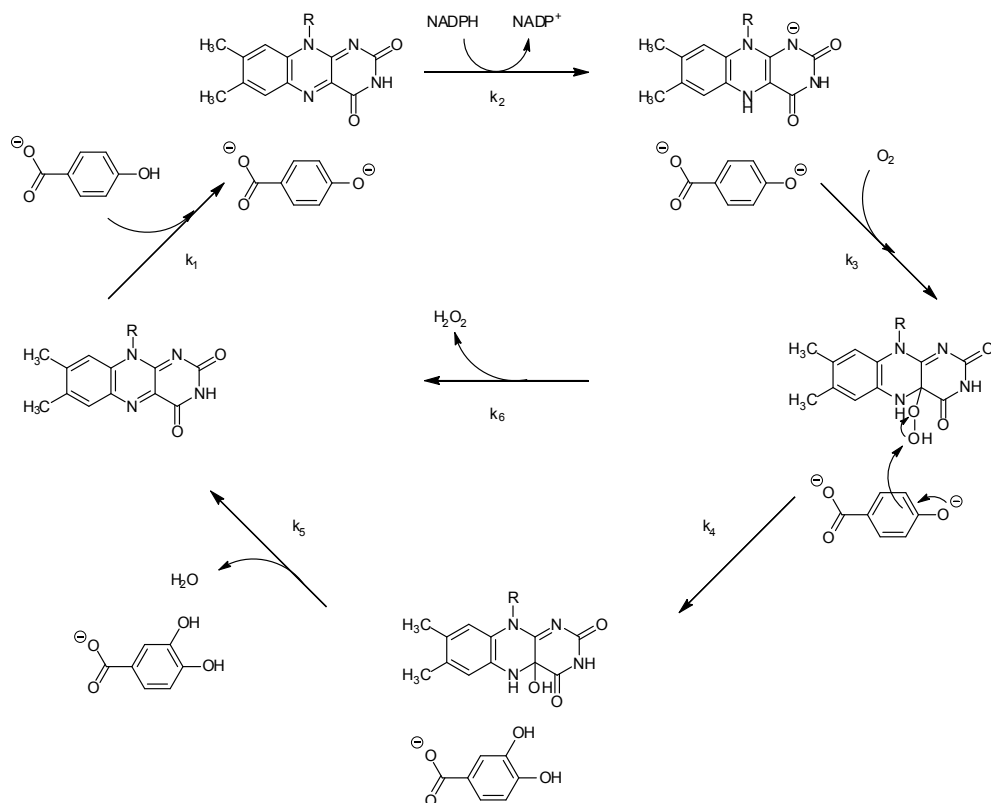


Figure 2. Catalytic cycle of PHBH.

Table 2. Substrates and effectors of PHBH.

	Compound	Main Product
<b>Substrate</b>	4-hydroxybenzoate	3,4-dihydroxybenzoate
	2,4-dihydroxybenzoate	2,3,4-trihydroxybenzoate
	4-mercaptopbenzoate	4,4'-ditiobisbenzoate
	2-fluoro-4-hydroxybenzoate	2-fluoro-3,4-hydroxybenzoate <sup>a</sup>
	3-fluoro-4-hydroxybenzoate	5-fluoro-3,4-hydroxybenzoate <sup>a</sup>
	3,5-difluoro-4-hydroxybenzoate	5-fluoro-3,4-hydroxybenzoate <sup>a</sup>
	2,3,5,6-tetrafluoro-4-hydroxybenzoate	2,5,6-trifluoro-3,4-dihydroxybenzoate <sup>a</sup>
	2-chloro-4-hydroxybenzoate	2-chloro-3,4-dihydroxybenzoate <sup>a</sup>
	3-chloro-4-hydroxybenzoate	5-chloro-3,4-dihydroxybenzoate <sup>a</sup>
<b>Non-substrate effectors</b>	3,4-dihydroxybenzoate	H <sub>2</sub> O <sub>2</sub>
	4-fluorobenzoate	H <sub>2</sub> O <sub>2</sub>
	benzoate	H <sub>2</sub> O <sub>2</sub>
	6-hydroxynicotinate	H <sub>2</sub> O <sub>2</sub>
	5-hydroxypicolinate	H <sub>2</sub> O <sub>2</sub>
<b>Inhibitors</b>	4-aminobenzoate	3-hydroxy-4-aminobenzoate <sup>b</sup>

<sup>a</sup> Regioselectivity dependent on the bacterial strain (Jadan *et al.*, 2004)

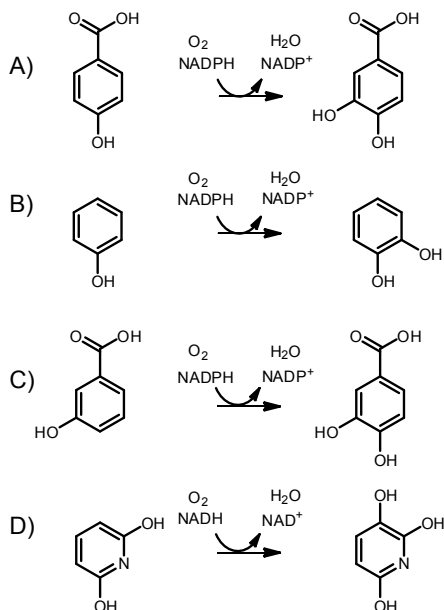
<sup>b</sup> If FAD is reduced chemically

*al.*, 2005). After reduction, the anionic flavin moves to the inner position in the active site where the reactions with oxygen and substrate occur. Oxygen might enter the protein *via* guided paths (Baron *et al.*, 2009) to react with the reduced FAD. The rate of such a reaction in the active site is 2–4 orders of magnitude faster than with free flavin in solution. Binding of oxygen takes place only on the *re* side of the isoalloxazine ring while the other side (*si* side) is in direct contact with the protein and therefore blocked.

The reaction with oxygen occurs in three steps (Palfey and McDonald, 2010). Briefly, one electron moves from FADH<sup>•</sup> to O<sub>2</sub> forming superoxide: this is the rate-limiting step of the reaction. Then radical recombination between the FAD radical and superoxide produces the covalent C4a-peroxyflavin adduct which is eventually protonated to yield the flavin C4a-hydroperoxide. Reduced flavin in the *in* orientation is shielded from solvent, a necessary condition for the stabilization of the flavin C4a-hydroperoxide. Studies with active site mutants have revealed how poor stabilization of the oxygenated flavin species results in inefficient substrate hydroxylation (Entsch *et al.*, 2005; Entsch and van Berkel, 1995).

Substrate hydroxylation in flavoprotein aromatic hydroxylases involves splitting of the oxygen-oxygen bond (Ridder *et al.*, 2000) and proceeds via electrophilic aromatic substitution: the C4a-hydroperoxide acts as the electrophile and the aromatic substrate as nucleophile (Ortiz-Maldonado *et al.*, 1999). In PHBH, the H-bond network connecting Tyr201, Tyr385 and His72 enhances substrate nucleophilicity via deprotonation of the 4-hydroxy group (Entsch *et al.*, 1991; Ortiz-Maldonado *et al.*, 2004). As explained above, deprotonation is also important for the effector role of the substrate.

Due to the limited stability of the oxygenated flavin species, no crystallographic



**Scheme 1. Reactions catalyzed by A) PHBH B)PHHY C)MHBH D) DHP hydroxylase.**

snapshots have been obtained of the events during the oxidative half reaction. After substrate hydroxylation, the C4a-hydroxyflavin is formed (Entsch, Ballou and Massey, 1976a). In the final stage of the reaction (Fig.2), this intermediate releases water and the aromatic product exchanges with substrate through movement of the flavin into the *open* conformation.

### Phenol 2-Monooxygenase: The First Eukaryotic Flavoprotein Hydroxylase.

Phenol 2-monooxygenase (PHHY) from the yeast *Trichosporum cutaneum* catalyzes the hydroxylation of phenol to catechol (Scheme 1B). The strictly NADPH-dependent enzyme can accept hydroxy, amino, halogen or methyl derivatives of phenol (Neujahr and Kjellén, 1978; Peelen *et al.*, 1995; Peelen *et al.*, 1993). In contrast to PHBH, PHHY

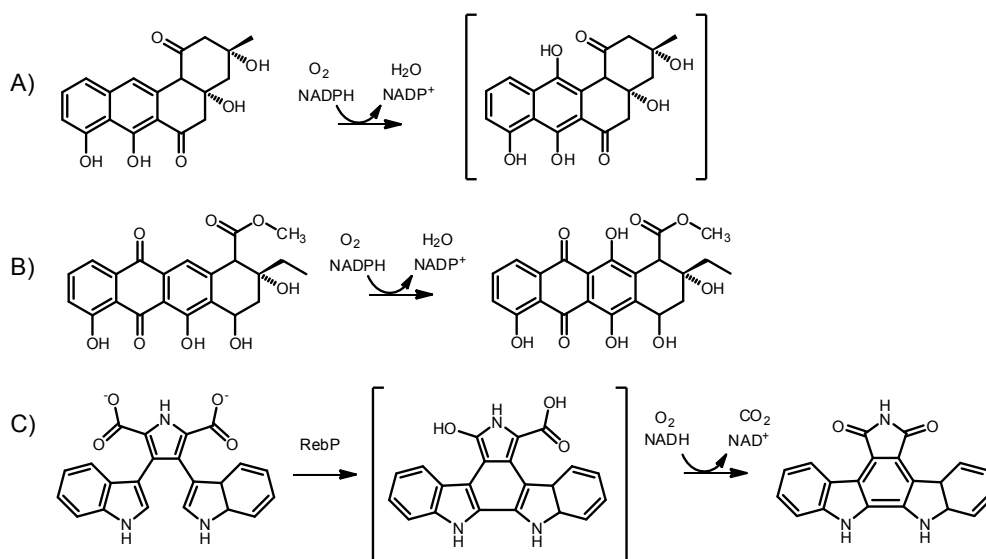
shows significant uncoupling of substrate hydroxylation, even with the physiological substrate (Neujahr and Kjellén, 1978). A slow hydroxylation rate is the main cause of the unproductive formation of hydrogen peroxide (Maeda-Yorita and Massey, 1993).

The PHHY structure (PDB: 1FOH and 1PN0) contains a third domain similar to a thioredoxin domain, present in other flavoprotein hydroxylases as well (Enroth, 2003; Enroth *et al.*, 1998). However, no real function for this domain was observed. Structural studies confirmed and explained further more previous biochemical data. Flavin mobility, as first reported for PHBH, is visible in the tetrameric PHHY structure. In different monomers of the enzyme-substrate complex, FAD is present in the *in* or *out* conformation. Moreover, the presence of a flexible lid that regulates substrate entry excludes solvent from the active site (Enroth *et al.*, 1998).

Studies performed with fluorinated phenols pointed at pH dependence in the regioselectivity of substrate hydroxylation (Peelen *et al.*, 1993; Peelen *et al.*, 1995). At low pH, hydroxylation was more favoured at C-6 than at C-2. One possible explanation would be the presence of a catalytic base able to abstract a proton from the hydroxy group of phenol. However, Xu *et al.* studied some PHHY variants in relation to the catalytic base with no correlation with PHBH results (Xu *et al.*, 2002; Xu *et al.*, 2001). Residues involved in the catalytic functions of PHHY are very different from those of PHBH, even though the two enzymes have similar reaction intermediates.

## New Flavoprotein Hydroxylases

**3-Hydroxybenzoate 4-Hydroxylase.** 3-Hydroxybenzoate 4-hydroxylase (MHBH) from *Comamonas testosteroni* converts 3-hydroxybenzoate into 3,4-dihydroxybenzoate at the expense of NADPH and O<sub>2</sub> (Scheme 1C). MHBH folds in a three-domain fashion with dimerization mediated by the thioredoxin domain (Hiromoto *et al.*, 2006). The enzyme is closely related to PHHY with 38% identity according to a DALI structural alignment. Residues in the active sites are also well conserved. Nevertheless, attempts to switch the substrate specificity of MHBH from 3-hydroxybenzoate to phenol by directed evolution did not show the expected change (Chang and Zylstra, 2008). The result stresses how mechanisms concerning the substrate and effector specificity of flavoprotein hydroxylases may have evolved in a more complicated way.



Scheme 2. Reactions catalyzed by A) PgaE/CabE B) RdmE C) RebC.

Based on the MHBH three-dimensional structure, Hiromoto and colleagues hypothesized that the recognition of the 3-hydroxybenzoate substrate starts at the surface of the protein with the same type of residues present in the active site. Moreover, they proposed the existence of a hydrophobic tunnel, not present in PHBH or PHHY, for the transport of the substrate to the active site, and a hydrophilic channel for oxygen diffusion (Hiromoto *et al.*, 2006).

PHBH, PHHY and MHBH perform *ortho*-hydroxylation reactions on related substrates. Nevertheless, their active sites are highly tuned for the conversion of a specific substrate. In this context it should be noted here that a detailed catalytic and structural comparison among *ortho*- and *para*-hydroxylating enzymes that are active

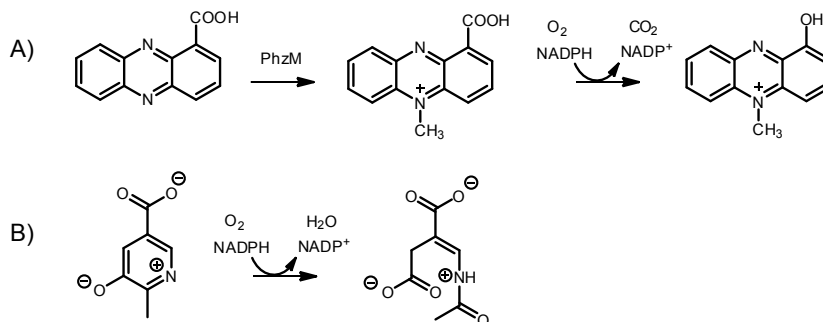


with the same substrate would add another level of information about the mechanisms and active site topologies of flavoprotein hydroxylases.

**DHP Hydroxylase.** Many flavoprotein hydroxylases are involved in the degradation of xenobiotics in the soil. Nicotine is degraded through multiple hydroxylations, oxidations and ring opening reactions producing  $\gamma$ -*N*-methylaminobutyric acid and 2,6-dihydroxypyridine (DHP). The latter compound is converted by 2,6-dihydroxypyridine-3-hydroxylase (DHP hydroxylase) to 2,3,6-trihydroxypyridine (Scheme 1D).

The hydroxylation product spontaneously oxidizes and dimerizes to a blue pigment. Biochemical data show how specific the enzyme is for the physiological substrate, but the information is not sufficient to fully understand the chemistry behind the reaction (Baitsch *et al.*, 2001). In 2008, the structure of DHP hydroxylase was solved at 2.6 Å resolution (Treiber and Schulz, 2008), showing an overall topology related to other subclass A structures. Knowledge on enzymes involved in nicotine metabolism could provide novel applied tools for solving environmental and health issues in the tobacco industry (Schmid, Dordick, Hauer, Kiener, Wubbolts and Witholt, 2001a).

**UWM16 Hydroxylase/Aklavinone 11-Hydroxylase.** Aromatic polyketides constitute an important class of secondary metabolites produced by Actinomycetes, fungi and plants. Angucyclines and anthracyclines belong to this class and are antibiotics produced by *Actinomycetales* and *Streptomyces* species. Flavoprotein hydroxylases are especially involved in early tailoring steps, which modify the common UW16 and aglycone cores (Scheme 2).



Scheme 3. Reactions catalyzed by A) PhzS B) MHPCO.

Tailoring steps (oxygenation, hydroxylations, dehydrogenations, dehydrations and carbon–carbon bond rearrangements) produce different compounds depending of the set of enzymes present; consequently, polyketide hydroxylases are an interest research subject for enzymologists. Recently, several structures for flavoprotein polyketide hydroxylases were solved (Koskiniemi *et al.*, 2007; Lindqvist *et al.*, 2009).



Among these enzymes, PgaE and CabE are involved in gaudimycin C biosynthesis in *Streptomyces* species (Scheme 2A), whereas aklavinone 11-hydroxylase (RdmE) is involved in the biosynthesis of rhodomycin in *Streptomyces purpurascens* (Scheme 2B).

PgaE, CabE and RdmE share the three-domain folding topology. This organization seems required for proper folding, as suggested by inclusion bodies formation of the PgaE C-terminal truncation mutant. The PgaE and CabE proteins were crystallized in the absence of substrate while RdmE gave crystals in complex with the substrate. In RdmE, a chemical match between substituents and binding pockets ensures stereospecific recognition of the C-9 *R* isomer. Inversion of the stereochemistry would result in a hydrophilic group of the substrate pointing into a hydrophobic patch of the enzyme. In contrast to other tailoring enzymes, RdmE does not accept substrates glycosylated at C-7. This selectivity is explained by the presence of a pocket next to the C-7 hydroxy group that produces several clashes if carbohydrate atoms are modeled (Lindqvist *et al.*, 2009).

*In vitro* studies with PgaE illustrate that conversion of UWM6 into gaudimycin C requires multiple coupled reactions to prevent intermediate degradation, complicating detailed biochemical studies (Kallio *et al.*, 2008). Nevertheless, more information regarding the substrate specificity and evolution potential could help in determining the synthetic and catalytic value of these polyketide hydroxylases.

**Flavoprotein Hydroxylase RebC.** Rebeccamycin is an antitumour agent that binds topoisomerase I complexes to prevent replication of DNA. Rebeccamycin biosynthesis recruits several enzymes able to build the aglycone scaffold from tryptophan, among them the flavoprotein hydroxylase RebC. RebC works in concert with the P450 cytochrome RebP to produce the rebeccamycin precursor arciriaflavin A (Scheme 2C). The individual reactions of RebP and RebC were unknown until Ryan and co-workers solved the RebC structure with the putative substrate trapped in the active site (Ryan *et al.*, 2007). Since 7-carboxy-K252c is assumed to be the nearest physiological substrate of RebC, attempts were made to elucidate the RebC reaction mechanism and its ability to tune the reaction into one single product (Ryan *et al.*, 2007; Howard-Jones and Walsh, 2006). Groom and coworkers (Groom *et al.*, 2011) were able to switch the regioselectivity of RebC from rebeccamycin to staurosporine production through exchanging a pair of active-site residues important in indolocarbazole ring contact. Among different indolocarbazole biosynthetic enzymes, Arg239 and Phe216 emerged as the key residues, mediating repeated regioselective substrate oxidation.

In 2008 a study about flavin movement and protein rearrangement drew up a new hypothesis about substrate entrance in the RebC active site. Ryan and colleagues crystallized RebC in substrate free (2R0C), substrate bound (2R0P) and cofactor reduced (2R0G) forms (Ryan *et al.*, 2008). The free enzyme shows a disordered helix in the back of the protein that gets ordered upon substrate binding and reduction of

the flavin. The current view is that the flexible loop permits substrate entrance. Once the substrate is bound, the loop folds into a helix that acts as a lid, ensuring exclusion of water from the active site. Reversible helix melting during catalysis guarantees substrate binding, entrapment and product release.

## 2

**Flavoprotein Hydroxylase PhzS: Pigment Biosynthesis.** Pyocyanin, a blue-pigmented phenazine derivative, is a virulence factor in *Pseudomonas aeruginosa*. Pyocyanin is involved in redox reactions consuming NADH, glutathione and other cell antioxidants. The reactive oxygen species thereby produced help *P. aeruginosa* to survive. The latest step in pyocyanin biosynthesis involves the flavoprotein PhzS, the action of which is tightly coupled with the adenosylmethionine-dependent methyltransferase PhzM. A recent review on secondary metabolites redox activity highlights the importance of both enzymes as drug targets in cancer or inflammatory diseases (Jacob *et al.*, 2011).

PhzS catalyzes the decarboxylative hydroxylation of phenazine 1-carboxylate (PCA), together with PhzM (Scheme 3A). From a mechanistic point of view, PhzS is quite an intriguing enzyme. 5-MethylPCA is an electron-poor substrate unlikely to participate in an electrophilic aromatic substitution reaction. Deuterium incorporation experiments suggest that the enzyme does not perform proton abstraction from the methyl group inserted by PhzM to increase electron density at the carboxyl group. Therefore, a nucleophilic substitution mechanism is proposed (Greenhagen *et al.*, 2008).

The overall structure of substrate free PhzS resembles those of other flavoprotein hydroxylases with FAD oriented in a rather contorted *out* conformation. Like RebC, PhzS has a disordered region near the substrate binding site, which might become ordered upon substrate binding. Structure and biochemical data of the interacting enzyme PhzM are also available (Parsons *et al.*, 2007), giving the possibility to study the complex in further detail.

**MHPCO: Unusual Pyridine Ring-Opening Reaction.** 2-Methyl-3-hydroxypyridine 5-carboxylic acid oxygenase (MHPCO) catalyzes two reactions: a pyridine hydroxylation and an unique ring-opening reaction (Scheme 3B) (Chaiyen, Brissette, Ballou and Massey, 1997c). The structure of MHPCO from *Mesorhizobium loti* MAFF303099 and the mechanism of the enzyme from *Pseudomonas* MA1 have been studied in quite some detail (McCulloch *et al.*, 2009; Chaiyen, Brissette, Ballou and Massey, 1997b; Chaiyen *et al.*, 2004). The overall MHPCO structure resembles that of PHBH, but the flavin occupies the *in* conformation in both free and substrate bound structures. Interestingly, the active site is larger than that in PHBH and contains nine water molecules deputized to form most of the bonds with the substrate. Even if the overall reaction mechanism is conserved, it seems that MHPCO behaves differently than PHBH. None of the charge-transfer species typical of the reductive half reaction

were observed and flavin movement is not the rate-limiting factor for hydride transfer (Chaiyen *et al.*, 2004). Nevertheless, NADPH binding seems unlikely with the flavin in the *in* conformation.

MHPCO selectively binds the tri-ionic form of the substrate (Chaiyen, Brissette, Ballou and Massey, 1997a), suitable already for electrophilic aromatic substitution, and does not contain a PHBH-type of hydrogen-bond network to activate the substrate. Nevertheless, the role of water in the ring-opening process is still under debate (Chaiyen, 2010).

## Recurrent Features And Open Questions

**Flavin-Dependent Hydroxylases In Biocatalysis.** Despite the intrinsic diversity among flavoprotein hydroxylases, general guidelines can be drawn about typical conditions for enzyme assays and HPLC product analysis (Jadan *et al.*, 2004; van Berkel *et al.*, 1999).

Standard flavoprotein hydroxylase activities are measured spectrophotometrically by following the consumption of NADH or NADPH ( $\epsilon_{340} = 6.22 \text{ mM}^{-1}\text{cm}^{-1}$ ), in air-saturated buffer at pH 7–8. Most flavoprotein hydroxylases are inhibited by monovalent anions (Steennis *et al.*, 1973; van Berkel and van den Tweel, 1991; van Berkel and Muller, 1991); therefore the use of chloride-containing buffers should be avoided. For standard assays and product analysis, enzyme concentrations may vary between 20 and 200 nM. Enzymes like RebC and PhzS need to interact with RebP and PhzM to perform proper catalysis, therefore enzyme ratio optimization is required. HPLC product analysis is usually done with  $C_{18}$  reverse phase columns, running in 0.1% TFA or acetic acid and gradient elution with methanol or acetonitrile (Jadan *et al.*, 2004). Whole cell catalysis, as developed for Baeyer-Villiger monooxygenases (de Gonzalo *et al.*, 2010) and styrene monooxygenase (*vide infra*), is not commonly applied for flavoprotein hydroxylases, but synthesis of valuable polyketide antibiotics may need this kind of approach.

**Flavin Mobility.** Cofactor movement during catalysis is one of the surprising features of flavoprotein hydroxylases. It was discovered in PHBH and turns out to be a general mechanism. Recent studies revealed that, in some hydroxylases, the aromatic substrate is not necessary for flavin movement. An example is the substrate-free RebC where a loop-helix transition helps FAD to swing *in* after reduction (Ryan *et al.*, 2008).

**Electrophilic Aromatic Substitution And Substrate Activation.** Oxygen insertion in flavoprotein monooxygenases is a tightly controlled mechanism. Highly reactive oxygen species are generated by adduct formation between the cofactor and oxygen. Flavoprotein monooxygenases adopt different strategies to perform oxygenation: Baeyer–Villiger monooxygenases (subclass B) react according to nucleophilic

(aromatic) substitution while hydroxylases perform electrophilic aromatic substitution (van Berkel *et al.*, 2006). In the latter case, the substrate acts as the nucleophile and the C4a-hydroperoxyflavin as the electrophile. The increased number of flavoprotein hydroxylase structures has given new insights on how these enzymes deal with substrate and flavin activation. To increase substrate nucleophilicity, PHBH has evolved a hydrogen bond network for substrate deprotonation (Entsch and van Berkel, 1995). In contrast, MHPCO selectively binds only the substrate tri-ionic form, ensuring enough electron density at the oxygenated carbon (Chaiyen, Brissette, Ballou and Massey, 1997b). Enzymes reacting with poor nucleophiles, such as PhzS, work in concert with another protein (PhzM, Scheme 3A). Such an interaction could ensure the formation of a transient substrate intermediate suitable for hydroxylation (Greenhagen *et al.*, 2008). The H-bond network ensuring proton storage during catalysis could be a peculiarity of PHBH or may be less tuned in other enzymes as in PHHY. Detailed rapid kinetics studies with enzyme variants might highlight such differences in substrate activation.

**Flavoprotein Hydroxylases: One Enzyme, Three Substrates.** Flavoprotein hydroxylases use three different substrates during catalysis: NAD(P)H, oxygen and an aromatic substrate. Questions about binding and transport of such substrates are partially without answer.

Flavoprotein monooxygenases use NAD(P)H as electron donor for flavin reduction. Rapid dissociation of the oxidized pyridine nucleotide discriminates flavoprotein hydroxylases from Baeyer–Villiger monooxygenases where the coenzyme remains bound throughout the catalysis and is needed for the stabilization of the anionic peroxyflavin (Malito *et al.*, 2004; Sheng *et al.*, 2001). A specific NAD domain ensures the tight interaction with the pyridine nucleotide in Baeyer–Villiger monooxygenases, while such domain is not present in hydroxylases. In fact, in the class A enzymes, the NAD(P)H can only react with the flavin in the *out* conformation, and is immediately released after oxidation. So far, it has been a challenge to structurally define the mode of binding of the pyridine nucleotide in flavoprotein hydroxylases. Protein engineering and crystallography studies of PHBH uncovered a plausible interdomain binding mode for NADPH (Eppink *et al.*, 1998; Wang *et al.*, 2002; Eppink *et al.*, 1999). Most flavoprotein hydroxylases are specific for either NADH or NADPH. Eppink *et al.* (Eppink *et al.*, 1999) were able to switch the PHBH coenzyme specificity by mutating residues belonging to helix H2 residing near the protein surface, far away from the active site. PHBH enzymes from Gram-negative bacteria are NADPH-specific while PHBH from Gram-positive strains show NADH preference. A consensus sequence in helix H2 seems indeed the key determinant for the coenzyme specificity in PHBH (Montersino *et al.*, 2008). Recently, Baron and colleagues studied the oxygen transport in flavoprotein oxidases and monooxygenases (Baron *et al.*, 2009). They showed that oxygen diffusion is protein guided via multiple pathways that funnel into discrete oxygen entry points in the active site. The entry

point is blocked in related dehydrogenases, explaining why these flavoenzymes poorly react with oxygen (Leferink *et al.*, 2009).

Flavoprotein hydroxylases may have evolved several strategies to permit substrate entrance into the active sites. In PHBH, the *open* conformation seems required to let the substrate enter directly from the FAD cleft. In PHHY, phenol may enter from the same side, but no FAD *open* conformation was observed. Instead, cofactor movement in PHHY is coupled to a major conformational change of a helix that acts as a lid, closing the FAD cleft after substrate binding. MHBH, PhzS and MHPCO display a tunnel probably needed to guide the substrate from the surface to the active site (Hiromoto *et al.*, 2006). Another adopted strategy is a loop-to-helix change observed in RebC and speculated in PhzS (Greenhagen *et al.*, 2008; Ryan *et al.*, 2008). Both hydroxylases act in concert with another enzyme (PhzM and RebP), leaving the possibility that the loop-to-helix transition is part of a substrate channeling process. Substrate recognition, transport and product release are intriguing elements of flavoprotein hydroxylase catalysis, with ingenious diversity displayed among the family members.

2

## Styrene Monooxygenase, A Versatile Catalyst

Styrene monooxygenases (SMOs) convert styrene into styrene oxide. Several styrene monooxygenases have been identified from different microorganisms (Mooney *et al.*, 2006; Lin *et al.*, 2010) or (meta)genomes (Lin *et al.*, 2010; van Hellemond *et al.*,

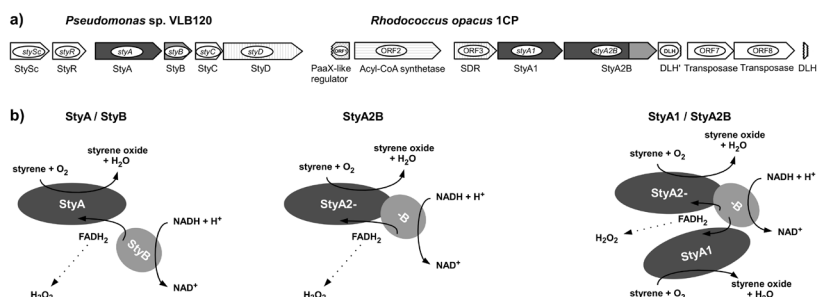


**Figure 3. Genetic organization and proposed mechanism of StyA/StyB from *Pseudomonas sp. VLB120* and StyA1/StyA2B from *R. opacus 1CP* (Tischler *et al.*, 2010). **A**) The gene cluster encoding the upper styrene degradation pathway: *stySc* and *styR* regulatory genes; *styA* and *styB* encoding a styrene monooxygenase, *styC* encoding a styrene oxide isomerase, and *styD* encoding phenylacetaldehyde dehydrogenase from *Pseudomonas sp. VLB120* and the organization of putative styrene-catabolic genes: *styA1* for an oxygenase component of a two-component SMO and *styA2B* for single-component SMO from *R. opacus 1CP* are shown. **B**) Proposed mechanisms of SMOs. From left to right: typical two-component SMO of *Pseudomonas* (Kantz *et al.*, 2005; Otto *et al.*, 2004) self-sufficient monooxygenase StyA2B from *R. opacus 1CP* (Tischler *et al.*, 2010), cooperative system of StyA2B and StyA1. Uncoupling-based FADH<sub>2</sub> autooxidation leading to the formation of hydrogen peroxide is indicated by dashed arrows.**

2007; Lin *et al.*, 2011; Tischler *et al.*, 2009), expressed, isolated and biochemically characterized, as native and/or recombinant enzyme, and applied in different forms for biotechnological purposes.

All characterized bacterial SMOs are flavin-dependent two-component proteins comprising a reductase (SMOB, StyB) and a monooxygenase (SMOA, StyA, StyA1). Remarkably, in few cases the enzyme occurs as a fusion protein (StyA2B) (Bernasconi *et al.*, 2000; Tischler *et al.*, 2009). The NADH-dependent reductase (SMOB) provides reduced FAD for the oxygenase-component (SMOA), where molecular oxygen reacts with the reduced flavin to form a peroxyflavin, which subsequently oxidizes the substrate styrene (Archer, 1997; Kantz *et al.*, 2005; Kantz and Gassner, 2011). Interestingly, bacterial SMOs show a high enantioselectivity and in almost all cases solely the (*S*)-enantiomer of styrene oxide is formed (Archelas and Furstoss, 1997; van Hellemond *et al.*, 2007; Tischler *et al.*, 2009; Tischler *et al.*, 2010; Lin *et al.*, 2010; Otto *et al.*, 2004). Excellent protein expression and therewith the unlimited access to this biocatalysts in combination with its capability to produce enantiopure styrene oxide and analogous epoxides as well as aryl sulfoxides have resulted in a high biotechnological interest in SMOs (Schmid, Hofstetter, Feiten, Hollmann and Witholt, 2001b; Kuhn *et al.*, 2010; Schmid, Dordick, Hauer, Kiener, Wubbolts and Witholt, 2001a; Mooney *et al.*, 2006; van Hellemond *et al.*, 2007). Herein, we focus on the best studied and recombinant accessible flavin-dependent SMOs, which are highly promising tools for various biotechnological approaches.

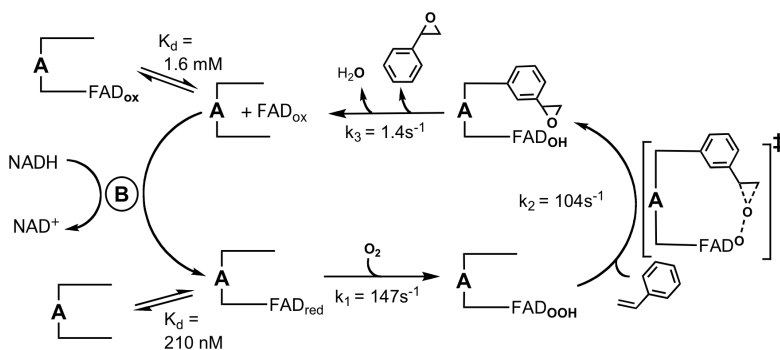
### Two Groups Of Flavin-Dependent Styrene Monooxygenases.

The distribution of SMOs among bacteria is supposed to be rather low considering the representatives per genome (Torres Pazmino *et al.*, 2010; van Berkel *et al.*, 2006). First characterized SMOs are from pseudomonadales and part of a catabolic gene cluster for styrene degradation yielding the central intermediate phenylacetic acid (Fig.3A) (Schmid, Hofstetter, Feiten, Hollmann and Witholt, 2001b; Mooney *et al.*, 2006; Schmid, Dordick, Hauer, Kiener, Wubbolts and Witholt, 2001a; O'Leary *et al.*, 2002). Further SMOs of this type were identified and characterized mostly in respect to biotechnological applicability (Panke *et al.*, 1998; Lin *et al.*, 2010; Mooney *et al.*, 2006; van Hellemond *et al.*, 2007). They all comprise a single NADH-dependent flavin reductase and a single styrene epoxidizing monooxygenase (Fig.3B). The reductase is able to reduce various flavins at the expense of NADH, whereas NADPH does not serve as electron donor (Schmid, Hofstetter, Feiten, Hollmann and Witholt, 2001b; Otto *et al.*, 2004; Panke *et al.*, 2000). The monooxygenase component accepts solely reduced FAD as coenzyme and uses molecular oxygen for subsequent stereoselective substrate oxygenation (Scheme 4) (Panke *et al.*, 2002; Otto *et al.*, 2004; Kantz *et al.*, 2005). Recently, we characterized the first representative of a new type of SMOs in which the reductase component is fused to the monooxygenase component (Gursky



*et al.*, 2010; Tischler *et al.*, 2009; Qaed *et al.*, 2011). The fusion protein StyA2B is the first self-sufficient styrene monooxygenase reported. However, a low epoxidizing activity of the fused monooxygenase as well as the occurrence of a second single monooxygenase gene (*styA1*) encoded directly upstream to *styA2B* raised questions on a functional dependence of both proteins (Fig.3A). Indeed it could be demonstrated that StyA1 and StyA2B together are a more efficient SMO using solely NADH as electron donor and FAD as coenzyme (Fig.3B). Additionally, StyA1 accepts reduced FAD also from other reductases yielding a similar or even higher monooxygenase activity (Panke *et al.*, 1999; Tischler *et al.*, 2010; Han *et al.*, 2006; Bae *et al.*, 2008; Bae *et al.*, 2010; Park *et al.*, 2006b), demonstrating that this component is the main monooxygenase in this SMO-type and that StyA2B is mainly acting as an FAD reductase. Based on genome mining only few representatives of this fusion-type SMO were identified yet. Interestingly, most of them are found among the Gram-positive Actinobacteria (*Arthrobacter aurescens* TC1, *Nocardia farcinica* IFM10152, and *Streptomyces platensis* CR50) and only one in a genome of a Gram-negative beta-proteobacterium (*Variovorax paradoxus* EPS).

Considering the gene/protein organization and subunit characteristics, two groups of subclass E flavoprotein monooxygenases (Schmid, Hofstetter, Feiten, Hollmann and Witholt, 2001b; van Berkel *et al.*, 2006; Panke *et al.*, 2000; Panke *et al.*, 2002; Park *et al.*, 2006a; Park *et al.*, 2006b) can be designated: E1 comprising StyA/StyB typically from *Pseudomonas*-species and E2 represented by StyA1/StyA2B from *Rhodococcus opacus* 1CP (Fig.3A).



**Scheme 4. Styrene-epoxidation and FAD-recycling reactions of styrene monooxygenase.** In catalysis SMOA binds tightly to reduced FAD and reacts with molecular oxygen to form a stable FAD C4a-hydroperoxide. This intermediate catalyzes the stereoselective addition of oxygen to styrene to yield the styrene oxide and FAD C4a-hydroxyflavin product complex. The nature of the oxygen transfer from peroxy-FAD to styrene is likely an electrophilic attack. Subsequent release of styrene oxide and elimination of water yields a weakly interacting SMOA-oxidized flavin complex. Oxidized FAD is recycled in the NADH-dependent flavin reduction reaction of SMOB. Given rate constants were derived from rapid reaction studies at 25°C. Residues of SMOA active site likely involved in binding the FAD intermediates are highlighted in Fig.4-5.

## Structure And Mechanism Of Styrene Monooxygenase

**Structure Of *Pseudomonas* SMO.** The three-dimensional structure of the dimeric FAD specific styrene monooxygenase (SMOA) from *Pseudomonas* investigated by molecular modeling and by X-ray crystallographic analysis indicates that it has an overall fold that is quite homologous to that of PHBH (Fig.4) (Kuhn *et al.*, 2010; Feenstra *et al.*, 2006; Ukaegbu *et al.*, 2010). The evolutionary relationship linking SMOA and PHBH is particularly apparent in comparing the FAD-binding Rossmann fold of each protein, which identifies them as both belonging to the GR2 family of FAD-binding proteins (Panke *et al.*, 2002; Dym and Eisenberg, 2001). Additional FAD-binding consensus sequences of the flavoprotein hydroxylase family are found in structurally homologous regions of the SMOA and PHBH (Gross *et al.*, 2007; Eppink *et al.*, 1997). Comparison of the apo-SMOA structure with wild-type and mutant structures of PHBH provides insight into both the overall structural homology and in identifying amino acid side chains that are thought to define the substrate and flavin-binding pockets of SMOA (Torres Pazmino *et al.*, 2010; Feenstra *et al.*, 2006; Ukaegbu *et al.*, 2010).

**Flavin And Styrene Binding Pocket.** A main difference between flavoprotein hydroxylases and styrene monooxygenases is that the latter enzymes only weakly interact with oxidized FAD (Tischler *et al.*, 2009; Ukaegbu *et al.*, 2010; Otto *et al.*, 2004; Hollmann *et al.*, 2003). FAD is thought to bind in SMOA in a large solvent filled cleft observed in the apo-enzyme structure based on sequence conservation and alignment of the apo-enzyme crystal structure of SMOA with holoenzyme structures

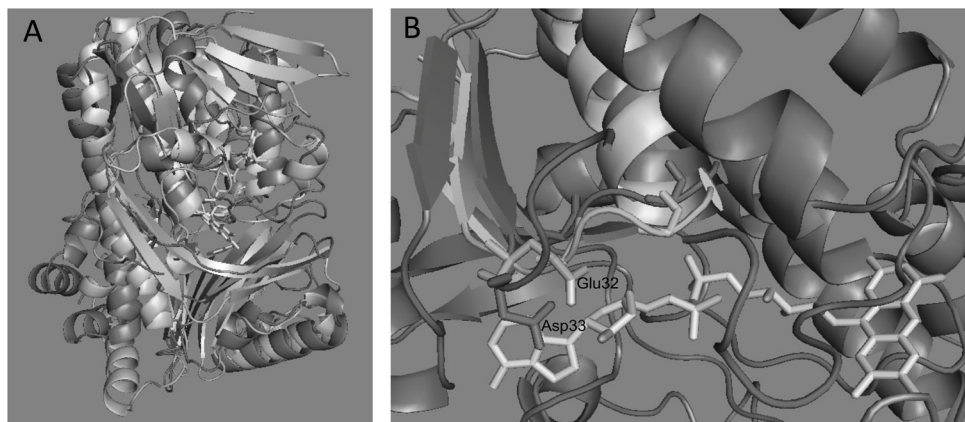


**Figure 4. Structural relationship of PHBH and SMOA. A)** Superposition of the crystallographically resolved structures of SMOA (PDB ID 3IHM) (dark gray) and PHBH (PDB ID 1cc6)(light gray). **B)** N-terminal regions of SMOA and PHBH highlighting the conserved FAD binding motif GxGxxGx<sub>17</sub>E (PHBH, light gray) and GxGxxGx<sub>22</sub>D (SMOA dark gray) bridging  $\beta$ -strand 1 and  $\alpha$ -helix 1 of the Rossmann fold of each protein.



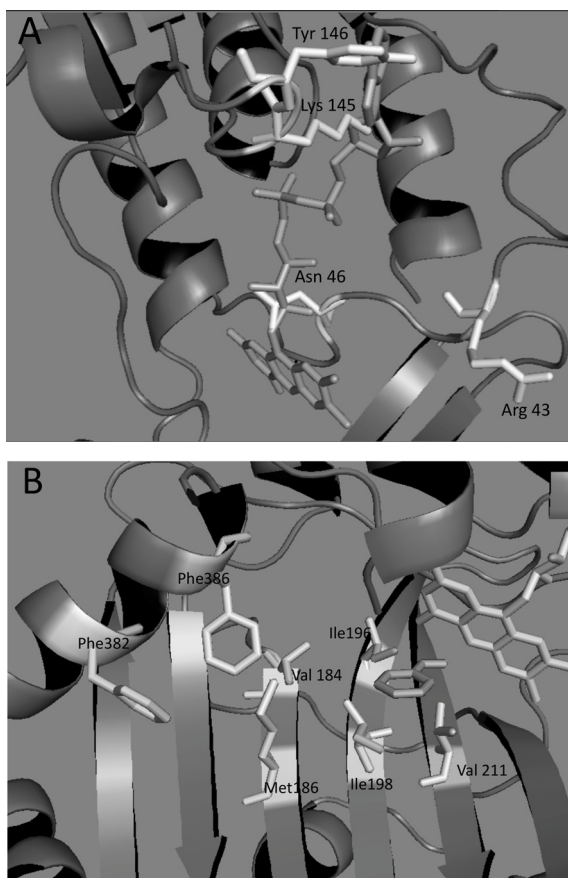


**Figure 5. Amino acid side chains in the FAD- and styrene-binding pockets of SMOA.** A) Amino acid side chains, which interfere with the projected mode of FAD-binding observed in PHBH (PDB ID 1cc6) are shown. B) Projection of oxidized FAD and bound substrate locations observed in PHBH onto the active site of SMOA. Hydrophobic side chains lining the proposed styrene-binding pocket of SMOA are shown

interferes with the FAD-binding pocket defined by the structure of PHBH (Fig.5A). The apparently unfavorable orientations of these side chains may contribute to the weak binding affinity of oxidized FAD for SMOA ( $K_d \sim 1.6$  mM), and suggest that significant structural reorganization may be required to account for the observed high affinity binding of reduced FAD to SMOA ( $K_d \sim 206$  nM) (Sheldon, 2007; Ukaegbu *et al.*, 2010). Differences in the substrate binding pockets of SMOA and PHBH further distinguish the structural architecture of these enzymes. Notably His72, which is thought to engage in a proton shuttling mechanism in the aromatic ring hydroxylation reaction of PHBH, is not conserved in SMOA and Tyr201, Arg220, and Tyr222, which

of PHBH with the FAD in the *in*, *open* and *out* configurations (Hollmann *et al.*, 2003; Ballou *et al.*, 2005; Ukaegbu *et al.*, 2010; Entsch *et al.*, 2005). Comparison of the apo-SMOA and holo-PHBH in configurations suggests that Ala13 of SMOA may function similarly to Ser13 of PHBH in binding to the pyrophosphate of FAD. Amino acid side chains Val47, Ala48, Gly307, Leu299 and Asn309 of SMOA are located at positions similar to the side chains Gly46, Val47, Gly298, Ala308, and Asn300 of holo-PHBH where they are thought to interact with the flavin-isoalloxazine ring system (Torres Pazmino *et al.*, 2010; Ukaegbu *et al.*, 2010; Hollmann *et al.*, 2003). Interestingly, the side chain Arg43 of SMOA points away from the FAD-binding pocket, whereas Arg44 in the homologous PHBH structure assists in cofactor binding through electrostatic interaction with the pyrophosphate backbone. The amino acid side chains of Asn46, Lys145 and Tyr146 in the structure of SMOA are positioned in a way that

Table 3. Valuable substrates of styrene monooxygenases.

Oxygenase	StyA1+ StyA2B <i>R. opacus</i> 1CP	StyA <i>Pseudomonas</i> sp. VLB120	SMO Unknown, metagenome
Reductase	StyA2B <i>R. opacus</i> 1CP	electrochemical FAD reduction	PheA2 <i>Geobacillus thermoglucosidans</i>
Substrate	Relative activity (%) % enantiomeric excess (preferred enantiomer)		
Styrene	100, > 94 ( <i>S</i> )	100, 98 ( <i>S</i> )	100, > 99 ( <i>S</i> )
2-Chlorostyrene	3	n.d.	49, 94 ( <i>S</i> )
3-Chlorostyrene	88	100, > 99 ( <i>S</i> )	70, > 99 ( <i>S</i> )
4-Chlorostyrene	38	153, 98	29, >99 ( <i>S</i> )
4-Methylstyrene	46	153, 99	n.d.
$\beta$ -trans Methylstyrene	n.d.	137, 98	n.d.
Indene	n.d.	158, 98 ( <i>1S</i> , <i>2R</i> )	n.d.
Dihydronaphthalene	78	184, 99	n.d.
Methylphenylsulfide	145	111, 26	14, 75 ( <i>R</i> )
Ethylphenylsulfide	n.d.	not declared, 13	29, 92 ( <i>R</i> )
References	(Tischler <i>et al.</i> , 2010)	(Hollmann <i>et al.</i> , 2003)	(van Hellemond <i>et al.</i> , 2007)

line the floor of the *para*-hydroxybenzoate binding pocket have been replaced with the more hydrophobic side chains of Met186, Ala209, and Val211 in conserved locations in the proposed styrene binding pocket of SMOA (Fig.5B). In addition, the C-terminus of SMOA includes  $\alpha$ -helical structure, which is absent in the PHBH structure.

The observed differences in the structures of SMOA and PHBH reflect fundamental differences in the mechanisms of these enzymes. PHBH binds tightly to both oxidized and reduced FAD and interacts directly with NADPH in catalysis, whereas SMOA is completely reliant on an external source of reduced FAD in catalysis.

**Engineering The Active Site Of SMO.** The functional significance of several amino acid side chains of SMOA has been investigated through evaluation of the relative catalytic activities of site-directed mutants of the epoxidase and used to assist in evaluating computational models of SMOA (Alfieri *et al.*, 2007; Feenstra *et al.*, 2006; Sucharitakul *et al.*, 2007). Subsequent engineering efforts to improve or alter the catalytic activity of SMOA have met with some success (Torres Pazmino *et al.*, 2010; Gursky *et al.*, 2010; Qaed *et al.*, 2011). SMO genes were subjected to error-prone mutagenesis and the resulting mutant enzymes were selected based on improved epoxidation activity assayed by indigo production. This approach proved successful in increasing the epoxidation activity of SMO for both styrene and indole and efforts to explain the changes in activity were made with reference to the computational model structure of SMO (Schreuder *et al.*, 1989; Gursky *et al.*, 2010; Wierenga *et al.*, 1979). Site-directed mutagenesis guided by the results of docking substrate analogues into the apo-enzyme crystal structure of SMOA, have successfully led to the identification of mutant enzymes forms with higher substrate specificity for  $\alpha$ -methyl- and  $\alpha$ -ethylstyrenes (Enroth, 2003; Qaed *et al.*, 2011; Enroth *et al.*, 1998). These results suggest that there is a bright future for the production of SMO variants

with enhanced catalytic activity and alternate substrate specificities.

**Styrene Epoxidation Mechanism.** The FAD-binding affinity of SMOA is tightly linked to the redox state of the flavin such that reduced flavin binds 8000-fold more tightly than does oxidized flavin. In turnover, reduced FAD supplied by SMOB, binds firmly as a substrate to apo-SMOA but then reacts catalytically with molecular oxygen as a coenzyme to form tightly-bound flavin-oxygen intermediates associated with the synthesis of styrene oxide. FAD then dissociates from SMOA as a product of the epoxidation reaction (Scheme 4). As noted above for other flavoprotein monooxygenases, the flavin C4a-hydroperoxide has been demonstrated through mechanistic and structural studies to be the key reactive intermediate responsible for substrate oxygenation (Hiromoto *et al.*, 2006; Palfey and McDonald, 2010).

Small molecule organic model systems indicate that oxaziradines are more enantioselective than organic peroxides as epoxidation reagents and in considering the unique enantioselective synthesis of (*S*)-styrene oxide by SMOA, it was postulated that the oxygen atom transfer reaction could occur through either an FAD-hydroperoxide or FAD-oxaziridine intermediates (Koskiniemi *et al.*, 2007; Kantz *et al.*, 2005; Kantz and Gassner, 2011). Stopped-flow and rapid chemical quench techniques; have now demonstrated that the epoxidation reaction occurs through the direct attack of the styrene to the flavin hydroperoxide (Scheme 4). This result further demonstrates the versatility of the flavin C4a-hydroperoxide intermediate in flavoenzyme-catalyzed epoxidation reactions and emphasizes the important role of the enzyme active site in carefully orientating and poisoning styrene and flavin-hydroperoxide to allow the exquisite, enantioselective delivery of oxygen observed in the SMOA-catalyzed epoxidation of styrene.

The monooxygenation reaction results in the production of a highly fluorescent C4a-hydroxyflavin intermediate, which eliminates water in a base-catalyzed reaction to regenerate oxidized flavin in the final rate-limiting step of turnover. The chemical stability and electronic spectrum of the C4a-hydroxyflavin intermediate indicate its similarity to the corresponding intermediates observed in the mechanisms of related flavoprotein monooxygenases (Ryan *et al.*, 2007; Kantz and Gassner, 2011).

**Mechanism Of Reduced Flavin Transfer From SMOB To SMOA.** The dimeric NADH-specific flavin reductase SMOB serves as the primary supply line for reduced FAD required in the SMOA-catalyzed epoxidation reaction (Treiber and Schulz, 2008; Kantz *et al.*, 2005; Otto *et al.*, 2004). The three-dimensional structure of SMOB is currently unavailable, but homology modeling suggests that it is closely related to the reported structure of PheA2, the flavin reductase of the two-component phenol hydroxylase PheA (Greenhagen *et al.*, 2008; Kirchner *et al.*, 2003; van den Heuvel *et al.*, 2004). In steady-state turnover, SMOB catalyzes the rapid and indiscriminate reduction of oxidized FAD, FMN, and riboflavin (Lindqvist *et al.*,

2009; Otto *et al.*, 2004). This apparent lack of specificity is interesting, considering that the flavin-catalyzed epoxidation reaction of SMOA is FAD-specific, and it supports the possibility that electrons maybe delivered to SMOA either directly in the form of reduced FAD or indirectly through intermolecular electron transfer from a pool of reduced flavin to FAD. When FAD is in excess over the enzyme active site concentration and SMOA and SMOB are present in equimolar concentrations, the rate at which SMOB catalyzes the reduction of the FAD pool greatly exceeds the rate at which SMOA can employ it in styrene epoxidation. This uncoupling of flavin reduction and styrene epoxidation is inefficient and results in the production of reactive oxygen species, mainly in the form of hydrogen peroxide. Rates of NADH consumption by SMOB and styrene oxide synthesis by SMOA can be matched if SMOA is present in excess over SMOB or at equal SMOA and SMOB concentrations if the FAD concentration is less than or equal to the concentration of available active sites. Under the latter conditions FAD species, occurring during catalysis (Scheme 4), are predominantly bound to the SMO components (McCulloch *et al.*, 2009; Kantz *et al.*, 2005).

Although efficient coupling of the NADH consumption and styrene epoxidation reactions is possible over a range of protein and flavin concentrations, there may be an additional need for SMOA-SMOB complex formation to explain the full range of reaction coupling efficiency (Ukaegbu *et al.*, 2010; Kantz *et al.*, 2005). This possibility that a protein-protein complex may form during catalysis is an area of current research.

**Proposed Mechanism Of StyA1/StyA2B-Type SMO.** StyA1 was shown to be the major styrene oxidizing component of the StyA1/StyA2B system by exchanging the natural partner StyA2B against another FAD reductase while maintaining a high epoxidation rate (Jadan *et al.*, 2004; Tischler *et al.*, 2010). Dependence on the applied reductase type was also demonstrated since PheA2 could not deliver sufficient reducing equivalents. A kind of reductase recognition or even protein-protein cross-talk was suggested. Sequence comparison of StyA1 and SMOA from *Pseudomonas* species revealed that all amino acids involved in catalysis are conserved (Tischler *et al.*, 2010; Tischler *et al.*, 2009). Therefore, a similar reaction sequence of epoxidation after binding of reduced FAD as drawn in Scheme 4 can be expected. The low epoxidation activity of StyA2B indicates that this fusion protein mainly serves a reductase function in this SMO type (Fig.3B). The A2 part of StyA2B shows high sequence similarity to SMOA from *Pseudomonas* species as well as to StyA1. Slight differences as well as the fusion character may impair efficient epoxidation by A2. The reductase subunit of StyA2B is sufficient to deliver reducing equivalents to both monooxygenases (A1 and A2).

Furthermore, a kind of protein cross-talk or transient complex formation between both proteins during which reduced FAD is channeled from reductase to monooxygenases was supposed since highest epoxidation activity and efficiency was observed at an

equimolar ratio of both components (Hollmann *et al.*, 2003; Tischler *et al.*, 2010).

The nature and possible advantages of the self-sufficient one-component SMO (StyA2B) needs further investigation. Elucidation of the structure and mechanism of this protein might help to design highly active and selective one-component SMOs for biotechnological purposes.

## Styrene Monooxygenases In Biocatalysis

Enantiopure terminal epoxides are high-value targets for fine chemistry, pharmaceutical and agrochemical industry, where they are used as building blocks for various syntheses (van Hellemond *et al.*, 2007; Rao *et al.*, 1992; Badone *et al.*, 1994; Besse *et al.*, 1994; Hattori *et al.*, 1995; Schulze and Wubbolts, 1999). Since enantioselective epoxidation of terminal alkenes is difficult to achieve with traditional chemical methods, several procedures applying asymmetric catalysts or chemo enzymatic approaches were investigated to yield the desired epoxides. Styrene monooxygenases allow regio- and stereoselective oxidation of styrene and analogous compounds under mild conditions (Fig.7) (Tischler *et al.*, 2010; Torres Pazmino *et al.*, 2010; Joosten and van Berkel, 2007; van Berkel *et al.*, 2006). Other monooxygenases are able to convert styrene(s) directly into the corresponding epoxide(s), but yield and enantiopurity are not comparable to those from SMOs (Kantz *et al.*, 2005; Mooney *et al.*, 2006; Otto *et al.*, 2004; Archelas and Furstoss, 1997).

**Enantioselective Biocatalysis With Styrene Monooxygenases.** So far all reported SMOs show a high enantioselectivity in substrate oxygenation (Tischler *et al.*, 2010; van Hellemond *et al.*, 2007; Tischler *et al.*, 2009; Tischler *et al.*, 2010; Lin *et al.*, 2010; Bernasconi *et al.*, 2000; Hollmann *et al.*, 2003; Lin *et al.*, 2011). Besides the natural substrate styrene also numerous derivatives like (i) ring substituted (chloro, bromo, fluoro, hydroxy, methoxy, methyl, monocycle), (ii) vinyl chain substituted ( $\alpha$ - or  $\beta$ - substitutions: methyl, ethyl, propyl; indole, indene and dihydronaphthalene), (iii) (ring substituted) aromatic sulfides, (iv) heterocyclic compounds (pyridine-like styrenes), and (v) non-conjugated alkenes (1-allylbenzene analogues) are converted in more or less stereoselective manner (Fig.7). Table 3 shows an overview of valuable substrates converted by different SMOs and activities compared to the conversion of styrene. Recently, an interesting SMO from a styrene-degrading pseudomonad was identified and characterized (Kuhn *et al.*, 2010; Lin *et al.*, 2010; Lin *et al.*, 2011). This enzyme is the most distinct SMO from pseudomonads based on sequence analysis. It converts a range of more bulky styrene derivatives and non-conjugated alkenes. Some of these compounds were previously reported as non-SMO substrates (Tischler *et al.*, 2010; Bernasconi *et al.*, 2000; Eppink *et al.*, 1999; Gursky *et al.*, 2010; Bernasconi *et al.*, 2000; Archer, 1997). Thus, a broader substrate spectrum for SMOs can be expected and might be exploited for valuable biotransformation in future.



The capability of SMOs to convert indene into enantiopure indene oxide (Archer, 1997), which serves as a precursor for the HIV protease inhibitor indinavir (Crixivan®), is a valuable process, especially since the access to this compound or to the precursor is hard to realize by chemical approaches. The company ‘Merck’ established a biotechnological route applying epoxide hydrolase to produce the desired (*1S,2R*)-indene oxide from racemic indene oxide (Archelas and Furstoss, 1997). However, using SMOs and therewith a direct stereoselective oxidation represents a promising alternative to the already established biotechnological process.

**Whole-Cell Biotransformation: A Large-Scale Application.** The application of biocatalysts for highly regio- or stereo-selective oxygenation reactions often attends with several problems such as long-term stability, solvent incompatibility, and complex down-stream processing (Schmid, Hofstetter, Feiten, Hollmann and Witholt, 2001b; Schmid, Dordick, Hauer, Kiener, Wubbolts and Witholt, 2001a). Another important issue concerns the cofactor-dependency of oxygenases (Torres Pazmino *et al.*, 2010). Thus, the capability of whole-cell processes for *in situ* NADH-regeneration favors these approaches for cofactor-dependent (styrene) monooxygenase-based biotransformations (Schmid, Hofstetter, Feiten, Hollmann and Witholt, 2001b; Schmid, Dordick, Hauer, Kiener, Wubbolts and Witholt, 2001a). In the case of styrene epoxidation, the low octanol/water partition coefficients of styrene (3.02 log P value) and styrene oxide (1.61 log P value) as well as the high reactivity of the epoxide make these compounds toxic for the biocatalyst expressing cells. Therefore a two-liquid phase bioconversion is most suited since the second organic phase serves as substrate reservoir and product trap.

Using a recombinant StyA/StyB from *Pseudomonas* sp. strain VLB120 (Panke *et al.*, 1998) expressed in *E. coli*, first a gram scale [2 L, 22.2 g (*S*)-styrene oxide; yield 71% in 10 h] was achieved (Schmid, Hofstetter, Feiten, Hollmann and Witholt, 2001b; Panke *et al.*, 2000), and later a multi-100 g scale [30 L, 388 g (*S*)-styrene oxide; yield 50% in 16 h] pilot fermentative production of enantiopure (*S*)-styrene oxide (Fig.6) (Panke *et al.*, 2002). After purification, 307 g pure (*S*)-styrene oxide (yield of 40%) were isolated by means of centrifugation to separate the aqueous cell suspension from the organic phase and subsequent distillation.

Within the last decade several approaches to improve the whole-cell biotransformation for (*S*)-styrene oxide production were reported. Optimization of the biocatalyst by protein engineering (Gursky *et al.*, 2010; Qaed *et al.*, 2011) or optimized expression systems (Panke *et al.*, 1999; Han *et al.*, 2006; Bae *et al.*, 2008; Bae *et al.*, 2010; Park *et al.*, 2006b), development of the fermentation process in respect to media, performance, and downstream processing (Schmid, Hofstetter, Feiten, Hollmann and Witholt, 2001b; Panke *et al.*, 2000; Panke *et al.*, 2002; Park *et al.*, 2006b; Park *et al.*, 2006a) were evaluated. Kuhn *et al.* (Kuhn *et al.*, 2010) reported a slightly modified approach from the original pilot-process of Panke *et al.* (Panke

*et al.*, 2002) and evaluated it in respect to economical as well as ecological aspects together with established chemical syntheses. The use of toxic and environmentally harmful bis(2-ethylhexyl) phthalate as organic phase was found to be the major drawback. Thus an alternative organic phase with similar compatibility to whole cells and suited partition coefficients for styrene and styrene oxide allow further

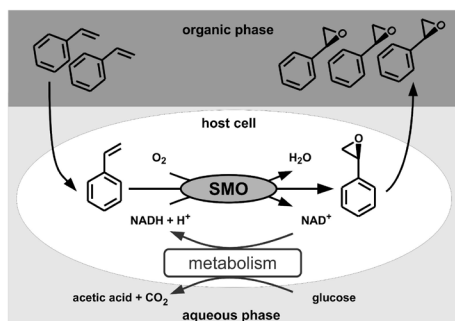


**Figure 6. A two-liquid phase biotransformation process for styrene epoxidation** (Kuhn *et al.*, 2010). The organic phase (e.g. bis(2-ethylhexyl) phthalate) serves as substrate reservoir (styrene) and allows a continuous product extraction. The biotransformation is carried out in the aqueous phase by a recombinant host expressing styrene monooxygenase (SMO). The biocatalyst produces enantiopure (*S*)-styrene oxide at the expense of NADH, which is delivered by the hosts glucose-metabolism.

2

improvement. In terms of product costs the bioprocess was already most competitive, demonstrating advantages of biotransformation for fine chemical production.

Bacteria growing in biofilms show a remarkable high tolerance against toxic substances and can be exploited for biotechnological applications. An SMO-expressing *Pseudomonas*-biofilm for (*S*)-styrene oxide production was established and represents in combination with in situ product extraction an alternative approach (Gross *et al.*, 2007). A lower volumetric productivity [16 g/ (L<sub>aq</sub> day)] compared to two-phase systems with suspended cells [continuous culture: 47 g/ (L<sub>aq</sub> day); fed-batch culture: 101 g/(L<sub>aq</sub> day)] was compensated by the now possible long-term performance of this approach (55 days). Optimization in oxygen supply and biofilm growth for a more reproducible and competitive process is needed.

**A Promising Cell-Free System.** Alternatively to whole-cell biotransformations, cell extracts containing a suitable biocatalyst or purified enzyme preparations can be used in chemical syntheses. In case of monooxygenases, the necessity of cofactors [e.g., NAD(P)H, FAD] and *in vitro* regeneration makes this approach a challenge (Torres Pazmino *et al.*, 2010). Several systems for cofactor regeneration have been established and in most cases enzyme-coupled systems such as formate dehydrogenase (FDH) or glucose-6-phosphate dehydrogenase (G6PDH) for NAD(P)<sup>+</sup> reduction are used. For SMOs, the application of FDH is suited to deliver reducing equivalents to SMOB which allows a subsequent reduction of the FAD cofactor (Tischler *et al.*, 2009; Otto *et al.*, 2004; Hollmann *et al.*, 2003). Some uncoupling depending on the applied monooxygenase occurs while the reduced FAD is channeled to the SMOA component (Fig.3B). The enzymatic regeneration systems are costly and might be affected by the organic nature of the substrate/ product of epoxidation. In

order to minimize uncoupling and avoid a further enzyme such as FDH, a system for direct electrochemical FAD reduction was introduced by Hollmann and coworkers (Hollmann *et al.*, 2003). Herein the only enzymatic component is SMOA for styrene epoxidation. The complete system for FADH<sub>2</sub> regeneration, composed of natural FAD reductase SMOB, the artificial NADH regeneration system, and NAD<sup>+</sup>, were replaced by the organometallic complex (pentamethylcyclopentadienyl)rhodium(bipyridine) [Cp\*Rh(bpy)(H<sub>2</sub>O)]<sub>2</sub><sup>+</sup>. The redox catalyst receives electrons for direct FAD reduction from formate oxidation and allows a cyclic FADH<sub>2</sub> production. In comparison to the fully enzymatic system this approach yielded about 70% epoxidation activity with similar (enantio)selectivity. Thus this cell-free system is at least suitable for small-scale applications. In order to achieve preparative-scale synthesis, the catalyst itself, a more productive redox catalyst, and the reaction conditions have to be optimized (Torres Pazmino *et al.*, 2010; Hollmann *et al.*, 2003). Stability and overall lifetime of the biocatalyst can be increased by enzyme immobilization techniques (Sheldon, 2007). In analogy to the above-mentioned whole-cell system a second organic phase could be applied to limit interaction of reactive substrates/products.

## General Conclusions And Perspectives

The structural and mechanistic studies on flavoprotein hydroxylases have revealed that these enzymes use a number of strategies to perform efficient catalysis. Tightly controlled FAD reduction avoids the unproductive consumption of NAD(P)H, and active sites are optimized for the regioselective incorporation of a hydroxy group. So far, relatively few hydroxylases have been described that consist of a reductase and a monooxygenase component (Alfieri *et al.*, 2007; Sucharitakul *et al.*, 2007). It is anticipated that many more of these enzymes will be uncovered from the metagenome, either in free form or fused as in StyA2B. The progress in chemical, electrochemical, and light-driven cofactor regeneration shows the general applicability for monooxygenases in small-scale cell-free biocatalysis (Torres Pazmino *et al.*, 2010).

The underrepresented monooxygenase-based bioprocesses might be overcome by SMO-based approaches since it was recently demonstrated that a whole-cell application competes well with other chemical approaches in terms of productivity as well as expense factor. Furthermore, the broad substrate range converted by these flavoproteins provides access to many valuable building blocks for chemical syntheses. The recently published structures and insights in mechanisms allow further approaches in protein engineering in order to alter active sites for higher activities or acceptance of more recalcitrant substrates.



## Acknowledgements

Dirk Tischler was supported by two predoctoral fellowships from the Deutsche Bundesstiftung Umwelt and Fulbright. We thank the Netherlands Organization for Scientific Research (NWO) for funding the work of Stefania Montersino within the IBOS (Integration of Biosynthesis and Organic Synthesis) program.

## References

- Alfieri, A., Fersini, F., Ruangchan, N., Prongjit, M., Chaiyen, P. and Mattevi, A., (2007) Structure of the monooxygenase component of a two-component flavoprotein monooxygenase. *Proceedings of the National Academy of Sciences of the United States of America*, 104(4), 1177–1182.
- Archelas, A. and Furstoss, R., (1997) Synthesis of enantiopure epoxides through biocatalytic approaches. *Annual Reviews in Microbiology*, 51, 491–525.
- Archer, I.V.J., (1997) Epoxide hydrolases as asymmetric catalysts. *Tetrahedron*, 53(46), 15617–15661.
- Badone, D., Badone, D., Guzzi, U. and Guzzi, U., (1994) Synthesis of the potent and selective atypical  $\beta$ -adrenergic agonist SR 59062A. *Journal of Medicinal Chemistry*, 37(16), 1921–1924.
- Bae, J.W., Doo, E.H., et al., (2010) Development of a recombinant *Escherichia coli*-based biocatalyst to enable high styrene epoxidation activity with high product yield on energy source. *Process Biochemistry*, 45(2), 147–152.
- Bae, J.W., Shin, S., Mohan Raj, S., Lee, S.E., Lee, S.-G., Jeong, Y.-J. and Park, S., (2008) Construction and characterization of a recombinant whole-cell biocatalyst of *Escherichia coli* expressing styrene monooxygenase under the control of arabinose promoter. *Biotechnology and Bioengineering*, 101(1), 69–76.
- Baitsch, D., Sandu, C., Brandsch, R. and Igloi, G.L., (2001) Gene cluster on pAO1 of *Arthrobacter nicotinovorans* involved in degradation of the plant alkaloid nicotine: cloning, purification, and characterization of 2, 6-dihydropyridine 3-hydroxylase. *Journal of Bacteriology*, 183(18), 5262–5267.
- Ballou, D.P., Entsch, B. and Cole, L.J., (2005) Dynamics involved in catalysis by single-component and two-component flavin-dependent aromatic hydroxylases. *Biochemical and Biophysical Research Communications*, 338(1), 590–598.
- Baron, R., Riley, C., Chenprakhon, P., et al., (2009) Multiple pathways guide oxygen diffusion into flavoenzyme active sites. *Proceedings of the National Academy of Sciences of the United States of America*, 106(26), 10603–10608.
- Bernasconi, S., Orsini, F., Sello, G., Colmegna, A., Galli, E. and Bestetti, G., (2000) Bioconversion of substituted styrenes to the corresponding enantiomerically pure epoxides by a recombinant *Escherichia coli* strain. *Tetrahedron Letters*, 41(47), 9157–9161.
- Besse, P., Besse, P., Besse, P., Veschambre, H., Veschambre, H. and Veschambre, H., (1994) Chemical and biological synthesis of chiral epoxides. *Tetrahedron*, 50, 8885–8927.
- Chaiyen, P., (2010) Flavoenzymes catalyzing oxidative aromatic ring-cleavage reactions. *Archives of Biochemistry and Biophysics*, 493(1), 62–70.
- Chaiyen, P., Brissette, P., Ballou, D.P. and Massey, V., (1997a) Reaction of 2-methyl-3-hydroxypyridine-5-carboxylic acid (MHPC) oxygenase with *N*-methyl-5-hydroxynicotinic acid: studies on the mode of binding, and protonation status of the substrate. *Biochemistry*, 36(45), 13856–13864.
- Chaiyen, P., Brissette, P., Ballou, D.P. and Massey, V., (1997b) Thermodynamics and reduction kinetics properties of 2-methyl-3-hydroxypyridine-5-carboxylic acid oxygenase. *Biochemistry*, 36(9), 2612–2621.
- Chaiyen, P., Brissette, P., Ballou, D.P. and Massey, V., (1997c) Unusual mechanism of oxygen atom transfer and product rearrangement in the catalytic reaction of 2-methyl-3-hydroxypyridine-5-carboxylic acid oxygenase. *Biochemistry*, 36(26), 8060–8070.
- Chaiyen, P., Sucharitakul, J., Svasti, J., Entsch, B., Massey, V. and Ballou, D.P., (2004) Use of 8-substituted-FAD analogues to investigate the hydroxylation mechanism of the flavoprotein 2-methyl-3-hydroxypyridine-5-carboxylic acid oxygenase. *Biochemistry*, 43(13), 3933–3943.
- Chang, H.-K. and Zylstra, G.J., (2008) Examination and expansion of the substrate range of *m*-hydroxybenzoate hydroxylase. *Biochemical and Biophysical Research Communications*, 371(1), 149–153.
- de Gonzalo, G., Mihovilovic, M.D. and Fraaije, M.W., (2010) Recent developments in the application of Baeyer-Villiger monooxygenases as biocatalysts. *ChemBioChem*, 11(16), 2208–2231.
- Dym, O. and Eisenberg, D., (2001) Sequence-structure analysis of FAD-containing proteins. *Protein Science*, 10(9), 1712–1728.
- Enroth, C., (2003) High-resolution structure of phenol hydroxylase and correction of sequence errors. *Acta Crystallographica. Section D, Biological Crystallography*, 59(Pt 9), 1597–1602.
- Enroth, C., Neujahr, H., Schneider, G. and Lindqvist, Y., (1998) The crystal structure of phenol hydroxylase in complex with FAD and phenol provides evidence for a concerted conformational change in the enzyme and its cofactor during catalysis. *Structure (London, England : 1993)*, 6(5), 605–617.
- Entsch, B. and van Berkel, W.J.H., (1995) Structure and mechanism of *para*-hydroxybenzoate hydroxylase. *FASEB Journal*, 9(7), 476–483.

- Entsch, B., Ballou, D.P. and Massey, V., (1976a) Flavin-oxygen derivatives involved in hydroxylation by *p*-hydroxybenzoate hydroxylase. *Journal of Biological Chemistry*, 251(9), 2550–2563.
- Entsch, B., Ballou, D.P., Husain, M. and Massey, V., (1976b) Catalytic mechanism of *p*-hydroxybenzoate hydroxylase with *p*-mercaptobenzoate as substrate. *Journal of Biological Chemistry*, 251(23), 7367–7369.
- Entsch, B., Cole, L.J. and Ballou, D.P., (2005) Protein dynamics and electrostatics in the function of *p*-hydroxybenzoate hydroxylase. *Archives of Biochemistry and Biophysics*, 433(1), 297–311.
- Entsch, B., Palfey, B.A., Ballou, D.P. and Massey, V., (1991) Catalytic function of tyrosine residues in *para*-hydroxybenzoate hydroxylase as determined by the study of site-directed mutants. *Journal of Biological Chemistry*, 266(26), 17341–17349.
- Eppink, M. and van Berkel, W.J., (1999) Crystal structure of “unactivated” *p*-hydroxybenzoate hydroxylase. In S Ghisla, P Macheroux, P Kroneck, H Sund, eds *Flavins and Flavoproteins* 1999. Agency for Scientific Publications, Berlin, 239–242.
- Eppink, M.H., Overkamp, K.M., Schreuder, H.A. and van Berkel, W.J.H., (1999) Switch of coenzyme specificity of *p*-hydroxybenzoate hydroxylase. *Journal of Molecular Biology*, 292(1), 87–96.
- Eppink, M.H.M., Schreuder, H.A. and van Berkel, W.J.H., (1998) Interdomain binding of NADPH in *p*-hydroxybenzoate hydroxylase as suggested by kinetic, crystallographic and modeling studies of histidine 162 and arginine 269 variants. *Journal of Biological Chemistry*, 273(33), 21031–21039.
- Eppink, M.H.M., van Berkel, W.J.H. and Schreuder, H.A., (1997) Identification of a novel conserved sequence motif in flavoprotein hydroxylases with a putative dual function in FAD/NAD(P) H binding. *Protein Science*, 6(11), 2454–2458.
- Feenstra, K.A., Hofstetter, K., Bosch, R., Schmid, A., Commandeur, J.N.M. and Vermeulen, N.P.E., (2006) Enantioselective substrate binding in a monooxygenase protein model by molecular dynamics and docking. *Biophysical Journal*, 91(9), 3206–3216.
- Gatti, D.L., Palfey, B.A., Lah, M.S., Entsch, B. and Massey, V., (1994) The mobile flavin of 4-OH benzoate hydroxylase. *Science*.
- Greenhagen, B.T., Shi, K., Robinson, H., Gamage, S., Bera, A.K., Ladner, J.E. and Parsons, J.F., (2008) Crystal structure of the pyocyanin biosynthetic protein PhzS. *Biochemistry*, 47(19), 5281–5289.
- Groom, K., Bhattacharya, A. and Zechel, D.L., (2011) Rebeccamycin and staurosporine biosynthesis: insight into the mechanisms of the flavin-dependent monooxygenases RebC and StaC. *ChemBioChem*, 12(3), 396–400.
- Gross, R., Hauer, B., Otto, K. and Schmid, A., (2007) Microbial biofilms: new catalysts for maximizing productivity of long-term biotransformations. *Biotechnology and Bioengineering*, 98(6), 1123–1134.
- Gursky, L.J., Nikodinovic-Runic, J., Feenstra, K.A. and O'Connor, K.E., (2010) *In vitro* evolution of styrene monooxygenase from *Pseudomonas putida* CA-3 for improved epoxide synthesis. *Applied Microbiology and Biotechnology*, 85(4), 995–1004.
- Han, J.H., Park, M.S., Bae, J.W., Lee, E.Y., Yoon, Y.J., Lee, S.G. and Park, S., (2006) Production of ( *S*)-styrene oxide using styrene oxide isomerase negative mutant of *Pseudomonas putida* SN1. *Enzyme and Microbial Technology*, 39(6), 1264–1269.
- Hattori, K., Nagano, M., Kato, T., Nakanishi, I., Imai, K., Kinoshita, T. and Sakane, K., (1995) Asymmetric synthesis of FR165914: A novel  $\beta$  3-adrenergic agonist with a benzocycloheptene structure. *Bioorganic & Medicinal Chemistry Letters*, 5(23), 2821–2824.
- Hiramoto, T., Fujiwara, S., Hosokawa, K. and Yamaguchi, H., (2006) Crystal structure of 3-hydroxybenzoate hydroxylase from *Comamonas testosteroni* has a large tunnel for substrate and oxygen access to the active site. *Journal of Molecular Biology*, 364(5), 878–896.
- Hollmann, F., Lin, P.-C., Witholt, B. and Schmid, A., (2003) Stereospecific biocatalytic epoxidation: the first example of direct regeneration of a FAD-dependent monooxygenase for catalysis. *Journal of the American Chemical Society*, 125(27), 8209–8217.
- Howard-Jones, A.R. and Walsh, C.T., (2006) Staurosporine and rebeccamycin aglycones are assembled by the oxidative action of StaP, StaC, and RebC on chromopyrrolic acid. *Journal of the American Chemical Society*, 128(37), 12289–12298.
- Husain, M. and Massey, V., (1979) Kinetic studies on the reaction of *p*-hydroxybenzoate hydroxylase. *Journal of Biological Chemistry*, 254(14), 6657–6666.
- Husain, M., Entsch, B., Ballou, D.P., Massey, V. and Chapman, P.J., (1980) Fluoride elimination from substrates in hydroxylation reactions catalyzed by *p*-hydroxybenzoate hydroxylase. *Journal of Biological Chemistry*, 255(9), 4189–4197.
- Jacob, C., Jamier, V. and Ba, L.A., (2011) Redox active secondary metabolites. *Current Opinion in Chemical Biology*, 15(1), 149–155.
- Jadan, A.P., Moonen, M.J.H., Boeren, S., Golovleva, L.A., Rietjens, I. and van Berkel, W.J.H., (2004) Biocatalytic potential of *p*-hydroxybenzoate hydroxylase from *Rhodococcus rhodnii* 135 and *Rhodococcus opacus* 557. *Advanced Synthesis & Catalysis*, 346(2-3), 367–375.
- Joosten, V. and van Berkel, W.J., (2007) Flavoenzymes. *Current Opinion in Chemical Biology*, 11(2), 195–202.
- Kallio, P., Liu, Z., Mäntsälä, P., Niemi, J. and Metsä-Ketelä, M., (2008) Sequential action of two flavoenzymes, PgaE and PgaM, in angucycline biosynthesis: chemoenzymatic synthesis of gaudimycin C. *Chemistry & Biology*, 15(2), 157–166.
- Kantz, A. and Gassner, G.T., (2011) Nature of the reaction intermediates in the flavin adenine dinucleotide-dependent epoxidation mechanism of styrene monooxygenase. *Biochemistry*, 50(4), 523–532.
- Kantz, A., Chin, F., Nallamotheu, N., Nguyen, T. and Gassner, G.T., (2005) Mechanism of flavin transfer and oxygen activation by the two-component flavoenzyme styrene monooxygenase. *Archives of Biochemistry and Biophysics*, 442(1), 102–116.
- Kirchner, U., Westphal, A.H., Müller, R. and van Berkel, W.J.H., (2003) Phenol hydroxylase from *Bacillus thermoglucosidasius* A7, a two-protein component monooxygenase with a dual role for FAD. *Journal of Biological Chemistry*, 278(48), 47545–47553.
- Koskiniemi, H., Metsä-Ketelä, M., Dobritzsch, D., Kallio, P., Korhonen, H., Mäntsälä, P., Schneider, G. and Niemi, J., (2007) Crystal structures of two aromatic hydroxylases involved in the early tailoring steps of angucycline biosynthesis. *Journal of Molecular Biology*, 372(3), 633–648.

- Kuhn, D., Kholiq, M.A., Heinze, E., Buhler, B. and Schmid, A., (2010) Intensification and economic and ecological assessment of a biocatalytic oxyfunctionalization process. *Green Chemistry*, 12(5), 815–827.
- Leferink, N.G.H., Fraaije, M.W., Joosten, H.-J., Schaap, P.J., Mattevi, A. and van Berkel, W.J.H., (2009) Identification of a gatekeeper residue that prevents dehydrogenases from acting as oxidases. *Journal of Biological Chemistry*, 284(7), 4392–4397.
- Lin, H., Liu, Y. and Wu, Z.-L., (2011) Highly diastereo- and enantio-selective epoxidation of secondary allylic alcohols catalyzed by styrene monooxygenase. *Chemical Communications*, 47(9), 2610–2612.
- Lin, H., Qiao, J., Liu, Y. and Wu, Z.L., (2010) Styrene monooxygenase from *Pseudomonas* sp. LQ26 catalyzes the asymmetric epoxidation of both conjugated and unconjugated alkenes. *Journal of Molecular Catalysis B: Enzymatic*, 67(3-4), 236–241.
- Lindqvist, Y., Koskiniemi, H., Jansson, A., Sandalova, T., Schnell, R., Liu, Z., Mäntsälä, P., Niemi, J. and Schneider, G., (2009) Structural basis for substrate recognition and specificity in akilavone-11-hydroxylase from rhodomycin biosynthesis. *Journal of Molecular Biology*, 393(4), 966–977.
- Maeda-Yorita, K. and Massey, V., (1993) On the reaction mechanism of phenol hydroxylase. *Journal of Biological Chemistry*, 268(6), 4134–4144.
- Malito, E., Alfieri, A., Fraaije, M.W. and Mattevi, A., (2004) Crystal structure of a Baeyer-Villiger monooxygenase. *Proceedings of the National Academy of Sciences of the United States of America*, 101(36), 13157–13162.
- Mattevi, A., (1998) The PHBH fold: not only flavoenzymes. *Biophysical Chemistry*, 70(3), 217–222.
- McCulloch, K.M., Mukherjee, T., Begley, T.P. and Ealick, S.E., (2009) Structure of the PLP degradative enzyme 2-methyl-3-hydroxypyridine-5-carboxylic acid oxygenase from *Mesorhizobium loti* MAFF303099 and its mechanistic implications. *Biochemistry*, 48(19), 4139–4149.
- Montersino, S., Golovleva, L., Schlömann, M. and van Berkel, W.J.H., (2008) Another look at *p*-hydroxybenzoate hydroxylase. In S Frago, C Gómez-Moreno, M Medina, eds, *Flavins and Flavoprotein 2008*. Prentice Hall, Zaragoza, Zaragoza, pp. 51–56.
- Mooney, A., Ward, P.G. and O'Connor, K.E., (2006) Microbial degradation of styrene: biochemistry, molecular genetics, and perspectives for biotechnological applications. *Applied Microbiology and Biotechnology*, 72(1), 1–10.
- Neujahr, H.Y. and Kjellén, K.G., (1978) Phenol hydroxylase from yeast. *Journal of Biological Chemistry*, 253(24), 8835–8841.
- O'Leary, N.D., O'Connor, K.E. and Dobson, A.D.W., (2002) Biochemistry, genetics and physiology of microbial styrene degradation. *FEMS Microbiology Reviews*, 26(4), 403–417.
- Ortiz-Maldonado, M., Ballou, D.P. and Massey, V., (1999) Use of free energy relationships to probe the individual steps of hydroxylation of *p*-hydroxybenzoate hydroxylase: studies with a series of 8-substituted flavins. *Biochemistry*, 38(25), 8124–8137.
- Ortiz-Maldonado, M., Entsch, B. and Ballou, D.P., (2004) Oxygen reactions in *p*-hydroxybenzoate hydroxylase utilize the H-bond network during catalysis. *Biochemistry*, 43(48), 15246–15257.
- Otto, K., Hofstetter, K., Röthlisberger, M., Witholt, B. and Schmid, A., (2004) Biochemical characterization of StyAB from *Pseudomonas* sp. strain VLB120 as a two-component flavin-diffusible monooxygenase. *Journal of Bacteriology*, 186(16), 5292–5302.
- Palfey, B.A. and McDonald, C.A., (2010) Control of catalysis in flavin-dependent monooxygenases. *Archives of Biochemistry and Biophysics*, 493(1), 26–36.
- Palfey, B.A., Moran, G.R., Entsch, B., Ballou, D.P. and Massey, V., (1999) Substrate recognition by “password” in *p*-hydroxybenzoate hydroxylase. *Biochemistry*, 38(4), 1153–1158.
- Panke, S., de Lorenzo, V., Kaiser, A., Witholt, B. and Wubbolts, M.G., (1999) Engineering of a stable whole-cell biocatalyst capable of (*S*)-styrene oxide formation for continuous two-liquid-phase applications. *Applied and Environmental Microbiology*, 65(12), 5619–5623.
- Panke, S., Held, M., Wubbolts, M.G., Witholt, B. and Schmid, A., (2002) Pilot-scale production of (*S*)-styrene oxide from styrene by recombinant *Escherichia coli* synthesizing styrene monooxygenase. *Biotechnology and Bioengineering*, 80(1), 33–41.
- Panke, S., Witholt, B., Schmid, A. and Wubbolts, M.G., (1998) Towards a biocatalyst for (*S*)-styrene oxide production: characterization of the styrene degradation pathway of *Pseudomonas* sp. strain VLB120. *Applied and Environmental Microbiology*, 64(6), 2032–2043.
- Panke, S., Wubbolts, M.G., Schmid, A. and Witholt, B., (2000) Production of enantiopure styrene oxide by recombinant *Escherichia coli* synthesizing a two-component styrene monooxygenase. *Biotechnology and Bioengineering*, 69(1), 91–100.
- Park, J.-B., Bühler, B., Habicher, T., Hauer, B., Panke, S., Witholt, B. and Schmid, A., (2006a) The efficiency of recombinant *Escherichia coli* as biocatalyst for stereospecific epoxidation. *Biotechnology and Bioengineering*, 95(3), 501–512.
- Park, M.S., Bae, J.W., Han, J.H., Lee, E.Y., Lee, S.G. and Park, S., (2006b) Characterization of styrene catabolic genes of *Pseudomonas putida* SN1 and construction of a recombinant *Escherichia coli* containing styrene monooxygenase gene for the production of (*S*)-styrene oxide. *Journal of microbiology and biotechnology*, 16(7), 1032–1040.
- Parsons, J.F., Greenhagen, B.T., Shi, K., Calabrese, K., Robinson, H. and Ladner, J.E., (2007) Structural and functional analysis of the pyocyanin biosynthetic protein PhzM from *Pseudomonas aeruginosa*. *Biochemistry*, 46(7), 1821–1828.
- Peelen, S., Rietjens, I.M., van Berkel, W.J.H., van Workum, W.A. and Vervoort, J., (1993) 19F-NMR study on the pH-dependent regioselectivity and rate of the *ortho*-hydroxylation of 3-fluorophenol by phenol hydroxylase from *Trichosporon cutaneum*. Implications for the reaction mechanism. *European journal of biochemistry*, 218(2), 345–353.
- Peelen, S., Rietjens, I.M.C.M., Boersma, M.G. and Vervoort, J., (1995) Conversion of phenol derivatives to hydroxylated products by phenol hydroxylase from *Trichosporon cutaneum*. *European journal of biochemistry*, 227(1-2), 284–291.
- Qaed, A.A., Lin, H., Tang, D.-F. and Wu, Z.-L., (2011) Rational design of styrene monooxygenase mutants with altered substrate preference. *Biotechnology Letters*, 33(3), 611–616.
- Rao, V.R., Rao, V.R., Rao, V.R., Gurjar, M.K., Gurjar, M.K., Gurjar, M.K., Kaiwar, V., Kaiwar, V. and Kaiwar, V., (1992)

- Enantioselective catalytic reductions of ketones with new four membered oxazaborolidines: Application to (*S*)-tetramisole. *Tetrahedron: Asymmetry*, 3(7), 859–862.
- Ridder, L., Palfey, B.A., Vervoort, J. and Rietjens, I.M., (2000) Modelling flavin and substrate substituent effects on the activation barrier and rate of oxygen transfer by *p*-hydroxybenzoate hydroxylase. *FEBS Letters*, 478(1-2), 197–201.
- Ryan, K.S., Chakraborty, S., Howard-Jones, A.R., Walsh, C.T., Ballou, D.P. and Drennan, C.L., (2008) The FAD cofactor of RebC shifts to an IN conformation upon flavin reduction. *Biochemistry*, 47(51), 13506–13513.
- Ryan, K.S., Howard-Jones, A.R., Hamill, M.J., Elliott, S.J., Walsh, C.T. and Drennan, C.L., (2007) Crystallographic trapping in the rebeccamycin biosynthetic enzyme RebC. *Proceedings of the National Academy of Sciences of the United States of America*, 104(39), 15311–15316.
- Schmid, A., Dordick, J.S., Hauer, B., Kiener, A., Wubbolts, M. and Witholt, B., (2001a) Industrial biocatalysis today and tomorrow. *Nature*, 409(6817), 258–268.
- Schmid, A., Hofstetter, K., Feiten, H.J., Hollmann, F. and Witholt, B., (2001b) Integrated biocatalytic synthesis on gram scale: the highly enantioselective preparation of chiral oxiranes with styrene monooxygenase. *Advanced Synthesis & Catalysis*, 343(6-7), 732–737.
- Schreuder, H.A., Mattevi, A., Obmolova, G., Kalk, K.H., Hol, W.G.J., van der Bolt, F.J.T. and van Berkel, W.J.H., (1994) Crystal structures of wild-type *p*-hydroxybenzoate hydroxylase complexed with 4-aminobenzoate, 2, 4-dihydroxybenzoate, and 2-hydroxy-4-aminobenzoate and of the Tyr222Ala mutant complexed with 2-hydroxy-4-aminobenzoate. Evidence for a proton channel and a new binding mode of the flavin ring. *Biochemistry*, 33(33), 10161–10170.
- Schreuder, H.A., Prick, P.A., Wierenga, R.K., Vriend, G., Wilson, K.S., Hol, W.G. and Drenth, J., (1989) Crystal structure of the *p*-hydroxybenzoate hydroxylase-substrate complex refined at 1.9 Å resolution. Analysis of the enzyme-substrate and enzyme-product complexes. *Journal of Molecular Biology*, 208(4), 679–696.
- Schulze, B. and Wubbolts, M.G., (1999) Biocatalysis for industrial production of fine chemicals. *Current Opinion in Biotechnology*, 10(6), 609–615.
- Sheldon, R.A., (2007) Enzyme immobilization: the quest for optimum performance. *Advanced Synthesis & Catalysis*, 349(8-9), 1289–1307.
- Sheng, D., Ballou, D.P. and Massey, V., (2001) Mechanistic studies of cyclohexanone monooxygenase: chemical properties of intermediates involved in catalysis. *Biochemistry*, 40(37), 11156–11167.
- Shoun, H., Beppu, T. and Arima, K., (1979) On the stable enzyme-substrate complex of *p*-hydroxybenzoate hydroxylase. *Journal of Biological Chemistry*, 254(3), 899–904.
- Spector, T. and Massey, V., (1972) Studies on the effector specificity of *p*-hydroxybenzoate hydroxylase from *Pseudomonas fluorescens*. *Journal of Biological Chemistry*, 247(14), 4679–4687.
- Steennis, P.J., Cordes, M.M., Hilken, J.H. and Muller, F., (1973) On the interaction of *para*-hydroxybenzoate hydroxylase from *Pseudomonas fluorescens* with halogen ions. *FEBS Letters*, 36(2), 177.
- Sucharitakul, J., Phongsak, T., Entsch, B., Svasti, J., Chaiyen, P. and Ballou, D.P., (2007) Kinetics of a two-component *p*-hydroxyphenylacetate hydroxylase explain how reduced flavin is transferred from the reductase to the oxygenase. *Biochemistry*, 46(29), 8611–8623.
- Tischler, D., Eulberg, D., Lakner, S., Kaschabek, S.R., van Berkel, W.J.H. and Schlömann, M., (2009) Identification of a novel self-sufficient styrene monooxygenase from *Rhodococcus opacus* 1CP. *Journal of Bacteriology*, 191(15), 4996–5009.
- Tischler, D., Kermer, R., Gröning, J.A.D., Kaschabek, S.R., van Berkel, W.J.H. and Schlömann, M., (2010) StyA1 and StyA2B from *Rhodococcus opacus* 1CP: a multifunctional styrene monooxygenase system. *Journal of Bacteriology*, 192(19), 5220–5227.
- Torres Pazmino, D.E., Winkler, M., Glieder, A. and Fraaije, M.W., (2010) Monooxygenases as biocatalysts: Classification, mechanistic aspects and biotechnological applications. *Journal of Biotechnology*, 146(1-2), 9–24.
- Treiber, N. and Schulz, G.E., (2008) Structure of 2,6-dihydroxypyridine 3-hydroxylase from a nicotine-degrading pathway. *Journal of Molecular Biology*, 379(1), 94–104.
- Ukaegbu, U.E., Kantz, A., Beaton, M., Gassner, G.T. and Rosenzweig, A.C., (2010) Structure and ligand binding properties of the epoxidase component of styrene monooxygenase. *Biochemistry*, 49(8), 1678–1688.
- van Berkel, W.J. and Muller, F., (1989) The temperature and pH dependence of some properties of *p*-hydroxybenzoate hydroxylase from *Pseudomonas fluorescens*. *European journal of biochemistry*, 179(2), 307–314.
- van Berkel, W.J.H. and Muller, F., (1991) Flavin-dependent monooxygenases with special reference to *p*-hydroxybenzoate hydroxylase. *Chemistry and Biochemistry of Flavoenzymes 2*, 2–29.
- van Berkel, W.J.H. and van den Tweel, W.J., (1991) Purification and characterisation of 3-hydroxyphenylacetate 6-hydroxylase: a novel FAD-dependent monooxygenase from a Flavobacterium species., 201(3), 585–592.
- van Berkel, W.J.H., Benen, J.A.E., Eppink, M.H.M. and Fraaije, M.W., (1999) Flavoprotein kinetics. *Methods in Molecular Biology*, 131, 61–86.
- van Berkel, W.J.H., Eppink, M.H. and Schreuder, H.A., (1994) Crystal structure of *p*-hydroxybenzoate hydroxylase reconstituted with the modified FAD present in alcohol oxidase from methylotrophic yeasts: evidence for an arabinoflavin. *Protein Science*, 3(12), 2245–2253.
- van Berkel, W.J.H., Kamerbeek, N.M. and Fraaije, M.W., (2006) Flavoprotein monooxygenases, a diverse class of oxidative biocatalysts. *Journal of Biotechnology*, 124(4), 670–689.
- van den Heuvel, R.H.H., Westphal, A.H., Heck, A.J.R., Walsh, M.A., Rovida, S., van Berkel, W.J.H. and Mattevi, A., (2004) Structural studies on flavin reductase PheA2 reveal binding of NAD in an unusual folded conformation and support novel mechanism of action. *Journal of Biological Chemistry*, 279(13), 12860–12867.
- van Hellemond, E.W., Janssen, D.B. and Fraaije, M.W., (2007) Discovery of a novel styrene monooxygenase originating from the

- metagenome. *Applied and Environmental Microbiology*, 73(18), 5832–5839.
- Wang, J., Ortiz-Maldonado, M., Entsch, B., Massey, V., Ballou, D. and Gatti, D.L.**, (2002) Protein and ligand dynamics in 4-hydroxybenzoate hydroxylase. *Proceedings of the National Academy of Sciences of the United States of America*, 99(2), 608–613.
- Wierenga, R.K., de Jong, R.J., Kalk, K.H., Hol, W.G. and Drenth, J.**, (1979) Crystal structure of *p*-hydroxybenzoate hydroxylase. *Journal of Molecular Biology*, 131(1), 55–73.
- Xu, D., Ballou, D.P. and Massey, V.**, (2001) Studies of the mechanism of phenol hydroxylase: mutants Tyr289Phe, Asp54Asn, and Arg281Met. *Biochemistry*, 40(41), 12369–12378.
- Xu, D., Enroth, C., Lindqvist, Y., Ballou, D.P. and Massey, V.**, (2002) Studies of the mechanism of phenol hydroxylase: effect of mutation of proline 364 to serine. *Biochemistry*, 41(46), 13627–13636.
- Yamamoto, S., Katagiri, M., Maeno, H. and Hayaishi, O.**, (1965) Salicylate hydroxylase, a monooxygenase requiring flavin adenine dinucleotide. *Journal of Biological Chemistry*, 240, 3408–3413.



**Functional annotation and  
characterization of  
3-hydroxybenzoate 6-hydroxylase from  
*Rhodococcus jostii* RHA1**

Stefania Montersino<sup>1</sup> and Willem J. H. van Berkel<sup>1</sup>

<sup>1</sup> Laboratory of Biochemistry, Wageningen University,  
Dreijenlaan 3, 6703 HA Wageningen, The Netherlands

*BBA Protein and proteomics* (2012) 1824:433-442

## Abstract

The genome of *Rhodococcus jostii* RHA1 contains an unusually large number of oxygenase encoding genes. Many of these genes have yet unknown function, implying that a notable part of the biochemical and catabolic biodiversity of this Gram-positive soil actinomycete is still elusive. Here we present a multiple sequence alignment and phylogenetic analysis of putative *R. jostii* RHA1 flavoprotein hydroxylases. Out of 18 candidate sequences, three hydroxylases are absent in other available *Rhodococcus* genomes. In addition, we report the biochemical characterization of 3-hydroxybenzoate 6-hydroxylase (3HB6H), a gentisate-producing enzyme originally mis-annotated as salicylate hydroxylase. *R. jostii* RHA1 3HB6H expressed in *Escherichia coli* is a homodimer with each 47 kDa subunit containing a non-covalently bound FAD cofactor. The enzyme has a pH optimum around pH 8.3 and prefers NADH as external electron donor. 3HB6H is active with a series of 3-hydroxybenzoate analogues, bearing substituents in *ortho*- or *meta*-position of the aromatic ring. Gentisate, the physiological product, is a non-substrate effector of 3HB6H. This compound is not converted but strongly stimulates the NADH oxidase activity of the enzyme.

3

**Keywords:** fingerprint, flavoprotein, functional annotation, 3-hydroxybenzoate 6-hydroxylase, monooxygenase, *Rhodococcus jostii* RHA1



## Introduction

*Rhodococcus jostii* RHA1 is a Gram-positive soil actinomycete able to degrade a wide range of organic compounds (Ahmad *et al.*, 2011; Larkin *et al.*, 2005; Larkin *et al.*, 2006; Martínková *et al.*, 2009). It possesses one of the largest bacterial genomes ever sequenced and encodes an exceptional amount of oxygenases (203 putative genes), in particular flavoprotein monooxygenases (88 putative genes) (McLeod *et al.*, 2006).

Flavoprotein monooxygenases (EC 1.14.13.x) perform a wide range of regio- and enantioselective reactions and can be divided in six subclasses (van Berkel *et al.*, 2006). Subclass A comprises a family of single-component flavoprotein hydroxylases, which are crucially involved in microbial degradation of natural and anthropogenic aromatics (Hammann and Kutzner, 1998; Harwood and Parales, 1996; Phale *et al.*, 2007), polyketide antibiotics biosynthesis (Kallio *et al.*, 2008; Lindqvist *et al.*, 2009; Ryan *et al.*, 2007), and antibiotic resistance (Andersen *et al.*, 1997; Hoshino *et al.*, 2010; Volkens *et al.*, 2011).

Flavoprotein hydroxylases can be identified on the basis of three fingerprint sequences, first defined in 4-hydroxybenzoate 3-hydroxylase (PHBH) (Fig. 1) (Eppink, van Berkel and Schreuder, 1997b). The GxGxxG sequence motif maps the ADP moiety of FAD (Wierenga *et al.*, 1986), while the GD consensus motif represents the residues that interact with the riboflavin moiety of FAD (Eggink *et al.*, 1990). Both of these FAD fingerprints are common for many flavoproteins (Macheroux *et al.*, 2011). The third, DG consensus motif, is specific for subclass A enzymes and serves a dual role of recognition of both FAD and NADPH (Eppink, van Berkel and Schreuder, 1997b).

Here we used the above mentioned fingerprints to detect putative flavoprotein hydroxylase sequences in the *R. jostii* RHA1 genome (Fig. 1; Table 1). Since most of the retrieved sequences are annotated without a particular function, we performed a multiple sequence alignment and phylogenetic analysis with a large set of known flavoprotein hydroxylases. Among the newly assigned functions, we present the biochemical characterization of 3-hydroxybenzoate 6-hydroxylase (3HB6H), a flavoprotein involved in the gentisate (2,5-dihydroxybenzoate) degradation pathway (Fuenmayor *et al.*, 1998; Jeon *et al.*, 2006). Notably, the gene encoding for this flavoenzyme is mis-annotated as a salicylate (2-hydroxybenzoate) hydroxylase. *R. jostii* RHA1 3HB6H expressed in *E. coli* is specific for 3-hydroxybenzoate derivatives and does not interact with salicylate.

## Materials And Methods

**Chemicals.** DNaseI was from Boehringer Mannheim GmbH (Mannheim, Germany). Restriction endonucleases and dNTPs were purchased from Invitrogen (Carlsbad, CA, USA). Phusion High Fidelity DNA polymerase was from Finnzymes (Espoo, Finland). In-Fusion PCR cloning System was purchased from Clontech (Mountain View, CA, USA). Oligonucleotides were synthesised by Eurogentec (Liege, Belgium). *E. coli* TOP10 was from Invitrogen (Carlsbad, CA, USA). The pBAD/*Myc*-His (*Nde*I) expression vector was kindly provided by Prof. M.W. Fraaije (University of Groningen).

Nickel nitrilotriacetic acid (Ni-NTA) agarose was purchased from Qiagen (Valencia, CA, USA) and Bio-Gel P-6DG was from Bio-Rad (Hercules, CA, USA). HiLoad 26/10 Q-Sepharose HP, Superdex 200 HR10/30, low molecular weight protein marker, prestained kaleidoscope protein standards, and catalase (232 kDa), aldolase (158 kDa), BSA (68 kDa) and ovalbumin (43 kDa) were obtained from Pharmacia Biotech (Uppsala, Sweden).

Aromatic compounds were purchased from Sigma-Aldrich (St Louis, MO, USA) and Acros Organics (New Jersey, US). Catalase, FAD, FMN, riboflavin and arabinose were from Sigma-Aldrich (St Louis, MO, USA). Pefabloc SC was obtained from Roche Diagnostics GmbH (Mannheim, Germany). All other chemicals were from commercial sources and of the purest grade available.

**Sequence Analysis.** The genome of *R. jostii* RHA1 was analysed for the presence of flavoprotein hydroxylases at the European Bioinformatic Institute ([www.ebi.ac.uk](http://www.ebi.ac.uk)). FASTA analysis ([www.ebi.ac.uk/Tools/sss/fasta](http://www.ebi.ac.uk/Tools/sss/fasta)) was performed to determine protein sequence homology. Multiple sequence alignments were made using CLUSTALW (Thompson *et al.*, 1994). DNA cluster comparison and database searches were carried out using Nucleotide and Protein resources from the National Center for Biotechnology Information ([www.ncbi.nlm.nih.gov](http://www.ncbi.nlm.nih.gov)) and UniProt Database ([www.uniprot.org](http://www.uniprot.org)). Phylogenetic analysis was performed using FigTree ([tree.bio.ed.ac.uk](http://tree.bio.ed.ac.uk)).

### Cloning, Expression And Purification Of 3-Hydroxybenzoate 6-Hydroxylase In *E. coli*.

A 1.2 kb DNA fragment encoding a putative salicylate hydroxylase (Gene ID: 4218663) was PCR amplified from *R. jostii* RHA1 genomic DNA, using the oligonucleotides SM\_1869fwd (5'AGGAGGAATTACATATGTCGAATCTGCAGGACGCAC3') and SM\_1869rev (5'GTTCGGGCCCCAAGCTTTGACGCGCGATCGGACG3'), introducing *Nde*I and *Hind*III restriction sites (underlined), respectively and containing the start codon (bold). The amplified fragment was cloned into the pBAD/*Myc*-His expression vector containing a C-terminal His<sub>6</sub>-tag by using the In-Fusion PCR Cloning System. The resulting construct (pBAD-3HB6H-His<sub>6</sub>) was verified by automated sequencing of both strands and electroporated to *E. coli* TOP10 cells for recombinant expression.

The Äkta Explorer FPLC system (Pharmacia Biotech) was used for protein chromatography. For enzyme production, *E. coli* TOP10 cells, harbouring a pBAD-3HB6H-His<sub>6</sub> plasmid, were grown in TB medium supplemented with 100 µg·mL<sup>-1</sup> ampicillin until an optical density (OD<sub>600 nm</sub>) of 0.8 was reached. Expression was induced by the addition of 0.02% (w/v) arabinose and the incubation was continued for 16 h at 37 °C. Cells (36 g wet weight) were harvested by centrifugation, resuspended in 120 mL of 20 mM potassium phosphate, 300 mM NaCl (pH 7.4), containing 1 mM Pefabloc SC, 1 mg DNase, 100 µM MgCl<sub>2</sub> and subsequently passed twice through a precooled French Pressure cell (SLM Aminco, SLM Instruments, Urbana, IL, USA) at 16 000 psi. The resulting homogenate was centrifuged at 25000 g for 45 min at 4 °C to remove cell debris, and the supernatant was applied onto a Ni-NTA agarose column (13 × 1.6 cm) equilibrated with 20 mM sodium phosphate, 300 mM NaCl (pH 7.4). The column was washed with two volumes of equilibration buffer. The enzyme was eluted with 300 mM imidazole in equilibration buffer. The active pool, containing an added excess of free FAD, was desalted using a Biogel column (14 × 2.6 cm), running in 50 mM BisTris-HCl, 0.1 mM EDTA (pH 7.2). The desalted protein was loaded onto a HiLoad 26/10 Q-Sepharose HP column equilibrated with the same buffer. After washing with two column volumes of starting buffer, the protein was eluted with a linear gradient of NaCl (0–1 M) in the same buffer. Active fractions were pooled and concentrated

to 8 mg/ml by using Amicon filters (30 kDa cutoff), and dialysed at 4°C against 50 mM BisTris–HCl (pH 7.2). Purified 3HB6H was frozen in liquid nitrogen and stored at - 80 °C.

**Protein Analysis.** SDS/PAGE was performed using 12.5% acrylamide slab gels essentially as described by Laemmli (Laemmli, 1970). Proteins were stained using Coomassie Brilliant Blue R-250. Total protein concentrations were estimated using the BCA protein kit from Thermo Scientific Pierce with BSA as standard. Analytical gel filtration to investigate the hydrodynamic properties of 3HB6H was performed on a Superdex 200 HR 10/30 column running in 50 mM potassium phosphate, 150 mM KCl (pH 7.4). Desalting or buffer exchange of small aliquots of enzyme was performed with Bio-Gel P-6DG columns and Amicon Ultra-0.5 filters (30 kDa cut off) (Millipore).

**Spectral Analysis.** Absorption spectra were recorded at 25 °C on a Hewlett Packard (Loveland, CO, USA) 8453 diode array spectrophotometer in 50 mM Tris-SO<sub>4</sub> (pH 8.0). Spectra were analysed using the UV-Visible CHEMSTATION software package (Hewlett Packard).

The molar absorption coefficient of protein-bound FAD was determined by recording the absorption spectrum of 3HB6H in the presence and absence of 0.1% (w/v) SDS, assuming a molar absorption coefficient for free FAD of 11.3 mM<sup>-1</sup> cm<sup>-1</sup> at 450 nm. Purified enzyme concentrations were routinely determined by measuring the absorbance at 453 nm using the molar absorption coefficient for protein-bound FAD (10.3 mM<sup>-1</sup> cm<sup>-1</sup>).

**HPLC Product Analysis.** The enzymatic conversions were analyzed by HPLC using an Applied Biosystems 400 pump equipped with a Waters 996 photodiode-array detector. Reaction products were separated with a 4.0 × 60 mm C18 reverse-phase column (Spherisorb, ODS 2, Pharmacia). Reaction mixtures contained 2 mM substrate, 5 mM of NADH and 2 μM 3HB6H in 1.5 mL air saturated 20 mM Tris-SO<sub>4</sub> (pH 8.0). At the end of the reaction, 10 kDa spin filters were used to separate the enzyme from the reaction mixture. HPLC analysis of the resulting supernatant was carried out by gradient elution with 0.8% acetic acid and 20% methanol (pH 2.9) as mobile phase (flow rate 0.8 ml/min).

**Cofactor Determination.** The flavin cofactor of 3HB6H was identified by thin layer chromatography (TLC). The cofactor was released from the protein by boiling for 5 min or acid treatment. The protein precipitate was removed by centrifugation and the supernatant was applied together with the reference compounds FAD, FMN and riboflavin onto a TLC plate (Baker-flex Silica Gel 1B2; JT Baker Inc., Phillipsburg, NY, USA). Butanol/acetic acid/water (5:3:3) served as the mobile phase.

**Enzyme Activity.** 3HB6H activity was routinely assayed by following the decrease in absorbance of NADH at 360 nm at 25 °C on a Hewlett Packard 8453 diode array spectrophotometer. Initial velocity values were calculated using a molar absorption coefficient ( $\epsilon_{360}$ ) of 4.31 mM<sup>-1</sup> cm<sup>-1</sup>. The standard assay mixture contained 50 mM Tris-SO<sub>4</sub> (pH 8.0), 200 μM 3-hydroxybenzoate and 250 μM NADH; the reaction was started by addition of 45 nM enzyme. One unit of enzyme activity (U) is defined as the

$$A_{490} = \epsilon_{ES} * ES + \epsilon_E * (E_t - ES) \quad (1)$$

$$ES = \frac{(E_t + S_t + K_d) - \sqrt{(E_t + S_t + K_d)^2 - 4ES}}{2}$$

amount of enzyme that consumes 1 μmol of NADH per min. The optimal pH for activity of 3HB6H was determined using 25 mM MES, HEPES and CHES buffers with varying pH (pH 5.5-9.5) and adjusted to an ionic strength of 0.1 M with Na<sub>2</sub>SO<sub>4</sub> (Wijnands *et al.*, 1984).

The activity of 3HB6H with 3-hydroxybenzoate, 2,3-dihydroxybenzoate, 3,5-dihydroxybenzoate and 2,5-dihydroxybenzoate followed Michaelis-Menten kinetics (Johnson and Goody, 2011). Kinetic parameters were calculated from multiple measurements with various substrate concentrations using a direct nonlinear regression fit to the data.

**Oxygen Consumption.** An OxyTherm Clark-type oxygen electrode system (Hansatech, Norfolk, UK) was used to determine the hydroxylation efficiency of 3HB6H towards different substrates. The assay solution (final volume 1.0 ml) contained 350 μM substrate, 250 μM NADH and 1 μM 3HB6H in 50

mM air saturated Tris-SO<sub>4</sub> (pH 8.0) at 25 °C. At the end of the reaction, the amount of hydrogen peroxide produced was determined by adding 0.02 mg/ml of catalase ( $2 \text{ H}_2\text{O}_2 \rightarrow \text{O}_2 + 2 \text{ H}_2\text{O}$ ).

**Substrates binding studies.** The interaction of 3HB6H (25 μM) with substrate analogues was studied in 50 mM Tris-SO<sub>4</sub> (pH 8.0). Dissociation constants ( $K_d$ ) of enzyme/substrate complexes were determined from flavin absorption difference spectra. The  $K_d$  was calculated from the changes in absorbance at 490 nm using a direct nonlinear regression fit to the data with IGOR (Wavemetrics, Lake Oswego, OR, USA). Apparent dissociation constants were calculated by fitting the relative absorbencies to Eq. (1), a modified equation compared with the one described elsewhere (Bollen *et al.*, 2005):

and  $A_{490}$ ,  $E_T$ ,  $S_T$ ,  $ES$ ,  $K_d$ ,  $\epsilon_{ES}$ ,  $\epsilon_E$  are the absorbance observed at 490 nm, the total enzyme concentration, the total substrate concentration, the enzyme-substrate complex concentration, the dissociation constant of the enzyme-substrate complex, the molar absorption coefficient of the enzyme-substrate complex and the molar absorption coefficient of the free enzyme, respectively.

# 3

## Results

### Analysis Of *R. jostii* RHA1 Genome

**Identification Of *R. jostii* RHA1 Flavoprotein Hydroxylases.** By searching the *R. jostii* RHA1 genome with the three flavoprotein hydroxylase fingerprints of PHBH from *Pseudomonas fluorescens* (Fig.1) (Eppink, van Berkel and Schreuder, 1997b), we retrieved eighteen candidate sequences (Fig.1 and Table 1). Out of the candidate sequences, fifteen are present in other sequenced *Rhodococcus* strains with highest similarities found in *Rhodococcus opacus* B4. Q0S9S6, Q0S6Z5 and Q0RV68 are only present in *R. jostii* RHA1. From the alignments it is clear that the consensus sequences of the selected proteins are well conserved, even though small deviations occur.

**Multiple Sequence Alignment And Phylogenetic Tree Analysis.** Most of the retrieved sequences are not linked to a clear annotated function. To predict protein functions, we performed a multiple sequence alignment and phylogenetic analysis with characterised flavoprotein hydroxylases from different bacterial orders and some eukaryotic systems. The neighbour joining method was used to draw the phylogenetic tree (Fig.2).

Among the retrieved sequences, only two annotated functions (Q0SJD0 and Q0SPD2) were confirmed by phylogenetic analysis. Q0SJD0 encodes for 3-(2-hydroxyphenyl) propionate hydroxylase, an enzyme characterised solely in *Rhodococcus aetherivorans* (Powell and Archer, 1998). Q0SPD2 encodes for 4-hydroxybenzoate 3-hydroxylase, the prototype of the flavoprotein hydroxylase family (Entsch and van Berkel, 1995). Q0SAU3 and Q0SFD6 are annotated as pentachlorophenol monooxygenases but neither cluster with the characterised pentachlorophenol-converting enzymes.

Eleven sequences are annotated either as putative monooxygenase, FAD binding monooxygenase or aromatic ring hydroxylase. From our analysis, putative functions

can be assigned to Q0SJG8, Q0S9K8 and Q0S0L2. Q0SJG8 clusters with a group of flavoproteins acting on activated substrates, including among others salicylyl-CoA 5-hydroxylase (Q7X281) and 2-aminobenzoyl-CoA monooxygenase/ reductase (Q93FB38, Q93FC6), acting on CoA-activated salicylate and CoA-activated 2-aminobenzoate, respectively. Another member of this group is the newly identified enzyme SibG that acts on an activated form of sibiromycin (Giessen *et al.*, 2011). Q0S9K8 might encode for 6-hydroxynicotinate 3-monooxygenase (39% sequence identity and 56% similarity), since it belongs to the 6-hydroxynicotinate 3-monooxygenase clade, where two enzymes both from *Pseudomonas* have been characterised (Jiménez *et al.*, 2008; Nakano *et al.*, 1999). Q0S0L2 has high sequence homology with rifampicin monooxygenase, an enzyme present in actinomycetes such as *Rhodococcus equi* and *Nocardia farcinica* (Andersen *et al.*, 1997; Hoshino *et al.*, 2010).

Three sequences have been annotated with a probable enzymatic function but all of them seem mis-annotated. According to the phylogenetic tree, Q0RW34 encodes for a 3-(2-hydroxyphenyl) propionate hydroxylase instead of 2,4-dichlorophenol 6-monooxygenase. Three different types of 2,4-dichlorophenol 6-monooxygenases are known (Huong *et al.*, 2007), but Q0RW34 does not cluster with any of them. Q0SFL5

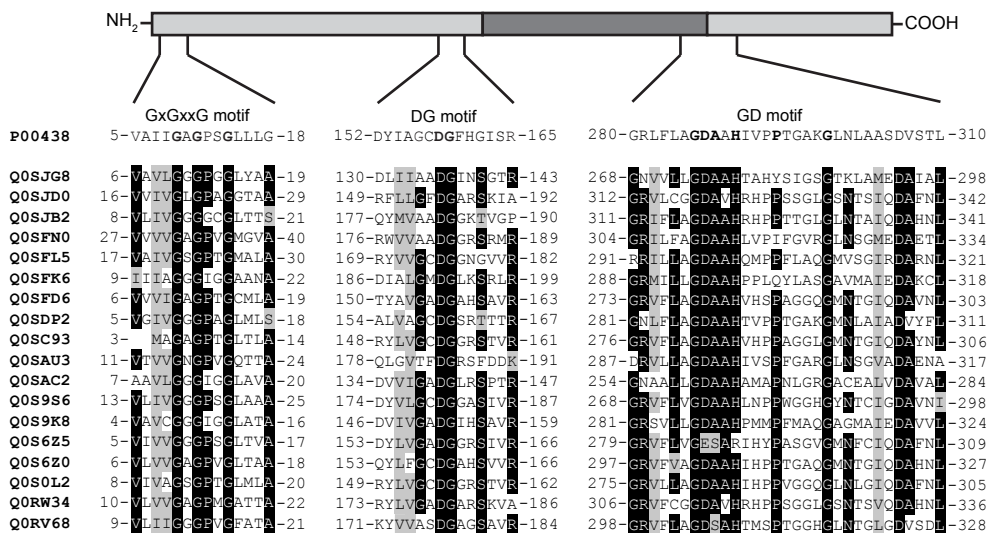


**Figure 1. Sequence comparison of putative flavoprotein hydroxylases from *Rhodococcus jostii* RHA1.** Upper panel: Schematic representation of the primary structure of PHBH from *P. fluorescens* (UniProt ID: P00438) with the FAD-binding domain in light gray and the substrate binding domain in dark gray. Middle panel: schematic representation of the flavoprotein hydroxylase fingerprints of PHBH from *P. fluorescens* used in this study. Bold characters represent residues used for fingerprint acronyms. Lower panel: Sequence alignment of flavoprotein hydroxylase fingerprint regions among putative flavoprotein hydroxylases from *R. jostii* RHA1. Identical residues are shaded in black, similar residues are shaded in gray.

does not seem to encode for a 3-(3-hydroxyphenyl) propionate hydroxylase, since the sequence outgroups from the clade quite early. Therefore, no putative function for Q0SFL5 can be addressed. Finally, Q0SFK6 is annotated as a putative salicylate hydroxylase, but both sequence alignment and cluster analysis (Fig.2) support another function (*vide infra*).

3

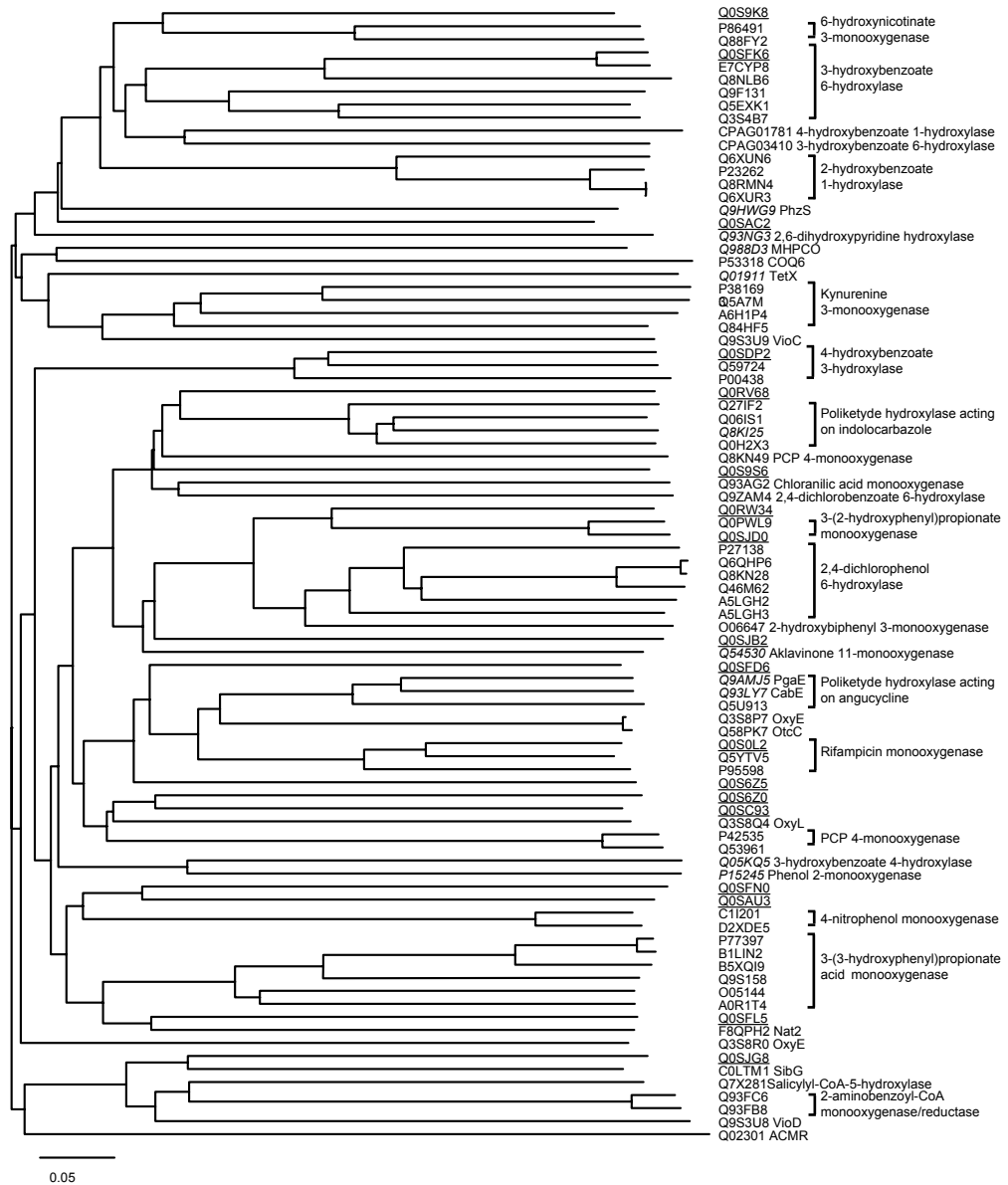




**Figure 2.** (Previous page) **Neighbour-joining tree of flavoprotein hydroxylases.** Underlined UniProt IDs represent hydroxylases from *R. jostii* RHA1. Italics UniProt IDs are sequences of hydroxylases with known crystal structures. On the right, enzymatic function has been reported.

## Functional Annotation Of 3HB6H

**Gene Order Conservation.** Putative salicylate monooxygenase (RHA1\_01869, GENE ID: 4218663) DNA locus region contains genes belonging to the gentisate degradation pathway (Fig.3): RHA1\_01866 (GENE ID: 4218660) encodes for a ring-fission dioxygenase that converts gentisate to maleylpyruvate.

This product is further converted to fumarylpyruvate by a maleylpyruvate isomerase

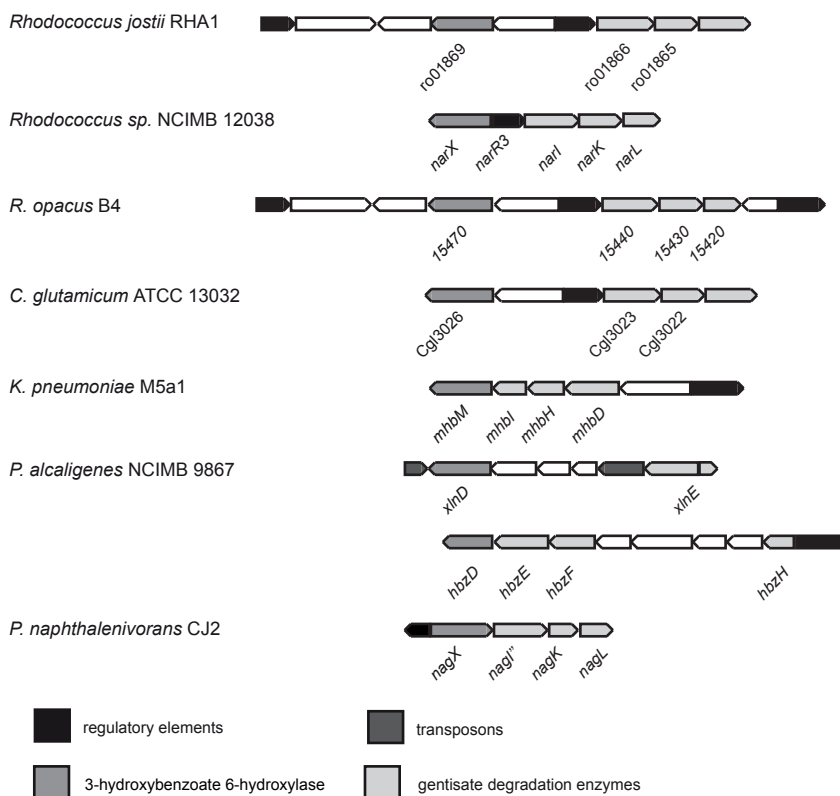


**Figure 3. Physical maps of gene clusters for 3-hydroxybenzoate and gentisate degradation.** ORFs annotated as unknown function are depicted in white. The sequences were taken from (GenBank ID) *R. jostii* RHA1 (CP000431), *Rhodococcus* sp. NCIMB 12083 (HM852512), *R. opacus* B4 (NC\_012522), *C. glutamicum* ATCC13032 (BA000036), *K. pneumoniae* M5a1 (AY648560), *P. alcaligenes* NCIMB 9867 (AF173167, DQ394580) and *P. naphthalenivorans* CJ2 (DQ167474).

Table 1. Flavoprotein hydroxylases from *R. jostii* RHAI.

Locus name	Tr-EMBL	Annotated name	Putative function from NJ-tree <sup>a</sup> (EC number)	Presence in other sp (percentage identity)
RHAI_rod00462	Q0S1G8	Monoxygenase/aromatic ring hydroxylase	acting on activated substrate	<i>R. opacus</i> B4 (74)
RHAI_rod00520	Q0S1D0	3-(2-hydroxyphenyl) propionate monooxygenase	3-(2-hydroxyphenyl) propionate hydroxylase (EC 1.14.13.x)	<i>R. aetherivorans</i> (90) <i>R. opacus</i> B4 (96)
RHAI_rod00538	Q0S1B2	Aromatic ring hydroxylase		<i>R. erythropolis</i> TA421 (78) <i>R. opacus</i> B4 (93)
RHAI_rod01845	Q0SFN0	Probable aromatic ring hydroxylase		<i>R. equi</i> ATCC 33707 (72)
RHAI_rod01860	Q0SFL5	Probable 3-(3-hydroxyphenyl) propionate hydroxylase		<i>R. equi</i> 103S (72)
RHAI_rod01869	Q0SFK6	Probable salicylate monooxygenase		<i>R. erythropolis</i> SK121 (71)
RHAI_rod01939	Q0SFD6	Pentachlorophenol monooxygenase	3-hydroxybenzoate 6-hydroxylase (EC 1.14.13.24)	<i>R. erythropolis</i> PR4 (70) <i>R. opacus</i> B4 (40)
RHAI_rod02539	Q0SPD2	4-hydroxybenzoate 3-monoxygenase	4-hydroxybenzoate 3-hydroxylase (EC 1.14.13.2)	<i>R. opacus</i> B4 (96) <i>Rhodococcus</i> NCIMB12038 (93)
RHAI_rod03040	Q0SC93	Probable aromatic ring hydroxylase		<i>R. opacus</i> B4 (90)
RHAI_rod03540	Q0SAU3	Pentachlorophenol monooxygenase		<i>R. opacus</i> B4 (97)
RHAI_rod03714	Q0SAC2	Possible aromatic ring hydroxylase		<i>R. equi</i> ATCC33707 (88)
RHAI_rod03910	Q0S9S6	FAD-binding monooxygenase		<i>R. equi</i> 103S (87)
RHAI_rod03981	Q0S9K8	Probable aromatic ring monooxygenase		<i>R. erythropolis</i> SK121 (89)
RHAI_rod04910	Q0S6Z5	Monoxygenase		<i>R. erythropolis</i> PR4 (87)
RHAI_rod04915	Q0S6Z0	Monoxygenase		<i>R. opacus</i> B4 (90) <i>R. opacus</i> B4 (95)
RHAI_rod07160	Q0S0L2	Probable FAD-dependent monooxygenase	6-hydroxymicoinate 3-monoxygenase (EC 1.14.13.114)	<i>R. equi</i> ATCC33707 (60) <i>R. equi</i> 103S (60)
RHAI_rod10313	Q0RW34	Probable 2,4-dichlorophenol 6-monoxygenase		<i>R. opacus</i> B4 (93)
RHAI_rod11171	Q0RV68	Possible monooxygenase/hydroxylase		<i>R. opacus</i> B4 (94) <i>R. erythropolis</i> SK121 (63)
				<i>R. erythropolis</i> PR4 (63)
				<i>R. opacus</i> B4 (73)
				<i>R. equi</i> ATCC 33707 (73)
				<i>R. equi</i> 103S (73)
				<i>R. erythropolis</i> SK121 (69)
				<i>R. erythropolis</i> PR4 (69)
				<i>Rhodococcus</i> NCIMB 9874 (80)
				<i>R. aetherivorans</i> (59)

<sup>a</sup> Neighbour joining tree (Fig.2)



encoded by RHA1\_rop1865 (GENE ID: 4218659). DNA regions encoding for known 3HB6Hs possess the same gene order organization as the RHA1\_rop1869 DNA region, especially the 3HB6H degradation operon from *Corynebacterium glutamicum* (Fig.3) (Shen *et al.*, 2005; Yang *et al.*, 2010). Q0SFK6 shares 93% amino acid sequence identity with 3HB6H from *Rhodococcus* NCIMB 12038 (*narX*, GenBank: HM852512.1) (Liu *et al.*, 2010) and 96% with putative 3HB6H from *Rhodococcus opacus* B4 (ROP\_15470, GENE ID: 7741586). Thus, based on protein sequence similarity, phylogenetic tree clustering and gene order conservation, we hypothesised that Q0SFK6 encodes for 3HB6H instead of salicylate hydroxylase. Very recently, a homologue 3HB6H gene was identified in *Candida parapsilosis* (Holesova *et al.*, 2011). The *C. parapsilosis* 3HB6H sequence does not cluster with bacterial 3HB6Hs (Fig.2). Instead, it forms a separate clade together with 4-hydroxybenzoate 1-hydroxylase from the same fungus (Holesova *et al.*, 2011; Eppink, Boeren, Vervoort and van Berkel, 1997a), probably due to the common eukaryotic origin.

**Cloning, Expression And Purification Of Q0SFK6.** To assess the activity of Q0SFK6, the gene was cloned into vector pBAD/*Myc*-His under control of the inducible *ara* promoter. The expression vector was transformed in *E. coli* TOP10 cells and overexpression of the His-tagged protein was induced by adding 0.02% (w/v) arabinose to the Terrific Broth medium. High level of expression was found after 16 h of induction at 37 °C. No expression was achieved in Luria Bertani medium.

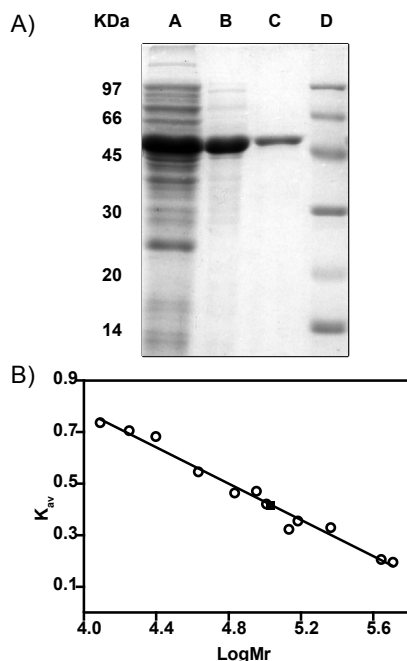


**Table 2. Purification of *R. jostii* RHA1 Q0SFK6 expressed in *E. coli*.**

Step	Protein (mg)	Activity (U)	Specific activity (U/mg <sup>-1</sup> )	Yield (%)
Cell extract	3360	18718	6	100
Ni-NTA agarose	780	14997	19	80
Q-Sepharose	450	10738	24	57

**Figure 4. Hydrodynamic properties of 3HB6H.**

A) SDS/PAGE analysis of the purification of 3HB6H from *R. jostii* RHA1 expressed in *E. coli*. Lane A, cell extract; Lane B, Ni-NTA pool; Lane C, Q-sepharose pool; Lane D, low molecular weight marker. B) Analytical gel filtration. Reference proteins used to calibrate the column and calculate the 3HB6H apparent molecular mass: cytochrome c (12.3 kDa), myoglobin (17.8 kDa), α-chymotrypsin (25 kDa), ovalbumin (43 kDa), bovine serum albumin (68 and 136 kDa), 4-hydroxybenzoate 3-hydroxylase (90 kDa), lipoamide dehydrogenase (102 kDa), phenol 2-hydroxylase (152 kDa), catalase (232 kDa), ferritin (440 kDa) and vanillyl-alcohol oxidase (510 kDa); ■ 3HB6H.

The recombinant protein was purified to apparent homogeneity by two successive chromatographic steps (Table 2). Approximately 420 mg of recombinant Q0SFK6 protein could be purified from 6 L batch culture containing 36 g (wet weight) of cells. SDS-PAGE showed a single band with an apparent molecular mass of 47 kDa (Fig.4A), in agreement with the Q0SFK6 amino acid sequence. The relative molecular mass of the native recombinant protein was estimated to be ~108 kDa by analytical gel filtration (Fig.4B), which indicates a dimer conformation in solution.

**Spectral Properties.** Recombinant Q0SKF6 showed a typical flavoprotein absorption spectrum with maxima at 274 nm, 383 nm and 453 nm and a shoulder at 480 nm. (Fig.5A) The molar absorption coefficient of protein-bound flavin was determined to be  $10.3 \text{ mM}^{-1} \text{ cm}^{-1}$  at 453 nm. The  $A_{274}/A_{453}$  ratio of the FAD-saturated protein preparation was 11.9. The  $A_{383}/A_{453}$  ratio (Fig.5A) is 1.2, a rather high value for flavoproteins. The flavin cofactor could be released from the protein by boiling or acid treatment and was identified as FAD by TLC.

**Table 3. Substrate and effector specificity of 3HB6H.**

Substrate	$K_d$ ( $\mu\text{M}$ )	$K_m$ ( $\mu\text{M}$ )	$k_{\text{cat}}$ ( $\text{s}^{-1}$ )	$k_{\text{cat}}/K_m$ ( $\mu\text{M}^{-1} \text{ s}^{-1}$ )	Uncoupling (%)
3-hydroxybenzoate	$48 \pm 2$	$46 \pm 3$	$35 \pm 1$	$8 \times 10^{-1}$	5
3,5-dihydroxybenzoate	$310 \pm 60$	$250 \pm 10$	$13 \pm 1$	$5 \times 10^{-2}$	10
2,3-dihydroxybenzoate	$63 \pm 9$	$51 \pm 7$	$10 \pm 1$	$2 \times 10^{-1}$	20
2,5-dihydroxybenzoate	$190 \pm 10$	$140 \pm 30$	$7 \pm 1$	$5 \times 10^{-2}$	99

Apparent kinetic constants were determined at 25 °C in 50 mM Tris- $\text{SO}_4$  (pH 8.0). Values are presented as the mean of three experiments. The percentage of uncoupling of hydroxylation was determined from polarographic measurements using a Clarke-type electrode. The percentage of uncoupling equals twice the amount of oxygen produced at the end of the reaction, after addition of catalase ( $2 \text{ H}_2\text{O}_2 \rightarrow \text{O}_2 + \text{H}_2\text{O}$ ).

### Catalytic Properties Of 3HB6H

**Enzyme Activity And Product Analysis.** Enzyme activity was assayed by measuring the consumption of NADH spectrophotometrically. Q0SFK6 showed a very low NADH oxidase activity ( $< 1 \text{ U mg}^{-1}$ ). No increase in enzyme activity was detected in the presence of salicylate, while NADH consumption was strongly stimulated by 3-hydroxybenzoate. The aromatic product was identified as gentisate (2,5-dihydroxybenzoate) by absorption spectral analysis, and HPLC (Table 4). Thus, enzyme activity and product analysis confirms the new annotation of Q0SKF6 as 3-hydroxybenzoate 6-hydroxylase (3HB6H).

**Kinetic Parameters.** 3HB6H from *R. jostii* RHA1 catalyses the *para*-hydroxylation of 3-hydroxybenzoate with the consumption of NAD(P)H and oxygen. The enzyme displayed a maximum activity around pH 8.0 in Tris- $\text{SO}_4$  buffer and around pH 8.6 in HEPES buffer (data not shown). Like other flavoprotein hydroxylases (Steennis *et al.*,

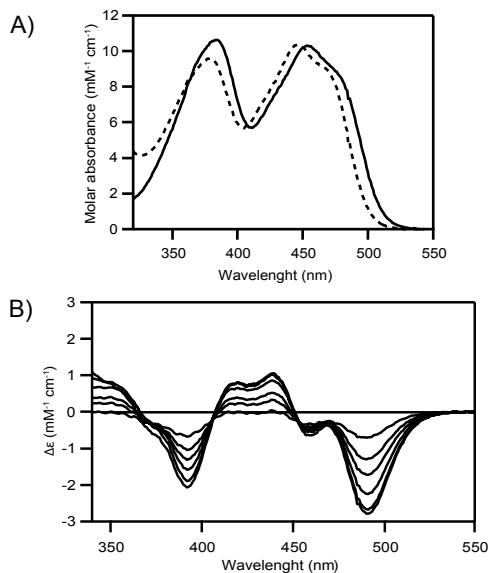


**Figure 5. Spectral properties of recombinant 3HB6H.** **A)** Spectral properties of free 3HB6H (solid line) and 3HB6H in complex with 890  $\mu\text{M}$  3-hydroxybenzoate (dashed line). **B)** Absorption difference spectra observed upon binding of 3-hydroxybenzoate to 25  $\mu\text{M}$  3HB6H. The curves shown are the difference spectra, the corrected enzyme spectra in the presence of 17, 50, 82, 177, 455 and 890  $\mu\text{M}$  3-hydroxybenzoate, minus the enzyme spectrum in the absence of 3-hydroxybenzoate

enzyme transformed the initial product of the reaction with 3,5-dihydroxybenzoate (2,3,5-trihydroxybenzoate) to 2,3,5,6-tetrahydroxybenzoate (Table 4).

To discriminate between true substrates and non-substrate effectors, oxygen consumption experiments were performed in the absence and presence of catalase. With all substrates, a certain degree of uncoupling of hydroxylation was observed, as evidenced by the production of hydrogen peroxide (Table 3). Gentisate, the physiological product, is a good effector of 3HB6H. This compound is not converted but strongly stimulates the NADH oxidase activity of the enzyme (Fig.6).

**Substrate Binding.** Upon titration of 3HB6H with 3-hydroxybenzoate derivatives, characteristic perturbations in the absorption properties of the FAD cofactor were observed (Fig.5B). From the absorption differences around 490 nm, dissociation constants ( $K_d$  values) were estimated for the binary enzyme-substrate complexes

1973; van Berkel and Tweel, 1991; van Berkel and Muller, 1991), the enzyme was strongly inhibited by chloride ions. The steady-state kinetic parameters of 3HB6H were determined at 25°C in 50 mM Tris- $\text{SO}_4$  (pH 8.0) (Table 3). This analysis revealed that the enzyme clearly prefers NADH ( $K_m = 48 \pm 4 \mu\text{M}$ ) over NADPH ( $K_m = 391 \pm 76 \mu\text{M}$ ) as external electron donor.

### Substrate And Effector Specificity.

3HB6H from *R. jostii* RHA1 catalyses the regioselective *para*-hydroxylation of 3-hydroxybenzoate forming gentisate (Fig.6). Besides from the parent substrate, 3HB6H was most active with 2,3-dihydroxybenzoate and 3,5-dihydroxybenzoate (Table 3; Fig.6). Next to that, the enzyme slowly converted ( $k_{\text{cat}} < 5 \text{ s}^{-1}$ ) a number of 3-hydroxybenzoate derivatives with substituents at the 4-position (Table 4). Among these compounds, 3,4-dihydroxybenzoate is a very poor substrate (Table 4). In analogy with the conversion of 2,3,4-trihydroxybenzoate to 2,3,4,6-tetrahydroxybenzoate, the

(Table 3). Similar titration experiments with salicylate established that this compound does not induce any flavin absorption change (data not shown).

**Table 4. HPLC product analysis of the 3HB6H reactions.**

Substrate	Retention time	Product(s)	Retention time
3-hydroxybenzoate	19	2,5-dihydroxybenzoate	12.3
2,5-dihydroxybenzoate	11.7	-	12.3
3,5-dihydroxybenzoate	7.2	2,3,5-trihydroxybenzoate	4
		2,3,5,6-tetrahydroxybenzoate	2.7
2,3-dihydroxybenzoate	19.5	2,3,6-trihydroxybenzoate	4.1
3,4-dihydroxybenzoate	8.3	-	7.8
2,3,4-trihydroxybenzoate	8.6	2,3,4,6-tetrahydroxybenzoate	2.9
3-hydroxy-4-aminobenzoate	5.1	4-amino-2,5-dihydroxybenzoate	5.8
3-hydroxy-4-methylbenzoate	22.8	4-methyl-2,5-dihydroxybenzoate	17.5
3-hydroxy-4-methoxybenzoate	21.5	4-methoxy-2,5-dihydroxybenzoate	4.7

## 3

## Discussion

*R. jostii* RHA1 is a versatile Gram-positive soil bacterium degrading a wide range of organic compounds, including lignin (Ahmad *et al.*, 2011). It contains an impressive amount of oxygenases, especially flavoprotein monooxygenases. Recently, Szolkowy and colleagues characterised the Baeyer-Villiger monooxygenase (BVMO) subclass of *R. jostii* RHA1 pointing out an exceptional diversity in regio- and enantioselectivity (Szolkowy *et al.*, 2009).

In the present study, we searched for new flavoprotein hydroxylases in the *R. jostii* RHA1 genome. Most of these enzymes are single-component proteins that form a specific class of flavoprotein monooxygenases (subclass A). By using three different fingerprints we were able to retrieve eighteen candidate flavoprotein hydroxylase sequences. Three of these sequences turned out to be *R. jostii* RHA1 specific, while the others are present also in other available *Rhodococcus* genomes, especially in *R. opacus* strain B4. The highest sequence similarity with flavoprotein hydroxylases from *R. opacus* strain B4 is in agreement with the overall synteny between these *Rhodococcus* strains.

Most of the candidate flavoprotein hydroxylase sequences have been annotated without a specific function or are mis-annotated. From multiple sequence alignment and phylogenetic analysis we could assess some new putative functions.

Q0S0L2 encodes for a rifampicin monooxygenase, an enzyme able to decompose the antibiotic *via* *N*-hydroxylation. This type of decomposition mechanism is driven by flavoprotein monooxygenases in *Nocardia farcinica* and *Rhodococcus equi*, both pathogen strains (Andersen *et al.*, 1997; Hoshino *et al.*, 2010). Rifampicin is used for tuberculosis treatment and drug inactivation in *Mycobacterium* is driven by decomposition as in *Rhodococcus* and *Nocardia* species (Hoshino *et al.*, 2010). *N*-hydroxylation is an unusual reaction for flavoprotein hydroxylases, usually

performed by subclass B monooxygenases (Torres Pazmiño *et al.*, 2010; Chocklett and Sobrado, 2010; Ge and Seah, 2006; Mayfield *et al.*, 2010; Meneely *et al.*, 2009; Meneely and Lamb, 2007). However, a hybrid kinetic mechanism between flavoprotein hydroxylases and subclass B monooxygenases has been reported for L-ornithine N5-oxygenase (Meneely *et al.*, 2009; Olucha and Lamb, 2011).

Q0RW34 and Q0S9K8 are predicted to be a 3-(2-hydroxyphenyl) propionate hydroxylase and 6-hydroxynicotinate 3-monooxygenase, respectively. The first enzyme plays a role in lignin degradation (Powell and Archer, 1998), whereas the latter is involved in the metabolism of nicotinic acid in *Pseudomonas fluorescens* T5 and *Pseudomonas putida* KT2400 (Jiménez *et al.*, 2008; Nakano *et al.*, 1999), performing decarboxylative hydroxylation of 6-hydroxynicotin acid into 2,5-dihydroxypyridine.

Q0SJG8 most likely acts on an activated substrate, similarly to SibG (Giessen *et al.*, 2011; Ishiyama *et al.*, 2004; Schühle *et al.*, 2001), 2-aminobenzoylCoA monooxygenase/reductase (ACMR) and salicylyl-CoA 5-hydroxylase. Interestingly, all the latter enzymes cluster in the same part of the tree (Fig.2), suggesting that they might have a conserved mode of CoA-substrate recognition.

Q0SFK6 represents a clear mis-annotation in the *R. jostii* genome. From comparing several known 3HB6H amino acid sequences and gene clusters with the Q0SFK6 *Rhodococcus* DNA locus, we conclude that Q0SFK6 encodes for a 3HB6H which is involved in the gentisate degradation pathway. The organization of the gene cluster is conserved in *Corynebacterium glutamicum* and in *Rhodococcus opacus* B4, and to a lesser extent in *Rhodococcus* NCIMB 12038 (Fig.3). The presence of many regulatory elements or transposase-like elements surrounding most of the 3HB6H clusters could be viewed as an element of plasticity of this cluster, since gentisate formation could involve also salicylate 5-hydroxylase.

The enzymatic activity of Q0SKF6 was addressed with the recombinant protein. In agreement with the above proposition derived from sequence data, activity was found with 3-hydroxybenzoate and not with salicylate. Product analysis confirmed that Q0SFK6 encodes for 3HB6H and thus is mis-annotated as a salicylate hydroxylase.

Analytical gel filtration indicated that 3HB6H from *R. jostii* RHA1 is a homodimer. So far, a monomeric (Suárez *et al.*, 1995) or trimeric (Yang *et al.*, 2010; Liu *et al.*, 2010; Gao *et al.*, 2005; Park *et al.*, 2007) nature has been reported for 3HB6H enzymes. 3HB6H from *R. jostii* RHA1 has narrow substrate specificity. Besides the parent substrate, the enzyme accepts 3-hydroxybenzoate compounds with substituents in *ortho*- and *meta*-position. Importantly, it was established here for the first time that gentisate is a non-substrate effector of 3HB6H, stimulating FAD reduction and NADH consumption with production of hydrogen peroxide. Such behaviour of the aromatic product is also seen with the prototype of this flavoprotein subfamily, PHBH (Entsch and van Berkel, 1995). In case of 3HB6H, waste of NADH consumption will be negligible under physiological conditions, since gentisate dioxygenases convert gentisate very efficiently (Adams *et al.*, 2006), preventing hydrogen peroxide

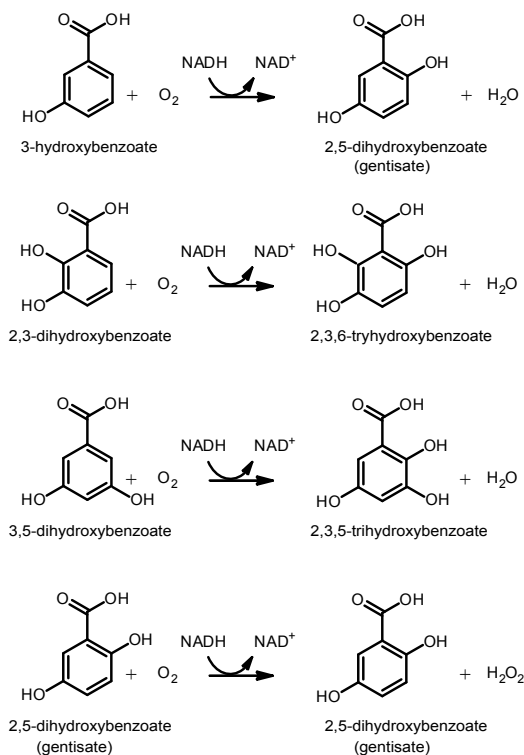


**Figure 6. Reactions catalyzed by 3HB6H.** From top to bottom: reactions with the best substrates (3-hydroxybenzoate, 2,3-dihydroxybenzoate and 3,5-dihydroxybenzoate) and the best non-substrate effector (2,5-dihydroxybenzoate).

B4 cell extracts (Grund *et al.*, 1992) and Di Gennaro and colleagues (Di Gennaro *et al.*, 2010) described a gene cluster in *Rhodococcus* R7 containing a salicylyl-CoA 5-hydroxylase gene. However, in both cases, no sequence or evidence at the enzyme level was reported. By using the *R. jostii* 3HB6H sequence as bait among the *Rhodococcus* genomes available, we found a putative 3HB6H in *R. opacus* B4 contained in a conserved 3-hydroxybenzoate/gentisate-degradation operon (Fig.3). In contrast, with salicylyl-CoA 5-hydroxylase (Q7X281) and salicylate 5-hydroxylase (Q3S4D3) as baits, no *Rhodococcus* homologues were found. Recently, a 3HB6H was described in *Rhodococcus* sp. NCIMB 12038 (Liu *et al.*, 2010). 3HB6H from *R. jostii* RHA1 shares 93% amino acid sequence with 3HB6H from *Rhodococcus* sp. NCIMB 12038. To our best knowledge, these are the only *Rhodococcus* gentisate producing enzymes characterised thus far.

production in the cell.

Three different microbial enzymes that produce gentisate have been reported: flavin-dependent salicylyl-CoA 5-hydroxylase, Rieske (2Fe-2S) dependent salicylate 5-hydroxylase, and flavin-dependent 3HB6H. Salicylyl-CoA 5-hydroxylase has been characterised in *Streptomyces* WA46 (Ishiyama *et al.*, 2004), while two-component Rieske type salicylate 5-hydroxylase has been studied in *Ralstonia* sp. U2 and *Polaromonas naphthalenivorans* CJ2 (Jeon *et al.*, 2006; Zhou *et al.*, 2002). Different 3HB6Hs have been described in Gram-positive (Yang *et al.*, 2010; Liu *et al.*, 2010) and Gram-negative bacteria (Suárez *et al.*, 1995; Gao *et al.*, 2005; Park *et al.*, 2007), and recently in *C. parapsilosis* (Holesova *et al.*, 2011).

Among *Rhodococcus* species, gentisate formation has been mostly related to salicylate 5-hydroxylase activity. Grund and colleagues measured salicylyl-CoA 5-hydroxylase activity in *R. opacus*



## Conclusion

In conclusion, we have retrieved a pool of flavoprotein hydroxylases in *R. jostii* RHA1 that share conserved flavoprotein fingerprints but can act on diverse aromatic substrates. Furthermore, from multiple sequence alignments and phylogenetic analysis, a number of functional annotations have been resolved.

Q0SFK6 is an example of a successful functional annotation. From biochemical analysis we obtained clear evidence that Q0SFK6 was mis-annotated as a salicylate hydroxylase, an enzyme related to 3HB6H but with different substrate specificity.

3HB6H is one of the few *para*-hydroxylating flavoprotein monooxygenases characterised. Recently, Hiromoto and coworkers (Hiromoto *et al.*, 2006) obtained the crystal structure of 3-hydroxybenzoate 4-hydroxylase (3HB4H) from *Comamonas testosteroni*. 3HB4H is using the same substrate as 3HB6H but performs an *ortho*-hydroxylation reaction. Comparison between structure and mechanism of 3HB4H and 3HB6H might help in understanding the striking regioselectivity of flavoprotein aromatic hydroxylases.

3

## Acknowledgements

We are grateful to Anette Riebel and Daniel Torres Pazmiño for In-Fusion PCR Cloning System optimization, Laura de Hoon for experimental contributions and Adrie Westphal for technical assistance. This study was supported by the Integrated Biosynthesis Organic Synthesis (IBOS) project of the Netherlands Organization for Scientific Research (NWO).

## References

- Adams, M.A., Singh, V.K., Keller, B.O. and Jia, Z., (2006) Structural and biochemical characterization of gentisate 1,2-dioxygenase from *Escherichia coli* O157:H7. *Molecular Microbiology*, 61(6), 1469–1484.
- Ahmad, M., Roberts, J.N., Hardiman, E.M., Singh, R., Eltis, L.D. and Bugg, T.D.H., (2011) Identification of DypB from *Rhodococcus jostii* RHA1 as a lignin peroxidase. *Biochemistry*, 50(23), 5096–5107.
- Andersen, S.J., Quan, S., Gowan, B. and Dabbs, E.R., (1997) Monooxygenase-like sequence of a *Rhodococcus equi* gene conferring increased resistance to rifampin by inactivating this antibiotic. *Antimicrobial agents and chemotherapy*, 41(1), 218–221.
- Bollen, Y.J.M., Nabuurs, S.M., van Berkel, W.J.H. and van Mierlo, C.P.M., (2005) Last in, first out: the role of cofactor binding in flavodoxin folding. *Journal of Biological Chemistry*, 280(9), 7836–7844.
- Chocklett, S.W. and Sobrado, P., (2010) *Aspergillus fumigatus* SidA is a highly specific ornithine hydroxylase with bound flavin cofactor. *Biochemistry*, 49(31), 6777–6783.
- Di Gennaro, P., Terreni, P., Masi, G., Botti, S., De Ferra, F. and Bestetti, G., (2010) Identification and characterization of genes involved in naphthalene degradation in *Rhodococcus opacus* R7. *Applied Microbiology and Biotechnology*, 87(1), 297–308.
- Eggink, G., Engel, H., Vriend, G., Terpstra, P. and Witholt, B., (1990) Rubredoxin reductase of *Pseudomonas oleovorans*. Structural relationship to other flavoprotein oxidoreductases based on one NAD and two FAD fingerprints. *Journal of Molecular Biology*, 212(1), 135–142.
- Entsch, B. and van Berkel, W.J.H., (1995) Structure and mechanism of *para*-hydroxybenzoate hydroxylase. *FASEB Journal*, 9(7), 476–483.
- Eppink, M.H.M., Boeren, S.A., Vervoort, J. and van Berkel, W.J.H., (1997a) Purification and properties of 4-hydroxybenzoate 1-hydroxylase (decarboxylating), a novel flavin adenine dinucleotide-dependent monooxygenase from *Candida parapsilosis* CBS604. *Journal of Bacteriology*, 179(21), 6680–6687.
- Eppink, M.H.M., van Berkel, W.J.H. and Schreuder, H.A., (1997b) Identification of a novel conserved sequence motif in flavoprotein hydroxylases with a putative dual function in FAD/NAD (P) H binding. *Protein Science*, 6(11), 2454–2458.

- Fuenmayor, S.L., Wild, M., Boyes, A.L. and Williams, P.A., (1998) A gene cluster encoding steps in conversion of naphthalene to gentisate in *Pseudomonas* sp. strain U2. *Journal of Bacteriology*, 180(9), 2522–2530.
- Gao, X., Tan, C.L., Yeo, C.C. and Poh, C.L., (2005) Molecular and biochemical characterization of the *xlnD*-encoded 3-hydroxybenzoate 6-hydroxylase involved in the degradation of 2,5-xyleneol via the gentisate pathway in *Pseudomonas alcaligenes* NCIMB 9867. *Journal of Bacteriology*, 187(22), 7696–7702.
- Ge, L. and Seah, S.Y.K., (2006) Heterologous expression, purification, and characterization of an l-ornithine N(5)-hydroxylase involved in pyoverdine siderophore biosynthesis in *Pseudomonas aeruginosa*. *Journal of Bacteriology*, 188(20), 7205–7210.
- Giessen, T.W., Kraas, F.I. and Marahiel, M.A., (2011) A four-enzyme pathway for 3,5-dihydroxy-4-methylanthranilic acid formation and incorporation into the antitumor antibiotic sibiromycin. *Biochemistry*, 50(25), 5680–5692.
- Grund, E., Denecke, B. and Eichenlaub, R., (1992) Naphthalene degradation via salicylate and gentisate by *Rhodococcus* sp. strain B4. *Applied and Environmental Microbiology*, 58(6), 1874–1877.
- Hammann, R. and Kutzner, H.J., (1998) Key enzymes for the degradation of benzoate, *m*- and *p*-hydroxybenzoate by some members of the order *Actinomycetales*. *Journal of Basic Microbiology*, 38(3), 207–220.
- Harwood, C.S. and Parales, R.E., (1996) The beta-ketoadipate pathway and the biology of self-identity. *Annual Reviews in Microbiology*, 50, 553–590.
- Hirohito, T., Fujiwara, S., Hosokawa, K. and Yamaguchi, H., (2006) Crystal structure of 3-hydroxybenzoate hydroxylase from *Comamonas testosteroni* has a large tunnel for substrate and oxygen access to the active site. *Journal of Molecular Biology*, 364(5), 878–896.
- Holesova, Z., Jakubkova, M., Zavadikova, I., Zeman, I., Tomaska, L. and Nosek, J., (2011) Gentisate and 3-oxoadipate pathways in the yeast *Candida parapsilosis*: identification and functional analysis of the genes coding for 3-hydroxybenzoate 6-hydroxylase and 4-hydroxybenzoate 1-hydroxylase. *Microbiology*, 157(Pt 7), 2152–2163.
- Hoshino, Y., Fujii, S., Shinonaga, H., Arai, K., Saito, F., Fukai, T., Satoh, H., Miyazaki, Y. and Ishikawa, J., (2010) Monoxygenation of rifampicin catalyzed by the *rox* gene product of *Nocardia farcinica*: structure elucidation, gene identification and role in drug resistance. *Journal of Antibiotics*, 63(1), 23–28.
- Huang, N.L., Itoh, K., Miyamoto, M., Suyama, K. and Yamamoto, H., (2007) Chlorophenol hydroxylase activity encoded by TfdB from 2,4-dichlorophenoxyacetic acid (2,4-D)-degrading *Bradyrhizobium* sp. strain RD5-C2. *Bioscience, Biotechnology, and Biochemistry*, 71(7), 1691–1696.
- Ishiyama, D., Vujaklija, D. and Davies, J., (2004) Novel pathway of salicylate degradation by *Streptomyces* sp. strain WA46. *Applied and Environmental Microbiology*, 70(3), 1297–1306.
- Jeon, C.O., Park, M., Ro, H.-S., Park, W. and Madsen, E.L., (2006) The naphthalene catabolic (*nag*) genes of *Polaromonas naphthalenivorans* CJ2: evolutionary implications for two gene clusters and novel regulatory control. *Applied and Environmental Microbiology*, 72(2), 1086–1095.
- Jiménez, J.L., Canales, A., Jiménez Barbero, J., Ginalski, K., Rychlewski, L., García, J.L. and Díaz, E., (2008) Deciphering the genetic determinants for aerobic nicotinic acid degradation: the nic cluster from *Pseudomonas putida* KT2440. *Proceedings of the National Academy of Sciences of the United States of America*, 105(32), 11329–11334.
- Johnson, K.A. and Goody, R.S., (2011) The original Michaelis constant: translation of the 1913 Michaelis–Menten paper. *Biochemistry*, 50(39), 8264–8269.
- Kallio, P., Liu, Z., Mäntsälä, P., Niemi, J. and Metsä-Ketelä, M., (2008) Sequential action of two flavoenzymes, PgaE and PgaM, in angucycline biosynthesis: chemoenzymatic synthesis of gaudimycin C. *Chemistry & Biology*, 15(2), 157–166.
- Laemmli, U.K., (1970) Cleavage of structural proteins during the assembly of the head of bacteriophage T4. *Nature*, 227(5259), 680–685.
- Larkin, M.J., Kulakov, L.A. and Allen, C.C.R., (2005) Biodegradation and *Rhodococcus*—masters of catabolic versatility. *Current Opinion in Biotechnology*, 16(3), 282–290.
- Larkin, M.J., Kulakov, L.A. and Allen, C.C.R., (2006) Biodegradation by members of the genus *Rhodococcus*: biochemistry, physiology, and genetic adaptation. *Advances in applied microbiology*, 59, 1–29.
- Lindqvist, Y., Koskineniemi, H., Jansson, A., Sandalova, T., Schnell, R., Liu, Z., Mäntsälä, P., Niemi, J. and Schneider, G., (2009) Structural basis for substrate recognition and specificity in aklavinone-11-hydroxylase from rhodomycin biosynthesis. *Journal of Molecular Biology*, 393(4), 966–977.
- Liu, T.-T., Xu, Y., Liu, H., Luo, S., Yin, Y.-J., Liu, S.-J. and Zhou, N.Y., (2010) Functional characterization of a gene cluster involved in gentisate catabolism in *Rhodococcus* sp. strain NCIMB 12038. *Applied Microbiology and Biotechnology*, 90(2), 671–678.
- Macheroux, P., Kappes, B. and Ealick, S.E., (2011) Flavogenomics—a genomic and structural view of flavin-dependent proteins. *FEBS Journal*, 278(15), 2625–2634.
- Martinková, L., Uhnáková, B., Pátek, M., Nešvera, J. and Křen, V., (2009) Biodegradation potential of the genus *Rhodococcus*. *Environment international*, 35(1), 162–177.
- Mayfield, J.A., Frederick, R.E., Streit, B.R., Wenciewicz, T.A., Ballou, D.P. and DuBois, J.L., (2010) Comprehensive spectroscopic, steady state, and transient kinetic studies of a representative siderophore-associated flavin monoxygenase. *Journal of Biological Chemistry*, 285(40), 30375–30388.
- McLeod, M.P., Warren, R.L., Hsiao, W.W.L., et al., (2006) The complete genome of *Rhodococcus* sp. RHA1 provides insights into a catabolic powerhouse. *Proceedings of the National Academy of Sciences of the United States of America*, 103(42), 15582–15587.
- Meneely, K.M. and Lamb, A.L., (2007) Biochemical characterization of a flavin adenine dinucleotide-dependent monoxygenase, ornithine hydroxylase from *Pseudomonas aeruginosa*, suggests a novel reaction mechanism. *Biochemistry*, 46(42), 11930–11937.
- Meneely, K.M., Barr, E.W., Bollinger, J.M. and Lamb, A.L., (2009) Kinetic mechanism of ornithine hydroxylase (PvdA) from *Pseudomonas aeruginosa*: substrate triggering of O<sub>2</sub> addition but not flavin reduction. *Biochemistry*, 48(20), 4371–4376.
- Nakano, H., Wieser, M., Hurh, B., Kawai, T., Yoshida, T., Yamane, T. and Nagasawa, T., (1999) Purification, characterization and



- gene cloning of 6-hydroxynicotinate 3-monooxygenase from *Pseudomonas fluorescens* TN5. *European journal of biochemistry*, 260(1), 120–126.
- Olucha, J. and Lamb, A.L.**, (2011) Mechanistic and structural studies of the *N*-hydroxylating flavoprotein monooxygenases. *Bioorganic Chemistry*, 39(5-6), 171–177.
- Park, M., Jeon, Y., Jang, H.H., Ro, H.-S., Park, W., Madsen, E.L. and Jeon, C.O.**, (2007) Molecular and biochemical characterization of 3-hydroxybenzoate 6-hydroxylase from *Polaromonas naphthalenivorans* CJ2. *Applied and Environmental Microbiology*, 73(16), 5146–5152.
- Phale, P.S., Basu, A., Majhi, P.D., Deveryshetty, J., Vamsee-Krishna, C. and Shrivastava, R.**, (2007) Metabolic diversity in bacterial degradation of aromatic compounds. *Omics : a journal of integrative biology*, 11(3), 252–279.
- Powell, J.A. and Archer, J.A.**, (1998) Molecular characterisation of a *Rhodococcus ohp* operon. *Antonie van Leeuwenhoek*, 74(1-3), 175–188.
- Ryan, K.S., Howard-Jones, A.R., Hamill, M.J., Elliott, S.J., Walsh, C.T. and Drennan, C.L.**, (2007) Crystallographic trapping in the rebeccamycin biosynthetic enzyme RebC. *Proceedings of the National Academy of Sciences of the United States of America*, 104(39), 15311–15316.
- Schühle, K., Jahn, M., Ghisla, S. and Fuchs, G.**, (2001) Two similar gene clusters coding for enzymes of a new type of aerobic 2-aminobenzoate (anthranilate) metabolism in the bacterium *Azoarcus evansii*. *Journal of Bacteriology*, 183(18), 5268–5278.
- Shen, X.-H., Jiang, C.-Y., Huang, Y., Liu, Z.-P. and Liu, S.-J.**, (2005) Functional identification of novel genes involved in the glutathione-independent gentisate pathway in *Corynebacterium glutamicum*. *Applied and Environmental Microbiology*, 71(7), 3442–3452.
- Steennis, P.J., Cordes, M.M., Hilken, J.H. and Muller, F.**, (1973) On the interaction of *para*-hydroxybenzoate hydroxylase from *Pseudomonas fluorescens* with halogen ions. *FEBS Letters*, 36(2), 177.
- Suárez, M., Ferrer, E., Garrido-Pertierra, A. and Martín, M.**, (1995) Purification and characterization of the 3-hydroxybenzoate 6-hydroxylase from *Klebsiella pneumoniae*. *FEMS Microbiology Letters*, 126(3), 283–290. Available at: <http://onlinelibrary.wiley.com/doi/10.1111/j.1574-6968.1995.tb07431.x/abstract>.
- Szolkowy, C., Eltis, L.D., Bruce, N.C. and Grogan, G.**, (2009) Insights into sequence-activity relationships amongst Baeyer-Villiger monooxygenases as revealed by the intragenomic complement of enzymes from *Rhodococcus jostii* RHA1. *ChemBioChem*, 10(7), 1208–1217.
- Thompson, J.D., Higgins, D.G. and Gibson, T.J.**, (1994) CLUSTAL W: improving the sensitivity of progressive multiple sequence alignment through sequence weighting, position-specific gap penalties and weight matrix choice. *Nucleic Acids Research*, 22(22), 4673–4680.
- Torres Pazmiño, D.E., Dudek, H.M. and Fraaije, M.W.**, (2010) Baeyer-Villiger monooxygenases: recent advances and future challenges. *Current Opinion in Chemical Biology*, 14(2), 138–144.
- van Berkel, W.J.H. and Muller, F.**, (1991) Flavin-dependent monooxygenases with special reference to *p*-hydroxybenzoate hydroxylase. *Chemistry and Biochemistry of Flavoenzymes 2*, 2–29.
- van Berkel, W.J.H. and Tweel, W.J.J.**, (1991) Purification and characterisation of 3-hydroxyphenylacetate 6-hydroxylase: a novel FAD-dependent monooxygenase from a *Flavobacterium* species. *European journal of biochemistry*, 201(3), 585–592.
- van Berkel, W.J.H., Kamerbeek, N.M. and Fraaije, M.W.**, (2006) Flavoprotein monooxygenases, a diverse class of oxidative biocatalysts. *Journal of Biotechnology*, 124(4), 670–689.
- Volkers, G., Palm, G.J., Weiss, M.S., Wright, G.D. and Hinrichs, W.**, (2011) Structural basis for a new tetracycline resistance mechanism relying on the TetX monooxygenase. *FEBS Letters*, 585(7), 1061–1066.
- Wierenga, R.K., Terpstra, P. and Hol, W.G.**, (1986) Prediction of the occurrence of the ADP-binding beta alpha beta-fold in proteins, using an amino acid sequence fingerprint. *Journal of Molecular Biology*, 187(1), 101–107.
- Wijnands, R.A., van der Zee, J., Van Leeuwen, J.W., van Berkel, W.J. and Muller, F.**, (1984) The importance of monopole-monopole and monopole-dipole interactions on the binding of NADPH and NADPH analogues to *p*-hydroxybenzoate hydroxylase from *Pseudomonas fluorescens*. *European journal of biochemistry*, 139(3), 637–644.
- Yang, Y.-F., Zhang, J.-J., Wang, S.-H. and Zhou, N.-Y.**, (2010) Purification and characterization of the ncgl2923 -encoded 3-hydroxybenzoate 6-hydroxylase from *Corynebacterium glutamicum*. *Journal of Basic Microbiology*, 50(6), 599–604.
- Zhou, N.Y., Al-Dulayymi, J., Baird, M.S. and Williams, P.A.**, (2002) Salicylate 5-hydroxylase from *Ralstonia* sp. strain U2: a monooxygenase with close relationships to and shared electron transport proteins with naphthalene dioxygenase. *Journal of Bacteriology*, 184(6), 1547–1555.



**Crystal structure of  
the flavoprotein monooxygenase  
3-hydroxybenzoate 6-hydroxylase:  
identification of a mysterious guest**

Stefania Montersino<sup>1</sup>, Roberto Orrú<sup>2</sup>, Arjan Barendregt<sup>3</sup>, Esther van Duijn<sup>3</sup>,  
Andrea Mattevi<sup>2</sup> and Willem J. H. van Berkel<sup>1</sup>

<sup>1</sup> Laboratory of Biochemistry, Wageningen University,  
Dreijenlaan 3, 6703 HA Wageningen, The Netherlands

<sup>2</sup> Department of Genetics and Microbiology, University of Pavia,  
Via Ferrata 1, 27100 Pavia, Italy

<sup>3</sup> Biomolecular Mass Spectrometry and Proteomics Group,  
Bijvoet Centre for Biomolecular Research, Utrecht University,  
Padualaan 8, 3584 CH Utrecht, The Netherlands

## Abstract

3-Hydroxybenzoate hydroxylase (3HB6H) from *Rhodococcus jostii* RHA1 is a soluble flavoprotein that catalyzes the NADH and oxygen dependent *para*-hydroxylation of 3-hydroxybenzoate to 2,5-dihydroxybenzoate. In this study, we report the crystal structure of *R. jostii* 3HB6H, as expressed in *Escherichia coli*. The overall fold of 3HB6H is similar to that of *p*-hydroxybenzoate hydroxylase (PHBH) and other flavoprotein aromatic hydroxylases. The isoalloxazine ring of the FAD cofactor is located *in* the active site. 3HB6H crystallizes in the substrate-free form, and co-crystallized chloride ions give a hint about possible substrate and oxygen binding sites.

Unexpectedly, a lipid ligand is bound to each 3HB6H monomer at the dimerization interface. ESI-MS identifies the lipid guest as a mixture of phosphatidylglycerol (PG) and phosphatidylethanolamine (PE), the major lipid components of the *E. coli* membrane. PE and PG binding might stabilize the 3HB6H dimer.

The 3HB6H structure opens new avenues for the investigation of the structural basis of the regioselectivity of hydroxylation of flavoprotein aromatic hydroxylases.

4

**Keywords:** crystal structure, flavoprotein, gentisate, hydroxylase, monooxygenase, phospholipid, *Rhodococcus*.

## Introduction

Flavoprotein aromatic hydroxylases are involved in diverse biological processes, ranging from lignin degradation to the synthesis of polyketides antibiotics (van Berkel *et al.*, 2006; Montersino *et al.*, 2011). They perform regioselective *ortho*- or *para*-hydroxylation reactions on a narrow subset of substrates with a tight regulated oxygen and coenzyme consumption (Palfey and McDonald, 2010). The reaction cycle of flavoprotein hydroxylases consists of two half-reactions according to the redox state of the flavin. In the reductive half-reaction, the oxidized flavin of the enzyme-substrate complex gets reduced by NAD(P)H. The oxidative half-reaction involves the reaction of reduced FAD with oxygen, the hydroxylation of the substrate and the reoxidation of the flavin.

Most biochemically characterized flavoprotein hydroxylases act on monophenols. Members with known structure include *p*-hydroxybenzoate hydroxylase (PHBH) (Schreuder *et al.*, 1989), phenol hydroxylase (PHHY) (Enroth *et al.*, 1998) and 3-hydroxybenzoate 4-hydroxylase (3HB4H) (Hiromoto *et al.*, 2006). More recently, structural and biochemical data have become available about flavoprotein hydroxylases that are active with pyridines (Treiber and Schulz, 2008; McCulloch *et al.*, 2009), phenazines (Greenhagen *et al.*, 2008), and polyketides (Koskiniemi *et al.*, 2007; Ryan *et al.*, 2007; Lindqvist *et al.*, 2009; Volkens *et al.*, 2011).

The actinomycete *R. jostii* RHA1 is a rich source of flavoprotein hydroxylases (Montersino and van Berkel, 2012). One of these enzymes, 3-hydroxybenzoate 6-hydroxylase (3HB6H), participates in the gentisate pathway where it catalyzes the *para*-hydroxylation of 3-hydroxybenzoate to gentisate (Fig.1). We found that *R. jostii* 3HB6H is a dimeric flavoprotein with each subunit containing a tightly non-covalently bound FAD. 3HB6H uses NADH as electron donor and has narrow substrate specificity. Besides 3-hydroxybenzoate, the enzyme converts a limited number of 3-hydroxybenzoate analogs to the corresponding gentisates (Montersino and van Berkel, 2012).

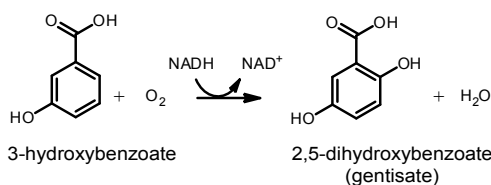


**Figure 1. Reaction catalyzed by 3-hydroxybenzoate 6-hydroxylase (3HB6H).**

3-hydroxypyridine-5-carboxylic acid oxygenase (MHPCO) (McCulloch *et al.*, 2009), phenazine-1-carboxylate hydroxylase (PhzS) (Greenhagen *et al.*, 2008), and 2,6-dihydroxypyridine hydroxylase (DHPH) (Treiber and Schulz, 2008).

Here we present the 3HB6H crystal structure and the identification of a natively bound phospholipid molecule. The structural analysis reveals that 3HB6H shares a common three-domain fold with other flavoprotein aromatic hydroxylases and that the overall architecture is closest to that of 2-methyl-

## Materials And Methods

**Chemicals.** Aromatic compounds were purchased from Sigma-Aldrich (St Louis, MO, USA) and Acros Organics (New Jersey, US). All other chemicals were from commercial sources and of the purest grade available. Crystallization kits were purchased from New Hampton (Aliso Viejo, CA).

**Protein Production.** 3HB6H from *R. jostii* RHA1 was expressed in *E. coli* and purified as C-terminal His<sub>6</sub>-tag protein as described previously (Monterisino and van Berkel, 2012).

**Crystallization And Structure Determination.** Crystals for structure determination were obtained by the sitting drop vapour diffusion method at 20 °C by mixing equal volumes (2 µL) of protein and reservoir solutions. Protein solutions consisted of 30 mg enzyme/ml in 1 mM FAD, 2 mM 3-hydroxybenzoate, and 50 mM Bis-Tris (pH 7.2), whereas precipitant solutions consisted of 28% PEG 4000, 0.2 M sodium acetate, and 0.1 M Tris-HCl (pH 8.5). Yellow crystals grew in one day. For data collection, a platinum derivative was obtained by soaking the crystals for 16 h in 20 µl reservoir solution containing 0.5 mM of K<sub>2</sub>Pt(NO<sub>2</sub>)<sub>4</sub> dissolved in DMSO.

X-ray diffraction data were collected at D14eh4 in the European Synchrotron Radiation Facility (Grenoble, France) and processed with the CCP4 package (Collaborative Computational Project, Number 4, 1994). The structure was solved by the single-wavelength anomalous dispersion (SAD) method by using the pipeline SHELX C/D/E (Sheldrick, 2010) and ARP/wARP for the model building (Langer *et al.*, 2008), refined with REFMAC5 (Murshudov *et al.*, 1997) and COOT (Emsley *et al.*, 2010). Pictures were generated with the program Pymol (DeLano, 2010) and CCP4mg (Potterton *et al.*, 2004). Data collection parameters and final refinement statistics are listed in Table 1.

**Analytical Methods.** Protein concentrations of purified enzyme were determined by measuring the absorption of protein-bound FAD at 453 nm ( $\epsilon_{453} = 10.3 \text{ mM}^{-1} \text{ cm}^{-1}$ ) (Monterisino and van Berkel, 2012).

**Apoprotein Preparation.** Release of flavin from 3HB6H was achieved by metal-chelating affinity chromatography (Hefti *et al.*, 2003). 3HB6H His<sub>6</sub>-tagged protein (4 mg) was bound to a 1 ml Ni-affinity column (HisGraviTrap, GE Healthcare Bioscience AB, Uppsala, Sweden) in 100 mM HEPES (pH 8.0), containing 0.2 M NaCl. After equilibrating, the column was washed with twenty volumes of the same buffer, containing 1 M urea and 2 M KBr. Apoprotein was collected by elution with 300 mM imidazole in starting buffer. The collected fractions were desalted and analyzed for 3HB6H activity in the absence and presence of FAD.

**ESI-MS Experiments.** For nanoflow ESI-MS analysis under native conditions, enzyme samples were prepared in 50 mM ammonium acetate (pH 6.8). For analysis under denaturing conditions, enzyme samples were diluted either in 50% acetonitrile with 0.2% formic acid or in 5% formic acid. Analysis was performed on a LC-T nanoflow ESI orthogonal TOF mass spectrometer (Micromass, Manchester, UK), equipped with a Z-spray nano-electrospray ionization source. All measurements were performed by operating in the positive ion mode and by using gold-coated needles, made with borosilicate glass capillaries (Kwik-Fill; World precision Instruments, Sarasota) on a P-97 puller (from Sutter Instruments, Novato). The needles were coated with a gold layer, which was performed by an Edwards Scancoat six Pirani 501 sputter coater (Edwards laboratories, Milpitas). Mass spectra were recorded with a capillary voltage of 1.2 kV and cone voltage of 70 V. The source pressure was raised to 6.8 mbar (Tahallah *et al.*, 2001), and the pressure in the ToF was 10<sup>-6</sup> mbar. All spectra were mass calibrated by using an aqueous solution of cesium iodide (25 mg/mL).

**Lipid Identification.** Identification of protein-bound lipid was performed as follows: extraction of lipid was achieved by mixing 100 µl buffer exchanged protein solution (50 mM ammonium acetate pH 6.8) with chloroform:methanol:sample (8:4:3) in a glass reaction tube. Once phase separation was reached, chloroform phase was extracted by Pasteur pipette and collected in a new reaction tube. Evaporation of the organic phase was done by flushing with nitrogen gas, and dry sample was dissolved in 15 µl isopropanol and analyzed.

## Results

### Structural Properties Of 3HB6H.

The structure of 3HB6H was solved at 1.55 Å resolution using SAD phasing (Table 1). The final model of the 3HB6H monomer (Fig.2A) contains one molecule of FAD, five chloride ions and a phospholipid ligand-like molecule (*vide infra*). All protein residues (except the N-terminal 1-2 and C-terminal 25 residues containing a spacer and the His<sub>6</sub>-tag) have well defined ordered conformations. 3HB6H is composed of 14  $\alpha$ -helices and 16  $\beta$ -sheets organized in three domains: the FAD binding domain (green, residues 1-73 and 94-175), the substrate binding domain (red, residues 74-93 and 176-302), composed of six  $\beta$ -sheets and four  $\alpha$ -helices, and the dimerization domain (blue, residues 303-398), built along four  $\alpha$ -helices.

The three-dimensional structure of 3HB6H is similar to that of PHBH and other flavoprotein hydroxylases (van Berkel *et al.*, 2006; Montersino *et al.*, 2011). A DALI structural homologue search (Table 2) reveals that the overall architecture of 3HB6H is closest to that of MHPCO (McCulloch *et al.*, 2009), PhzS (Greenhagen *et al.*, 2008) and DPHH (Treiber and Schulz, 2008). Despite a relatively low sequence identity (14-26 %), most part of the protein can be structurally aligned (Fig.3). Some flavin-dependent hydroxylases contain a thioredoxin-like domain with yet unknown function (Koskiniemi *et al.*, 2007), therefore in some cases 100-200 amino acids near the C-terminus do not align with 3HB6H.

**FAD Binding Domain.** The FAD binding domain contains a Rossmann fold for binding the ADP moiety of the cofactor. The isoalloxazine ring of FAD is located in the interior of the protein at the interface between the FAD and substrate binding domains. FAD contacts around thirty residues along the polypeptide chain (Fig.3 yellow dots and Fig.4A), resulting in a tight protein-cofactor interaction. One third of the protein-FAD contacts are strictly conserved among flavoprotein hydroxylases and cluster around the three fingerprint sequences (Eppink *et al.*, 1997).

For PHBH it was observed that the isoalloxazine ring of FAD occupies different

**Table 1. Crystallographic data collection and refinement statistics.**

	Pt soaking	Wild-type
Unit cell (Å)	$a=b=106.65$ $c=142.25$	$a=b=106.78$ $c=142.67$
Space group	$I4_122$	$I4_122$
Resolution (Å)	1.59	1.55
$R_{\text{sym}}^{\text{a,b}}$ (%)	5.8 (28.1)	9.1 (48.4)
Completeness <sup>b</sup> (%)	100 (99.9)	99.2 (99.4)
Unique reflections	55136	59071
Redundancy <sup>b</sup>	9.1 (6.8)	3.6 (3.6)
$I/\sigma^{\text{b}}$	21.6 (5.7)	8.7 (2.5)
N° of atoms	3423	3467
Average $B$ value (Å <sup>2</sup> )	18.4	18.2
$R_{\text{cryst}}^{\text{c}}$ (%)	19.2	20.2
$R_{\text{free}}^{\text{c}}$ (%)	22.3	23.8
Rms bond length (Å)	0.014	0.014
Rms bond angles (°)	1.6	1.6

<sup>a</sup>  $R_{\text{sym}} = \sum |I_i - \langle I \rangle| / \sum I_i$ , where  $I_i$  is the intensity of  $i^{\text{th}}$  observation and  $\langle I \rangle$  is the mean intensity of the reflection.

<sup>b</sup> Values in parentheses are for reflections in the highest

<sup>c</sup>  $R_{\text{cryst}} = \sum |F_{\text{obs}} - F_{\text{calc}}| / \sum F_{\text{obs}}$ , where  $F_{\text{obs}}$  and  $F_{\text{calc}}$  are observed and calculated structure factor amplitudes, respectively.  $R_{\text{cryst}}$  and  $R_{\text{free}}$  were calculated using the working and test set, respectively.

4



conformations *in* and *out* of the active site (Entsch and van Berkel, 1995; Entsch *et al.*, 2005): the *out* conformation is suitable for flavin reduction, the *in* conformation ensures proper hydroxylation during the oxidative half reaction, and the *open* conformation allows substrate/product binding and release. In 3HB6H, the flavin ring has a well defined electron density and was refined with full occupancy with the *in* conformation (Fig.4A), similarly to the FAD conformation of the uncomplexed forms of MHPCO and DHPH.

Earlier studies with PHBH have indicated that the FAD domain plays a crucial role in NADPH binding (Eppink *et al.*, 1998; Wang *et al.*, 2002) and that a small helix near the protein surface is the key determinant for the coenzyme specificity (Eppink *et al.*, 1999; Montersino *et al.*, 2008). This surface helix is absent in 3HB6H, providing no clue for the NADH preference of the enzyme.

**Table 2. DALI alignment.**

PDB	Z-score <sup>a</sup>	RSDM	lali <sup>b</sup>	nres <sup>c</sup>	%id <sup>d</sup>	Name
3ALL	39.8	2.5	345	371	23	MHPCO
3C96	39	2.2	340	381	26	PhzS
2VOU	37.1	2.6	349	393	21	DHPH
1D7L	34.7	3	352	394	14	PHBH
2Y6Q	34.3	3.2	344	368	15	TetX2
2X3N	33.5	3.1	342	364	20	FAD-dependent monooxygenase
3IHG	32	3.1	350	535	15	Aklavinone 11-hydroxylase
3E1T	31.7	3.2	344	437	17	CndH halogenase
3FMW	31.6	3.2	348	489	20	MtmOIV
3NIX	31.6	3.1	348	407	15	Flavoprotein dehydrogenase
2DKI	31.4	3.3	342	615	17	3HB4H
1FOH	30.5	3.1	357	656	14	PHHY

<sup>a</sup> Calculated on DALI server on 11 october 2011 (Holm and Rosenström, 2010)

<sup>b</sup> Number of aligned positions

<sup>c</sup> Number of residues in matched structure

<sup>d</sup> Sequence identity of aligned positions

**Substrate Binding Domain.** The substrate binding domain of 3HB6H is composed mainly of  $\beta$ -sheets and four surface-exposed  $\alpha$ -helices (Fig.2A). The secondary structure of the domain is conserved among flavoprotein hydroxylases, but not the primary sequence (Fig.3). The last twenty amino acids of the substrate domain are conserved among structural aligned hydroxylases. This region contains the GD fingerprint sequence involved in dual binding of NAD(P)H and FAD (Eppink *et al.*, 1997).

The active site of 3HB6H is formed by residues of the FAD and substrate binding domain. A clear homology with other hydroxylases is not evident, likely because each family member needs its own architecture to ensure proper substrate binding. Structural comparison between PHBH and 3HB6H presents a *re*-side of the flavin where chloride binding takes place and a *si*-side of the flavin less structurally constrained. Instead of

the conserved PHBH loop containing Arg45 in direct contact with the isoalloxazine ring (Entsch *et al.*, 2005), 3HB6H possesses a short  $\beta$ -sheet (residues 47-50) with a structurally aligned Leu48. Although 3HB6H crystals were prepared with excess 3-hydroxybenzoate in the crystallization drop, no electron density for the aromatic substrate is found in the active site (Fig.4B).

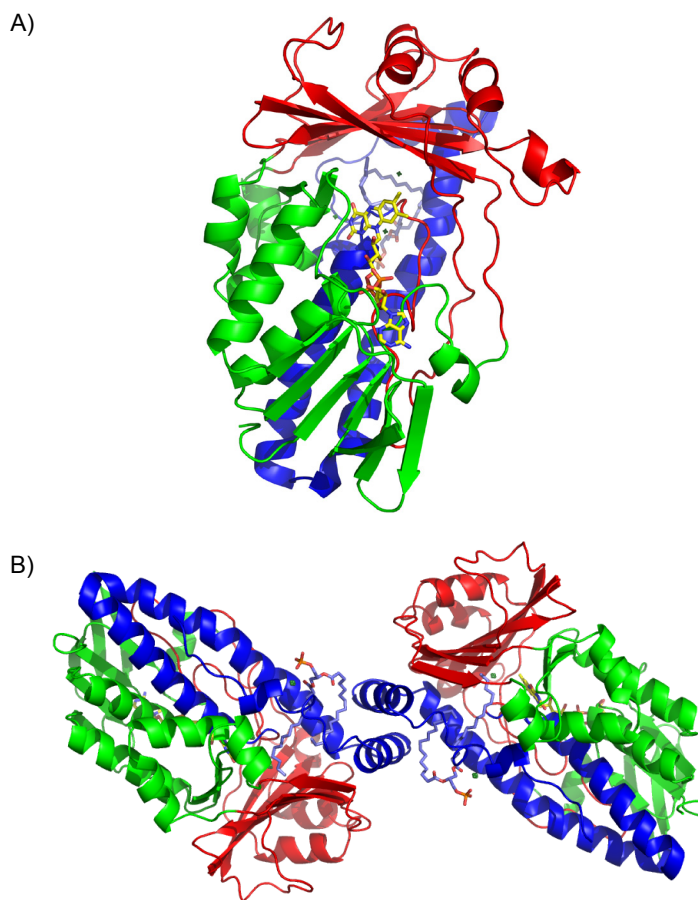


**Figure 2. 3HB6H native structure and domain organization.** A) Schematic view of the monomer and B) dimer of 3HB6H. FAD binding domain is depicted in green, substrate binding domain in red and dimerization domain in blue. FAD is shown as a stick model in yellow. Lipid ligand is shown as a stick model in blue.

**Dimerization Domain.** 3HB6H is a dimer, both in solution (Montersino and van Berkel, 2012) and in crystal form. In the crystal structure, the active sites are facing opposite direction and the two subunits are oriented antiparallel to each other (Fig.2B). Among the structurally related proteins, PHBH shows the most similar dimer association.

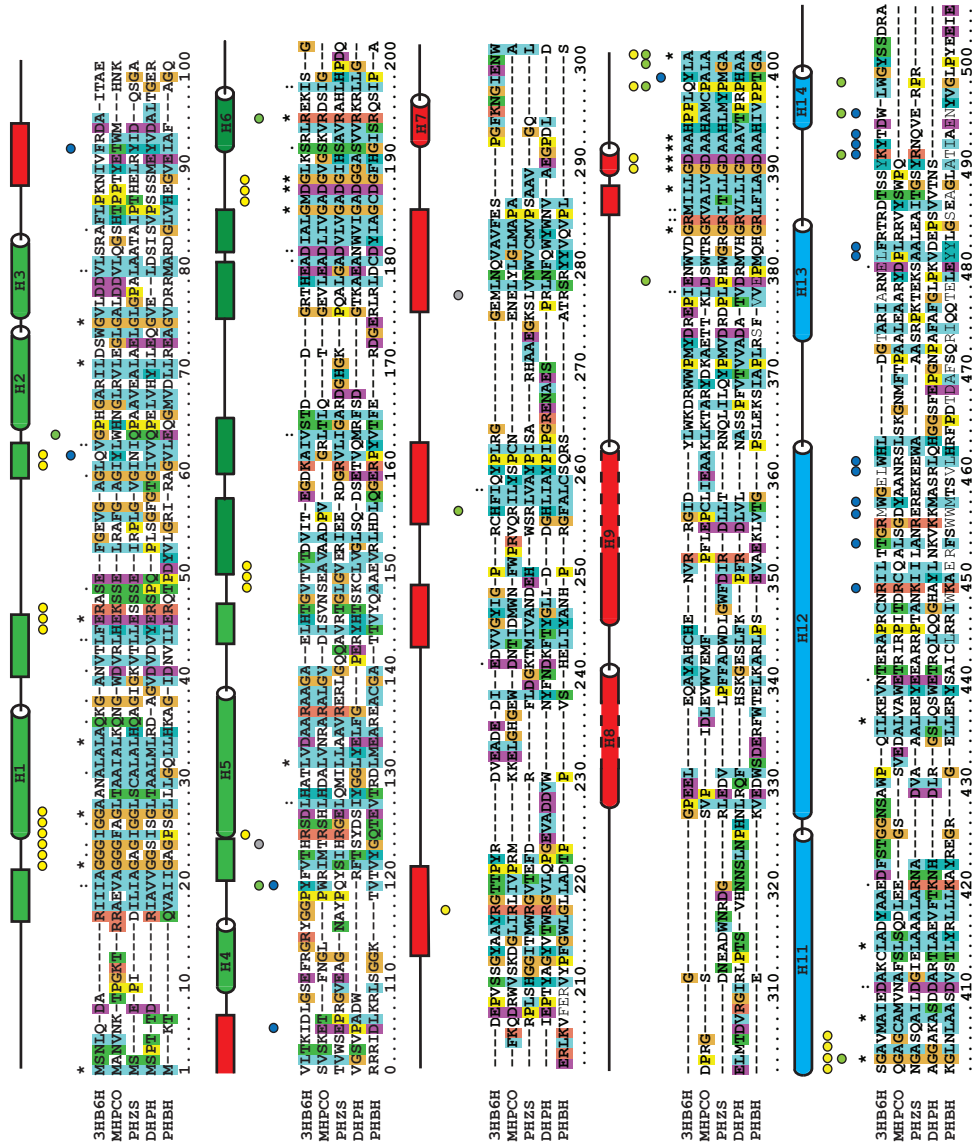


**Figure 3.** Structure-based sequence alignment of flavoprotein aromatic hydroxylases. From top: 3HB6H, MHPCO (PDB: 3ALL), PHZS (PDB: 3C96), DHPH (PDB: 2VOU) and PHBH (PDB: 1D7L). Structural alignment was done by STRAP (Gille and Frömmel, 2001) and edited in CLUSTALW (Thompson *et al.*, 1994). Secondary structure elements of 3HB6H are indicated above the alignment, and coloured according to the respective domain. Residues involved in direct FAD contact (yellow dots), chloride and platinum contact (green and grey dots) and lipid contact (blue dots) are indicated. 3HB6H and PHBH residues involved in dimerization are in regular font. Shading of amino acid residues depends on their chemical characteristics

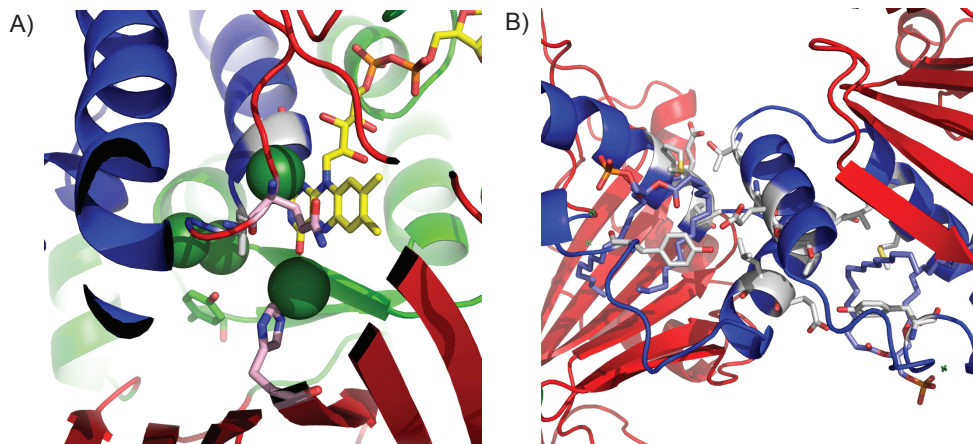


**Figure 4. 3HB6H domains.** A) Substrate binding pocket B) Dimerization domain. Chlorides are represented in green spheres and amino acid residues involved in chloride binding and dimerization are depicted in sticks.

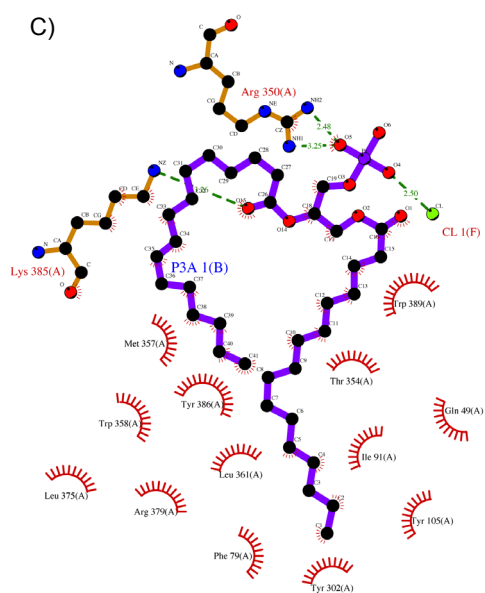
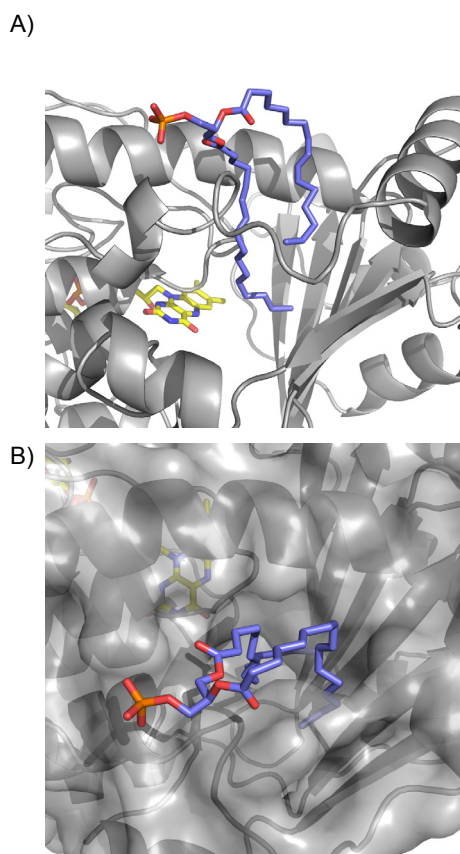


**Figure 5. Lipid binding to 3HB6H.** A) Lipid insertion B) Tunnel surface C) Maps of protein-lipid interactions.

PHBH uses several helices to form a hydrophobic dimerization interface with few important salt bridges (Weijer *et al.*, 1983; Montersino *et al.*, 2008). The 3HB6H dimerization domain shows the same secondary structure organization. Compared to PHBH, less contacts are formed among monomers and dimer interactions occur *via* H12H13\*, H13H13\* (Fig.4C), and *via* the tightly bound lipid molecule (*vide infra*).

**Ion And Metal Binding.** Platinum atoms interacting with Met224 and His109 on the protein surface permitted phase solving. Both native and Pt-soaked crystals contain chloride ions in the active site interacting with Gly51, Tyr105, His213, Gln301, Ala304 and Gly306. The presence of these anions on the flavin *re*-side (Fig.4B) might give a hint about the orientation of the aromatic substrate and the oxygen binding site.

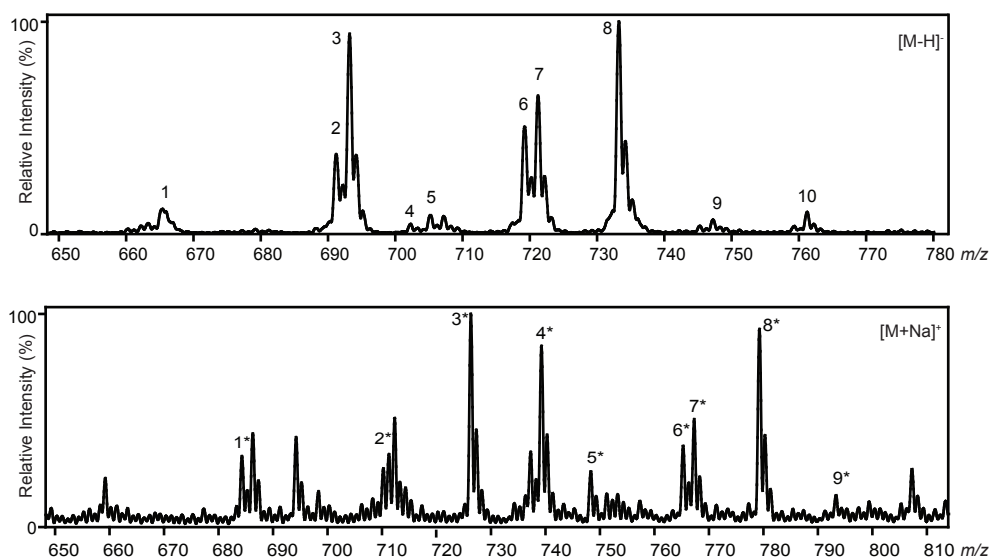


**Figure 6. Lipids extraction and identification.** ESI-MS spectrum in negative (top) and positive (bottom) mode, in the mass range 600–800 m/z. Identification of the numbered peaks is listed in Table 3.

**Lipid Binding And Identification.** Electron density of a lipid-like ligand was observed both in the native and Pt-derivative 3HB6H data set (Fig.5A). Tentatively, a phospholipid with two chains of sixteen carbons was modelled on the basis of the electron density (Fig.5A). The lipid guest is inserted in a tunnel, which runs from the protein surface to the active site (Fig.5B). In the tunnel, the lipid contacts hydrophobic and aliphatic residues (Fig.3 and Fig.5C). Some interaction occurs between the phospholipid and the opposite monomer (Fig.5), moreover, at the surface, the phosphate group resides with the same occupancy in two opposite positions stabilized by Arg350 and Lys385 (Fig.5). From the crystal structure the exact identity of the phospholipid is difficult to assign, as the density of the head group is poorly defined.

Detailed assignment of the phospholipid was achieved by mass spectral analysis of the low molecular weight components extracted from denatured 3HB6H. The mass spectrum (Fig.6) showed four main peaks with  $m/z$  values of 693, 719, 721 and 733 (Fig.6 3,6-8) in the negative mode, and three main peaks in the positive mode with  $m/z$  values of 726, 739 and 779, respectively (Fig.6 3\*,4\*,8\*). Fragmentation analysis and comparison with *E. coli* lipids MS spectra (Pulfer and Murphy, 2003; Oursel *et al.*, 2007; Fahy *et al.*, 2009; Fahy *et al.*, 2011) led to the matching of the mass peaks with either phosphatidylglycerol (PG) or phosphatidylethanolamine (PE) with aliphatic chains ranging from 14 to 19 carbons (Table 3). PGs were visible both in negative and positive mode as complexes with two sodium molecules, while PEs in the positive mode mostly were found in complex with one sodium ion.

**Table 3. Lipids identification.**

	$m/z$	[M-H] <sup>-</sup>	Abbreviation	
	1	665	PG C14:0/C14:0	
	2	691	PG C14:0/C16:1	
	3	693	PG C14:0/C14:0	
	4	702	PE C16:0/cyC17:0	
	5	705	PG C14:0/cyC17:0	
[M-H] <sup>-</sup>	6	719	PG C15:0/C16:1 PG C14:0/C18:1 PG C15:0/cyC17:0 PG C16:0/C16:1	
	7	721	PG C16:0/C16:0	
	8	733	PG C16:0/cyC17:0	
	9	747	PG C16:0/C18:1	
	10	761	PG C16:0/cyC19:0	
	1*	684	Na n.d.	PE C14:0/C16:1 (661)
	2*	711	2Na	1
	3*	726	Na	4
	4*	739	2Na	3
[M+Na] <sup>+</sup>	5*	748	2Na	4
	6*	765	2Na	6
	7*	767	2Na	7
	8*	779	2Na	8
	9*	793	2Na	9

**Protein Oligomeric Composition.** To understand the abundance of the interaction between 3HB6H and bound phospholipid, we determined the 3HB6H oligomeric composition using mass spectrometry (Fig.7). The experimental mass of denatured 3HB6H ( $46766 \pm 4$  Da) agreed with the primary sequence lacking the N-terminal methionine (Table 4 and Fig.7A). Native MS showed five major charge state distributions (Fig.7A) present in different ratio. The first charge state distribution (Fig.7A, red triangle) represents the apoprotein ( $46835 \pm 5$  Da). Two charge state distributions are similar to the molecular mass of the apo-3HB6H monomer



**Table 4. Determination of 3HB6H oligomeric state by ESI-MS**

Peak	<i>m/z</i>	Average mass Da	$\Delta$ mass Da	Intensity %
1	3603	46835 $\pm$ 5		7 <sup>c</sup>
2	3663	47603 $\pm$ 6	767 <sup>a</sup>	15 <sup>c</sup>
3	3717	48312 $\pm$ 7	1477 <sup>a</sup>	16 <sup>c</sup>
4	5048	95868 $\pm$ 16	2198 <sup>b</sup>	28 <sup>d</sup>
5	5088	96643 $\pm$ 14	2973 <sup>b</sup>	72 <sup>d</sup>

<sup>a</sup> calculated using apo-3HB6H monomer (peak 1)

<sup>b</sup> calculated using apo-3HB6H dimer (2  $\times$  peak 1 93671 Da)

<sup>c</sup> based on 12+, 13+ and 14+ charge state distribution ions

<sup>d</sup> based on 17+, 18+, 19+, 20+ and 21+ charge state distribution ions

(Fig. 7A, green and blue triangle), and two charge state distributions are similar to the apo-3HB6H dimer mass (Fig. 7A, orange and yellow triangle).

Mass increase is due to the presence of the cofactor FAD (783 Da) and/or the presence of PG/PE molecules (average mass 712 Da). Tandem MS experiments revealed that one, two, three, and four ligands can be expelled from 3HB6H, but due to peak broadening and similar molecular mass, ligand identification was difficult (data not shown). An assignment

of ligands was made on the basis of total mass increase and comparison with native oligomeric composition of apo-3HB6H and reconstituted-3HB6H (data not shown). The first monomer species corresponds to the holo-3HB6H monomer (47603  $\pm$  6 Da).

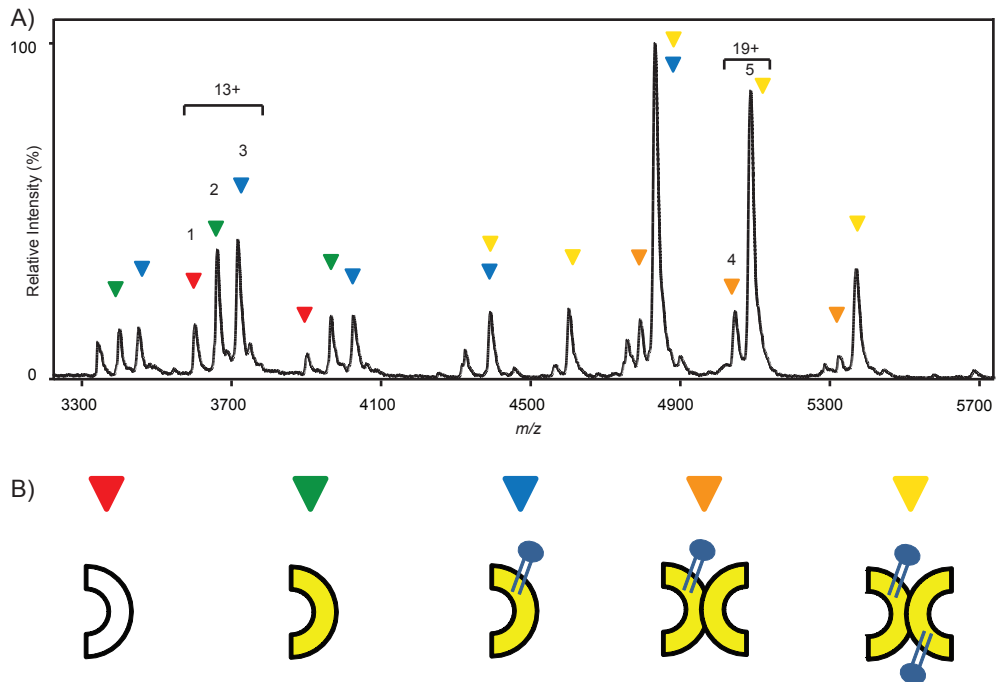


**Figure 7. 3HB6H oligomeric composition as determined by native ESI-MS. A)** Mass spectrum in 50 mM ammonium acetate (pH 6.8). **B)** 3HB6H subunit composition. Mass and intensity of numbered peaks are listed in Table 4. Apoprotein is indicated in white, holoprotein in yellow and lipid molecules in blue sticks.



The second monomer species ( $48312 \pm 7$  Da) contains two ligands assigned as FAD and PG/PE. The two dimeric species are holo-3HB6H dimer with PG/PE bound to one subunit ( $95868 \pm 16$  Da) and holo-3HB6H dimer with PG/PE bound to both subunits ( $96643 \pm 14$  Da) (Table 4 and Fig. 7B).

## Discussion

3HB6H crystal structure reveals that the enzyme possesses many characteristic features of single-component flavoprotein aromatic hydroxylases: the overall structure and domain organization are conserved and around 25 residues are identical among structurally related proteins. Most of these conserved residues belong to the FAD binding domain, with a special conservation cluster in the region of the GD fingerprint. This short amino acid sequence motif is involved in the binding of the pyrophosphate moieties of FAD and NAD(P)H and is specific for flavoprotein hydroxylases (Eppink *et al.*, 1997). Flavoprotein hydroxylases show poor sequence conservation in their substrate binding sites, despite a conserved  $\beta$ -sheet secondary structure organization. This explains the strict substrate specificity and lack of substrate promiscuity of these enzymes. Each hydroxylase requires a specific active site architecture to orient the substrate in a suitable position for either *ortho*- or *para*-hydroxylation. Possibly, each regioselectivity shares a pattern of residues not yet evident, but more apparent by the fact that structural alignment gave a top list score to *para*-hydroxylases regardless the type of substrate involved.

No electron density for bound substrate was observed in the 3HB6H structure, despite soaking and co-crystallization with 3-hydroxybenzoate. Instead, three chloride ions were found in the active site of the native structure. One chloride ion interacts with His213, another with Tyr105 and the third chloride ion, present also in Pt-soaked crystals, is localized on top of FAD facing the *re*-side of the isoalloxazine ring. Based on the available space (and the active sites of other flavoprotein hydroxylases), this chloride binding pocket likely represents the substrate binding site. Chloride anions could mimic the hydroxyl and carboxyl group of the substrate and the oxygen binding site.

Many flavoprotein hydroxylases are inhibited by chloride ions (van Berkel and Muller, 1991; van Berkel and Tweel, 1991). Studies with PHBH showed a competitive mode of inhibition with respect to NADPH and a non-competitive or mixed-type inhibition with respect to the physiological substrate 4-hydroxybenzoate (Steennis *et al.*, 1973). 3HB6H shows mixed-type inhibition with respect to the substrate as well (data not shown).

A key requirement for the action of flavoprotein hydroxylases is the stabilization of the C4a-hydroperoxyflavin oxygenating species (Palfey and McDonald, 2010). Studies of oxygen diffusion of phenylacetate monooxygenase C2 component revealed that a small hydrophobic cavity near flavin C4a constitutes the oxygen binding site

(Baron *et al.*, 2009). Chloride in the 3HB6H native and Pt-soaked structure shows the same position as oxygen on top of the flavin with 4 Å distance to flavin C4a. Pro299, Ala304, Gly306 and the carbon chain of Glu301 could form a possible oxygen binding cavity. Moreover, the anion is positioned in front of the N-terminus of H11 with possible helix dipole stabilization (Wierenga *et al.*, 1979; Schreuder *et al.*, 1989).

Intriguingly, a non-covalently bound phospholipid molecule was found in each monomer of 3HB6H in the crystallographic model. The fatty acid chains occupy hydrophobic channels that penetrate deep into the interior of the substrate-binding domain of each subunit, while the hydrophilic portion of the molecule exposes out of the protein surface, connecting the dimerization domains *via* few interactions. Any attempt to delipidate the protein by using beads (Crawford *et al.*, 2009), detergents or by reversible unfolding failed. Soaking the FAD-reduced enzyme with substrate as shown for 6-hydroxy-L-nicotine oxidase (Kachalova *et al.*, 2010) was also not successful.

Mass spectrometry identification of bound phospholipid revealed the presence of two phospholipid species (PG and PE) with carbon chains varying from 14 to 19 carbon atoms. PG and PE are the major components of the *E. coli* membrane, and their presence correlates with other MS analysis (Oursel *et al.*, 2007). From the crystal structure, determination of the exact nature of the bound phospholipid is not possible, since the head group is not visible. We therefore refer to PG/PE as the phospholipid bound to the enzyme with an average mass of 712 Da. From the kinks present in the modelled aliphatic chain of PG/PE, we assumed that each C16 chain contains one double bond although from MS/MS identification it seems more reasonable that only one fatty acid chain is unsaturated.

According to native ESI-MS, PG/PE is natively bound to 3HB6H either to one or two monomers of the dimeric enzyme in 1:3 ratio. 40% of the protein in the gas phase splits into a small fraction of apoprotein and monomers with two different *m/z* values. Since the two peaks have equal intensity, and a mass difference corresponding to approximately 700 Da, we conclude that they originate from the 3HB6H dimers containing only one PG/PE bound. Summing up, the ratio between fully saturated PG/PE dimers and dimers that contain one PG/PE molecule is about 1:1.

Protein-bound phospholipids with a regulatory role have been described in different enzyme systems (Forneris and Mattevi, 2008). Cytochrome *bc*<sub>1</sub> complex (Lange *et al.*, 2001), pyruvate oxidase (Neumann *et al.*, 2008; Bertagnolli and Hager, 1991) and  $\beta$ -hydroxysteroid dehydrogenase (Rajapaksha *et al.*, 2011) are just a few examples in which binding of lipids lead to enzyme activation. In 3HB6H, PE/PG binding seems to have no influence on the binding of substrates and cofactors. The enzyme behaves as a homogeneous competent hydroxylase in kinetic studies (Sucharitakul *et al.*, 2012). The protein microheterogeneity is only detectable by native MS, since the enzyme elutes as single peak in gel filtration and ionic exchange chromatography (Montersino and van Berkel, 2012). Fully saturated PG/PE 3HB6H is more stable in the gas phase

and prone to crystallize. As shown in the crystal structure model, 3HB6H presents a different dimerization interface than PHBH, despite similar secondary structure organization. Most of the hydrophobic residues involved in PHBH dimerization are not conserved in 3HB6H and the few protein-protein interactions are primarily made by H13 contacts. We hypothesize that PG/PE functions as glue, promoting and stabilizing dimer formation. 3HB6H dimers containing only one PG/PE bound are less stable in the gas phase and easier to split in monomers than 3HB6H dimers containing two PG/PE molecules. Phospholipid contribution to dimer stability has been proposed for 6-hydroxy-L-nicotine oxidase (6HNLO) (Kachalova *et al.*, 2010), a flavoprotein oxidase containing a similar phospholipid bound at the interface between the monomers. Further investigations are required to assess a possible role of PE/PG binding to 3HB6H.

In conclusion, the 3HB6H crystal structure presents the first three-dimensional model of flavin-dependent *para*-hydroxylase acting on hydroxybenzoic compounds. The 3HB6H structure reveals close similarity in domain architecture and topology to other flavoprotein hydroxylases. Although 3HB6H crystallizes only in the free-state, the structure might disclose new insight in substrate binding and regioselective hydroxylation of flavoprotein monooxygenases.

## Acknowledgments

We are grateful to Stefano Rovida for assistance during crystallization screening experiments. This study was supported by the Integrated Biosynthesis Organic Synthesis (IBOS) project of the Netherlands Organization for Scientific Research (NWO).

## References

- Baron, R., Riley, C., Chenprakhon, P., et al., (2009) Multiple pathways guide oxygen diffusion into flavoenzyme active sites. *Proceedings of the National Academy of Sciences of the United States of America*, 106(26), 10603–10608.
- Bertagnolli, B.L. and Hager, L.P., (1991) Minimum requirements for protease activation of flavin pyruvate oxidase. *Biochemistry*, 30(33), 8131–8137.
- Collaborative Computational Project, Number 4, (1994) The CCP4 suite: programs for protein crystallography. *Acta crystallographica. Section D, Biological crystallography*, 50(5), 760–763.
- Crawford, J.M., Korman, T.P., Labonte, J.W., Vagstad, A.L., Hill, E.A., Kamari-Bidkorpheh, O., Tsai, S.-C. and Townsend, C.A., (2009) Structural basis for biosynthetic programming of fungal aromatic polyketide cyclization. *Nature*, 461(7267), 1139–1143.
- DeLano, W.L., (2010) The PyMOL Molecular Graphics System, Version 1.3r1 L. Schroedinger, ed.
- Emsley, P., Lohkamp, B., Scott, W.G. and Cowtan, K., (2010) Features and development of Coot. *Acta crystallographica. Section D, Biological crystallography*, 66(Pt 4), 486–501.
- Enroth, C., Neujahr, H., Schneider, G. and Lindqvist, Y., (1998) The crystal structure of phenol hydroxylase in complex with FAD and phenol provides evidence for a concerted conformational change in the enzyme and its cofactor during catalysis. *Structure (London, England : 1993)*, 6(5), 605–617.
- Entsch, B. and van Berkel, W.J.H., (1995) Structure and mechanism of *para*-hydroxybenzoate hydroxylase. *FASEB Journal*, 9(7), 476–483.
- Entsch, B., Cole, L.J. and Ballou, D.P., (2005) Protein dynamics and electrostatics in the function of *p*-hydroxybenzoate hydroxylase. *Archives of Biochemistry and Biophysics*, 433(1), 297–311.
- Eppink, M.H., Overkamp, K.M., Schreuder, H.A. and van Berkel, W.J.H., (1999) Switch of coenzyme specificity of *p*-hydroxybenzoate hydroxylase. *Journal of Molecular Biology*, 292(1), 87–96.

- Eppink, M.H.M., Schreuder, H.A. and van Berkel, W.J.H., (1998) Interdomain binding of NADPH in *p*-hydroxybenzoate hydroxylase as suggested by kinetic, crystallographic and modeling studies of histidine 162 and arginine 269 variants. *Journal of Biological Chemistry*, 273(33), 21031–21039.
- Eppink, M.H.M., van Berkel, W.J.H. and Schreuder, H.A., (1997) Identification of a novel conserved sequence motif in flavoprotein hydroxylases with a putative dual function in FAD/NAD (P) H binding. *Protein Science*, 6(11), 2454–2458.
- Fahy, E., Cotter, D., Sud, M. and Subramaniam, S., (2011) Lipid classification, structures and tools. *Biochimica et Biophysica Acta*, 1811(11), 637–647.
- Fahy, E., Subramaniam, S., Murphy, R.C., et al., (2009) Update of the LIPID MAPS comprehensive classification system for lipids. *Journal of Lipid Research*, 50 Suppl, S9–14.
- Fornieris, F. and Mattevi, A., (2008) Enzymes without borders: mobilizing substrates, delivering products. *Science*, 321(5886), 213–216.
- Gille, C. and Frömmel, C., (2001) STRAP: editor for STRuctural Alignments of Proteins. *Bioinformatics*, 17(4), 377–378.
- Greenhagen, B.T., Shi, K., Robinson, H., Gamage, S., Bera, A.K., Ladner, J.E. and Parsons, J.F., (2008) Crystal structure of the pyocyanin biosynthetic protein PhzS. *Biochemistry*, 47(19), 5281–5289.
- Hefti, M.H., Milder, F.J., Boeren, S., Vervoort, J. and van Berkel, W.J.H., (2003) A His-tag based immobilization method for the preparation and reconstitution of apoflavoproteins. *Biochimica et Biophysica Acta*, 1619(2), 139–143.
- Hiromoto, T., Fujiwara, S., Hosokawa, K. and Yamaguchi, H., (2006) Crystal structure of 3-hydroxybenzoate hydroxylase from *Comamonas testosteroni* has a large tunnel for substrate and oxygen access to the active site. *Journal of Molecular Biology*, 364(5), 878–896.
- Holm, L. and Rosenström, P., (2010) Dali server: conservation mapping in 3D. *Nucleic Acids Research*, 38(Web Server issue), W545–9.
- Kachalova, G.S., Bourenkov, G.P., Mengesdorf, T., Schenk, S., Maun, H.R., Burghammer, M., Riekel, C., Decker, K. and Bartunik, H.D., (2010) Crystal structure analysis of free and substrate-bound 6-hydroxy-L-nicotine oxidase from *Arthrobacter nicotinovorans*. *Journal of Molecular Biology*, 396(3), 785–799.
- Koskiniemi, H., Metsä-Ketelä, M., Dobritzsch, D., Kallio, P., Korhonen, H., Mäntsälä, P., Schneider, G. and Niemi, J., (2007) Crystal structures of two aromatic hydroxylases involved in the early tailoring steps of angucycline biosynthesis. *Journal of Molecular Biology*, 372(3), 633–648.
- Lange, C., Nett, J.H., Trumpower, B.L. and Hunte, C., (2001) Specific roles of protein-phospholipid interactions in the yeast cytochrome bc<sub>1</sub> complex structure. *EMBO Journal*, 20(23), 6591–6600.
- Langer, G., Cohen, S.X., Lamzin, V.S. and Perrakis, A., (2008) Automated macromolecular model building for X-ray crystallography using ARP/wARP version 7. *Nature Protocols*, 3(7), 1171–1179.
- Lindqvist, Y., Koskiniemi, H., Jansson, A., Sandalova, T., Schnell, R., Liu, Z., Mäntsälä, P., Niemi, J. and Schneider, G., (2009) Structural basis for substrate recognition and specificity in aklavinone-11-hydroxylase from rhodomycin biosynthesis. *Journal of Molecular Biology*, 393(4), 966–977.
- McCulloch, K.M., Mukherjee, T., Begley, T.P. and Ealick, S.E., (2009) Structure of the PLP degradative enzyme 2-methyl-3-hydroxypyridine-5-carboxylic acid oxygenase from *Mesorhizobium loti* MAFF303099 and its mechanistic implications. *Biochemistry*, 48(19), 4139–4149.
- Montersino, S. and van Berkel, W.J.H., (2012) Functional annotation and characterization of 3-hydroxybenzoate 6-hydroxylase from *Rhodococcus jostii* RHA1. *Biochimica et Biophysica Acta*, 1824(3), 433–442.
- Montersino, S., Golovleva, L., Schlömann, M. and van Berkel, W.J.H., (2008) Another look at *p*-hydroxybenzoate hydroxylase. In S Frago, C Gómez-Moreno, M Medina, eds, *Flavins and Flavoprotein 2008*. Prensas Universitarias de Zaragoza, Zaragoza, pp. 51–56.
- Montersino, S., Tischler, D., Gassner, G.T. and van Berkel, W.J.H., (2011) Catalytic and structural features of flavoprotein hydroxylases and epoxidases. *Advanced Synthesis & Catalysis*, 353(13), 2301–2319.
- Murshudov, G.N., Vagin, A.A. and Dodson, E.J., (1997) Refinement of Macromolecular Structures by the Maximum-Likelihood Method. *Acta Crystallographica. Section D. Biological Crystallography*, 53(3), 240–255.
- Neumann, P., Weidner, A., Pech, A., Stubbs, M.T. and Tittmann, K., (2008) Structural basis for membrane binding and catalytic activation of the peripheral membrane enzyme pyruvate oxidase from *Escherichia coli*. *Proceedings of the National Academy of Sciences of the United States of America*, 105(45), 17390–17395.
- Oursel, D., Loutelier-Bourhis, C., Orange, N., Chevalier, S., Norris, V. and Lange, C.M., (2007) Lipid composition of membranes of *Escherichia coli* by liquid chromatography/tandem mass spectrometry using negative electrospray ionization. *Rapid Communications in Mass Spectrometry*, 21(11), 1721–1728.
- Palfey, B.A. and McDonald, C.A., (2010) Control of catalysis in flavin-dependent monooxygenases. *Archives of Biochemistry and Biophysics*, 493(1), 26–36.
- Potterton, L., McNicholas, S., Krissinel, E., et al., (2004) Developments in the CCP4 molecular-graphics project. *Acta Crystallographica. Section D. Biological Crystallography*, 60(Pt 12 Pt 1), 2288–2294.
- Pulfer, M. and Murphy, R.C., (2003) Electrospray mass spectrometry of phospholipids. *Mass Spectrometry Reviews*, 22(5), 332–364.
- Rajapaksha, M., Thomas, J.L., Streeter, M., Prasad, M., Whittal, R.M., Bell, J.D. and Bose, H.S., (2011) Lipid-mediated unfolding of 3 $\beta$ -hydroxysteroid dehydrogenase 2 is essential for steroidogenic activity. *Biochemistry*, 50(51), 11015–11024.
- Ryan, K.S., Howard-Jones, A.R., Hamill, M.J., Elliott, S.J., Walsh, C.T. and Drennan, C.L., (2007) Crystallographic trapping in the rebecamycin biosynthetic enzyme RebC. *Proceedings of the National Academy of Sciences of the United States of America*, 104(39), 15311–15316.
- Schreuder, H.A., Prick, P.A., Wierenga, R.K., Vriend, G., Wilson, K.S., Hol, W.G. and Drenth, J., (1989) Crystal structure of the *p*-hydroxybenzoate hydroxylase-substrate complex refined at 1.9 Å resolution. Analysis of the enzyme-substrate and enzyme-

- product complexes. *Journal of Molecular Biology*, 208(4), 679–696.
- Sheldrick, G.M.**, (2010) Experimental phasing with SHELXC/D/E: combining chain tracing with density modification. *Acta crystallographica. Section D, Biological crystallography*, 66(Pt 4), 479–485.
- Steennis, P.J., Cordes, M.M., Hilkens, J.H. and Muller, F.**, (1973) On the interaction of *para*-hydroxybenzoate hydroxylase from *Pseudomonas fluorescens* with halogen ions. *FEBS Letters*, 36(2), 177.
- Sucharitakul, J., Wongnate, T., Montersino, S., van Berkel, W.J.H. and Chaiyen, P.**, (2012) Reduction kinetics of 3-hydroxybenzoate 6-hydroxylase from *Rhodococcus jostii* RHA1. *Biochemistry*. dx.doi.org/10.1021/bi201823c
- Tahallah, N., Pinkse, M., Maier, C.S. and Heck, A.J.R.**, (2001) The effect of the source pressure on the abundance of ions of noncovalent protein assemblies in an electrospray ionization orthogonal time-of-flight instrument. *Rapid Communications in Mass Spectrometry*, 15(8), 596–601.
- Thompson, J.D., Higgins, D.G. and Gibson, T.J.**, (1994) CLUSTAL W: improving the sensitivity of progressive multiple sequence alignment through sequence weighting, position-specific gap penalties and weight matrix choice. *Nucleic Acids Research*, 22(22), 4673–4680.
- Treiber, N. and Schulz, G.E.**, (2008) Structure of 2,6-dihydroxypyridine 3-hydroxylase from a nicotine-degrading pathway. *Journal of Molecular Biology*, 379(1), 94–104.
- van Berkel, W.J.H. and Muller, F.**, (1991) Flavin-dependent monooxygenases with special reference to *p*-hydroxybenzoate hydroxylase. *Chemistry and Biochemistry of Flavoenzymes* 2, 2–29.
- van Berkel, W.J.H. and Tweel, W.J.J.**, (1991) Purification and characterization of 3-hydroxyphenylacetate 6-hydroxylase: a novel FAD dependent monooxygenase from a *Flavobacterium* species. *European journal of biochemistry*, 201(3), 585–592.
- van Berkel, W.J.H., Kamerbeek, N.M. and Fraaije, M.W.**, (2006) Flavoprotein monooxygenases, a diverse class of oxidative biocatalysts. *Journal of Biotechnology*, 124(4), 670–689.
- Volkers, G., Palm, G.J., Weiss, M.S., Wright, G.D. and Hinrichs, W.**, (2011) Structural basis for a new tetracycline resistance mechanism relying on the TetX monooxygenase. *FEBS Letters*, 585(7), 1061–1066.
- Wang, J., Ortiz-Maldonado, M., Entsch, B., Massey, V., Ballou, D. and Gatti, D.L.**, (2002) Protein and ligand dynamics in 4-hydroxybenzoate hydroxylase. *Proceedings of the National Academy of Sciences of the United States of America*, 99(2), 608–613.
- Weijer, W.J., Hofsteenge, J., Beintema, J.J., Wierenga, R.K. and Drenth, J.**, (1983) *p*-Hydroxybenzoate hydroxylase from *Pseudomonas fluorescens*. *European journal of biochemistry*, 133(1), 109–118.
- Wierenga, R.K., de Jong, R.J., Kalk, K.H., Hol, W.G. and Drenth, J.**, (1979) Crystal structure of *p*-hydroxybenzoate hydroxylase. *Journal of Molecular Biology*, 131(1), 55–73.



**Phosphatidylinositol is  
the natural phospholipid ligand  
of *Rhodococcus jostii* RHA1  
3-hydroxybenzoate 6-hydroxylase**

Stefania Montersino<sup>1</sup>, Eveliene te Poele<sup>2</sup>, Roberto Orrú<sup>3</sup>, Arjan Barendregt<sup>4</sup>,  
Esther van Duijn<sup>4</sup>, Robert van der Geize<sup>2</sup>, Lubbert Dijkhuizen<sup>2</sup>,  
Andrea Mattevi<sup>3</sup> and Willem J. H. van Berkel<sup>1</sup>

- <sup>1</sup> Laboratory of Biochemistry, Wageningen University,  
Dreijenlaan 3, 6703 HA Wageningen, The Netherlands
- <sup>2</sup> Department of Microbial Physiology, University of Groningen,  
Nijenborgh 7, 9747 AG Groningen, The Netherlands
- <sup>3</sup> Department of Genetics and Microbiology, University of Pavia,  
Via Ferrata 1, 27100 Pavia, Italy
- <sup>4</sup> Biomolecular Mass Spectrometry and Proteomics Group,  
Bijvoet Centre for Biomolecular Research, Utrecht University,  
Padualaan 8, 3584 CH Utrecht, The Netherlands



## Abstract

*Rhodococcus jostii* RHA1 3-hydroxybenzoate 6-hydroxylase (3HB6H) expressed in *Escherichia coli* is unique among flavoprotein hydroxylases in binding a mixture of phosphatidylglycerol and phosphatidylethanolamine, the major constituents of the *E. coli* inner membrane. To gain more insight into presence and possible role of the lipid guest, we here produced 3HB6H (3HB6H<sub>Rh</sub>) in a newly developed *R. jostii* RHA1#2 expression strain. *R. jostii* RHA1#2 produces reasonable amounts of 3HB6H<sub>Rh</sub>, opening a new scenario among Gram-positive expression systems. 3HB6H<sub>Rh</sub> possesses similar catalytic and structural properties as 3HB6H, but contains phosphatidylinositol as glycerophospholipid ligand. Lipid binding near the dimer interface stabilizes monomer contacts, but might also have a role in localizing 3HB6H at a specific spot at the plasma membrane to efficiently deal with breakdown of aromatic compounds. In conclusion, we demonstrate the intrinsic ability of 3HB6H from *R. jostii* RHA1 to bind phospholipids with different specificity according to the membrane composition of its bacterial host.

## Introduction

*Rhodococcus jostii* RHA1 is a biotechnologically and environmentally important bacterium from *Actinomycetales* order. Together with the genera *Nocardia*, *Corynebacterium* and *Mycobacterium*, *Rhodococcus* forms a distinct group of bacteria called mycolata (Chun *et al.*, 1996; Finnerty, 1992; Gürtler *et al.*, 2004), characterized by a complex cell envelope and an impressive catabolic diversity, permitting to adapt to different carbon sources (van der Geize and Dijkhuizen, 2004). In comparison with other mycolata, *R. jostii* RHA1 is particularly rich in oxygenases (203 putative genes) and ligases (192 putative genes), gained primarily through ancient gene duplications or acquisitions (McLeod *et al.*, 2006).

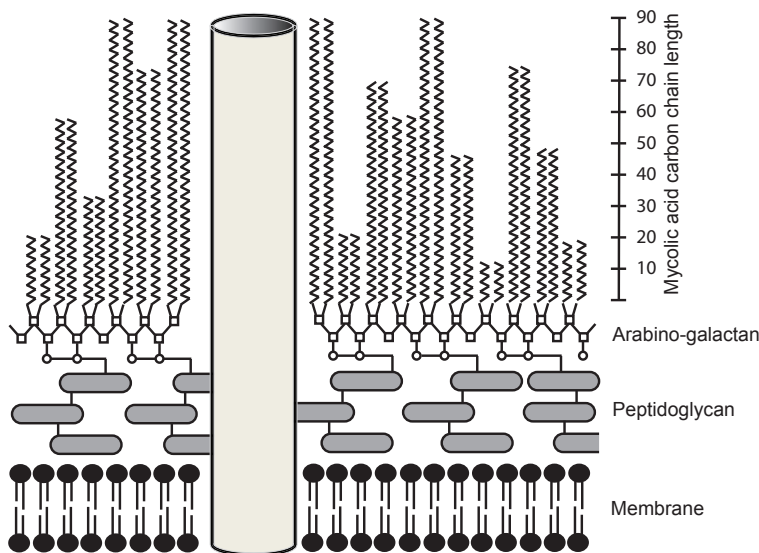


**Figure 1. Model of the cell envelope composition in mycolata (Sutcliffe, 1998).**

Mycolata exhibit a more complex cell envelope composition and organization than other Gram-positive bacteria (Fig.1) (Sutcliffe, 1998; Gürtler *et al.*, 2004). This is ascribed to the presence of mycolic acids connected to the cell wall (Hunter and Brennan, 1990; Nishiuchi *et al.*, 2000), and lipidoarabinomannans as main components of peptidoglycan (Nigou *et al.*, 2003; Guerin *et al.*, 2010). Mycolic acids confer hydrophobicity to the cell envelope and might form the basis of an outer lipid permeability barrier (Sutcliffe, 1998). Moreover, these natural biosurfactants are of commercial and biomedical interest (Lang and Philp, 1998). Lipidoarabinomannans have been studied mainly for their role in *Mycobacterium tuberculosis* and *Rhodococcus equi* virulence and immune host modulation activity (Nigou *et al.*, 2003).

The cell envelope of the genus *Rhodococcus* is composed of mycolic acids (34-52 carbons) in the "bound" form, where they are covalently linked to the cell wall matrix, and in "free" extractable form. The peptidoglycan matrix consists of *N*-acetylglucosamine, *N*-glycolylmuramic acid, D- and L-alanine, D-glutamic acid, and *meso*-diaminopimelic acid, while arabinose and galactose comprise the cell wall carbohydrates. The *Rhodococcus* membrane contains phospholipids as cardiolipin, phosphatidylethanolamine (PE), phosphatidylinositol (PI), and phosphatidylinositol mannosides esterified to saturated, unsaturated fatty and tuberculostearic acid (Finnerty, 1992; Sutcliffe, 1998).

We recently solved the structure of *R. jostii* RHA1 3-hydroxybenzoate 6-hydroxylase (3HB6H), as expressed in *Escherichia coli* (Chapter 4). 3HB6H catalyzes the *para*-hydroxylation of 3-hydroxybenzoate to 2,5-dihydroxybenzoate (gentisate). The 3HB6H structure appeared to be similar to other flavoprotein hydroxylase structures (Monterisino *et al.*, 2011), except for the binding of phospholipids at the dimer interface. The bound phospholipids were identified as a mixture of phosphatidylglycerol (PG) and PE, the major constituents of the *E. coli* inner membrane (Oursel *et al.*, 2007; Pulfer and Murphy, 2003).

3HB6H monomers interact via few residues of helices H12 and H13 and some interactions (Ile30 and Gln374) between the bound phospholipids and the opposite monomer. ESI-MS revealed that half of the native 3HB6H dimers bind only one phospholipid, while the other half binds two phospholipids. This microheterogeneity does not affect substrate binding nor enzyme activity, but causes a different stability of the 3HB6H molecules in the gas phase (Chapter 4).

Considering the different lipid composition of *R. jostii* and *E. coli*, and to gain more information about presence and possible role of the lipid guest, we here produced 3HB6H (3HB6H<sub>Rh</sub>) in a newly developed *R. jostii* RHA1#2 expression strain. We found that 3HB6H<sub>Rh</sub> possesses similar catalytic and structural characteristics compared to the *E. coli* expressed protein, but contains PI as glycerophospholipid ligand.

## Materials And Methods

**Chemicals.** Aromatic compounds were purchased from Sigma-Aldrich (St Louis, MO, USA) and Acros Organics (New Jersey, US). All other chemicals were from commercial sources and of the purest grade available. Crystallization kits were purchased from New Hampton (Aliso Viejo, CA).

**Strains.** *Escherichia coli* DH5 $\alpha$  was used as host for cloning procedures. *R. jostii* strain RHA1 #2 was used as a host for protein expression. This strain is a spontaneous mutant of *R. jostii* RHA1, carrying deletions of ~0.9 Mb on the 1.12 Mb linear plasmid pRHL1 and ~0.2 Mb on the 0.44 Mb linear plasmid pRHL2. The deletions together comprise ~11.3 % of the 9.7 Mb *R. jostii* genome (McLeod *et al.*, 2006).

**Construction Of *Rhodococcus* Overexpression Vector Q2+.** The *E. coli*-*Rhodococcus* shuttle vector pRESQ (van der Geize *et al.*, 2002) was modified by insertion of the RP4 *oriT* of pK18*mobsacB* (Schäfer *et al.*, 1994) enabling trans-conjugal transfer of the resulting vector. For this, the *oriT* region was amplified from pK18*mobsacB* by PCR (*Pfu* DNA polymerase, Fermentas; forward primer *oriT*-F 5'-CATAGTCCACGACGCCC-3', and reverse primer *oriT*-R 5'-TCTTTGGCATCGTCTCTCG-3'). The 549 bp PCR product was cloned into the *Sma*I site of pRESQ, resulting in pQmob. A duplicate region of 424 bp on pQmob was removed by deleting the 760 bp *Xba*I-*Bsp*HI fragment, yielding pQmobd. The *egfp* gene from pIJ8630 (Sun *et al.*, 1999) was amplified by PCR (High Fidelity DNA polymerase, Fermentas; forward primer *egfp*-*Pci*I-F 5'-GCACATGTCCGAGGTCC ATATGGCCATGGT-3', containing a *Pci*I restriction site, and reverse primer *egfp*-*Pci*I-R5'-GCACATGTACTTGTACAGCTCGTCCATGC-3', containing a *Pci*I restriction site). The 744 bp *Pci*I fragment containing *egfp* was cloned into the *Pci*I site of pQmobd, to generate pEGFPQ.

The *R. jostii* strain RHA1 genomic region consisting of gene *ro00440*, its promoter region and the *prmA* promoter (*PprmA*) (here referred to as region *reg1*-*PprmA*; GenBank accession number CP000431: nt 521,345-nt 523,358) was amplified from genomic DNA of *R. jostii* RHA1 by PCR using forward primer *reg1*-*Bgl*II-F 5'-GGAGATCTGACATTCGCGGATACG-3' (containing a *Bgl*II restriction site) and reverse primer *prmA*-*Nde*I-R 5'-GGCATATGTGCGCCTCCTGGATCG-3' (containing an *Nde*I restriction site). The 2,014 bp *Bgl*II-*Nde*I *reg1*-*PprmA* fragment was cloned into the *Bgl*II-*Nde*I sites of pEGFPQ, yielding prMOeGFPQ1.

The *R. jostii* RHA1 gene *ro00452* and its promoter region (here referred to as region *reg2*; CP000431: nt 534,363-nt 536,227) were amplified by PCR (*Pfu* DNA polymerase, Fermentas; *Taq* polymerase, Roche) using forward primer *reg2*-*Pci*I-F 5'-GGACATGTCCCGTCCCTCCACCACCCCGTCT-3' and reverse primer *reg2*-*Pci*I-R 5'-GGACATGTCCGGTGGGCGACGTCATATGTCG-3' (*Pci*I restriction sites underlined). The 1,880 bp PCR product was cloned into the *Pci*I-site of prMOeGFPQ1, resulting in prMOeGFPQ2.

For construction of the expression vector Q2+, the *egfp* gene of prMOeGFPQ2 was replaced with a multiple cloning site (MCS). For this, part of the MCS of pBluescriptKS- was amplified by PCR (*Pfu* DNA polymerase, Fermentas; *Taq* polymerase, Roche) using forward primer MCS-*Nde*I-F 5'-TTGCATATGCACCGCG-GTGGC-3' and reverse primer MCS-*Pci*I-R 5'-GGGAACATGTGCTGGGTACC-3' (*Nde*I and *Pci*I restriction sites underlined). The 125 bp PCR product was cloned into the *Nde*I-*Pci*I site of prMOeGFPQ2, replacing the *Nde*I-*Pci*I region containing *egfp*, to generate expression vector Q2+.

**Cloning And Expression Of 3HB6H In *R. jostii* RHA1 #2.** The 1,321 bp *Nde*I-*Xmn*I-fragment of pBAD-3HB6H-His<sub>6</sub> containing the complete 3HB6H gene was cloned into the *Nde*I-*Hind*III (Klenow-fragment treated) site of Q2+ to generate plasmid Q2+-3HB6H-His<sub>6</sub>. *Rhodococcus* cells were electroporated as described previously (Geize *et al.*, 2000). Prior to electroporation, plasmid DNA was desalted by dialyzing 10  $\mu$ l plasmid DNA for 30 min on a Millipore "V" Series filter disk (0.025 $\mu$ m) floating on milliQ water. Cultures of *R. jostii* RHA1 #2 were grown in LB broth (Sigma) supplemented

with 50  $\mu\text{g ml}^{-1}$  kanamycin at 30°C at 200 rpm. *R. jostii* RHA1 #2 cells harbouring Q2+3HB6H-His<sub>6</sub> were grown overnight in 3 ml LB broth, diluted 1:300 in 300 ml LB broth in a 3 l Erlenmeyer flask and grown for 20-24 h. Cultures were induced by adding 2 mM 4-androstene-3,17-dione (Merck, Oss, the Netherlands) dissolved in acetone. Growth was continued for 48 h after induction. Cells were harvested by centrifugation (4500 rpm; 15 min; 4°C) and pellets were washed once with ice-cold 20 mM potassium phosphate (pH 7.2), containing 300 mM NaCl.

**Protein Purification And Crystallization.** 3HB6H<sub>Rh</sub> was purified to apparent homogeneity in three chromatographic steps (Chapter 3). Approximately 3.7 mg of 3HB6H<sub>Rh</sub> was purified from 0.6 L batch culture containing 6 g of wet cells.

Crystals for structure determination were obtained by the sitting drop vapor diffusion method at 37 °C by mixing equal volumes (2  $\mu\text{L}$ ) of protein and reservoir solutions. Protein solutions consisted of 30 mg/ml enzyme in 1 mM FAD, 2 mM 3-hydroxybenzoate, and 50 mM Bis-Tris (pH 7.2), whereas precipitant solutions consisted of 30% PEG 4000, 0.2 M LiSO<sub>4</sub>, and 0.1 M Tris-HCl (pH 8.5). Yellow crystals grew in one day. X-ray diffraction data were collected at Grenoble and processed with the CCP4 package (Collaborative Computational Project, Number 4, 1994). The 3HB6H<sub>Rh</sub> structure was solved by molecular replacement using the structure of a monomer of 3HB6H as search model. Crystallographic computing and model analysis were performed with COOT (Emsley *et al.*, 2010) and programs of the CCP4 package (Collaborative Computational Project, Number 4, 1994). Pictures were generated with Pymol (DeLano, 2010) and CCP4mg (Potterton *et al.*, 2004). Data collection parameters and final refinement statistics are listed in Table 2.

**Biochemical Characterization.** The molar absorption coefficient of protein-bound FAD was determined by recording the absorption spectrum of 3HB6H<sub>Rh</sub> in the presence and absence of 0.1% (w/v) SDS, assuming a molar absorption coefficient for free FAD of 11.3 mM<sup>-1</sup> cm<sup>-1</sup> at 450 nm. Enzyme concentrations were routinely determined by measuring the absorbance at 453 nm using the molar absorption coefficient for protein-bound FAD (10.3 mM<sup>-1</sup> cm<sup>-1</sup>). 3HB6H<sub>Rh</sub> activity was assayed spectrophotometrically, by measuring NADH consumption (Montersino and van Berkel, 2012). The hydroxylation efficiency of 3HB6H<sub>Rh</sub> was determined by oxygen consumption experiments, essentially as described before (Chapter 3).

**Lipid Identification And Native ESI-MS Experiments.** Identification of protein-bound lipid was performed as follows: extraction of lipid was achieved by mixing 100  $\mu\text{l}$  buffer exchanged protein solution (50 mM ammonium acetate, pH 6.8, final concentration  $\sim 5 \mu\text{M}$ ) with chloroform:methanol:sample (8:4:3) in a glass reaction tube. Once phase separation was reached, chloroform phase was extracted by Pasteur pipette and collected in a new reaction tube. Evaporation of the organic phase was done by flushing with nitrogen gas, and dry sample was dissolved in 15  $\mu\text{l}$  isopropanol and analyzed.

For nanoflow ESI-MS analysis under native conditions, enzyme samples were prepared and analyzed as described in Chapter 4.

## Results

**Biochemical And Structural Characterization Of 3HB6H<sub>Rh</sub>.** Expression of 3HB6H from *R. jostii* RHA1 #2 (3HB6H<sub>Rh</sub>) yielded 6.2 mg/l of purified protein in the soluble fraction. During the second metal-affinity chromatography step, we noticed some unbound 3HB6H<sub>Rh</sub> during the washing step, probably due to loss of the His<sub>6</sub>-tag by protease cleavage during purification (Table 1).

3HB6H<sub>Rh</sub> displayed the same absorption spectrum with maxima at 274 nm, 383 nm and 453 nm and a shoulder at 480 nm, as 3HB6H (Chapter 3). The molar absorption coefficient of protein-bound flavin was determined to be 10.3 mM<sup>-1</sup> cm<sup>-1</sup> at 453 nm. 3HB6H<sub>Rh</sub> showed a very low NADH oxidase activity (< 1 U mg<sup>-1</sup>). The steady-state kinetic parameters were determined at 25°C in 50 mM Tris-SO<sub>4</sub> (pH 8.0). This analysis revealed that 3HB6H<sub>Rh</sub> behaves similarly as 3HB6H with 3-hydroxybenzoate ( $K_m = 35 \pm 3 \mu\text{M}$ ,  $k_{\text{cat}} = 20 \text{ s}^{-1}$ ,  $k_{\text{cat}}/K_m = 6 \times 10^5 \text{ s}^{-1} \text{ M}^{-1}$ ) as best substrate and NADH ( $K_m = 68 \pm 5 \mu\text{M}$ ,  $k_{\text{cat}} = 20 \text{ s}^{-1}$ ) as preferred coenzyme. Uncoupling of hydroxylation with 3-hydroxybenzoate is negligible, while gentisate is a good effector (data not shown), consuming NADH in H<sub>2</sub>O<sub>2</sub> production.

To investigate the lipid binding properties of 3HB6H as expressed in its original *R. jostii* host, we solved the structure of 3HB6H<sub>Rh</sub> by molecular replacement. 3HB6H<sub>Rh</sub> crystals grew in similar conditions as 3HB6H, with LiSO<sub>4</sub> present instead of sodium acetate. The 3HB6H<sub>Rh</sub> model is presented in Figure 2A. The isoalloxazine ring of FAD was refined with full occupancy of the *in* conformation. No substrate could be detected in the active site despite 2 mM 3-hydroxybenzoate being present in the crystallization drop. The protein crystallizes as a dimer as previously reported (Chapter 4), and retains the ability to bind a lipid-like molecule at the dimerization interface. Superimposition of the 3HB6H<sub>Rh</sub> and 3HB6H models showed minor deviations (RMSD= 0.217 Å) (Fig.2B)

**Table 1. Purification of 3HB6H expressed in *R. jostii* RHA1#2.**

Step	Protein (mg)	Activity (U)	Specific activity (U/mg <sup>-1</sup> )	Yield (%)
Cell extract	208	355	2	100
His <sub>6</sub> -GraviTrap	37	300	8	84
Mono-Q	16	230	14	65
His <sub>6</sub> -GraviTrap <sup>a</sup>	5.8	170	21	35

<sup>a</sup> fraction of unbound protein contained 3HB6H<sub>Rh</sub>

**Identification Of Protein-Bound Lipid Molecules.** Detailed assignment of protein-bound phospholipids was achieved by mass spectral analysis of the low molecular weight components extracted from denatured 3HB6H<sub>Rh</sub>. The mass spectrum in negative mode (Fig.3A) displayed three main peaks with m/z values of 823, 837,

and 851. From the MS pattern and the model of crystal structure it is evident that 3HB6H<sub>Rh</sub> binds another type of phospholipid than 3HB6H, with a bigger head group.

Fragmentation analysis and comparison with lipid MS spectra led to the tentative matching of the mass peaks with PI with aliphatic chains of 16 to 19 carbons (Table 2). Moreover, typical fragmentation of PI was visible in the MS/MS spectra by signature peaks at 153, 223, 241, 297 m/z representing glycerol phosphate water (153 m/z) and inositol head group fragments (Oursel *et al.*, 2007; Wenk *et al.*, 2003) (data not shown). Minor peaks at  $\pm 2$  m/z smaller than identified peaks represent the same PI, containing one unsaturated bond.

**3HB6H<sub>Rh</sub> Protein Oligomeric Composition.** To compare the abundance of interaction between 3HB6H<sub>Rh</sub> and bound phospholipids we determined the native oligomeric protein composition using mass spectrometry (Fig.4). The experimental mass of denatured 3HB6H<sub>Rh</sub> ( $46761 \pm 2$  Da) agreed with the primary sequence lacking the N-terminal methionine.

Differently than purified protein in *E. coli*, 3HB6H<sub>Rh</sub> suffers from proteolysis probably at both termini and/or small protein impurities still present in the final enzyme preparation. Native MS showed two minor and three major state distributions (Fig.4 and Table 4). Two charge state distributions are close to the molecular mass of apo-3HB6H<sub>Rh</sub> monomer (Fig.4, green and blue square), and one charge state distribution corresponds with the mass of apo-3HB6H<sub>Rh</sub> dimer (Fig.4, yellow square). One of the minor charge state distributions (3% relative abundance) (Fig.4, red square) represents the monomeric apoprotein ( $46829 \pm 1$  Da).

Mass increase in the ligand-bound state is due to the presence of the FAD cofactor (783 Da) and/or the presence of PI molecules (average mass 839 Da). An assignment of ligands was made on the basis of total mass increase and comparison with native oligomeric composition of 3HB6H (Chapter 4, Fig.7). The first monomer species (m/z 3683,  $47613 \pm 1$  Da) corresponds to holo-3HB6H monomer. A second monomer species (m/z 3728,  $48458 \pm 2$  Da) contains two ligands assigned as FAD and PI. This

**Table 2. Crystallographic data collection and refinement statistics.**

3HB6H <sub>Rh</sub>	
Unit cell (Å)	$a=b=106.94$ $c=143.33$
Space group	$I4_122$
Resolution (Å)	2.66
$R_{\text{sym}}^{\text{a,b}}$ (%)	13 (25.7)
Completeness <sup>b</sup> (%)	99.7 (100)
Unique reflections	12229
Redundancy <sup>b</sup>	7.7 (8.2)
$I/\sigma^b$	10.7 (6.3)
N° of atoms	3467
Average $B$ value (Å <sup>2</sup> )	18.3
$R_{\text{crist}}^{\text{c}}$ (%)	20.2
$R_{\text{free}}^{\text{c}}$ (%)	23.8
Rms bond length (Å)	0.014
Rms bond angles (°)	1.6

<sup>a</sup>  $R_{\text{sym}} = \sum |I_i - \langle I \rangle| / \sum I_i$ , where  $I_i$  is the intensity of  $i^{\text{th}}$  observation and  $\langle I \rangle$  is the mean intensity of the reflection.

<sup>b</sup> Values in parentheses are for reflections in the highest resolution shell.

<sup>c</sup>  $R_{\text{crist}} = \sum |F_{\text{obs}} - F_{\text{calc}}| / \sum F_{\text{obs}}$  where  $F_{\text{obs}}$  and  $F_{\text{calc}}$  are the observed and calculated structure factor amplitudes, respectively.

**Figure 2.** (Next page) **3HB6H<sub>Rh</sub> structure.** View of  $\alpha$ -carbon traces of the refined structures of 3HB6H expressed in *E. coli* (green) and 3HB6H<sub>Rh</sub> expressed in *R. jostii* RHA1#2 (red), following superposition of corresponding main chain atoms. FAD is shown as a stick model in yellow. Lipid ligand is shown as a stick model in blue in the back of the protein.



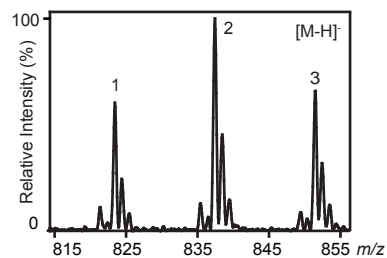
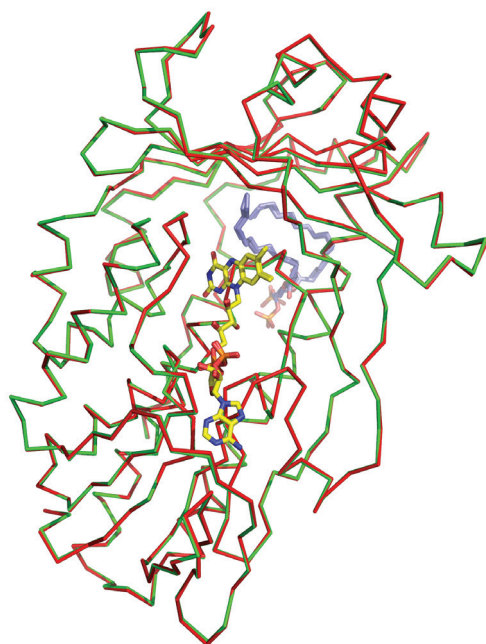
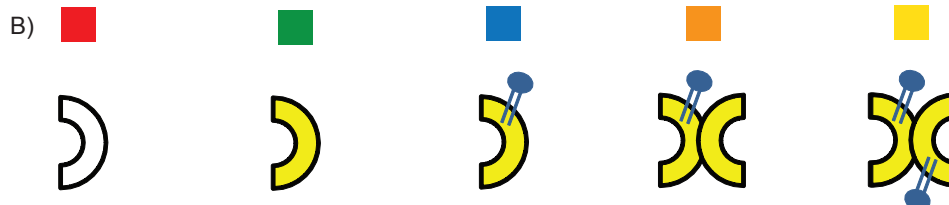
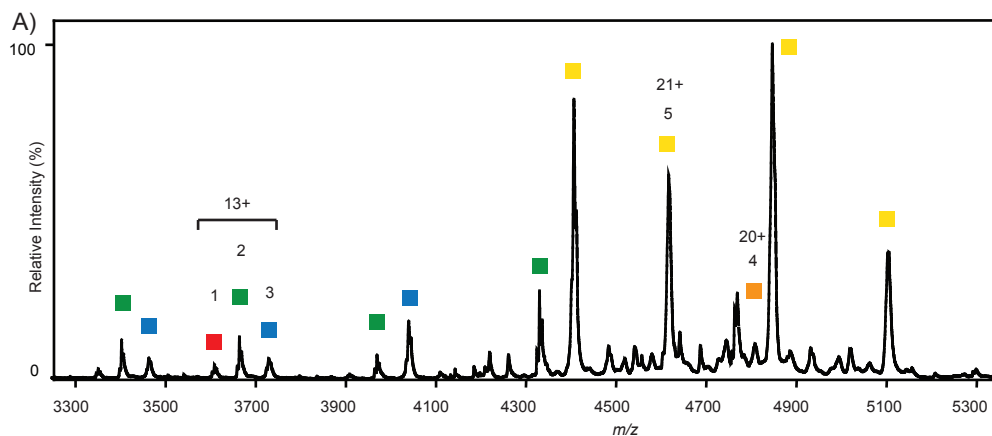


**Figure 3. 3HB6H<sub>Rh</sub> lipids extraction and identification.** ESI-MS spectrum in negative mode, in the mass range 815–855 *m/z*. Identification of the numbered peaks is listed in Table 3.

**Figure 4. 3HB6H<sub>Rh</sub> oligomer distribution and lipid composition as determined by native ESI-MS.** A) Mass spectrum in 50 mM ammonium acetate (pH 6.8). B) 3HB6H<sub>Rh</sub> subunit composition. Mass and intensity of numbered peaks are listed in Table 4. Apoprotein is indicated in white, holoprotein in yellow and lipid molecules in blue sticks.



species differs from comparable 3HB6H species (Chapter 4, Fig.7 blue triangle) for the bigger head group. The dimeric form contains only holo-3HB6H<sub>Rh</sub> dimer with PI bound to both subunits (96938 ± 32 Da), only by magnification it is possible to detect a minor peak representing the holo-3HB6H<sub>Rh</sub> dimer with one PI bound (Fig.4, orange square).

**Table 4. Determination of 3HB6H<sub>Rh</sub> oligomeric state by ESI-MS**

Peak	m/z	Average mass	Δ mass	Intensity
		Da	Da	
1	3608	46829 ± 1		3 <sup>c</sup>
2	3663	47613 ± 1	784 <sup>a</sup>	9 <sup>d</sup>
3	3728	48458 ± 2	1629 <sup>a</sup>	9 <sup>d</sup>
4	4807	96128 ± 5	2470 <sup>b</sup>	2 <sup>c</sup>
5	4616	96938 ± 32	3280 <sup>b</sup>	77 <sup>f</sup>

<sup>a</sup>calculated using apo-3HB6H monomer (peak 1)

<sup>b</sup>calculated using apo-3HB6H dimer (2 × peak 1 93658 Da)

<sup>c</sup>based on 12+, 13+ and 14+ charge state distribution ions

<sup>d</sup>based on 12+, 13+, 14+ and 15+ charge state distribution

<sup>e</sup>based on 13+ charge state distribution ions

<sup>f</sup>based on 19+, 20+, 21+ and 22+ charge state distribution ions

**Table 3. Lipids identification.**

	m/z	Abbreviation	
	1	823	PI (15:0/18:0)
[M-H] <sup>-</sup>	2	837	PI (16:0/18:0) <sup>a</sup>
	3	851	PI (16:0/19:0) <sup>b</sup>

<sup>a</sup>(Morita *et al.*, 2011; Wenk *et al.*, 2003)

<sup>b</sup>alternate acylate form (tuberculostearic acid) (Drage *et al.*, 2010)

## Discussion

# 5

The complexity of *Actinomycetes* (in particular mycolata) cell wall permits these bacteria to deal with harmful environmental conditions (Sutcliffe, 1998; Brennan and Nikaido, 1995) and specify their virulence (Drage *et al.*, 2010; Hunter and Brennan, 1990). The asymmetric, lipid-rich envelope has its similarities with the outer membranes of Gram-negative bacteria, although the specific lipid composition differs. Mycolic acids are exclusively produced by mycolata, which belong to the few bacteria able to synthesize inositol and the related glycolipid phosphatidylinositol (PI) (Guerin *et al.*, 2010; Morita *et al.*, 2011). PI is both the main membrane component (up to a quarter of total phospholipids) and the membrane anchor for glycolipids as lipidoarabinomannan (Nigou *et al.*, 2003). *E. coli*, the leading bacterial expression host, is unable to synthesize PI and its membrane is rich in PE, PG and cardiolipin (Oursel *et al.*, 2007). By solving the crystal structure of 3HB6H from *R. jostii* RHA1 as expressed in *E. coli* (Chapter 4), we found a mixture of PE and PG (32 carbons) bound at the dimerization interface. These tightly bound phospholipids do not interfere with catalysis of 3HB6H, but 3HB6H dimers containing two phospholipids seem to be more stable in the gas phase than dimers containing one phospholipid (Chapter 4).

By expressing *R. jostii* RHA1 3HB6H into the *R. jostii* RHA1#2 expression strain we wanted to unravel lipid binding abilities in the original host and compare expression and biochemical characteristics among the two expression systems. Even if 10 times less than in *E. coli*, significant quantities of homologously expressed

enzyme were obtained from the *R. jostii* RHA1 cells. Such difference could be linked to the type of induction and promoter strength used in the *R. jostii* RHA1#2 based on propane monooxygenase operon (Sharp *et al.*, 2007). Some proteolytic activity at the C-terminal His<sub>6</sub>-tag and probably N-terminus was observed during purification and native MS analysis.

3HB6H<sub>Rh</sub> showed similar catalytic properties as 3HB6H: NADH specificity, high turnover with substrate, and effector role of the gentisate. In addition, the overall structure of 3HB6H<sub>Rh</sub> was similar to that of the heterologously expressed protein in *E. coli* (RSMD deviation of 0.2 Å), also comprising a phospholipid bound at the dimerization interface.

MS analysis of extracted lipids and native 3HB6H<sub>Rh</sub> ESI-MS confirmed the presence of bound phospholipids. Based on MS/MS analysis and comparison with related MS spectra, we identified bound phospholipids as a mixture of phosphatidylinositols with carbon chains between 15 and 19 carbons. In particular, one of the identified peaks was containing tuberculostearic acid, an alternative acylated form of palmitate present in *Rhodococcus* and *Mycobacterium* (Drage *et al.*, 2010). Electron density of the phospholipid in the crystal structure was refined as two acyl chains of sixteen carbon units, but from extracted lipids only a small peak at m/z 709 could be assigned as PI (16:0/16:0).

3HB6H<sub>Rh</sub> is a dimer both in solution and in crystal form, but native MS shows a ratio of monomer to dimer of about 1:3. Binding of only one PI to the dimer resulted in monomerization in the gas phase. A similar observation was made with the binding of PG and PE to 3HB6H (Chapter 4), although in that case more dimers containing only one lipid bound were detected. The tight and specific binding of phospholipids seems to be determined only by the hydrophobic interaction between the protein and the acyl chains and not by the phospholipid head group. Moreover, 3HB6H point mutations of residues involved in phosphate interaction (K385A and K385D) did not interfere with binding of PG/PE (data not shown). This is in contrast with other recently characterized lipid-bound protein LprG in *Mycobacterium stegmatis* in which a point mutation at the portal of lipid binding pocket could impair PI binding (Drage *et al.*, 2010).

Like PG/PE in *E. coli*, PI is the major lipid membrane component in *Rhodococcus* (Morita *et al.*, 2011). This may explain why PG/PE are found as lipid ligands of 3HB6H heterologously expressed in *E. coli*, while PI is found in 3HB6H<sub>Rh</sub>. PI is the precursor for lipidoarabinomannan and phosphatidylinositol-mannoside synthesis. Glycolipid synthesis and reorganization of membrane composition allow *Rhodococcus* to adapt to environmental changes (Lang and Philp, 1998; Morita *et al.*, 2011; Guerin *et al.*, 2010). Binding of PI might localize 3HB6H at the plasma membrane, via inositol recognition of other proteins or specific phospholipid patching at the inner membrane (Morita *et al.*, 2011). At those specific spots, uptake of aromatic compounds from the environment might be coupled more efficiently to their hydroxylation in *R. jostii*

RHA1 metabolism.

Taking together, phospholipids do not have a direct catalytic role in 3HB6H, but are involved in stabilizing the dimer contact. At this stage, we cannot exclude that bound phospholipids have some other function, for instance in directing the plasma membrane localization or in guiding /protecting molecules from entering the active site.

The *R. jostii* RHA1#2 expression strain described here represents a useful alternative to available expression hosts both for purified proteins as well as whole-cell biocatalysts. Further expression trials with other representative monooxygenases from *R. jostii* RHA1 such as Baeyer-Villiger and cytochrome P450 enzymes are under study.

## References

- Brennan, P.J. and Nikaido, H., (1995) The envelope of mycobacteria. *Annual Review of Biochemistry*, 64, 29–63.
- Chun, J., Kang, S.O., Hah, Y.C. and Goodfellow, M., (1996) Phylogeny of mycolic acid-containing actinomycetes. *Journal of Industrial Microbiology & Biotechnology*, 17(3), 205–213.
- Collaborative Computational Project, Number 4, (1994) The CCP4 suite: programs for protein crystallography. *Acta crystallographica. Section D, Biological crystallography*, 50(5), 760–763.
- DeLano, W.L., (2010) The PyMOL Molecular Graphics System, Version 1.3r1 L. Schroedinger, ed.
- Drage, M.G., Tsai, H.-C., Pecora, N.D., et al., (2010) *Mycobacterium tuberculosis* lipoprotein LprG (*Rv1411c*) binds triacylated glycolipid agonists of Toll-like receptor 2. *Nature Structural & Molecular Biology*, 17(9), 1088–1095.
- Emsley, P., Lohkamp, B., Scott, W.G. and Cowtan, K., (2010) Features and development of Coot. *Acta crystallographica. Section D, Biological crystallography*, 66(Pt 4), 486–501.
- Finnerty, W.R., (1992) The biology and genetics of the genus *Rhodococcus*. *Annual Reviews in Microbiology*, 46(1), 193–218.
- Geize, R., Hessels, G., van Gerwen, R., Vrijbloed, J., van der Meijden, P. and Dijkhuizen, L., (2000) Targeted disruption of the *kstD* gene encoding a 3-ketosteroid  $\Delta 1$ -dehydrogenase isoenzyme of *Rhodococcus erythropolis* strain SQ1. *Applied and Environmental Microbiology*, 66(5), 2029–2036.
- Guerin, M.E., Korduláková, J., Alzari, P.M., Brennan, P.J. and Jackson, M., (2010) Molecular basis of phosphatidyl-*myo*-inositol mannoside biosynthesis and regulation in Mycobacteria. *Journal of Biological Chemistry*, 285(44), 33577–33583.
- Gürtler, V., Mayall, B.C. and Seviour, R., (2004) Can whole genome analysis refine the taxonomy of the genus *Rhodococcus*? *FEMS Microbiology Reviews*, 28(3), 377–403.
- Hunter, S.W. and Brennan, P.J., (1990) Evidence for the presence of a phosphatidylinositol anchor on the lipoarabinomannan and lipomannan of *Mycobacterium tuberculosis*. *Journal of Biological Chemistry*, 265(16), 9272–9279.
- Lang, S. and Philp, J.C., (1998) Surface-active lipids in rhodococci. *Antonie van Leeuwenhoek*, 74(1-3), 59–70.
- McLeod, M.P., Warren, R.L., Hsiao, W.W.L., et al., (2006) The complete genome of *Rhodococcus* sp. RHA1 provides insights into a catabolic powerhouse. *Proceedings of the National Academy of Sciences of the United States of America*, 103(42), 15582–15587.
- Montersino, S. and van Berkel, W.J.H., (2012) Functional annotation and characterization of 3-hydroxybenzoate 6-hydroxylase from *Rhodococcus jostii* RHA1. *Biochimica et biophysica acta*, 1824(3), 433–442.
- Montersino, S., Tischler, D., Gassner, G.T. and van Berkel, W.J.H., (2011) Catalytic and structural features of flavoprotein hydroxylases and epoxidases. *Advanced Synthesis & Catalysis*, 353(13), 2301–2319.
- Morita, Y.S., Fukuda, T., Sena, C.B.C., Yamaryo-Botte, Y., McConville, M.J. and Kinoshita, T., (2011) Inositol lipid metabolism in mycobacteria: biosynthesis and regulatory mechanisms. *Biochimica et biophysica acta*, 1810(6), 630–641.
- Nigou, J., Gilleron, M. and Puzo, G., (2003) Lipoarabinomannans: from structure to biosynthesis. *Biochimie*, 85(1-2), 153–166.
- Nishiuchi, Y., Baba, T. and Yano, I., (2000) Mycolic acids from *Rhodococcus*, *Gordonia*, and *Dietzia*. *Journal of microbiological methods*, 40(1), 1–9.
- Oursel, D., Loutelier-Bourhis, C., Orange, N., Chevalier, S., Norris, V. and Lange, C.M., (2007) Lipid composition of membranes of *Escherichia coli* by liquid chromatography/tandem mass spectrometry using negative electrospray ionization. *Rapid Communications in Mass Spectrometry*, 21(11), 1721–1728.
- Potterton, L., McNicholas, S., Krissinel, E., et al., (2004) Developments in the CCP4 molecular-graphics project. *Acta crystallographica. Section D, Biological crystallography*, 60(Pt 12 Pt 1), 2288–2294.
- Pulfer, M. and Murphy, R.C., (2003) Electrospray mass spectrometry of phospholipids. *Mass Spectrometry Reviews*, 22(5), 332–364.
- Schäfer, A., Tauch, A., Jäger, W., Kalinowski, J., Thierbach, G. and Pühler, A., (1994) Small mobilizable multi-purpose cloning vectors derived from the *Escherichia coli* plasmids pK18 and pK19: selection of defined deletions in the chromosome of *Corynebacterium glutamicum*. *Gene*, 145(1), 69–73.

- Sharp, J.O., Sales, C.M., LeBlanc, J.C., Liu, J., Wood, T.K., Eltis, L.D., Mohn, W.W. and Alvarez-Cohen, L., (2007) An inducible propane monooxygenase is responsible for N-nitrosodimethylamine degradation by *Rhodococcus* sp. strain RHA1. *Applied and Environmental Microbiology*, 73(21), 6930–6938.
- Sun, J., Kelemen, G.H., Fernández-Abalos, J.M. and Bibb, M.J., (1999) Green fluorescent protein as a reporter for spatial and temporal gene expression in *Streptomyces coelicolor* A3(2). *Microbiology*, 145 ( Pt 9), 2221–2227.
- Sutcliffe, I.C., (1998) Cell envelope composition and organisation in the genus *Rhodococcus*. *Antonie van Leeuwenhoek*, 74(1-3), 49–58.
- van der Geize, R. and Dijkhuizen, L., (2004) Harnessing the catabolic diversity of rhodococci for environmental and biotechnological applications. *Current opinion in microbiology*, 7(3), 255–261.
- van der Geize, R., Hessels, G.I., van Gerwen, R., van der Meijden, P. and Dijkhuizen, L., (2002) Molecular and functional characterization of *kshA* and *kshB*, encoding two components of 3-ketosteroid 9 $\alpha$ -hydroxylase, a class IA monooxygenase, in *Rhodococcus erythropolis* strain SQ1. *Molecular Microbiology*, 45(4), 1007.
- Wenk, M.R., Lucast, L., Di Paolo, G., et al., (2003) Phosphoinositide profiling in complex lipid mixtures using electrospray ionization mass spectrometry. *Nature Biotechnology*, 21(7), 813–817.



**Exploring natural diversity of  
3-hydroxybenzoate 6-hydroxylases:  
revisiting the properties of  
the enzyme from  
*Pseudomonas alcaligenes* NCIMB 9867**

Stefania Montersino<sup>1</sup>, Adrie H. Westphal<sup>1</sup> and Willem J. H. van Berkel<sup>1</sup>

<sup>1</sup> Laboratory of Biochemistry, Wageningen University,  
Dreijenlaan 3, 6703 HA Wageningen, The Netherlands



## Abstract

3-Hydroxybenzoate 6-hydroxylase (3HB6H, EC 1.13.14.26) is a flavoprotein monooxygenase that catalyzes the *para*-hydroxylation of 3-hydroxybenzoate to gentisate. Recent studies from protein crystallography and mass spectrometry revealed that each subunit of dimeric 3HB6H from *Rhodococcus jostii* RHA1 harbours a tightly bound glycerophospholipid molecule.

Here, we analysed the biochemical properties of 3HB6H from *Pseudomonas alcaligenes* NCIMB 9867 (3HB6H<sub>pa</sub>), as expressed in *Escherichia coli*. Sequence alignment highlighted amino acid substitutions in the interface domain that might be crucial for oligomerization and lipid binding. In contrast to the trimeric nature reported before, 3HB6H<sub>pa</sub> was found to be a homodimer. In common with 3HB6H from *R. jostii* RHA1, 3HB6H<sub>pa</sub> strongly binds membrane phospholipids near the dimer interface.

3HB6H<sub>pa</sub> is highly specific for NADH and shows considerable uncoupling of substrate hydroxylation. In contrast to 3HB6H from *R. jostii*, 3HB6H<sub>pa</sub> is highly active with 3-hydroxy-4-methylbenzoate and 4-hydroxybenzoate. The latter compound acts as a true non-substrate effector. The relatively high fluorescence of protein-bound FAD was used to determine the dissociation constant of the enzyme-substrate complex ( $K_d = 180 \mu\text{M}$ ).

## Introduction

3-Hydroxybenzoate 6-hydroxylase (3HB6H, EC 1.13.14.26) is a subclass A flavoprotein monooxygenase (van Berkel *et al.*, 2006) that catalyzes the pyridine nucleotide and oxygen dependent *para*-hydroxylation of 3-hydroxybenzoate to gentisate, a key intermediate in the catabolism of aromatic compounds in the soil (Pérez-Pantoja *et al.*, 2010). 3HB6H activity has been reported for Gram-positive and Gram-negative bacteria and for yeasts. So far, the enzyme has been partially characterized from *Klebsiella pneumonia* M5a1 (Suárez *et al.*, 1995; Liu *et al.*, 2005), *Pseudomonas alcaligenes* NCIMB 9867 (Gao *et al.*, 2005), *Polaromonas naphthalenivorans* CJ2 (Park *et al.*, 2007), *Corynebacterium glutamicum* ATCC 12032 (Yang *et al.*, 2010), *Rhodococcus* sp. NCIMB 12038 (Liu *et al.*, 2010) and *Candida parapsilosis* (Holesova *et al.*, 2011).

Recently, we reported the biochemical characterization of 3HB6H from *Rhodococcus jostii* RHA1 (Montersino and van Berkel, 2012). *R. jostii* RHA1 3HB6H expressed in *Escherichia coli* is a homodimer containing a non-covalently bound FAD cofactor. The enzyme prefers NADH as electron donor and is active with a series of 3-hydroxybenzoate analogs, bearing substituents in *ortho*- or *meta*-position of the aromatic ring. Gentisate, the physiological product, is a non-substrate effector of 3HB6H. This compound is not converted but strongly stimulates the NADH oxidase activity of the enzyme. Crystallographic data have provided important information about the 3HB6H structure (Chapter 4-5). The overall fold of 3HB6H is similar to that of *p*-hydroxybenzoate hydroxylase (PHBH) and other flavoprotein aromatic hydroxylases. 3HB6H crystallizes in substrate-free form with the isoalloxazine ring of the FAD cofactor located *in* the active site. Unexpectedly, a lipid molecule, phosphatidylglycerol (PG) or phosphatidylethanolamine (PE), is bound to each 3HB6H monomer near the dimer interface. 3HB6H expressed in the original strain *R. jostii* RHA1#2 retains the ability to bind phospholipids although, in the mycolata strain, PE and PG are replaced by phosphatidylinositol (PI). Based on native ESI-MS analysis we hypothesized that phospholipid binding is required for 3HB6H dimer stabilization (Chapter 4-5).

In this study, we analyzed the hydrodynamic and lipid binding properties of 3HB6H from *P. alcaligenes* NCIMB 9867 (3HB6H<sub>pa</sub>), as expressed in *E. coli*. Evidence is provided that 3HB6H<sub>pa</sub> is a dimer and not a trimer as postulated before (Gao *et al.*, 2005), and that each 3HB6H<sub>pa</sub> monomer binds a PE or PG molecule. The catalytic properties of 3HB6H<sub>pa</sub> are discussed as well.

## Materials And Methods

**Chemicals.** DNaseI was from Boehringer Mannheim GmbH (Mannheim, Germany). *E. coli* TOP10 was from Invitrogen (Carlsbad, CA, USA). Aromatic compounds were purchased from Sigma-Aldrich (St Louis, MO, USA) and Acros Organics (New Jersey, US). Catalase, FAD, FMN and arabinose were from Sigma-Aldrich (St Louis, MO, USA). Pefabloc SC was obtained from Roche Diagnostics GmbH (Mannheim, Germany). All other chemicals were from commercial sources and of the purest grade available.

**Amino Acid Sequence Analysis.** Protein sequences were retrieved using protein resources from the National Centre for Biotechnology Information ([www.ncbi.nlm.nih.gov](http://www.ncbi.nlm.nih.gov)) and UniProt Database ([www.uniprot.org](http://www.uniprot.org)). Multiple sequence alignments were made using CLUSTALW (Thompson *et al.*, 1994). Phylogenetic analysis was performed using FigTree ([tree.bio.ed.ac.uk](http://tree.bio.ed.ac.uk)).

**Expression And Purification Of 3HB6H From *P. alcaligenes* NCIMB 9867.** The *xlnD* gene sequence encoding for 3HB6H was synthesized and subcloned in pBAD/*Myc*-His(*Nde*I) vector by GeneArt (Invitrogen, CA). The resulting construct (pBAD-3HB6H<sub>pa</sub>-His<sub>6</sub>) was verified by automated sequencing of both strands and electroporated to *E. coli* TOP10 cells for recombinant expression.

For enzyme production, *E. coli* TOP10 cells, harbouring a pBAD-3HB6H<sub>pa</sub> plasmid, were grown in TB medium at 37 °C supplemented with 100 µg·mL<sup>-1</sup> ampicillin until an optical density (OD<sub>600 nm</sub>) of 0.8 was reached. Expression was induced by the addition of 0.02% (w/v) arabinose and incubation was continued for 40 h at 17 °C. Cells were harvested by centrifugation and recombinant protein was purified to apparent homogeneity by three successive chromatographic steps (Chapter 3). Purified 3HB6H<sub>pa</sub> was frozen in liquid nitrogen and stored at -80 °C. Before use, enzyme samples were incubated with FAD and excess flavin was removed by Biogel P-6DG gel filtration.

**Biochemical Characterization.** The molar absorption coefficient of protein-bound FAD was determined by recording the absorption spectrum of 3HB6H<sub>pa</sub> in the presence and absence of 0.1% (w/v) SDS, assuming a molar absorption coefficient for free FAD of 11.3 mM<sup>-1</sup> cm<sup>-1</sup> at 450 nm. Enzyme concentrations were determined by measuring the absorbance at 450 nm using the molar absorption coefficient for protein-bound FAD (11.0 mM<sup>-1</sup> cm<sup>-1</sup>). 3HB6H activity and oxygen consumption was assayed as described previously (Montersino and van Berkel, 2012). The substrate specificity of 3HB6H<sub>pa</sub> was analyzed by measuring the standard activity in the presence of 2 mM substrate (analog).

**Substrate Binding.** The interaction of 3HB6H<sub>pa</sub> with 3-hydroxybenzoate was studied in 50 mM Tris SO<sub>4</sub> (pH 8.0). The dissociation constant ( $K_d$ ) of the enzyme/substrate complex was determined from fluorescence titration experiments. Fluorescence measurements were carried out with a Cary Elipse spectrofluorimeter (Varian, Agilent Technologies). Excitation was at 450 nm while emission spectra were recorded from 460 to 700 nm using a 1 ml initial volume with 3-hydroxybenzoate additions. The fluorescence intensities were corrected for dilution due to the addition of 3-hydroxybenzoate and buffer fluorescence emission. The apparent dissociation constant of the enzyme-substrate complex was calculated from the increase in FAD fluorescence emission using a direct nonlinear regression fit to the data with IGOR (Wavemetrics, Lake Oswego, OR, USA).

The analysis assumed that the fraction of bound ligand is equal to the ratio of fluorescence observed ( $F = F_b - F_o$ ) to the maximum fluorescence ( $F_{max} = F_{bmax} - F_o$ ), where  $F_o$ ,  $F_b$ , and  $F_{bmax}$  are the fluorescence intensity at 525 nm in the absence of ligand, the fluorescence intensity in the presence of ligand, and the maximum fluorescence at saturating amounts of ligand, respectively. Apparent dissociation constants were calculated by fitting fluorescence to Eq. (1), a modified equation compared with the one described elsewhere (Bollen *et al.*, 2005; Ereemeeva *et al.*, 2009):

$$\frac{F}{F_{max}} = \frac{(C + L + K_d) - \sqrt{(C + L + K_d)^2 - 4CL}}{2} \quad (1)$$

where  $C$ ,  $L$ , and  $K_d$  are 3HB6H<sub>pa</sub> concentration, 3-hydroxybenzoate concentration, and apparent dissociation constant, respectively.

**ESI-MS Experiments.** MS analysis was performed on a LC-T nanoflow ESI orthogonal TOF mass spectrometer (Micromass, Manchester, UK), equipped with a Z-spray nano-electrospray ionization source. Native MS and identification of protein-bound lipids was performed as described previously (Chapter 4).

## Results

**Protein Sequence Analysis.** Multiple sequence alignment and phylogenetic analysis of (partially) characterized 3HB6H enzymes underlined a clustering of sequences from *Actinobacteria* towards *Proteobacteria*, and an outgroup of the eukaryotic *C. parapsilosis* sequence. The 3HB6H sequences originating from *Rhodococcus* species are most identical, while some variations are visible among *Proteobacteria* sequences, with an identity always above 30 % and amino acid similarities not less than 45 % (Fig.1). All known 3HB6H enzymes use NADH and show narrow substrate specificity. While 3HB6H from *R. jostii* RHA1 is poorly active with 3-hydroxybenzoic compounds containing functional groups in 4-position (Montersino and van Berkel, 2012), the enzyme from *P. alcaligenes* NCIMB 9867 was reported to use 3-hydroxy-4-methylbenzoate as one of the best substrates (Gao *et al.*, 2005; Yeo *et al.*, 2007). However, for the latter enzyme, no information about the efficiency of hydroxylation was presented.

3HB6Hs from *Rhodococcus* sp. NCIMB 12038, *C. glutamicum* ATCC 12031 and *P. alcaligenes* NCIMB 9867 were reported to be trimeric proteins (Liu *et al.*, 2010; Yang *et al.*, 2010; Gao *et al.*, 2005), while 3HB6H from *K. pneumoniae* M5a1 and *P. naphthalenivorans* CJ2 were stated to be monomers (Liu *et al.*, 2005; Park *et al.*, 2007) In contrast, we established that 3HB6H from *R. jostii* RHA1 is a dimer both in solution and in crystal form (Chapter 4). From multiple sequence alignment of known 3HB6H enzymes, we noticed that residues involved in dimer and lipid contact in *R. jostii* RHA1 are not always conserved, and that most sequence divergence occurs in 3HB6H from *P. alcaligenes* NCIMB 9867. In particular, residues involved in lipid binding in 3HB6H from *R. jostii* (Val204, Val205, Leu303, Trp358 and Phe376) are exchanged in the *P. alcaligenes* NCIMB 9867 enzyme with less hydrophobic residues (Ser202, Thr203, Met302, Ala350 and Met369) (Fig.1). Furthermore, in the *P. alcaligenes* NCIMB 9867 enzyme, a patch of residues on the protein surface (Chapter 4) harbors a bulky tryptophan (Trp380) instead of a tyrosine (Tyr386) that could interfere with lipid binding and oligomerization (Fig.1).

**Expression And Purification Of 3HB6H<sub>pa</sub>.** Expression of 3HB6H<sub>pa</sub> at 37 °C in *E. coli* TOP10 mainly yielded inclusion bodies. Soluble protein was obtained by decreasing the temperature during growth to 17 °C. Although suffering from precipitation, recombinant 3HB6H<sub>pa</sub> was purified to apparent homogeneity in three chromatographic

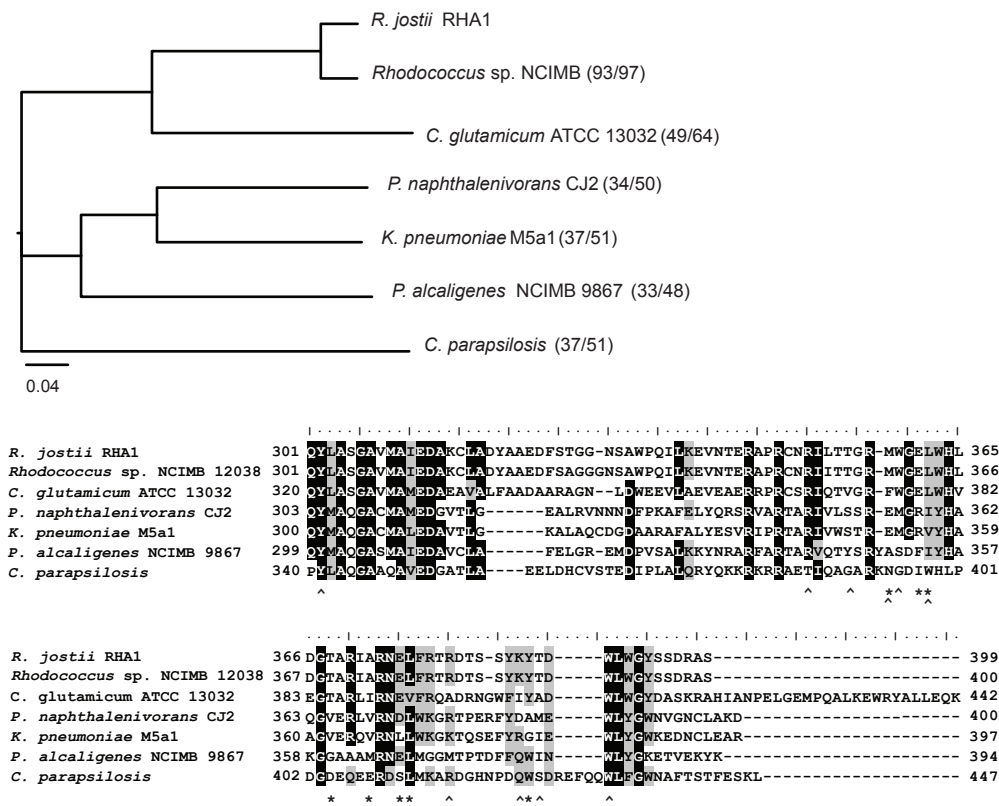


**Figure 1. ClustalW multiple sequence alignment of dimerization domains of known 3HB6H enzymes.** Upper panel: Phylogenetic tree of known 3HB6H enzymes. Percentage of identical and similar residues is indicated in brackets. Lower panel: Identical residues are shaded in black, similar residues are shaded in gray (60 % threshold for shading). The asterisk (\*) marks residues involved in dimerization contacts. The arrow (^) indicates residues involved in lipid binding. UniProt ID numbers: Q0SFK6, E7CYP8, Q8NLB6, Q3S4B7, Q6EXK1, Q9F131; for 3HB6H from *C. parapsilosis* we used the ID number : CPAG\_003410 (Holesova *et al.*, 2011).

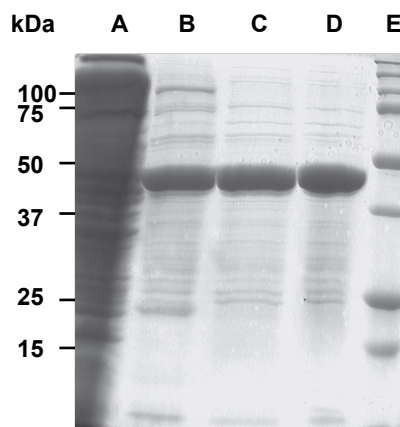
steps (Table 1 and Fig.2). About 12 mg of purified enzyme was obtained from a 1 L batch culture containing 10 g of wet cells. The final 3HB6H<sub>pa</sub> preparation had a specific activity of 26 U mg<sup>-1</sup> (Table 1). This 'as isolated' activity increased by a factor of 1.7 when the enzyme was treated with excess FAD and imidazole was removed (*vide infra*). Recombinant 3HB6H<sub>pa</sub> migrated in SDS-PAGE in a single band with an apparent molecular mass of around 47 kDa (Fig.2), in agreement with the theoretical subunit molecular mass. The 3HB6H<sub>pa</sub> oligomeric state was estimated as a dimer by ESI-MS (Table 2 and Fig.4) showing similar behaviour as 3HB6H from *R. jostii* RHA1 (Chapter 4).

**Spectral Properties Of 3HB6H<sub>pa</sub>.** Recombinant 3HB6H<sub>pa</sub> showed a typical flavoprotein absorption spectrum with maxima at 373 nm and 450 nm and a weak pronounced shoulder at 480 nm (Fig.3A). The molar absorption coefficient of protein-bound FAD was determined to be 11 mM<sup>-1</sup> cm<sup>-1</sup> at 450 nm. The A<sub>373</sub>/A<sub>450</sub> ratio (Fig.3A) is 1.1, a rather high value for flavoproteins. In contrast to *R. jostii* 3HB6H (Chapter 3), no perturbations of flavin absorbance were induced upon substrate binding.

**Table 1. Purification of *P. alcaligenes* NCIMB 9867 3HB6H expressed in *E. coli*.**

Step	Protein (mg)	Activity (U)	Specific activity (U/mg <sup>-1</sup> )	Yield (%)
Cell extract	1080	260	0.2	100
His <sub>6</sub> -GraviTrap	45	244	5	94
Mono-Q	12	225	19	87
His <sub>6</sub> -GraviTrap	5	170	34	66

**Figure 2. SDS/PAGE analysis of the purification of 3HB6H from *P. alcaligenes* NCIMB 9867 expressed in *E. coli*.** Lane A, cell extract; Lane B, His<sub>6</sub>-GraviTrap pool; Lane C, Mono-Q pool; Lane D, His<sub>6</sub>-GraviTrap pool; Lane E, Precision plus protein Standards (BioRad).



The FAD cofactor of 3HB6H<sub>pa</sub> showed a rather high fluorescence, a property not appreciable in *R. jostii* 3HB6H (Chapter 3). The relative flavin fluorescence quantum yield of 3HB6H<sub>pa</sub> was about 6% of free FMN and increased to 8% in the presence of substrate (Fig.3B). From the changes in fluorescence emission at 525 nm (Fig.3B), a dissociation constant,  $K_d = 180 \pm 30 \mu\text{M}$ , for the binary enzyme-substrate complex was estimated. This value compares favourably with the  $K_m$  value (*vide infra*), but is significantly higher than the corresponding value reported for *R. jostii* 3HB6H (Montersino and van Berkel, 2012).

**Catalytic Properties Of 3HB6H<sub>pa</sub>.** The steady-state kinetic parameters of 3HB6H were determined at 25°C in 50 mM Tris-SO<sub>4</sub> (pH 8.0). This analysis revealed that the enzyme is active with 3-hydroxybenzoate ( $K_m = 147 \pm 8 \mu\text{M}$ ;  $k_{\text{cat}} = 34 \pm 1 \text{ s}^{-1}$ ;  $k_{\text{cat}}/K_m = 2.3 \times 10^5 \text{ M}^{-1} \text{ s}^{-1}$ ) and prefers NADH ( $K_m = 48 \pm 4 \mu\text{M}$ ) over NADPH ( $K_m = 391 \pm 76 \mu\text{M}$ ) as coenzyme. 3HB6H<sub>pa</sub> showed a rather poor hydroxylation efficiency ( $25 \pm 4 \%$  uncoupling), thus producing significant amounts of hydrogen peroxide. Gentisate, the physiological product, is an effector of 3HB6H ( $K_m = 280 \pm 10 \mu\text{M}$ ;  $k_{\text{cat}} = 1.1 \pm 0.1 \text{ s}^{-1}$ ;  $k_{\text{cat}}/K_m = 4 \times 10^3 \text{ M}^{-1} \text{ s}^{-1}$ ). This compound is not converted but stimulates the NADH oxidase activity of the enzyme (99% uncoupling).

Some effort was made to test the substrate specificity of 3HB6H<sub>pa</sub>. In agreement with published data (Gao *et al.*, 2005; Yeo *et al.*, 2007), 3-hydroxy-4-methylbenzoate appeared to be a good substrate. At 2 mM substrate concentration, the activity with



this compound was  $13.7 \text{ U mg}^{-1}$  (compared to  $25.2 \text{ U mg}^{-1}$  for 3-hydroxybenzoate) and only  $12 \pm 1\%$  uncoupling was observed. 4-Hydroxybenzoate turned out to be a rather good effector for  $3\text{HB}6\text{H}_{\text{Pa}}$ . This compound was not converted (100% uncoupling), but strongly stimulated the NADH oxidase activity (specific activity =  $16.0 \text{ U mg}^{-1}$ ). 3-Aminobenzoate, on the other hand, was a poor effector (100% uncoupling; specific activity =  $1.7 \text{ U mg}^{-1}$ ).

**Lipid Analysis.** The lipid content of  $3\text{HB}6\text{H}_{\text{Pa}}$  was analyzed by ESI-MS (Table 2, Fig. 4). The mass spectrum of extracted lipids showed peaks with  $m/z$  values characteristic of phosphatidylglycerol (PG) and phosphatidylethanolamine (PE) with aliphatic chains ranging from 14 to 19 carbons, as previously identified in  $3\text{HB}6\text{H}$  from *R. jostii* RHA1 (Chapter 4).

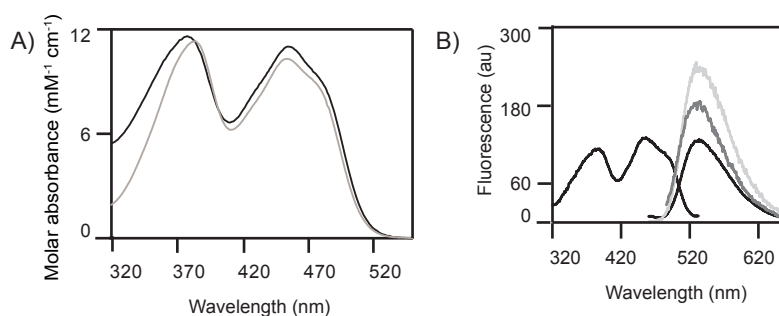


**Figure 3. Flavin absorption and fluorescence properties of  $3\text{HB}6\text{H}_{\text{Pa}}$ .** **A)** Absorption spectrum of  $3\text{HB}6\text{H}_{\text{Pa}}$  (black line) and  $3\text{HB}6\text{H}$  from *R. jostii* RHA1 (grey line). **B)** Fluorescence excitation and emission spectrum of free  $3\text{HB}6\text{H}_{\text{Pa}}$  (black line); emission spectrum of  $3\text{HB}6\text{H}_{\text{Pa}}$  complexed with 3-hydroxybenzoate (dark grey line); emission spectrum of free  $\text{FMN}_{\text{Pa}}$  (light gray line). Excitation was at 450 nm. Protein concentration was  $3 \mu\text{M}$ , FMN concentration was  $0.3 \mu\text{M}$  and 3-hydroxybenzoate concentration was  $583 \mu\text{M}$ . All spectra were recorded in  $50 \text{ mM TrisSO}_4$  (pH 8).

**Table 2. Determination of  $3\text{HB}6\text{H}_{\text{Pa}}$  oligomeric state by ESI-MS.**

Peak	$m/z$	Average mass	
		Da	$\Delta$ mass Da
1	3651 <sup>a</sup>	$47448 \pm 2$	790 <sup>c</sup>
2	3706 <sup>a</sup>	$48167 \pm 2$	1509 <sup>c</sup>
3	5035 <sup>b</sup>	$95662 \pm 7$	2346 <sup>d</sup>
4	5073 <sup>b</sup>	$96378 \pm 8$	3062 <sup>d</sup>

<sup>a</sup> based on 13+ charge state

<sup>b</sup> based on 19+ charge state

<sup>c</sup> calculated using apo-monomer ( $46658 \pm 2 \text{ Da}$ )

<sup>d</sup> calculated using apo-dimer ( $93316 \text{ Da}$ )



## Discussion

Gram-negative bacteria are able to degrade 2,5-xyleneol, 3,5-xyleneol and *m*-cresol via the 3HB6H-mediated conversion of 3-hydroxybenzoate to gentisate (Gao *et al.*, 2005; Yeo *et al.*, 2007; Yeo *et al.*, 2003). 3HB6H from *P. alcaligenes* NCIMB 9867 was partially characterized by Gao and coworkers (Gao *et al.*, 2005). They reported that 3HB6H<sub>pa</sub> contains FAD, is trimeric, NADH specific and, except for the physiological substrate, is active with 3-hydroxybenzoate analogs bearing methyl substituents in *ortho* and *meta* position.

We became interested in 3HB6H<sub>pa</sub> in view of the biochemical and structural properties of the related 3HB6H from *R. jostii* RHA1 (Chapter 3-5). Sequence alignment highlighted amino acid substitutions in the dimerization domain that might be crucial for oligomerization and lipid binding. Recombinant expression of His-tagged 3HB6H<sub>pa</sub> in *E. coli* resulted in formation of inclusion bodies at 37 °C, but active soluble protein was obtained when cells were grown at 17 °C.

3HB6H<sub>pa</sub> possessed relatively high flavin fluorescence, allowing the accurate determination of the dissociation constant of the enzyme-substrate complex. The interaction with the physiological substrate ( $K_d = 180 \mu\text{M}$ ), appeared to be much

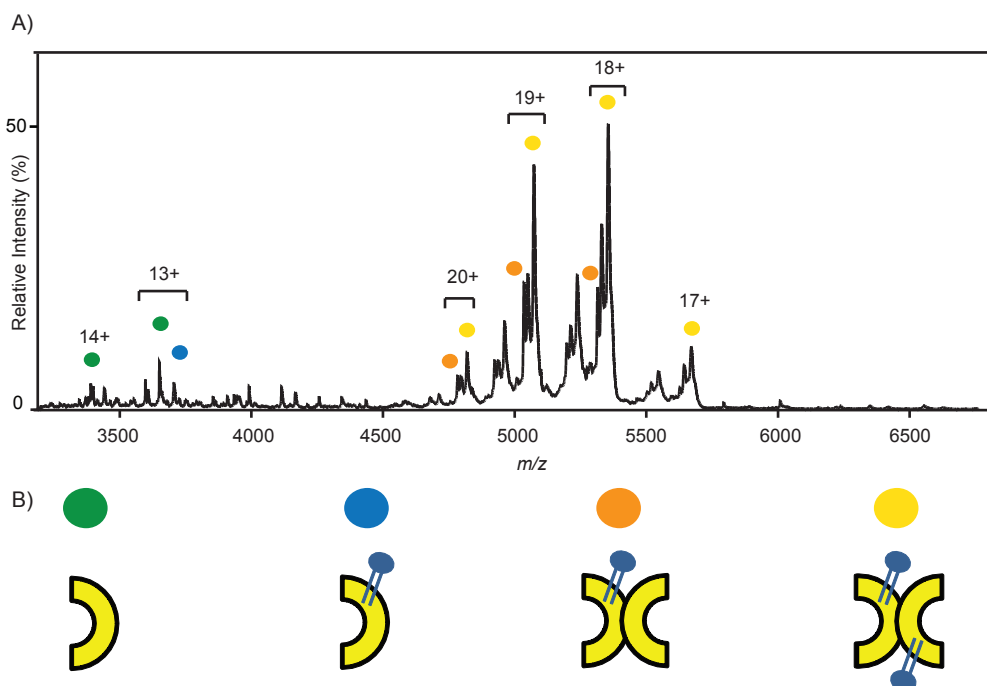


**Figure 4.** 3HB6H<sub>pa</sub> oligomer distribution and lipid composition as determined by native ESI-MS. **A)** Mass spectrum in 50 mM ammonium acetate (pH 6.8). **B)** 3HB6H<sub>pa</sub> subunit composition. Mass of 13+ and 19+.

weaker than with the *R. jostii* RHA1 enzyme (Montersino and van Berkel, 2012).

3HB6H<sub>pa</sub> preferred NADH as electron donor ( $K_m = 48 \pm 4 \mu\text{M}$ ), but the enzyme also accepted NADPH ( $K_m = 391 \pm 76 \mu\text{M}$ ). Kinetic results with 3-hydroxybenzoate agreed with published data (Gao *et al.*, 2005). However, we noticed an unusual high degree of uncoupling of substrate hydroxylation ( $25 \pm 4\%$ ). Several phenomena might account for this behavior: (i) significant production of hydrogen peroxide might be related to instability of the flavin-hydroperoxide oxygenating species (Massey, 1994) (ii) gentisate product binding might compete with weak binding of 3-hydroxybenzoate and result in accumulation of hydrogen peroxide. Significant less uncoupling ( $12 \pm 1\%$ ) and a reasonable high activity ( $14 \text{ U mg}^{-1}$ ) was observed with the substrate analog 3-hydroxy-4-methylbenzoate. This might indicate that this compound is a physiological substrate of 3HB6H<sub>pa</sub>, being an intermediate in 2,5-xylanol degradation (Gao *et al.*, 2005; Gao *et al.*, 2005; Yeo *et al.*, 2007).

4-Hydroxybenzoate turned out to be a strong effector of NADH oxidation. The relatively high specific activity ( $16 \text{ U mg}^{-1}$ ) observed with this compound suggests that 3HB6H<sub>pa</sub> is less well evolved for its specific tasks than the *R. jostii* enzyme. Future active site modeling of 3HB6H<sub>pa</sub> might provide a *rationale* for the different substrate and effector specificities observed (see also Chapter 7).

Native MS analysis showed that 3HB6H<sub>pa</sub> is a homodimer and not a trimer as postulated before (Gao *et al.*, 2005). The dimeric nature is in agreement with the structural properties of 3HB6H from *R. jostii* RHA1 (Chapter 4). MS analysis also revealed that, in spite of a less hydrophobic character of the dimerization domain, recombinant 3HB6H<sub>pa</sub> binds the same type of phospholipids as 3HB6H from *R. jostii* RHA1. This indicates that lipid binding is an intrinsic property of 3HB6Hs.

As a main result, it appears that the 3HB6H family uses phospholipids as a common tool to increase their dimerization strength. Phospholipid binding is independent of the type of lipid head group, but relies on the presence of hydrophobic tunnels running from protein surface to active site. Fluorescence localization (Holesova *et al.*, 2011) or lipid photo-crosslinking (Gubbens *et al.*, 2009) might be useful to determine the relevance of the observed protein-lipid interactions in an *in vivo* environment.

## 6

### Acknowledgements

We are grateful to Arjan Barendrecht for ESI-MS experimental contribution. This study was supported by the Integrated Biosynthesis Organic Synthesis (IBOS) project of the Netherlands Organization for Scientific Research (NWO).

## References

- Bollen, Y.J.M., Nabuurs, S.M., van Berkel, W.J.H. and van Mierlo, C.P.M., (2005) Last in, first out: the role of cofactor binding in flavodoxin folding. *Journal of Biological Chemistry*, 280(9), 7836–7844.
- Eremeeva, E.V., Markova, S.V., Westphal, A.H., Visser, A.J.W.G., van Berkel, W.J.H. and Vysotski, E.S., (2009) The intrinsic fluorescence of apo-obelin and apo-aequorin and use of its quenching to characterize coelenterazine binding. *FEBS Letters*, 583(12), 1939–1944.
- Gao, X., Tan, C.L., Yeo, C.C. and Poh, C.L., (2005) Molecular and biochemical characterization of the *xlnD*-encoded 3-hydroxybenzoate 6-hydroxylase involved in the degradation of 2,5-xyleneol via the gentisate pathway in *Pseudomonas alcaligenes* NCIMB 9867. *Journal of Bacteriology*, 187(22), 7696–7702.
- Gubbens, J., Ruijter, E., de Fays, L.E.V., Damen, J.M.A., de Kruijff, B., Slijper, M., Rijkers, D.T.S., Liskamp, R.M.J. and de Kroon, A.I.P.M., (2009) Photocrosslinking and click chemistry enable the specific detection of proteins interacting with phospholipids at the membrane interface. *Chemistry & Biology*, 16(1), 3–14.
- Holesova, Z., Jakubkova, M., Zavadiakova, I., Zeman, I., Tomaska, L. and Nosek, J., (2011) Gentisate and 3-oxoadipate pathways in the yeast *Candida parapsilosis*: identification and functional analysis of the genes coding for 3-hydroxybenzoate 6-hydroxylase and 4-hydroxybenzoate 1-hydroxylase. *Microbiology*, 157(Pt 7), 2152–2163.
- Liu, D.Q., Liu, H., Gao, X.L., Leak, D.J. and Zhou, N.Y., (2005) Arg169 is essential for catalytic activity of 3-hydroxybenzoate 6-hydroxylase from *Klebsiella pneumoniae* M5a1. *Microbiological Research*, 160(1), 53–59.
- Liu, T.-T., Xu, Y., Liu, H., Luo, S., Yin, Y.-J., Liu, S.-J. and Zhou, N.Y., (2010) Functional characterization of a gene cluster involved in gentisate catabolism in *Rhodococcus* sp. strain NCIMB 12038. *Applied Microbiology and Biotechnology*, 90(2), 671–678.
- Massey, V., (1994) Activation of molecular oxygen by flavins and flavoproteins. *Journal of Biological Chemistry*, 269(36), 22459–22462.
- Montersino, S. and van Berkel, W.J.H., (2012) Functional annotation and characterization of 3-hydroxybenzoate 6-hydroxylase from *Rhodococcus jostii* RHA1. *Biochimica et biophysica acta*, 1824(3), 433–442.
- Park, M., Jeon, Y., Jang, H.H., Ro, H.-S., Park, W., Madsen, E.L. and Jeon, C.O., (2007) Molecular and biochemical characterization of 3-hydroxybenzoate 6-hydroxylase from *Polaromonas naphthalenivorans* CJ2. *Applied and Environmental Microbiology*, 73(16), 5146–5152.
- Pérez-Pantoja, D., González, B. and Pieper, D., (2010) Aerobic degradation of aromatic hydrocarbons. *Handbook of Hydrocarbon and Lipid Microbiology*, 2, 800–837.
- Suárez, M., Ferrer, E., Garrido-Pertierra, A. and Martín, M., (1995) Purification and characterization of the 3-hydroxybenzoate-6-hydroxylase from *Klebsiella pneumoniae*. *FEMS Microbiology Letters*, 126(3), 283–290.
- Thompson, J.D., Higgins, D.G. and Gibson, T.J., (1994) CLUSTAL W: improving the sensitivity of progressive multiple sequence alignment through sequence weighting, position-specific gap penalties and weight matrix choice. *Nucleic Acids Research*, 22(22), 4673–4680.
- van Berkel, W.J.H., Kamerbeek, N.M. and Fraaije, M.W., (2006) Flavoprotein monooxygenases, a diverse class of oxidative biocatalysts. *Journal of Biotechnology*, 124(4), 670–689.
- Yang, Y.-F., Zhang, J.-J., Wang, S.-H. and Zhou, N.-Y., (2010) Purification and characterization of the *ncgl2923*-encoded 3-hydroxybenzoate 6-hydroxylase from *Corynebacterium glutamicum*. *Journal of Basic Microbiology*, 50(6), 599–604.
- Yeo, C.C., Tan, C.L., Gao, X., Zhao, B. and Poh, C.L., (2007) Characterization of *hbzE*-encoded gentisate 1,2-dioxygenase from *Pseudomonas alcaligenes* NCIMB 9867. *Research in microbiology*, 158(7), 608–616.
- Yeo, C.C., Wong, M.V.M., Feng, Y., Song, K.P. and Poh, C.L., (2003) Molecular characterization of an inducible gentisate 1,2-dioxygenase gene, *xlnE*, from *Pseudomonas alcaligenes* NCIMB 9867. *Gene*, 312, 239–248.





# **Mirror-image substrate binding directs regioselectivity of flavoprotein dependent 3-hydroxybenzoate hydroxylation**

Stefania Montersino<sup>1</sup>, Roberto Orrú<sup>2</sup>, Adrie H. Westphal<sup>1</sup>,  
Alexander M.J.J. Bonvin<sup>3</sup>, Andrea Mattevi<sup>2</sup> and Willem J. H. van Berkel<sup>1</sup>

<sup>1</sup> Laboratory of Biochemistry, Wageningen University,  
Dreijenlaan 3, 6703 HA Wageningen, The Netherlands

<sup>2</sup> Department of Genetics and Microbiology, University of Pavia,  
Via Ferrata 1, 27100 Pavia, Italy

<sup>3</sup> Computational Structural Biology Group,  
Bijvoet Centre for Biomolecular Research, Utrecht University,  
Padualaan 8, 3584 CH Utrecht, The Netherlands

## Abstract

NAD(P)H-dependent single-component flavoprotein hydroxylases convert monophenols in a truly regiospecific manner, but the structural basis of this selectivity is unclear. Recently, we determined the crystal structure of 3-hydroxybenzoate 6-hydroxylase (3HB6H) from *Rhodococcus jostii* RHA1, but no aromatic substrate was found in the active site. Here we addressed the regioselectivity of hydroxylation of 3HB6H by substrate docking and site-directed mutagenesis.

Data-driven substrate docking pointed to the involvement in substrate binding of a Tyr-His pair, present in mirror image fashion in 3-hydroxybenzoate 4-hydroxylase (3HB4H) from *Comamonas testosteroni*. Biochemical and structural analysis of active site mutant proteins revealed that His213 in 3HB6H is essential for catalysis and that Tyr105 is critically involved in substrate binding.

The results presented suggest that 3HB4H and 3HB6H possess functional mirror image binding sites. This strategy to control regioselectivity is of great interest for future redesign of flavoprotein hydroxylases.

## Introduction

Microbial aerobic degradation of aromatic compounds is organized in peripheral routes funnelling a broad range of substrates to few key intermediates entering in central pathways (Phale *et al.*, 2007; Harwood and Parales, 1996). Oxygenation is a major strategy to process aromatic intermediates by increasing their oxidative state (Fuchs *et al.*, 2011). In particular, flavoprotein hydroxylases convert phenolic compounds into catechols and hydroquinones (Fig.1) which are central ring-cleavage substrates for dioxygenases (Pérez-Pantoja *et al.*, 2010; Moonen *et al.*, 2008).

NAD(P)H-dependent single-component flavoprotein hydroxylases convert monophenols in a truly regioselective manner, but the structural basis of this selectivity is unclear (Montersino *et al.*, 2011). So far, structure-function relationships focused on the *ortho*-specific enzymes 4-hydroxybenzoate 3-hydroxylase (PHBH) from *Pseudomonas* species (Entsch *et al.*, 2005; Entsch and van Berkel, 1995; Schreuder *et al.*, 1989), phenol hydroxylase (PHHY) from *Trichosporum cutaneum* (Enroth, 2003; Enroth *et al.*, 1998), and 3-hydroxybenzoate 4-hydroxylase (3HB4H) from *Comamonas testosteroni* (Hiromoto *et al.*, 2006) (Fig.1 underlined).

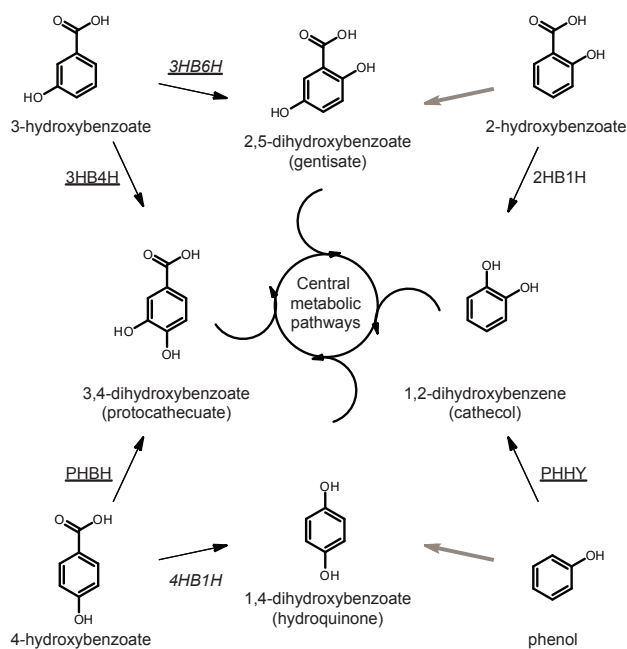


**Figure 1. Overview of single-component flavoprotein hydroxylases involved in the microbial degradation of monophenols.** 3-hydroxybenzoate 6-hydroxylase (3HB6H), 3-hydroxybenzoate 4-hydroxylase (3HB4H), 4-hydroxybenzoate 3-hydroxylase (PHBH), 4-hydroxybenzoate 1-hydroxylase (4HB1H), phenol 2-monooxygenase (PHHY), 2-hydroxybenzoate 1-hydroxylase (2HB1H). *para*-Hydroxylases are in italics, available crystal structures are underlined. Flavin-dependent hydroxylation reactions not yet characterized are in grey.



Recently, we determined the crystal structure of 3-hydroxybenzoate 6-hydroxylase (3HB6H) from *Rhodococcus jostii* RHA1 (Chapter 4). The 3HB6H three-dimensional model revealed a close similarity in domain architecture and topology to other flavoprotein hydroxylases, but no aromatic substrate was found in the active site. To gain insight into the structural determinants of the regioselectivity of flavoprotein-dependent 3-hydroxybenzoate hydroxylation, we here addressed the mode of substrate binding in 3HB6H and the role of putative active site residues in catalysis. Data-driven substrate docking pointed to the involvement in substrate binding of a Tyr-His pair, present in mirror image fashion in 3HB4H from *C. testosteroni*. Biochemical and structural analysis of active site mutant proteins revealed that His213 in 3HB6H is essential for catalysis and that Tyr105 is critically involved in substrate binding.

This is the first report that addresses the structural determinants of the regioselective reaction of flavoprotein aromatic hydroxylases. The results uncover a strategy in which *ortho* and *para*-hydroxylases that act on the same substrate employ a mirror-image binding site.

## Materials And Methods

**Chemicals.** *Pfu* DNA polymerase, *DpnI* and dNTPs were purchased from Invitrogen (Carlsbad, CA, USA). Oligonucleotides were synthesised by Eurogentec (Liege, Belgium). *E. coli* TOP10 was from Invitrogen (Carlsbad, CA, USA).

Aromatic compounds were purchased from Sigma-Aldrich (St Louis, MO, USA) and Acros Organics (New Jersey, US). All other chemicals were from commercial sources and of the purest grade available.

**Cloning And Site Directed Mutagenesis.** 3HB6H variants were constructed using pBAD-3HB6H-His<sub>6</sub> as template using the QuickChange II protocol (Stratagene, La Jolla, CA, USA). Oligonucleotides used were Y105F\_fw (5'-GCTACGGCGGACCGTTTTTCGTGACCCATCG-3'), H213A\_fw (5'-CGGACCGCGGTGCGCATTTCATCCAGTACCC-3'), H213S\_fw (5'-CGGACCGCGGTGCTCATTTCATCCAGTACCC-3') and Q301E\_fw (5'-GCACCCGCCACTGGAATACCTGGCCTCG-3') with the codon exchanged underlined. Successful mutagenesis was confirmed by automated sequencing. Resulting constructs were electroporated to *E. coli* TOP10 (Invitrogen) for recombinant expression.

**Enzyme Production And Purification.** The Äkta Explorer FPLC system (Pharmacia Biotech) was used for protein chromatography. For enzyme production, *E. coli* TOP10 cells, harbouring a pBAD-3HB6H plasmid, were grown in TB medium supplemented with 100 µg·mL<sup>-1</sup> ampicillin until an optical density (OD<sub>600 nm</sub>) of 0.8 was reached. Expression was induced by addition of 0.02% (w/v) arabinose and incubation was continued for 16 h at 37 °C. His<sub>6</sub>-tagged 3HB6H variants were purified using a similar procedure as described for wild-type enzyme (Montersino 2012). Desalting or buffer exchange of enzyme aliquots was performed with Bio-Gel P-6DG columns and Amicon Ultra-0.5 filters (30kDa cut off) (Millipore).

**Crystallization And Structure Determination.** Crystals for structure determination were obtained by the sitting drop vapour diffusion method at 20 °C by mixing equal volumes (2 µL) of protein and reservoir solutions. Protein solutions consisted of 28-30 mg enzyme/ml in 1 mM FAD, 2 mM 3-hydroxybenzoate, and 50 mM Bis-Tris (pH 7.2), while the reservoir solution consisted of 30% PEG 4K, 0.1 M Tris/HCl (pH 8.5) and 0.2 M LiSO<sub>4</sub>. X-ray diffraction data were collected at D14eh4 in

the European Synchrotron Radiation Facility (Grenoble, France) and processed with the CCP4 package (Collaborative Computational Project, Number 4, 1994). Structures of 3HB6H variants were solved by molecular replacement using the structure of a monomer of 3HB6H as search model. Crystallographic computing and model analysis were performed with COOT (Emsley *et al.*, 2010) and programs of the CCP4 package (Collaborative Computational Project, Number 4, 1994). Pictures were generated with Pymol (DeLano, 2010) and CCP4mg (Potterton *et al.*, 2004). Data collection parameters and final refinement statistics are listed in Table 1.

**Spectral Analysis.** Absorption spectra were recorded at 25 °C on a Hewlett Packard (Loveland, CO, USA) 8453 diode array spectrophotometer in 50 mM TrisSO<sub>4</sub> (pH 8.0). Spectra were analysed using the UV-Visible CHEMSTATION software package (Hewlett Packard).

Molar absorption coefficients of protein-bound FAD were determined by recording the absorption spectra of 3HB6H variants in the presence and absence of 0.1% (w/v) SDS, assuming a molar absorption coefficient for free FAD of 11.3 mM<sup>-1</sup> cm<sup>-1</sup> at 450 nm. Enzyme concentrations were determined by measuring the absorbance of protein-bound FAD using the following molar absorption coefficients: Y105F,  $\epsilon_{450}$  = 10.4 mM<sup>-1</sup> cm<sup>-1</sup>; H213A,  $\epsilon_{457}$  = 9.8 mM<sup>-1</sup> cm<sup>-1</sup>; H213S,  $\epsilon_{451}$  = 9.9 mM<sup>-1</sup> cm<sup>-1</sup>; Q301E,  $\epsilon_{446}$  = 10.8 mM<sup>-1</sup> cm<sup>-1</sup>.

**Thermal Stability.** Thermal unfolding of 3HB6H variants was followed by recording tryptophan and flavin fluorescence. Excitation was at 280 nm and 450 nm, while emission was recorded at 335, 350 and 525 nm, respectively. Protein concentrations were 2 μM in 100 mM HEPES (pH 7.5), containing 0.2 M NaCl. Individual thermal unfolding curves were fitted to a two-state mechanism according to a modified Gibbs-Helmholtz equation (Nabuurs *et al.*, 2009).

**Activity Measurements.** 3HB6H activity was routinely assayed by following the decrease in absorbance of NADH at 360 nm at 25 °C on a Hewlett Packard 8453 diode array spectrophotometer. Initial rates were calculated using a molar absorption coefficient ( $\epsilon_{360}$ ) of 4.31 mM<sup>-1</sup> cm<sup>-1</sup> (Montersino and van Berkel, 2012). One unit of enzyme activity (U) is defined as the amount of enzyme that consumes 1 μmol of NADH per min.

The activity of 3HB6H variants with 3-hydroxybenzoate followed Michaelis-Menten kinetics (Johnson and Goody, 2011). Kinetic parameters were calculated from multiple measurements with various substrate concentrations using a direct non-linear regression fit to the data.

**Oxygen Consumption.** An OxyTherm Clark-type oxygen electrode system (Hansatech, Norfolk, UK) was used to determine the hydroxylation efficiency of 3HB6H variants towards different aromatic substrates. The assay solution (final volume 1.0 ml) contained 350 μM aromatic substrate, 250 μM NADH, and 1-10 μM enzyme in 50 mM air-saturated Tris-SO<sub>4</sub> (pH 8.0), at 25 °C. At the end of the reaction, the amount of hydrogen peroxide produced was determined by adding 20 μg catalase (2H<sub>2</sub>O<sub>2</sub> → O<sub>2</sub> + 2H<sub>2</sub>O).

**Substrate Binding.** The interaction of 3HB6H (25 μM) with substrate analogues was studied in 50 mM Tris-SO<sub>4</sub> (pH 8.0). Dissociation constants ( $K_d$ ) of enzyme/substrate complexes were determined from flavin absorption difference spectra, essentially as described elsewhere (Montersino and van Berkel, 2012).

**Modeling Of The Complex Between 3HB6H And 3-Hydroxybenzoate.** The crystal structure of native monomer of 3HB6H was used to model the mode of 3-hydroxybenzoate binding. Docking was performed using HADDOCK 2.0 (de Vries *et al.*, 2010). The solvated docking was carried out with the recommended parameters of HADDOCK. Ambiguous interaction restraints were defined, based on the proposed substrate binding residues involved. A distance restraint of 4.0 Å was set between Tyr105-OH and any oxygen of the substrate, and between His231-ND1 and any oxygen of the substrate. Furthermore, a distance restraint of 6.0 Å was set between C7 of the substrate and C4a of the flavin cofactor. For rigid-body energy minimization, 1,000 structures were generated, with the 200 lowest energy solutions used for subsequent semi-flexible simulated annealing and water refinement. Resulting structures were sorted according to intermolecular energy and clustered using a 6.5 Å cut-off criterion. Subsequent cluster analysis was performed within a 2.0 Å cut-off criterion.

## Results

**Active Site Comparison Between 3HB4H And 3HB6H.** Recently, the 3HB6H crystal structure was solved and refined at 1.5 Å resolution (Chapter 4). Although 3HB6H crystals were prepared in the presence of 3-hydroxybenzoate, no electron density for the aromatic substrate was found in the active site (Fig.2). Chloride ions, present in the native 3HB6H structure, give a hint to the position of the substrate oxygen atoms in the active site (Chapter 4). Moreover, the putative binding site and orientation of the substrate can be inferred from comparison with other flavoprotein hydroxylases.

In 3HB4H, 3-hydroxybenzoate is located on the *re*-side of the flavin and maintained in the correct orientation by Tyr271, Lys247 and His135 (Hiromoto *et al.*, 2006). Lys247 and His135 interact with the carboxyl moiety of the substrate, whereas Tyr271 makes a hydrogen bond with the phenol (Fig.2). These interactions position the C4 atom of 3-hydroxybenzoate near the C4a atom of the isoalloxazine ring of the flavin, which is the site of hydroxylation during the oxidative half reaction (Massey, 1994). Indeed, the relative position of the reactive substrate carbon with respect to the flavin is functionally conserved among flavoprotein hydroxylases with known structure. Despite having similar folds, 3HB4H and 3HB6H share few conserved residues in their active sites (Fig.3). Phe79/106, Pro104/137, Val205/249, Val230/279 and Gly306/369 are conserved, but they are not directly involved in substrate binding.

**Modeling Of The 3HB6H Enzyme-Substrate Complex.** From comparing their substrate binding pockets, we hypothesized that the orientation of 3-hydroxybenzoate in 3HB6H mirrors the mode of substrate binding in 3HB4H, permitting the substrate C6 carbon to react with the flavin-C4a-hydroperoxide. In this geometry, the 3HB6H residues Tyr105 and His213 occupy mirror positions with respect to Tyr271 and His135 in 3HB4H (Fig.2).

Next, we modelled the 3HB6H enzyme-substrate complex, using HADDOCK. To collect substrate conformations suitable to hydroxylation, we introduced ambiguous restraints favouring the proximity of the substrate to the C4a environment of the flavin ring (*see* Materials and Methods). Since 3HB6H contains a tightly bound phospholipid molecule (Chapter 4), we performed the docking experiment both in presence and absence of phospholipid, but excluding chloride ions present in the native structure. We analysed the resulting models (Table 2), of which representative conformations of each cluster are shown in Figure 4. The docking results show that 3-hydroxybenzoate fits into the active site of 3HB6H, and no major protein conformational rearrangements are required to bind the substrate.

Including phospholipid into the docking procedure limited the results to only one cluster of conformations (Cluster 1P), in contrast to three clusters present in the run without phospholipid (Cluster 1-3). Although Cluster 2 possesses the better score

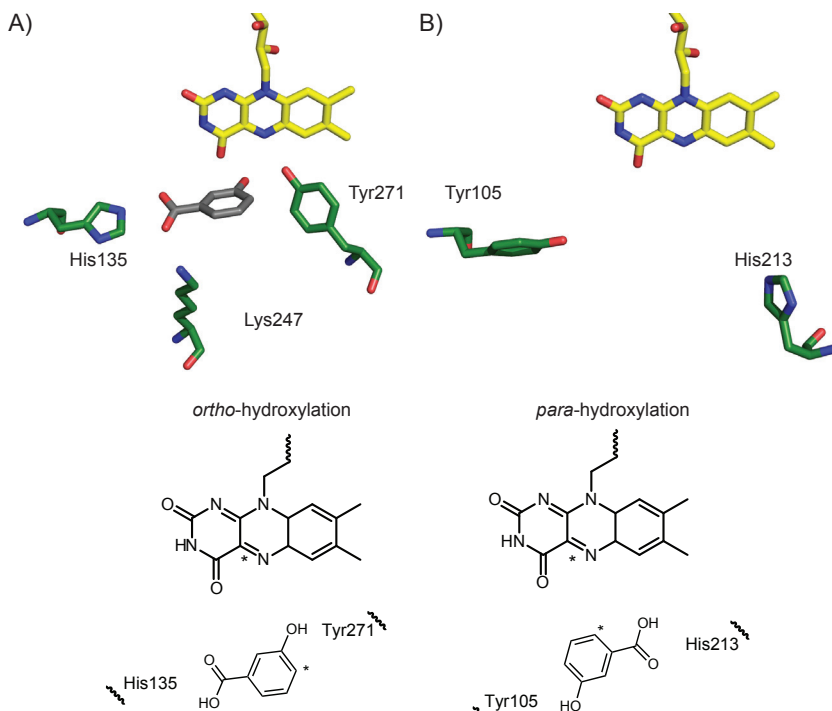


**Figure 2. Active sites comparison between 3HB6H and 3HB4H.** A) Crystal structure of the active site of 3HB4H with bound 3-hydroxybenzoate (PDB: 2DKI).

B) Crystal structure of the active site of 3HB6H. Residues are indicated in green stick, cofactor in yellow stick and substrate in grey stick. Lower panel: Scheme of mirror image binding site between 3HB4H and 3HB6H. C4a of the flavin and carbon subjected to hydroxylation are indicated with an asterisk (\*).

**Table 1. Crystallographic data collection and refinement statistics.**

	Y105F	H213S	Q301E
Unit cell (Å)	$a=b=106.52$ $c=142.8$	$a=b=105.79$ $c=142.29$	$a=b=106.45$ $c=142.72$
Space group	$I4_122$	$I4_122$	$I4_122$
Resolution (Å)	1.78	1.83	2.47
$R_{\text{sym}}^{\text{a,b}}$ (%)	9.1(29.6)	6.5 (13.0)	9.8 (22.1)
Completeness <sup>b</sup> (%)	99.2 (96.9)	97.1 (99.2)	99.9 (99.9)
Unique reflections	39391	34563	15029
Redundancy <sup>b</sup>	6.4 (6.0)	3.3 (3.4)	7.8 (7.8)
$I/\sigma^{\text{b}}$	14.5 (5.9)	13.7 (7.5)	15.2 (9.0)
N° of atoms	3408	3366	3281
Average $B$ value (Å <sup>2</sup> )	19.3	26.9	18.5
$R_{\text{cryst}}^{\text{c}}$ (%)	19.7	19.8	18.5
$R_{\text{free}}^{\text{c}}$ (%)	23.8	24.8	26.5
Rms bond length (Å)	0.017	0.019	0.014
Rms bond angles (°)	1.8	1.9	1.7

<sup>a</sup>  $R_{\text{sym}} = \sum |I_i - \langle I \rangle| / \sum I_i$ , where  $I_i$  is the intensity of  $i^{\text{th}}$  observation and  $\langle I \rangle$  is the mean intensity of the reflection.

<sup>b</sup> Values in parentheses are for reflections in the highest resolution shell.

<sup>c</sup>  $R_{\text{cryst}} = \sum |F_{\text{obs}} - F_{\text{calc}}| / \sum F_{\text{obs}}$ , where  $F_{\text{obs}}$  and  $F_{\text{calc}}$  are the observed and calculated structure factor amplitudes, respectively.  $R_{\text{cryst}}$  and  $R_{\text{free}}$  were calculated using the working and test set, respectively.

7

(Fig.4C), it represents a random orientation of the substrate in the active site, not catalytically relevant for *para*-hydroxylation. Cluster 3 results propose a substrate conformation similar to the one present in the 3HB4H active site, with opposite interactions between substrate substituents and active site residues, therefore not in agreement with the type of reaction performed by 3HB6H (Fig.4D).

The best HADDOCK scores in the runs with and without phospholipid are both in agreement with the hypothesis-driven active site comparison with 3HB4H and the hydroxylation mode (Fig.4A-B). Based on the strong interaction between the enzyme

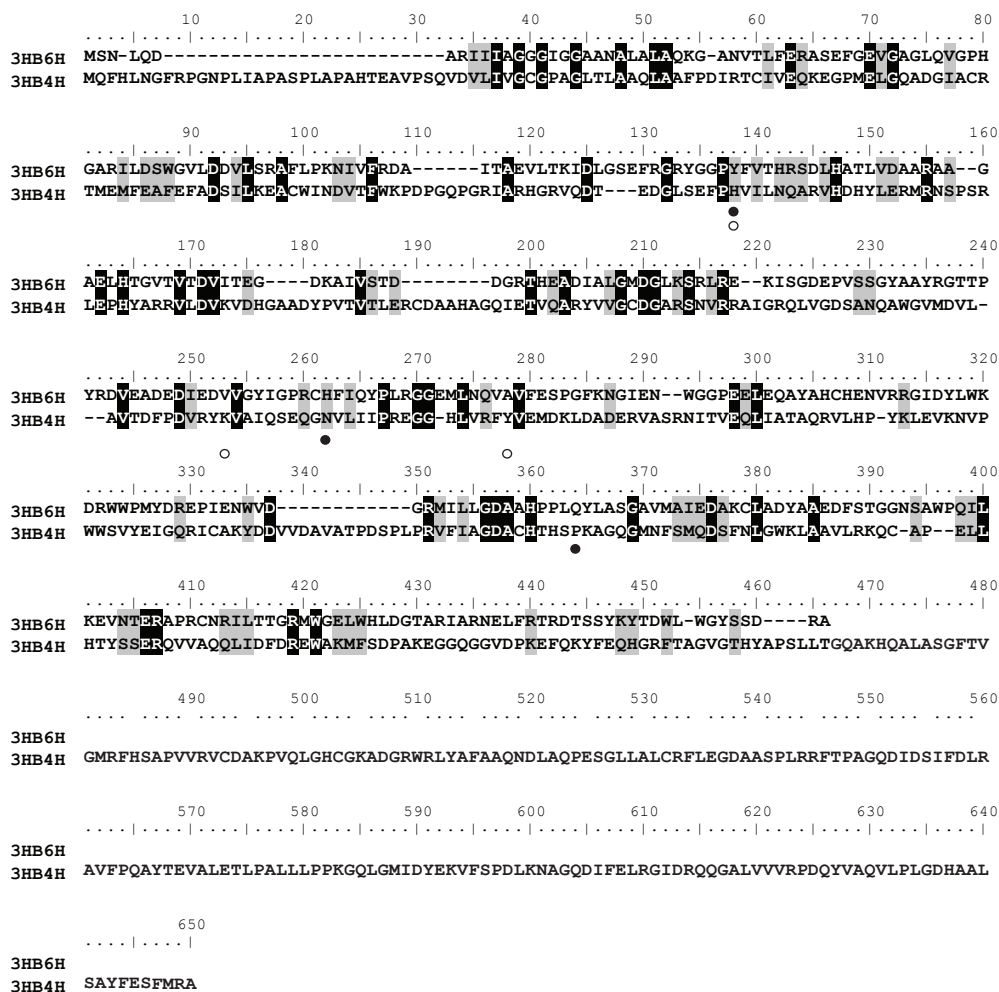


**Figure 3. Structural sequence alignment between 3HB6H and 3HB4H.** 3HB6H (PDB) and 3HB4H (PDB: 2DK1). Structural alignment was done by STRAP (Gille and Frömmel, 2001) and edited in CLUSTALW (Thompson *et al.*, 1994). Residues involved in substrate binding are highlighted in 3HB6H (black dots) and 3HB4H (white dots).

and the phospholipid (Chapter 4) we selected Cluster 1P as the representative model of 3-hydroxybenzoate binding in 3HB6H (Fig.5A). In this model, the hydroxyl group of Tyr105 is in hydrogen bond distance of the phenolic moiety of 3-hydroxybenzoate and the side chain of His213 interacts with one of the carboxyl oxygens of the substrate. Like in 3HB4H, aliphatic and hydrophobic residues such as Val228, Val230, Ile215, Trp358 and Trp362, constitute the boundaries of the substrate binding pocket. From the model, a possible role in substrate binding of Gln301 emerges, as the amide group interacts with one of the carboxyl oxygens of the substrate. Furthermore, the C6 atom of 3-hydroxybenzoate is at appropriate short distance ( $\sim 4.9$  Å) to C4A of the flavin, in agreement with *para*-hydroxylation.

Superimposition of the active site of substrate-bound 3HB6H with related flavoprotein hydroxylases fits the C6 atom of 3-hydroxybenzoate into the position of the reactive carbons of the substrates of TetX, DPHH, RebC, akalavinone 11-hydroxylase and MHPCO (data not shown, cf chapter 4).

**Characterization Of Active Site Variants.** To study the role of Tyr105, His213 and Gln301 in substrate binding and catalysis, the enzyme variants Y105F, H213A, H213S and Q301E were expressed and purified. Crystal structures were obtained of Y105F, H213S and Q301E.

All structures of the 3HB6H variants are essentially identical to the native protein, with exception of the site of mutation (Fig.5). In Y105F, no essential structural difference is observed with respect to wild-type enzyme. In H213S, the introduced serine causes the side chain of Gln301 to turn almost  $30^\circ$  degrees back in the active site (Fig.5C). Furthermore, the glutamine to glutamate replacement in Q301E leads to stacking of the glutamate side chain parallel to the isoalloxazine ring in front of flavin N3, avoiding chloride binding in that position as in wild-type enzyme (Fig.5D).

All 3HB6H variants have similar melting temperatures as wild-type enzyme ( $T_m$  between 45 and 50 °C). The mutations slightly affect the flavin absorption spectral properties of the substrate-free enzymes, especially the intensity of the maximum around 385 nm (Fig.6).

All 3HB6H variants were analyzed for their catalytic and binding properties with 3-hydroxybenzoate (Table 3 and Fig.7). Compared to wild type enzyme, Y105F shows less affinity for the aromatic substrate with a 14-fold increase in  $K_d$ . Weaker substrate binding does not affect the hydroxylation efficiency and turnover rate (Table 3). Due to a 4-fold higher apparent  $K_m$ , Y105F has a somewhat lower specificity constant ( $k_{cat}/K_m$ ) than wild-type enzyme.

H213A turns out to be almost completely inactive. No NADH oxidase activity is observed under standard assay conditions, but at higher enzyme concentration, NADH gets slowly consumed without coupling to hydroxylation. Intriguingly, the strength of substrate binding is not affected by the His213→Ala replacement. The same is true for the affinity with the substrate analogue 2,3-dihydroxybenzoate. Unfortunately, no

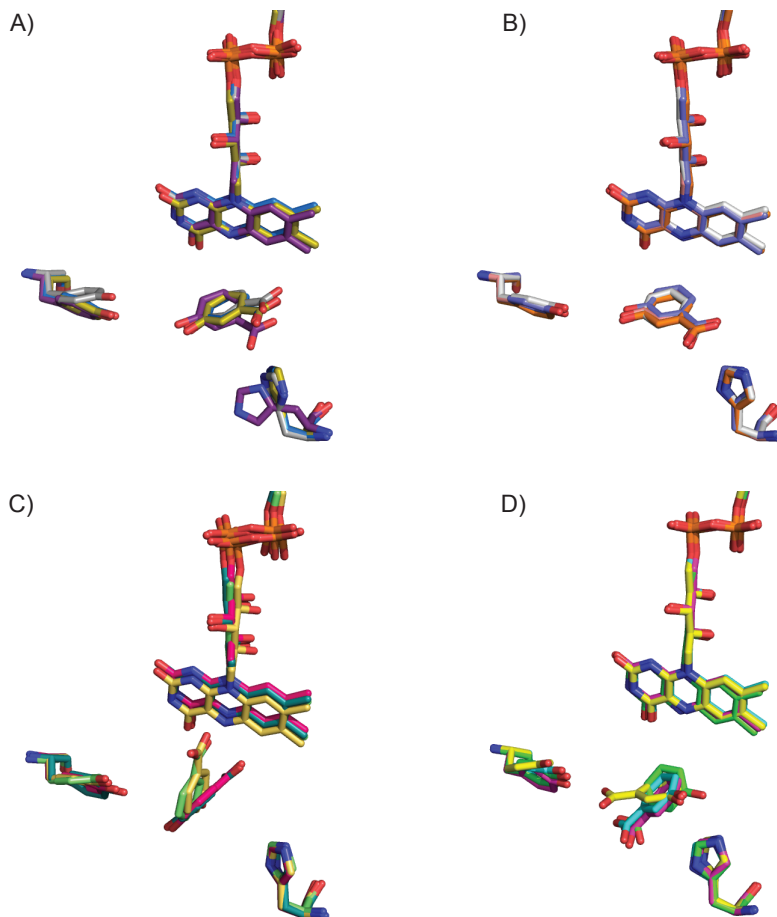


Figure 4. HADDOCK 3-hydroxybenzoate binding of 3HB6H. A) Cluster 1P, B-D) cluster 1-3.

Table 2. Statistics of HADDOCK results for the various clusters.

Cluster <sup>a</sup>	HADDOCK score (a.u) <sup>b</sup>	Ligand rmsd $E_{\min}$ (Å) <sup>c</sup>	No. of structures in the cluster	$E_{\text{vdw}}$ (kcal mol <sup>-1</sup> ) <sup>d</sup>	$E_{\text{elec}}$ (kcal mol <sup>-1</sup> )	$E_{\text{desol}}$ (kcal mol <sup>-1</sup> ) <sup>e</sup>	Buried surface area (Å <sup>2</sup> )
1	-7.4 ± 4.1	0.3 ± 0.2	103	-13.7 ± 0.6	-47.3 ± 1.4	15.9 ± 3.4	338.4 ± 6.0
2	-10.6 ± 1.2	0.4 ± 0.0	90	-9.0 ± 0.13	-113.5 ± 4.5	21.1 ± 1.1	335.9 ± 6.8
3	9.3 ± 5.8	0.4 ± 0.0	6	-12.1 ± 1.3	-25.7 ± 5.1	26.5 ± 4.9	358.2 ± 4.6
1P	-15 ± 2.1	0.3 ± 0.2	198	-14.9 ± 0.5	-60.2 ± 5.6	11.9 ± 1.5	339.4 ± 3.5

<sup>a</sup> Cluster in absence (1,2,3) or presence of phospholipid (1P)

<sup>b</sup> The HADDOCK score in arbitrary units (a.u) calculated as:

HADDOCK score = 1.0 \*  $E_{\text{vdw}}$  + 0.2 \*  $E_{\text{elec}}$  + 0.1 \*  $E_{\text{AIR}}$  + 1.0 \*  $E_{\text{desol}}$  \*  $E_{\text{vdw}}$ .  $E_{\text{vdw}}$  represents the Van der Waals energy,  $E_{\text{elec}}$  represents the electrostatic energy,  $E_{\text{AIR}}$  represents the energy from the ambiguous interaction restraints, and  $E_{\text{desol}}$  represents the empirical desolvation energy term.

<sup>c</sup> Average rmsd and SD from the overall lowest energy.

<sup>d</sup> The nonbonded energies were calculated with the OPLS parameters (Jorgensen and Tirado-Rives, 1988) using a 6.5 Å

<sup>e</sup> Empirical desolvation energy (Fernández-Recio *et al.*, 2004)



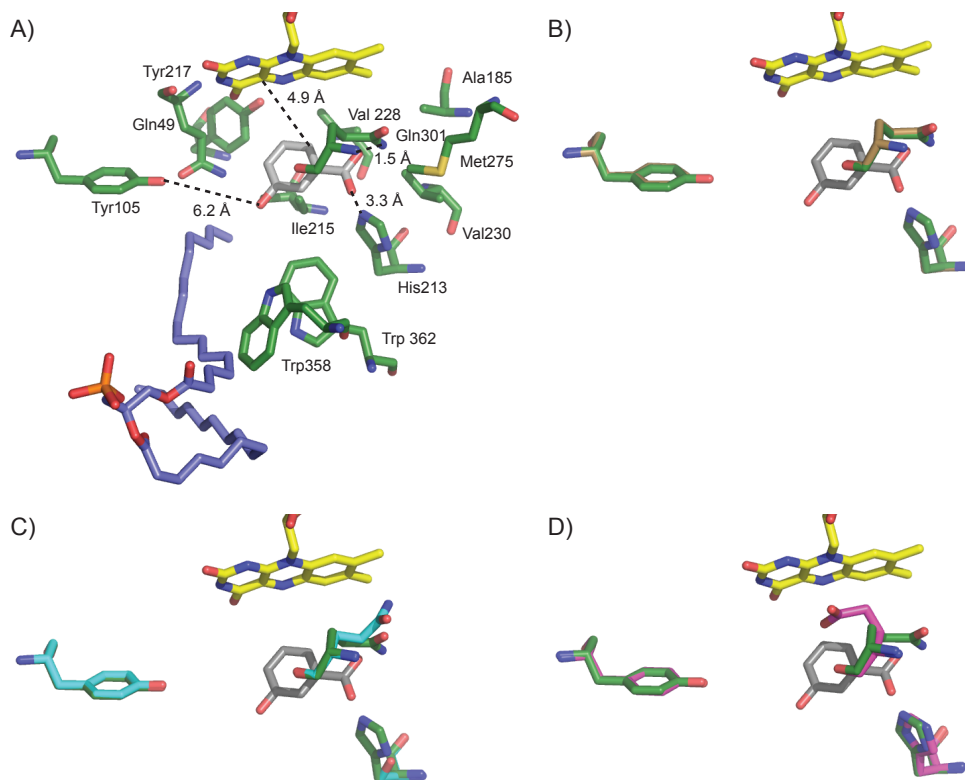


**Figure 5. Active site close-up of 3HB6H variants.** **A)** Wild-type 3HB6H with proposed substrate orientation. Bound phospholipid and FAD are represented in blue and yellow sticks, respectively. **B)** Superimposition Y105F (brown sticks) with WT active site (green sticks), **C)** Superimposition H213S (cyan sticks) with WT active site, **D)** Superimposition Q301E (magenta sticks) with WT active site.

**Table 3. Kinetic parameters and dissociation constants of enzyme-substrate complexes of 3HB6H variants.** Data are presented as the mean  $\pm$  SD of at least two independent experiments. 3-HB, 3-hydroxybenzoate; 2,3-DHB, 2,3-dihydroxybenzoate.

Enzyme	3-HB				2,3-DHB
	$K_d$ $\mu\text{M}$	$K_m$ $\mu\text{M}$	$k_{cat}$ $\text{s}^{-1}$	Uncoupling %	$K_d$ $\mu\text{M}$
WT	$48 \pm 2$	$46 \pm 3$	$35 \pm 1$	$4 \pm 0$	$63 \pm 9$
Tyr105Phe	$644 \pm 53$	$186 \pm 22$	$41 \pm 2$	$5 \pm 1$	-
His213Ala	$61 \pm 5$	-	-	$5 \pm 1$	$109 \pm 19$
His213Ser <sup>1</sup>	-	-	-	$47 \pm 12$	-
Gln301Glu <sup>1</sup>	-	-	-	$36 \pm 3$	-

<sup>1</sup>Dissociation constants and kinetic parameters not determinable due to very poor substrate binding.

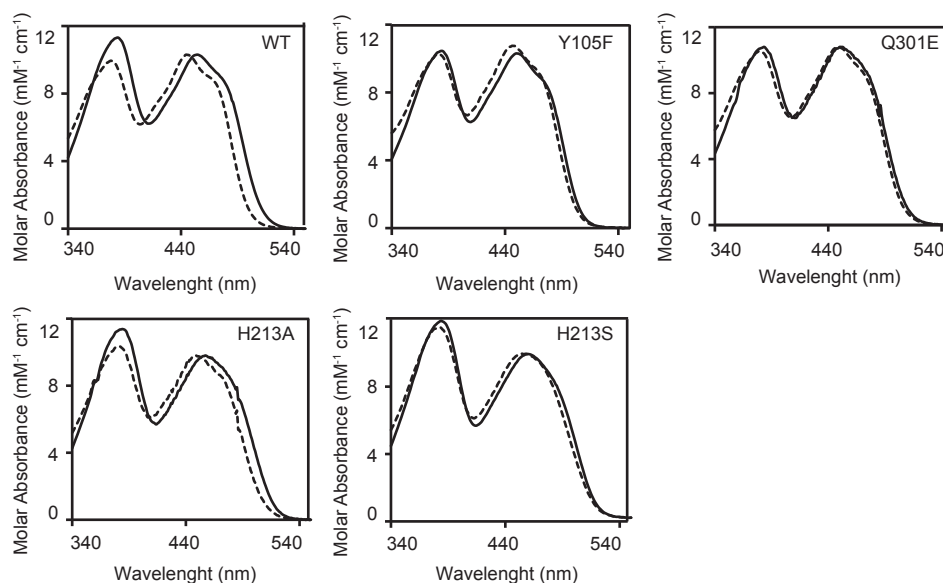


**Figure 6. Spectral properties of 3HB6H active site variants.** Optical spectra of 3HB6H<sub>WT</sub>, Y105F, H213A, H213S and Q301E. Solid line: free enzyme; dashed line: enzyme in complex with 3-hydroxybenzoate (1.3 mM).

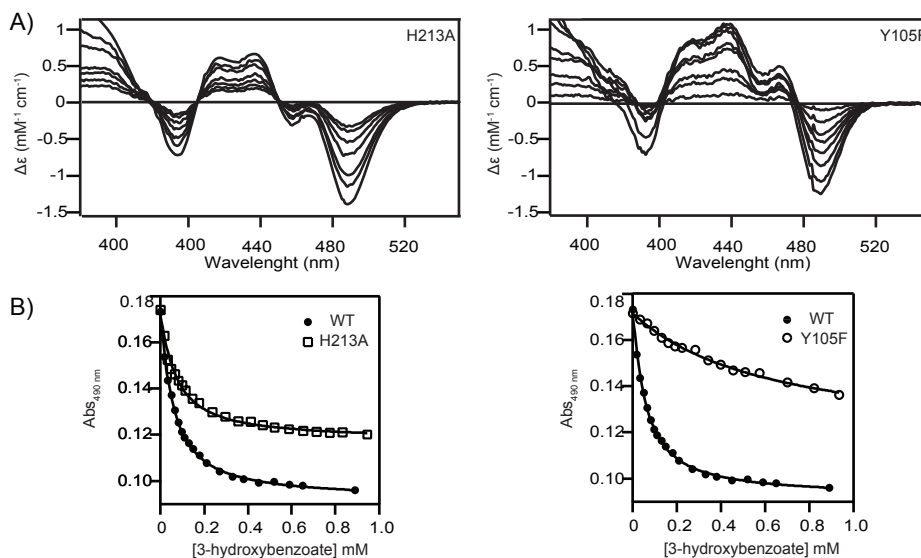


**Figure 7. Substrate binding properties of 3HB6H active site variants.** A) Absorbance difference spectra of H213A and Y105F. For clarity, only selected spectra are shown. B) Dissociation constants of H213A and Y105F variants compared to 3HB6H<sub>WT</sub>. All spectra were recorded in 50 mM TrisSO<sub>4</sub> (pH 8).

structural data are available for this 3HB6H variant. H213S deviates in behaviour from H213A. With this variant, substrate binding is strongly impaired and the enzyme acts as a poor NADH oxidase (Table 3).

The properties of Q301E are similar to those of H213S. Q301E shows increased NADH oxidase activity, no hydroxylation power and loss of substrate binding capacity. Perturbed substrate binding of Q301E is evidenced by the lack of characteristic spectral changes in the light-absorption difference spectra in the presence and absence of 3-hydroxybenzoate (Fig.6 and Fig.7).

## Discussion

Recently, the crystal structure of 3HB6H was solved (Chapter 4 and 5), but no structure of the enzyme-substrate complex was obtained. Here, we addressed the mode of 3-hydroxybenzoate binding of 3HB6H from *R. jostii* RHA1. Elucidation of the interaction between 3HB6H and its physiological substrate is particularly interesting in relation to the ability of the enzyme to perform an exclusive *para*-hydroxylation reaction. Most structurally characterized flavin-dependent hydroxylases that act on monophenols are *ortho*-hydroxylases (Monterisino *et al.*, 2011). Among them, 3HB4H represents the counterpart of 3HB6H, performing the *ortho*-hydroxylation of 3-hydroxybenzoate.

Structural comparison revealed that 3HB6H and 3HB4H share a Tyr-His pair in their active sites and that these residues might form mirror image substrate binding sites. This hypothesis was confirmed by data-driven docking, a method used to model large protein-protein complex structures (Bowyer *et al.*, 2009) and ligand-protein interactions (Rutten *et al.*, 2009; Marquer *et al.*, 2011). The docking results indicated a major role in substrate binding for Tyr105, His213 and Gln301. To probe the involvement of these residues in substrate binding and catalysis, we characterized a number of selected Tyr105, His213 and Gln301 variants.

The properties of Y105F revealed that Tyr105 has an exclusive role in binding and not in catalysis. The weak binding of the substrate in the Y105F variant indicates that the Tyr105→Phe replacement disrupts the hydrogen bond between the hydroxyl group of Tyr105 and the hydroxyl moiety of 3-hydroxybenzoate. The fact that Y105F is a competent hydroxylase suggests that Tyr105 is not needed for substrate activation and that the 3-hydroxyl moiety of the substrate does not necessarily become deprotonated during the course of the reaction. This is in line with pH-dependent binding studies (Monterisino and van Berkel, 2012) and resembles the situation reported for phenol hydroxylase (Ridder *et al.*, 2000; Xu *et al.*, 2002; Xu *et al.*, 2001), phenazine hydroxylase (Greenhagen *et al.*, 2008) and 3HB4H (Hiromoto *et al.*, 2006). A different mechanism for substrate activation applies for PHBH (Entsch and van Berkel, 1995). Here, a hydrogen bond network that extends to the protein surface is involved in ionization of the substrate phenol. This deprotonation is not only required

for substrate hydroxylation but also allows fast reduction of the flavin by NADPH (Entsch *et al.*, 1991; van Berkel *et al.*, 1994).

Substitution of His213 with Ala or Ser results into quite different 3HB6H behaviour. H213A is completely inactive but perfectly able to bind 3-hydroxybenzoate and 2,3-dihydroxybenzoate. As a consequence, His213 seems to have a primary role in catalysis. On the other hand, H213S has lost the ability to bind the substrate and acts as a poor NADH oxidase. The crystallographic data of H213S suggest that movement of the Gln301 side chain away from the 3-hydroxybenzoate carboxylic group impairs substrate binding in this variant. The important role of Gln301 in substrate binding is supported by the properties of Q301E. The Gln301→Glu replacement results in stacking of the glutamate residue parallel to the isoalloxazine ring, a position occupied in the native structure by chloride ion(s). Besides impairing substrate binding, the orientation of the Glu310 side chain next to the flavin likely disturbs the reactivity of the enzyme with oxygen and the stabilization of the flavin C4a-hydroperoxide. In the H213A variant, Gln301 apparently keeps the substrate firmly bound, suggesting that His213 mainly is needed for stabilizing the transition state during the hydroxylation reaction. Rapid kinetics of the reductive and oxidative half-reactions are needed to see if the His213→Ala replacement also affects the reaction of the enzyme with NADH and possibly other reaction steps.

The results presented here suggest that 3HB4H and 3HB6H possess functional mirror image binding sites. Mirror image enzymes are not uncommon in nature; they have been studied mainly in relation to enantiocomplementarity (Jorgensen and Tirado-Rives, 1988; Mattevi *et al.*, 1996; Fraaije and Mattevi, 2000; Mugford *et al.*, 2008). A good example of mirror image flavoenzymes is provided by D-amino acid oxidase (DAAO) and L-amino acid oxidase (LAAO) and vanillyl-alcohol oxidase (VAO) (Pawelek *et al.*, 2000) and *p*-cresol methylhydroxylase (PCMH) (Mattevi *et al.*, 1997). Based on structural insights it was possible to redesign the enantioselectivity of VAO to the one of PCMH by transferring the active site base to the other site of the substrate binding pocket (van den Heuvel *et al.*, 2000). Like above mentioned flavoproteins 3HB4H and 3HB6H possess the same protein fold and their active sites display mirror images. Furthermore, FAD represents the pivot around the active site is built to ensure regioselective hydroxylation.

3HB4H and 3HB6H represents the first example of a flavoenzyme pair for which regioselective hydroxylation is based on mirror image active sites. Recently, van Pée and collaborators (Lang *et al.*, 2011), tried to exchange the regioselectivity of the flavoprotein monooxygenases tryptophan 7-halogenase (PrnA) and tryptophan 5-halogenase (PyrH). Directed mutagenesis, supported by previous data on the role of residues in binding and catalysis (Dong *et al.*, 2005; Flecks *et al.*, 2008), permitted the production of a mixture of halogenated compounds with the expected regioselectivity. From the inspection of the model of bound tryptophan to PrnA and the suggested orientation of the substrate for 5-halogenation, we also noticed a mirroring among the

orientation of the tryptophan substrates, but not at the protein level.

In summary, the results presented here provide evidences for a different role of substrate binding residues in *ortho* and *para* 3-hydroxybenzoate hydroxylases. Several questions regarding the exact role of Tyr105, His213 and Gln301 in 3HB6H catalysis are still open, and rapid kinetics experiments may sort out unanswered points. Moreover, mirror-imaging as rationale behind the redesign of flavoprotein hydroxylase active sites could be a powerful tool for biocatalysis.

## Acknowledgments

This study was supported by the Integrated Biosynthesis Organic Synthesis (IBOS) project of the Netherlands Organization for Scientific Research (NWO). We thank the Dutch BiG Grid project (NWO) for the use of computing and storage facilities.

## References

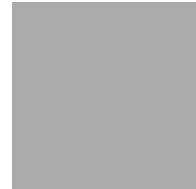
- Bowyer, A., Mikolajek, H., Stuart, J.W., Wood, S.P., Jamil, F., Rashid, N., Akhtar, M. and Cooper, J.B., (2009) Structure and function of the L-threonine dehydrogenase (TKTDH) from the hyperthermophilic archaeon *Thermococcus kodakaraensis*. *Journal of Structural Biology*, 168(2), 294–304.
- Collaborative Computational Project, Number 4, (1994) The CCP4 suite: programs for protein crystallography. *Acta crystallographica. Section D, Biological crystallography*, 50(5), 760–763.
- de Vries, S.J., van Dijk, M. and Bonvin, A.M.J.J., (2010) The HADDOCK web server for data-driven biomolecular docking. *Nature Protocols*, 5(5), 883–897.
- DeLano, W.L., (2010) The PyMOL Molecular Graphics System, Version 1.3r1 L. Schroedinger, ed.
- Dong, C., Flecks, S., Unversucht, S., Haupt, C., van Pée, K.-H. and Naismith, J.H., (2005) Tryptophan 7-halogenase (PmA) structure suggests a mechanism for regioselective chlorination. *Science*, 309(5744), 2216–2219.
- Emsley, P., Lohkamp, B., Scott, W.G. and Cowtan, K., (2010) Features and development of Coot. *Acta crystallographica. Section D, Biological crystallography*, 66(Pt 4), 486–501.
- Enroth, C., (2003) High-resolution structure of phenol hydroxylase and correction of sequence errors. *Acta crystallographica. Section D, Biological crystallography*, 59(Pt 9), 1597–1602.
- Enroth, C., Neujahr, H., Schneider, G. and Lindqvist, Y., (1998) The crystal structure of phenol hydroxylase in complex with FAD and phenol provides evidence for a concerted conformational change in the enzyme and its cofactor during catalysis. *Structure (London, England : 1993)*, 6(5), 605–617.
- Entsch, B. and van Berkel, W.J.H., (1995) Structure and mechanism of *para*-hydroxybenzoate hydroxylase. *FASEB Journal*, 9(7), 476–483.
- Entsch, B., Cole, L.J. and Ballou, D.P., (2005) Protein dynamics and electrostatics in the function of *p*-hydroxybenzoate hydroxylase. *Archives of Biochemistry and Biophysics*, 433(1), 297–311.
- Entsch, B., Palfey, B.A., Ballou, D.P. and Massey, V., (1991) Catalytic function of tyrosine residues in *para*-hydroxybenzoate hydroxylase as determined by the study of site-directed mutants. *Journal of Biological Chemistry*, 266(26), 17341–17349.
- Fernández-Recio, J., Totrov, M. and Abagyan, R., (2004) Identification of protein-protein interaction sites from docking energy landscapes. *Journal of Molecular Biology*, 335(3), 843–865.
- Flecks, S., Patallo, E.P., Zhu, X., Ernyei, A.J., Seifert, G., Schneider, A., Dong, C., Naismith, J.H. and van Pée, K.-H., (2008) New insights into the mechanism of enzymatic chlorination of tryptophan. *Angewandte Chemie*, 47(49), 9533–9536.
- Fraaije, M.W. and Mattevi, A., (2000) Flavoenzymes: diverse catalysts with recurrent features. *Trends in biochemical sciences*, 25(3), 126–132.
- Fuchs, G., Boll, M. and Heider, J., (2011) Microbial degradation of aromatic compounds - from one strategy to four. *Nature Reviews Microbiology*, 9(11), 803–816.
- Gille, C. and Frömmel, C., (2001) STRAP: editor for STRuctural Alignments of Proteins. *Bioinformatics*, 17(4), 377–378.
- Greenhagen, B.T., Shi, K., Robinson, H., Gamage, S., Bera, A.K., Ladner, J.E. and Parsons, J.F., (2008) Crystal structure of the pyocyanin biosynthetic protein PhzS. *Biochemistry*, 47(19), 5281–5289.
- Harwood, C.S. and Parales, R.E., (1996) The beta-ketoadipate pathway and the biology of self-identity. *Annual Reviews in Microbiology*, 50, 553–590.
- Hiramoto, T., Fujiwara, S., Hosokawa, K. and Yamaguchi, H., (2006) Crystal structure of 3-hydroxybenzoate hydroxylase from *Comamonas testosteroni* has a large tunnel for substrate and oxygen access to the active site. *Journal of Molecular Biology*, 364(5), 878–896.

- Johnson, K.A. and Goody, R.S., (2011) The original Michaelis constant: translation of the 1913 Michaelis–Menten paper. *Biochemistry*, 50(39), 8264–8269.
- Jorgensen, W.L. and Tirado-Rives, J., (1988) The OPLS [optimized potentials for liquid simulations] potential functions for proteins, energy minimizations for crystals of cyclic peptides and crambin. *Journal of the American Chemical Society*, 110(6), 1657–1666.
- Lang, A., Polnick, S., Nicke, T., William, P., Patallo, E.P., Naismith, J.H. and van Pée, K.-H., (2011) Changing the regioselectivity of the tryptophan 7-halogenase PrnA by site-directed mutagenesis. *Angewandte Chemie*, 50(13), 2951–2953.
- Marquer, C., Fruchart-Gaillard, C., Letellier, G., Marcon, E., Mourier, G., Zinn-Justin, S., Ménez, A., Servent, D. and Gilquin, B., (2011) Structural model of ligand-G protein-coupled receptor (GPCR) complex based on experimental double mutant cycle data. *Journal of Biological Chemistry*, 286(36), 31661–31675.
- Massey, V., (1994) Activation of molecular oxygen by flavins and flavoproteins. *Journal of Biological Chemistry*, 269(36), 22459–22462.
- Mattevi, A., Fraaije, M.W., Mozzarelli, A., Olivi, L., Coda, A. and van Berkel, W.J.H., (1997) Crystal structures and inhibitor binding in the octameric flavoenzyme vanillyl-alcohol oxidase: the shape of the active-site cavity controls substrate specificity. *Structure (London, England : 1993)*, 5(7), 907–920.
- Mattevi, A., Vanoni, M.A., Todone, F., Rizzi, M., Teplyakov, A., Coda, A., Bolognesi, M. and Curti, B., (1996) Crystal structure of D-amino acid oxidase: a case of active site mirror-image convergent evolution with flavocytochrome b2. *Proceedings of the National Academy of Sciences of the United States of America*, 93(15), 7496.
- Montersino, S. and van Berkel, W.J.H., (2012) Functional annotation and characterization of 3-hydroxybenzoate 6-hydroxylase from *Rhodococcus jostii* RHA1. *Biochimica et biophysica acta*, 1824(3), 433–442.
- Montersino, S., Tischler, D., Gassner, G.T. and van Berkel, W.J.H., (2011) Catalytic and structural features of flavoprotein hydroxylases and epoxidases. *Advanced Synthesis & Catalysis*, 353(13), 2301–2319.
- Moonen, M.J.H., Synowsky, S.A., Van Den Berg, W.A.M., Westphal, A.H., Heck, A.J.R., van den Heuvel, R.H.H., Fraaije, M.W. and van Berkel, W.J.H., (2008) Hydroquinone dioxygenase from *Pseudomonas fluorescens* ACB: a novel member of the family of nonheme-iron(II)-dependent dioxygenases. *Journal of Bacteriology*, 190(15), 5199–5209.
- Mugford, P.F., Wagner, U.G., Jiang, Y., Faber, K. and Kazlauskas, R.J., (2008) Enantiocomplementary enzymes: classification, molecular basis for their enantioselectivity, and prospects for mirror-image biotransformations. *Angewandte Chemie*, 47(46), 8782–8793.
- Nabuurs, S.M., Westphal, A.H., van den Toorn, M., Lindhoud, S. and van Mierlo, C.P.M., (2009) Topological switching between an alpha-beta parallel protein and a remarkably helical molten globule. *Journal of the American Chemical Society*, 131(23), 8290–8295.
- Pawelek, P.D., Cheah, J., Coulombe, R., Macheroux, P., Ghisla, S. and Vrielink, A., (2000) The structure of L-amino acid oxidase reveals the substrate trajectory into an enantiomerically conserved active site. *EMBO Journal*, 19(16), 4204–4215.
- Pérez-Pantoja, D., González, B. and Pieper, D., (2010) Aerobic degradation of aromatic hydrocarbons. *Handbook of Hydrocarbon and Lipid Microbiology*, 2, 800–837.
- Phale, P.S., Basu, A., Majhi, P.D., Deveryshtetty, J., Vamsee-Krishna, C. and Shrivastava, R., (2007) Metabolic diversity in bacterial degradation of aromatic compounds. *Omics : a journal of integrative biology*, 11(3), 252–279.
- Potterton, L., McNicholas, S., Krissinel, E., et al., (2004) Developments in the CCP4 molecular-graphics project. *Acta crystallographica. Section D. Biological crystallography*, 60(Pt 12 Pt 1), 2288–2294.
- Ridder, L., Palfey, B.A., Vervoort, J. and Rietjens, I.M., (2000) Modelling flavin and substrate substituent effects on the activation barrier and rate of oxygen transfer by *p*-hydroxybenzoate hydroxylase. *FEBS Letters*, 478(1–2), 197–201.
- Rutten, L., Mannie, J.-P.B.A., Stead, C.M., et al., (2009) Active-site architecture and catalytic mechanism of the lipid A deacylase LpxR of *Salmonella typhimurium*. *Proceedings of the National Academy of Sciences of the United States of America*, 106(6), 1960–1964.
- Schreuder, H.A., Prick, P.A., Wierenga, R.K., Vriend, G., Wilson, K.S., Hol, W.G. and Drenth, J., (1989) Crystal structure of the *p*-hydroxybenzoate hydroxylase-substrate complex refined at 1.9 Å resolution. Analysis of the enzyme-substrate and enzyme-product complexes. *Journal of Molecular Biology*, 208(4), 679–696.
- Thompson, J.D., Higgins, D.G. and Gibson, T.J., (1994) CLUSTAL W: improving the sensitivity of progressive multiple sequence alignment through sequence weighting, position-specific gap penalties and weight matrix choice. *Nucleic Acids Research*, 22(22), 4673–4680.
- van Berkel, W.J.H., Eppink, M.H. and Schreuder, H.A., (1994) Crystal structure of *p*-hydroxybenzoate hydroxylase reconstituted with the modified FAD present in alcohol oxidase from methylotrophic yeasts: evidence for an arabinoflavin. *Protein Science*, 3(12), 2245–2253.
- van den Heuvel, R.H., Fraaije, M.W., Ferrer, M., Mattevi, A. and van Berkel, W.J.H., (2000) Inversion of stereospecificity of vanillyl-alcohol oxidase. *Proceedings of the National Academy of Sciences of the United States of America*, 97(17), 9455–9460.
- Xu, D., Ballou, D.P. and Massey, V., (2001) Studies of the mechanism of phenol hydroxylase: mutants Tyr289Phe, Asp54Asn, and Arg281Met. *Biochemistry*, 40(41), 12369–12378.
- Xu, D., Enroth, C., Lindqvist, Y., Ballou, D.P. and Massey, V., (2002) Studies of the mechanism of phenol hydroxylase: effect of mutation of proline 364 to serine. *Biochemistry*, 41(46), 13627–13636.









# Summary and General Discussion

Stefania Montersino<sup>1</sup> and Willem J. H. van Berkel<sup>1</sup>

<sup>1</sup> Laboratory of Biochemistry, Wageningen University,  
Dreijenlaan 3, 6703 HA Wageningen, The Netherlands

## Summary

This thesis focuses on the structural and biochemical characterization of 3-hydroxybenzoate 6-hydroxylase (3HB6H), a flavoprotein monooxygenase that catalyzes the *para*-hydroxylation of 3-hydroxybenzoate to gentisate (2,5-dihydroxybenzoate).

As described in **Chapter 2**, flavoprotein hydroxylases are involved in many biological processes, having no enzymatic equivalent regarding substrate specificity. Substrate binding in flavoprotein hydroxylases tightly controls flavin reduction, increases the stability of flavin-oxygen adducts and creates an optimal environment for efficient and regioselective aromatic hydroxylation. Despite longstanding research, the structural basis of the regioselectivity of flavoprotein hydroxylases is not well understood.

Sequence-based discovery of flavoprotein hydroxylases makes use of three fingerprints mapping different parts of the FAD binding site. By using the oxygenase-rich actinomycete *Rhodococcus jostii* RHA1 as genome source, 18 putative flavoprotein hydroxylase sequences were retrieved (**Chapter 3**). Based on comparison with known enzymes and phylogenetic analysis, several genes were re-annotated and putative functions to different sequences were assigned. 3-Hydroxybenzoate 6-hydroxylase (3HB6H), originally misannotated as salicylate hydroxylase (Fig.1),

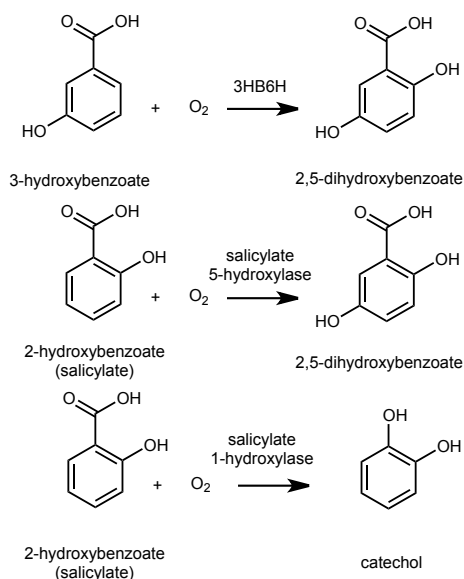


**Figure 1.** Overview of reaction catalyzed by 3-hydroxybenzoate 6-hydroxylase (3HB6H) and salicylate hydroxylases.

was biochemically characterized. *R. jostii* 3HB6H is a FAD-containing homodimer, preferring NADH as coenzyme. The enzyme displays a narrow substrate specificity, being most efficient with 3-hydroxybenzoate, 2,3-dihydroxybenzoate and 3,5-dihydroxybenzoate. The physiological product gentisate is a true effector, strongly stimulating NADH oxidation.

The structural properties of *R. jostii* 3HB6H were disclosed in **Chapter 4** and **Chapter 5**. In agreement with hydrodynamic data it was unambiguously established that the enzyme is a homodimer (Fig.2). High-resolution three-dimensional structures of substrate-free 3HB6H were obtained from protein produced in *E. coli* and in

the newly developed expression strain *R. jostii* RHA1#2. The overall 3HB6H structure shares a common fold with *p*-hydroxybenzoate hydroxylase and other flavoprotein hydroxylases. The isoalloxazine ring of the FAD cofactor of 3HB6H is located *in* the active site, with no hint for flavin mobility, as found with other family members. Next to the *re*-side of the flavin, electron density was found for chloride ions, pointing to a possible oxygen binding site.

**Chapter 4** and **Chapter 5** also describe a new feature of flavoprotein hydroxylases. It is demonstrated that 3HB6H from *R. jostii* RHA1 binds phospholipids at the dimerization interface (Fig.2). Moreover, evidence is provided that the type of phospholipid ligand depends on the bacterial membrane composition of the expression host. Phosphatidylinositol, the natural ligand in the Gram-positive *R. jostii* strain, is replaced by a mixture of phosphatidylethanolamine and phosphatidylglycerol when the enzyme is expressed in *E. coli*. The entrapped phospholipids might act as protein glue, since 3HB6H dimers containing only one lipid split easier to monomers in the gas phase.

3HB6H from *Pseudomonas alcaligenes* NCIMB 9867 shows 33 % sequence identity with 3HB6H from *R. jostii* RHA1. Several aminoacid substitutions are found in the dimerization domain. Nevertheless, the *P. alcaligenes* enzyme also contains phosphatidylethanolamine and phosphatidylglycerol when expressed in *E. coli* (**Chapter 6**). Thus, phospholipid binding seems to be a common feature of the 3HB6H family. Interesting differences between both 3HB6H enzymes were found regarding substrate specificity and hydroxylation capacity. *R. jostii* 3HB6H is most active with 3-hydroxybenzoate, while *P. alcaligenes* 3HB6H uses 3-hydroxy-4-methylbenzoate as best substrate.

In **Chapter 7** substrate docking and active site-directed mutagenesis were used to address the regioselectivity of hydroxylation of 3HB6H. Data-driven substrate docking pointed to the involvement of a His-Tyr pair in substrate binding. Such amino acid pair is present in a mirror image position in the sister enzyme 3HB4H from *Comamonas testosteroni* and provides a *rationale* for the regioselectivity of 3-hydroxybenzoate hydroxylation (Fig.3). Active site variants of *R. jostii* 3HB6H revealed that His213 is essential for catalysis and that Tyr105 is critically involved in substrate binding, raising questions about the mechanism of 3HB6H hydroxylation.

---

**Figure 3.** (Next page) **Active sites comparison between 3HB6H and 3HB4H.** **A)** Crystal structure of the active site of 3HB4H with bound 3-hydroxybenzoate (PDB: 2DKI). **B)** Crystal structure of the active site of 3HB6H. Residues are indicated in green stick, cofactor in yellow stick and substrate in grey stick. Lower panel: Scheme of mirror image binding site between 3HB4H and 3HB6H. C4a of the flavin and carbon subjected to hydroxylation are indicated with an asterisk (\*).

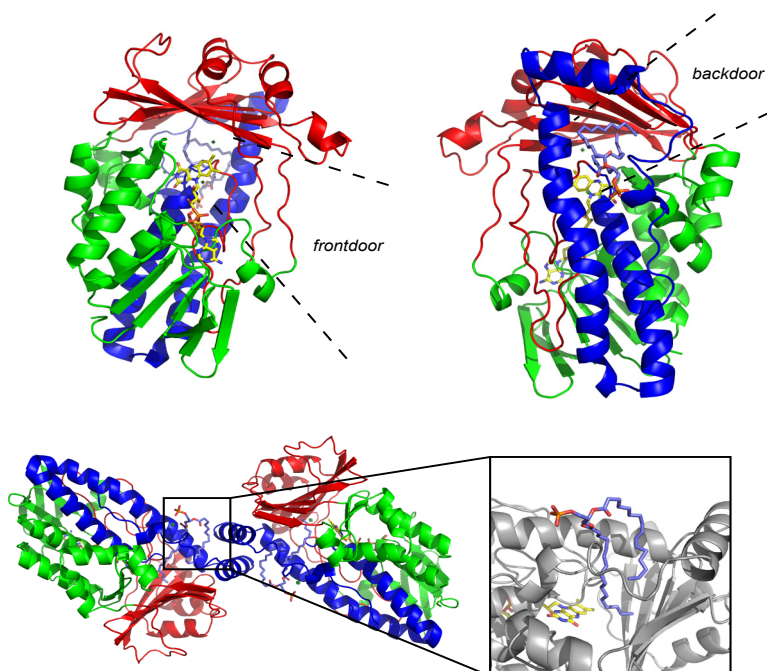
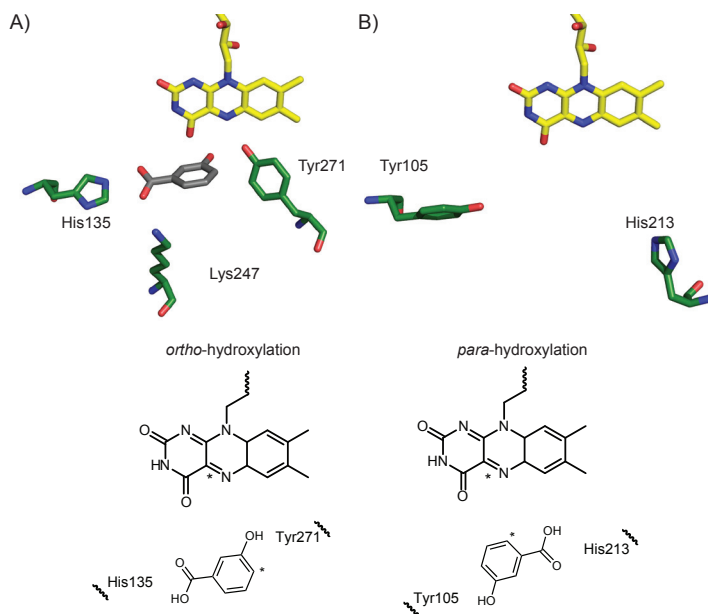


Figure 2. Overall structure of 3HB6H from *R. jostii* RHA1. Upper panel: monomer view from front side and back side. Lower panel: Dimer of 3HB6H and magnification of lipid binding pocket.



## General Discussion

### Prediction Of Function From Sequence

Coupling a function to a primary protein sequence is a challenge, and the huge number of unknown or misannotated protein sequences deposited in databases could at first complicate the assignment (Furnham *et al.*, 2009). The Enzyme Functional Initiative (EFI) is trying to build a multidisciplinary approach for functional assignment of unknown enzymes (Gerlt *et al.*, 2011). The strategy comprehends truly computational tools complemented with experimental activity screening, crystal structural assignment and *in vivo* studies. The approach will result in a breakthrough to deduce functional properties from large scale analysis of enzyme (super)families and from metagenomic samples (Brown and Babbitt, 2012).

On a smaller scale, effort has been put in flavoprotein monooxygenase genome mining thanks to different sequence fingerprints (Eppink *et al.*, 1997; Fraaije *et al.*, 2002; Macheroux *et al.*, 2011). Combination of optimized soluble protein expression and activity screening in cell extracts provided insight into the biocatalytic potential of Baeyer-Villiger monooxygenases from *R. jostii* RHA1 (Riebel *et al.*, 2012; Szolkowy *et al.*, 2009). Moreover, structure-based multiple sequence alignments highlighted a new fingerprint more discriminative for identifying BVMOs (Riebel *et al.*, 2012).

The innate narrow specificity of flavoprotein hydroxylases limited the use of the above described strategy for assigning functions to unknown family members in *R. jostii* RHA1. Even though multiple sequence alignments gave an initial clue about (im)possible function, including operon and genome context analysis was essential for reliable assignments (**Chapter 3**). Among different approaches, this strategy might be the most effective because prokaryotic flavoprotein hydroxylases are involved in many metabolic pathways, either conserved or combined in a patchwork fashion.

Based on our assignments (**Chapter 3**), interesting targets for future research are the putative rifampicin monooxygenase (Q0S0L2), an enzyme able to inactivate *Mycobacterium* and *Rhodococcus* antibiotics (Andersen *et al.*, 1997; Hoshino *et al.*, 2010), and a protein (Q0SJG8), most likely belonging to a subgroup of hydroxylases acting on Coenzyme A (CoA) activated substrates. Next to biomedical impact, rifampicin monooxygenase is of mechanistic interest because it might share catalytic features with *N*-hydroxylating enzymes (Meneely *et al.*, 2009; Olucha and Lamb, 2011). Addressing the properties of flavoprotein hydroxylases acting on CoA activated substrates could answer interesting questions about CoA recognition, fingerprint design and consequences of CoA activation on flavoprotein oxygenation power (Schühle *et al.*, 2001).

### 3HB6H Structure

In the last few years several new flavoprotein hydroxylase structures were solved ((Montersino *et al.*, 2011); **Chapter 2**). All these structures share a PHBH fold with a striking conservation of overall topology. This structural conservation stresses the capacity of this fold to adapt to different catalytic and binding abilities (Mattevi, 1998). Indeed, we found that 3HB6H contains a PHBH fold (**Chapter 4**). The overall architecture appeared to be closest to that of 2-methyl-3-hydroxypyridine-5-carboxylic acid oxygenase (MHPCO) (McCulloch *et al.*, 2009), phenazine-1-carboxylate hydroxylase (PhzS) (Greenhagen *et al.*, 2008), and 2,6-dihydroxypyridine hydroxylase (DHPH) (Treiber and Schulz, 2008). This shows that flavoprotein hydroxylases that use the same substrate, such as 3HB4H and 3HB6H, do not necessarily share the highest structural homology.

The PHBH fold arises interesting questions about oligomerization features of flavoprotein hydroxylases. The dimerization domain is built around three conserved helices, but quaternary structures show different trends: monomer (RebC, RdmE, TetX and PhzS), dimer (PHBH, PgaE, CabE and 3HB6H), tetramer (MHPCO), and unusual dimers (PHHY and 3HB4H and DHPH). Differences in dimerization among 3HB6H, CabE/PgaE and PHBH are caused by slipping of monomers towards one helix-helix contact surface, strengthened by lipid binding in 3HB6H (**Chapter 4**).

### Phospholipid Binding

A major finding of this thesis is that 3HB6H binds phospholipids at the dimer interface (**Chapter 4-6**). 3HB6H proteins from different origin were shown to have the intrinsic ability to bind phospholipids with acyl chains between C14 and C19, with a phospholipid of C32 (16:0/16:0) bound in all refined crystal structures. Phospholipid binding might stimulate dimerization, since 3HB6H containing only one phospholipid easier dissociates into monomers in the gas phase. Lipid binding is extremely tight and the lipid is only released under denaturing conditions. For instance, apo-dimer generated by urea treatment remains saturated with phospholipid.

In **Chapter 5** we showed that the membrane composition of the bacterial host modulates the type of phospholipids bound. As a result, phosphatidylinositol was found as natural ligand in *Rhodococcus*, while a mixture of phosphatidylethanolamine and phosphatidylglycerol was found as ligand in the *E. coli* expressed proteins. The hydrophilic head group and phosphate moiety of the phospholipid do no influence the interaction with 3HB6H. The head group is not visible in the crystal structure, suggesting that it protrudes out of the protein and is mobile. The phosphate ester interacts with Arg350 and Lys385, but K385D and K358A mutations do not affect lipid binding.

3HB6H from *P. alcaligenes* NCIMB 9816 contains a less hydrophobic lipid



binding tunnel, nevertheless lipid binding is retained (**Chapter 6**). It would be interesting to determine by scanning mutagenesis the minimal sequence required for lipid binding. Such signature sequence could be used to screen potential lipid-binding proteins with similar binding features as 3HB6H. A sequence signature has been proposed for sphingolipid binding of protein transmembrane domains (Contreras *et al.*, 2012).

### Substrate Binding

Substrate transport in flavoprotein hydroxylases is unclear. For PHBH it was proposed that the aromatic substrate enters the protein from the front (cf. Fig.2) and that conformational rearrangements including flavin movement are needed to guide the substrate to the active site (Entsch *et al.*, 2005). For 3HB4H it was proposed that substrate and oxygen use a specific entrance tunnel (Hiromoto *et al.*, 2006). In rebeccamycin hydroxylase (RebC), the substrate is believed to enter from the back (cf. Fig.2). The same helix portion that defines 3HB6H lipid binding is disordered in the unliganded form of RebC and gets ordered upon substrate binding or flavin reduction (Ryan *et al.*, 2008). The backdoor substrate entrance and ensuing helix formation in RebC represents an important novelty among flavoprotein hydroxylases. The same melting helix concept is probably shared by PhzS (Greenhagen *et al.*, 2008) as a system to lock and hide the substrate in the active site.

In 3HB6H, the phospholipid acts as a plug and closes the backdoor tunnel that runs from the surface till the active site (**Chapter 4-6**). This tunnel seems not to be involved in substrate transport because *R. jostii* 3HB6H behaves as fully active enzyme (Sucharitakul *et al.*, 2012). An intriguing possibility is the protecting role of phospholipid during catalysis. Once 3-hydroxybenzoate is bound and flavin gets reduced by NADH, formation of oxygen-flavin adduct in a solvent excluded environment is crucial for the stabilization of the C4a-hydroperoxyflavin. Phenol hydroxylase possesses a lid that, upon substrate binding, rolls over the FAD cleft (Enroth, 2003), while RebC closes off the active site *via* helix formation on top of substrate tunnel (Ryan *et al.*, 2008). Bound phospholipid in 3HB6H might prevent transport to the active site of water molecules, thus preventing fast decay of the flavin-oxygen adduct and subsequent formation of hydrogen peroxide.

### Regioselectivity Of Hydroxylation

3HB6H catalyzes the *para*-hydroxylation of 3-hydroxybenzoate, while 3HB4H hydroxylates the same substrate at the *ortho*-position. Insight into the structural determinants of regioselective 3-hydroxybenzoate hydroxylation was hampered by the lack of structural data of the 3HB6H enzyme-substrate complex. Comparison of the structure of unliganded 3HB6H with 3HB4H, chloride binding at the active site

and substrate docking filled the gap.

Chloride ions can be a valid surrogate of substrate oxygens (Kommoju *et al.*, 2011). 3HB6H crystallized in substrate-free form contains a few chloride atoms that bind at the re-side of the flavin in front of N5 and at the end of the dipole of helix H11. This location might be a preorganized site for oxygen binding and activation (Baron *et al.*, 2009; Kommoju *et al.*, 2011). Moreover, chlorides were mimicking quite well the position of the hydroxyl group of 3-hydroxybenzoate in the substrate-docking model, offering a further example of chloride as oxygen probe.

Data-driven docking suggested that 3HB6H and 3HB4H possess functional mirror image substrate binding sites (Fig.3). Biochemical and structural analysis of active site variants revealed that His213 in 3HB6H is essential for catalysis and that Tyr105 and Gln301 are critically involved in substrate binding. The estimated steady-state kinetic parameters of the active site variants provide an excellent starting point for detailed rapid kinetic experiments. Dissecting the two half-reactions will more clearly reveal which steps in the catalytic cycle are compromised. There is also a need to study the catalytic properties of other active site variants, as for example H213N, H213Y, Q301N and Q301A.

Although the elucidation of the 3HB6H hydroxylation mechanism must await further studies, an initial picture of substrate conversion can be drawn. Activation of the substrate by deprotonation is not a strategy for 3HB6H or 3HB4H; in fact both proteins do not influence the acidity of the 3-hydroxyl group of the substrate by shifting the  $pK_a$  (Hiromoto *et al.*, 2006). Sucharitakul and colleagues proposed that the reduction mechanism of 3HB6H involves an isomerization of the initial enzyme-ligand complex to a fully activated form before flavin reduction takes place (Sucharitakul *et al.*, 2012). Possible isomerization steps might involve positioning of residues for optimal substrate attack.

### NADH Binding And Flavin Mobility

The crystal structure of 3HB6H provides no clue for the binding mode of the NADH coenzyme. With substrate bound there is no room for the nicotinamide moiety to enter the active site. This suggests that flavin mobility, as observed in other flavoprotein hydroxylases (Montersino *et al.*, 2011), is an integral part of the catalytic process. However, with the information currently available, other conformational rearrangements cannot be excluded.

To conclude, the results emerged in this thesis provide a solid foundation for further structural and kinetic studies on 3HB6H and related enzymes. The knowledge acquired in this research improves our insight into the strategies of flavin-dependent regioselective hydroxylation, and adds a meaningful piece to the flavoprotein monooxygenase repertoire.

## References

- Andersen, S.J., Quan, S., Gowan, B. and Dabbs, E.R., (1997) Monooxygenase-like sequence of a *Rhodococcus equi* gene conferring increased resistance to rifampin by inactivating this antibiotic. *Antimicrobial agents and chemotherapy*, 41(1), 218–221.
- Baron, R., Riley, C., Chenprakhon, P., et al., (2009) Multiple pathways guide oxygen diffusion into flavoenzyme active sites. *Proceedings of the National Academy of Sciences of the United States of America*, 106(26), 10603–10608.
- Brown, S.D. and Babbitt, P.C., (2012) Inference of functional properties from large-scale analysis of enzyme superfamilies. *Journal of Biological Chemistry*, 287(1), 35–42.
- Contreras, F.X., Ernst, A.M., Haberkant, P., et al., (2012) Molecular recognition of a single sphingolipid species by a protein's transmembrane domain. *Nature*, 481(7382), 525–529.
- Enroth, C., (2003) High-resolution structure of phenol hydroxylase and correction of sequence errors. *Acta crystallographica. Section D, Biological crystallography*, 59(Pt 9), 1597–1602.
- Entsch, B., Cole, L.J. and Ballou, D.P., (2005) Protein dynamics and electrostatics in the function of *p*-hydroxybenzoate hydroxylase. *Archives of Biochemistry and Biophysics*, 433(1), 297–311.
- Eppink, M.H.M., van Berkel, W.J.H. and Schreuder, H.A., (1997) Identification of a novel conserved sequence motif in flavoprotein hydroxylases with a putative dual function in FAD/NAD (P) H binding. *Protein Science*, 6(11), 2454–2458.
- Fraaije, M.W., Kamerbeek, N.M., van Berkel, W.J.H. and Janssen, D.B., (2002) Identification of a Baeyer-Villiger monooxygenase sequence motif. *FEBS Letters*, 518(1-3), 43–47.
- Furnham, N., Garavelli, J.S., Apweiler, R. and Thornton, J.M., (2009) Missing in action: enzyme functional annotations in biological databases. *Nature chemical biology*, 5(8), 521–525.
- Gerlt, J.A., Allen, K.N., Almo, S.C., et al., (2011) The Enzyme Function Initiative. *Biochemistry*, 50(46), 9950–9962.
- Greenhagen, B.T., Shi, K., Robinson, H., Gamage, S., Bera, A.K., Ladner, J.E. and Parsons, J.F., (2008) Crystal structure of the pyocyanin biosynthetic protein PhzS. *Biochemistry*, 47(19), 5281–5289.
- Himoto, T., Fujiwara, S., Hosokawa, K. and Yamaguchi, H., (2006) Crystal structure of 3-hydroxybenzoate hydroxylase from *Comamonas testosteroni* has a large tunnel for substrate and oxygen access to the active site. *Journal of Molecular Biology*, 364(5), 878–896.
- Hoshino, Y., Fujii, S., Shinonaga, H., Arai, K., Saito, F., Fukai, T., Satoh, H., Miyazaki, Y. and Ishikawa, J., (2010) Monooxygenation of rifampicin catalyzed by the *rox* gene product of *Nocardia farcinica*: structure elucidation, gene identification and role in drug resistance. *Journal of Antibiotics*, 63(1), 23–28.
- Kommoju, P.-R., Chen, Z.-W., Bruckner, R.C., Mathews, F.S. and Jorns, M.S., (2011) Probing oxygen activation sites in two flavoprotein oxidases using chloride as an oxygen surrogate. *Biochemistry*, 50(24), 5521–5534.
- Macheroux, P., Kappes, B. and Ealick, S.E., (2011) Flavogenomics—a genomic and structural view of flavin-dependent proteins. *FEBS Journal*, 278(15), 2625–2634.
- Mattevi, A., (1998) The PHBH fold: not only flavoenzymes. *Biophysical Chemistry*, 70(3), 217–222.
- McCulloch, K.M., Mukherjee, T., Begley, T.P. and Ealick, S.E., (2009) Structure of the PLP degradative enzyme 2-methyl-3-hydroxypyridine-5-carboxylic acid oxygenase from *Mesorhizobium loti* MAFF303099 and its mechanistic implications. *Biochemistry*, 48(19), 4139–4149.
- Meneely, K.M., Barr, E.W., Bollinger, J.M. and Lamb, A.L., (2009) Kinetic mechanism of ornithine hydroxylase (PvdA) from *Pseudomonas aeruginosa*: substrate triggering of O<sub>2</sub> addition but not flavin reduction. *Biochemistry*, 48(20), 4371–4376.
- Montersino, S., Tischler, D., Gassner, G.T. and van Berkel, W.J.H., (2011) Catalytic and structural features of flavoprotein hydroxylases and epoxidases. *Advanced Synthesis & Catalysis*, 353(13), 2301–2319.
- Olucha, J. and Lamb, A.L., (2011) Mechanistic and structural studies of the *N*-hydroxylating flavoprotein monooxygenases. *Bioorganic Chemistry*, 39(5-6), 171–177.
- Riebel, A., Dudek, H.M., de Gonzalo, G., Stepniak, P., Rychlewski, L. and Fraaije, M.W., (2012) Expanding the set of rhodococcal Baeyer-Villiger monooxygenases by high-throughput cloning, expression and substrate screening. *Applied Microbiology and Biotechnology*.
- Ryan, K.S., Chakraborty, S., Howard-Jones, A.R., Walsh, C.T., Ballou, D.P. and Drennan, C.L., (2008) The FAD cofactor of RebC shifts to an IN conformation upon flavin reduction. *Biochemistry*, 47(51), 13506–13513.
- Schühle, K., Jahn, M., Ghisla, S. and Fuchs, G., (2001) Two similar gene clusters coding for enzymes of a new type of aerobic 2-aminobenzoate (anthranilate) metabolism in the bacterium *Azoarcus evansii*. *Journal of Bacteriology*, 183(18), 5268–5278.
- Sucharitakul, J., Wongnate, T., Montersino, S., van Berkel, W.J.H. and Chaiyen, P., (2012) Reduction kinetics of 3-hydroxybenzoate 6-hydroxylase from *Rhodococcus jostii* RHA1. *Biochemistry*. dx.doi.org/10.1021/bi201823c
- Szolkowy, C., Eltis, L.D., Bruce, N.C. and Grogan, G., (2009) Insights into sequence-activity relationships amongst Baeyer-Villiger monooxygenases as revealed by the intragenomic complement of enzymes from *Rhodococcus jostii* RHA1. *ChemBioChem*, 10(7), 1208–1217.
- Treiber, N. and Schulz, G.E., (2008) Structure of 2,6-dihydroxypyridine 3-hydroxylase from a nicotine-degrading pathway. *Journal of Molecular Biology*, 379(1), 94–104.



## Samenvatting

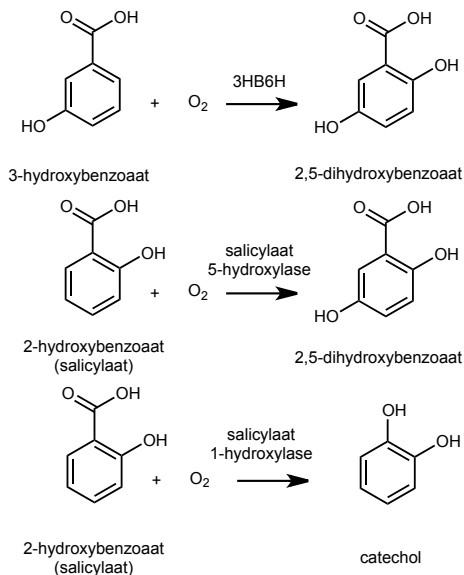
Dit proefschrift beschrijft de structurele en biochemische karakterisatie van 3-hydroxybenzoaat 6-hydroxylase (3HB6H), een flavine-afhankelijke monooxygenase die de omzetting katalyseert van 3-hydroxybenzoaat naar gentisaat (2,5-dihydroxybenzoaat)

Flavine-afhankelijke hydroxylases zijn betrokken bij vele biologische processen en hebben een unieke substraatspecificiteit (**hoofdstuk 2**). Binding van het substraat in deze enzymen zorgt o.a. voor: (i) een strikte controle van de reductieve half-reactie waarin het flavine elektronen ontvangt van NAD(P)H (ii) stabilisatie van de flavine-zuurstof adducten tijdens de oxidatieve half-reactie en (iii) een optimale omgeving voor regioselectieve hydroxylering. Ondanks uitgebreid onderzoek is er nog weinig bekend over hoe de diverse substraten in de actieve centra van flavine-afhankelijke hydroxylases worden gepositioneerd en hoe deze actieve centra zijn geëvolueerd.

Het ontdekken van (nieuwe) flavine-afhankelijke hydroxylases gebeurt aan de hand van drie karakteristieke aminozuurvolgordes die voorkomen in het FAD bindende domein van deze enzymen. Via deze vingerafdrukken zijn 18 flavine-afhankelijke hydroxylases opgespoord in de genom sequentie van de actinomyceet *Rhodococcus jostii* RHA1 (**hoofdstuk 3**). Deze Gram-positieve bodembacterie bevat vele oxidatieve

enzymen en is zeer geschikt voor het opruimen van organisch materiaal. Door phylogenetische en gencluster analyse kon de annotatie van de hydroxylase genen worden verbeterd en konden diverse functies worden toegekend.

3HB6H, oorspronkelijk foutief geannoteerd als salicylaathydroxylase (Fig.1), werd geselecteerd voor een uitvoerige biochemische analyse. *R. jostii* 3HB6H blijkt een homodimeer te zijn die een sterke voorkeur heeft voor NADH als coenzym. 3HB6H vertoont een nauwe substraatspecificiteit en reageert naast 3-hydroxybenzoaat het best met 2,3-dihydroxybenzoaat en 3,5-dihydroxybenzoaat. Gentisaat, het fysiologische product, ontkoppelt de hydroxyleringsreactie. Het is een zeer goede effector die de oxidatie van



**Figuur 1. Reactiesge katalyseerd door 3-hydroxybenzoaat 6-hydroxylase (3HB6H) en salicylaat hydroxylases.**

NADH stimuleert.

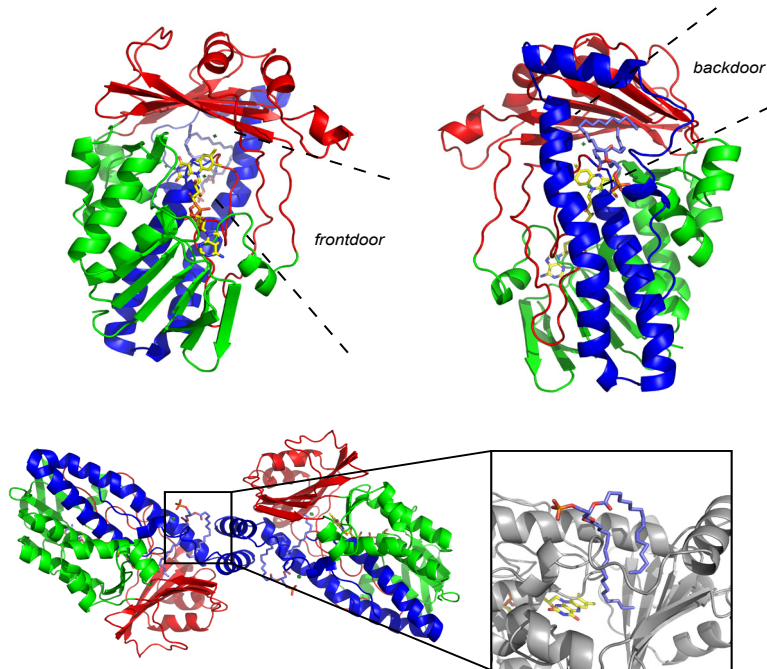
De structurele eigenschappen van *R. jostii* 3HB6H staan beschreven in **hoofdstuk 4 en 5**. Een hoge resolutie kristalstructuur werd verkregen van het vrije enzym, zowel na heterologe productie in *Escherichia coli* als na homologe productie in de nieuw ontwikkelde expressiestam *R. jostii* RHA1#2. De structuur opheldering bevestigde dat het enzym een homodimeer is (Fig.2). Het vouwingspatroon van 3HB6H komt overeen met dat van *p*-hydroxybenzoesuur hydroxylase en andere flavine-afhankelijke hydroxylases. De isoalloxazine ring van de FAD cofactor van 3HB6H is gelokaliseerd in het actieve centrum, en er zijn geen aanwijzingen voor flavine mobiliteit, zoals gevonden voor andere familieleden. Vlak naast de achterkant van het flavine zit electronen-dichtheid voor chloride ionen, wat kan duiden op een mogelijke bindingsplaats voor zuurstof.

**Hoofdstuk 4 en 5** beschrijven ook een nieuwe eigenschap van flavine-afhankelijke hydroxylases. Ieder monomeer van 3HB6H uit *R. jostii* RHA1 bindt een phospholipide in een tunnel in de buurt van het dimeer interactievlak (Fig.2). M.b.v. massaspectrometrie kon aangetoond worden dat het type phospholipide afhangt van de membraansamenstelling van de expressie gastheer. Phosphatidylinositol, de natuurlijke ligand in de Gram-positieve *R. jostii* stam, wordt in *E. coli* vervangen door een mengsel van phosphatidylethanolamine en phosphatidylglycerol. De ingevangen phospholipiden zouden als een soort lijm de dimeer interactie van 3HB6H kunnen versterken. Deze conclusie wordt ondersteund door natieve massaspectrometrie waarbij 3HB6H dimeren met slechts één gebonden lipide makkelijker tot monomeren dissociëren.

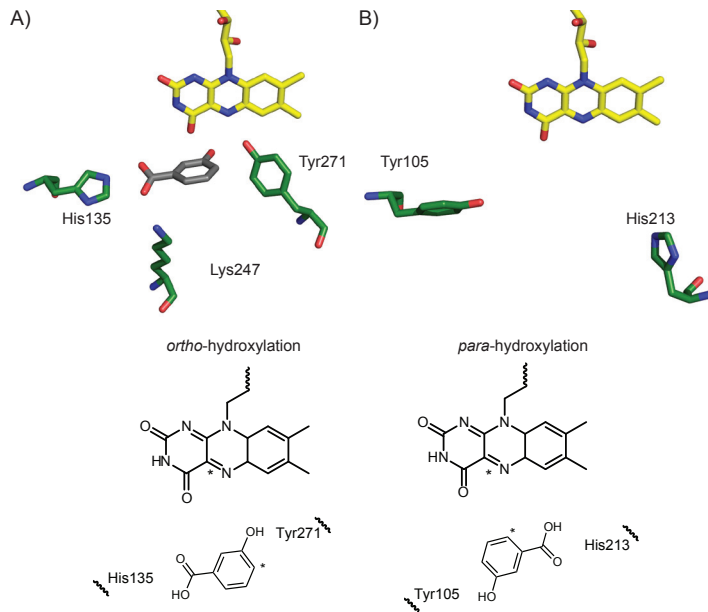
De aminozuurvolgorde van 3HB6H uit *Pseudomonas alcaligenes* NCIMB 9867 vertoont 33% identiteit met 3HB6H uit *R. jostii* RHA1. Het *P. alcaligenes* enzym bevat echter aanzienlijk meer zure groepen in het dimeer interactie domein. Niettemin bevat ook dit enzym een mengsel van phosphatidylethanolamine en phosphatidylglycerol wanneer het tot expressie wordt gebracht in *E. coli* (**hoofdstuk 6**). Dit rechtvaardigt de conclusie dat phospholipide binding een algemene eigenschap is van de 3HB6H familie. *R. jostii* 3HB6H en *P. alcaligenes* 3HB6H vertonen interessante verschillen in substraatspecificiteit en hydroxyleringscapaciteit. *R. jostii* 3HB6H is het meest actief met 3-hydroxybenzoesuur, terwijl *P. alcaligenes* 3HB6H een voorkeur heeft voor 3-hydroxy-4-methylbenzoesuur.

---

**Figuur 3.** (Volgende pagina) **Actieve centra van 3HB4H en 3HB6H.** **A)** Kristalstructuur van het actieve centrum van 3HB4H met gebonden 3-hydroxybenzoesuur. **B)** Kristalstructuur van het actieve centrum van 3HB6H. Aminozuur residuen zijn weergegeven in groen, cofactor in geel en substraat in grijs. Beneden: spiegeling van de actieve centra van 3HB4H en 3HB6H. Het C4a atoom van de flavine en het reactieve koolstof atoom van het substraat zijn aangeduid met een sterretje (\*).



Figuur 2. 3D-structuur van 3HB6H uit *R. jostii* RHA1. Boven: monomer gezien van voren en van achteren. Beneden: 3HB6H dimeer en uitvergroting lipide bindingplaats.





In **hoofdstuk 7** is de substraat binding van 3HB6H bestudeerd om inzicht te krijgen in de regioselectiviteit van 3-hydroxybenzoaat hydroxylering. Via een gerichte docking procedure werd duidelijk dat een His-Tyr paar een belangrijke rol speelt bij de binding van de carboxyl en hydroxyl groep van het substraat. Eenzelfde aminozuur paar is aanwezig in het actieve centrum van het zuster enzym 3HB4H uit *Comamonas testosteroni* en kan een verklaring geven voor de verschillen in regioselectiviteit van beide enzymen (Fig.2). Punt mutaties van *R. jostii* 3HB6H lieten zien dat His213 essentieel is voor de katalyse en dat Tyr105 belangrijk is voor de binding van het substraat. Studies van de reductieve en oxidatieve deelreacties zijn nodig om het mechanisme van hydroxylering nader te toetsen.

## Algemene Discussie

### Voorspelling Van Functie Van Een Primaire Eiwitstructuur

Het koppelen van een functie aan een primaire eiwitstructuur is een uitdaging. In eerste instantie lijken de grote aantallen van onbekende of foutief geannoteerde eiwitsequenties die gedeponeerd zijn in databanken de toekenning alleen maar te bemoeilijken (Furnham *et al.*, 2009). Het Enzyme Functional Initiative (EFI) probeert dit te doorbreken met een multidisciplinaire aanpak voor de functionele toekenning van onbekende enzymen (Gerlt *et al.*, 2011). De gekozen strategie combineert zuivere informatica gereedschappen met experimentele activiteitsscreening, kristal structuur toekenningen en *in vivo* studies. De verwachting is dat het op grote schaal analyseren van enzym (super)families en metagenoom monsters een doorbraak teweeg zal brengen in het vaststellen van functies van nieuwe enzymen (Brown and Babbitt, 2012).

Op kleinere schaal is reeds gewerkt aan het opsporen van nieuwe flavine-afhankelijke monooxygenases (Eppink *et al.*, 1997; Fraaije *et al.*, 2002; Macheroux *et al.*, 2011). Zo is via een combinatie van geoptimaliseerde expressie van oplosbaar eiwit en activiteitsscreening van celextracten inzicht verkregen in de biokatalytische potentie van Baeyer-Villiger monooxygenases uit *R. jostii* RHA1 (Riebel *et al.*, 2012; Szolkowy *et al.*, 2009). Verder is door het op basis van kristalstructuren vergelijken van aminozuurvolgordes een nieuw sequentie motief ontwikkeld welke Baeyer-Villiger monooxygenases beter kan onderscheiden van andere flavine-afhankelijke monooxygenases (Riebel *et al.*, 2012).

De van nature nauwe substraat specificiteit van flavine-afhankelijke hydroxylases beperkte het gebruik van de bovengenoemde strategie om de functie van onbekende familieleden in het genoom van *Rhodococcus jostii* RHA1 toe te kennen. Hoewel het uitvoerig vergelijken van aminozuurvolgordes een eerste aanwijzing gaf over een (on)mogelijke functie, was het incorporeren van operon en genoom context gegevens

essentieel voor een betrouwbare toekenning (**hoofdstuk 3**). Van de verschillende benaderingen is deze aanpak waarschijnlijk het meest effectief omdat prokaryote flavoproteïne hydroxylases betrokken zijn bij vele metabole routes die ofwel geconserveerd zijn, ofwel gecombineerd als een lappen deken.

Op basis van onze toekenningen (**hoofdstuk 3**) kunnen een aantal interessante eiwitten worden aangewezen. Zo is rifampicine monooxygenase (Q0S0L2) een enzym dat *Mycobacterium* and *Rhodococcus* antibiotica kan inactiveren (Andersen *et al.*, 1997; Hoshino *et al.*, 2010). Naast deze biomedische relevantie is rifampicin monooxygenase ook mechanistisch interessant omdat het katalytische eigenschappen deelt met *N*-hydroxylerende enzymen (Meneely *et al.*, 2009; Olucha and Lamb, 2011). Een ander voorbeeld van een interessant nieuw enzym is proteïne (Q0SJG8), dat actief is met een Coenzym A (CoA) geactiveerd substraat. Meer informatie over dit soort eiwitten kan antwoord geven op onopgeloste vragen over CoA herkenning en de consequenties van CoA activering voor de oxygeneringskracht van flavoenzymen (Schühle *et al.*, 2001).

### 3HB6H Structuur

In de afgelopen paar jaar zijn verschillende nieuwe kristalstructuren van flavine-afhankelijke hydroxylases opgelost ((Montersino *et al.*, 2011); **hoofdstuk 2**). Deze structuren bezitten allemaal een PHBH vouwingspatroon met een opmerkelijk goed geconserveerde topologie. Deze sterke overeenkomst in structuur onderschrijft het vermogen van deze enzymfamilie om zich aan te passen voor verschillende katalyse doeleinden (Mattevi, 1998).

We vonden inderdaad dat de drie-dimensionale structuur van 3HB6H sterk op die van PHBH lijkt (**hoofdstuk 4**). De globale architectuur van 3HB6H lijkt het meest op die van 2-methyl-3-hydroxypyridine-5-carboxylaat oxygenase (MHPCO) (McCulloch *et al.*, 2009), phenazine-1-carboxylaat hydroxylase (PhzS) (Greenhagen *et al.*, 2008), en 2,6-dihydroxypyridine hydroxylase (DHPH) (Treiber and Schulz, 2008). Dit toont aan dat flavine-afhankelijke hydroxylases die hetzelfde substraat gebruiken, zoals 3HB4H en 3HB6H, niet noodzakelijk de hoogste structurele homologie delen.

Het vouwingspatroon van de PHBH familie werpt interessante vragen op over de oligomerisatie eigenschappen van flavine-afhankelijke hydroxylases. Het dimerisatie domein is opgebouwd rond drie geconserveerde helix ketens, maar de quaternaire structuren vertonen verschillende trends: monomeer (RebC, Rdme, TetX en PhzS), dimeer (PHBH, PgaE, CabE en 3HB6H), tetrameer (MHPCO), en ongewone dimeren (PHHY, 3HB4H en DHPH). Verschillen in dimerisatie tussen 3HB6H, CabE/PgaE en PHBH worden veroorzaakt door het schuiven van de monomeren over het helix-helix contact oppervlak, en versterkt door lipide binding in 3HB6H (**hoofdstuk 4**).

## Phospholipide Binding

Een van de belangrijkste resultaten van dit proefschrift is dat 3HB6H phospholipiden bindt in de buurt van het dimeer interactievlak (**hoofdstuk 4-6**). Massaspectrometrie laat zien dat 3HB6H eiwitten van verschillende afkomst het intrinsieke vermogen bezitten om phospholipiden te binden met acyl ketens van 14 tot 19 koolstofatomen. Alle 3HB6H kristalstructuren die verfijnd zijn bezitten een gebonden C32 (16:0/16:0) phospholipide. Phospholipide binding stimuleert waarschijnlijk de dimerisatie van het enzym. 3HB6H dimeren die slechts één phospholipide keten gebonden hebben dissociëren nl. makkelijker in de gas fase tot monomeren. In oplossing is de 3HB6H-phospholipide interactie enorm sterk en alleen te verbreken na denaturatie van het enzym. Apo-dimeer, verkregen door ureum behandeling, blijft verzadigd met phospholipide.

In **hoofdstuk 5** hebben we laten zien dat de membraansamenstelling van de bacteriële gastheer het type gebonden phospholipide bepaalt. Phosphatidylinositol is de natuurlijke ligand in *Rhodococcus*, terwijl een mengsel van phosphatidylethanolamine en phosphatidylglycerol de ligand is in de in *E. coli* tot expressie gebrachte eiwitten. De kopgroep en fosfaat ester van de phospholipide hebben geen invloed op de interactie met 3HB6H. De polaire kopgroep is niet zichtbaar in de kristalstructuur, steekt waarschijnlijk uit het eiwit en is mobiel. De fosfaat ester is in interactie met Arg350 en Lys385, maar K385D en K358A mutaties hebben geen invloed op de phospholipide binding.

3HB6H uit *P. alcaligenes* NCIMB 9816 bevat een minder hydrophobe lipide bindingsplaats, niettemin blijft de lipide binding in dit enzym behouden (**Chapter 6**). Het zou interessant zijn om via scanning mutagenese de minimale sequentie te bepalen die nodig is voor lipide binding. Zo'n herkenningsequentie kan gebruikt worden om potentiële lipide bindende eiwitten op te sporen. Een soortgelijke sequentie is voorgesteld voor het binden van sphingolipiden aan eiwit transmembraan domeinen (Contreras *et al.*, 2012).

## Substrate Binding

Hoe substraten in flavine-afhankelijke hydroxylases worden getransporteerd is verre van duidelijk. Voor PHBH is voorgesteld dat het aromatische substraat het eiwit aan de voorkant binnen gaat (zie Fig.2) en dat dynamische verschuivingen in eiwit en flavine conformatie nodig zijn om het substraat naar het actieve centrum te leiden (Entsch *et al.*, 2005). Voor 3HB4H is voorgesteld dat het substraat en zuurstof een specifieke toegangstunnel gebruiken (Hiromoto *et al.*, 2006). Voor rebeccamycin hydroxylase (RebC) wordt aangenomen dat het substraat aan de achterkant binnenkomt (zie Fig.2). Hetzelfde deel van de helix die betrokken is bij de lipide binding in 3HB6H is niet gestructureerd in RebC en wordt geordend na substraat binding of flavine reductie

(Ryan *et al.*, 2008). Het aan de achterkant binnenkomen en de daarmee gepaard gaande helix vorming vertegenwoordigen een belangrijke nieuwe eigenschap van flavine-afhankelijke hydroxylases. Een soortgelijke smeltende helix die nodig is om het substraat toe te laten en stevig op te bergen is mogelijk ook aanwezig in PhzS (Greenhagen *et al.*, 2008).

In 3HB6H functioneert de phospholipide als een plug waarmee de toegangstunnel aan de achterkant van het enzym wordt afgesloten. Deze tunnel, die loopt van het enzym oppervlak tot aan het actieve centrum, lijkt niet betrokken te zijn bij het substraat transport. Substraat bindt nl. snel, ondanks de aanwezigheid van gebonden phospholipiden (Sucharitakul *et al.*, 2012). Een fascinerende mogelijkheid is dat het phospholipide een beschermende rol speelt tijdens de katalyse. Wanneer het substraat eenmaal gebonden is en de flavine door NADH is gereduceerd, moet na reactie met zuurstof de gevormde flavine-peroxide afgeschermd worden van oplosmiddel. Phenol hydroxylase bevat een deksel die na substraat binding de FAD kloof afsluit (Enroth, 2003). RebC doet hetzelfde door een helix te vormen bovenaan de substraat tunnel (Ryan *et al.*, 2008). De phospholipide in 3HB6H zou het transport van watermoleculen naar het actieve centrum kunnen verhinderen waardoor de flavine-peroxide wordt gestabiliseerd en ont koppeling van hydroxylering (vorming van waterstofperoxide) wordt voorkomen.

### Regioselectivity Of Hydroxylation

3HB6H katalyseert de *para*-hydroxylering van 3-hydroxybenzoesuur, terwijl 3HB4H hetzelfde substraat hydroxyleert op de *ortho*-positie. Inzicht in de structurele determinanten van deze regioselectiviteit werd bemoeilijkt doordat er geen structuur is van het enzym-substraat complex van 3HB6H. Door het vrije enzym te vergelijken met 3HB4H, de binding van chloride te bepalen in het actieve centrum, en dockings studies met het substraat is dit hiaat gevuld.

Chloride ionen kunnen een redelijk surrogaat vormen voor moleculaire zuurstof (Kommoju *et al.*, 2011). De kristalstructuur van de substraat-vrije vorm van 3HB6H bevat een paar chloride atomen aan het eind van de dipool van helix H11. Deze plek zou gereserveerd kunnen zijn voor zuurstof binding en activering (Baron *et al.*, 2009; Kommoju *et al.*, 2011). De chlorides zitten ook op de plek waar de hydroxyl groep van het substraat bindt in het substraat dockings model.

Aan de hand van data-gestuurde dockings experimenten kwamen we er achter dat 3HB6H en 3HB4H gespiegelde substraat bindingsplaatsen bezitten. Via biochemische analyses en structuur opheldering van actief centrum varianten kon worden vastgesteld dat His213 in 3HB6H essentieel is voor de katalyse en dat Tyr105 en Gln301 kritisch betrokken zijn bij de substraat binding. De steady-state kinetische parameters van H213A, H213S, Y105F en Q301E zijn een uitstekend uitgangspunt voor verder onderzoek d.m.v. snelle reactie kinetiek. Het opsplitsen van de deelreacties

zal uitsluitel geven over welke stap(pen) in de katalytische cyclus van de mutant eiwitten zijn aangetast. Onderzoek naar de katalytische eigenschappen van andere mutanten zoals H213N, H213Y, Q301N en Q301A is ook gewenst.

Hoewel de opheldering van het hydroxyleringsmechanisme verder onderzoek vereist, kunnen we al wel een voorzet geven van hoe het substraat wordt omgezet. Activering van het substraat via deprotonering lijkt voor 3HB6H en 3HB4H niet nodig. Beide enzymen beïnvloeden de  $pK_a$  van de 3-hydroxyl groep van het substraat niet (Hiromoto *et al.*, 2006). Sucharitakul en collega's hebben voorgesteld dat er tijdens de reductie van het enzym een isomerisatie optreedt van het initiële enzym-substraat complex naar een volledig geactiveerde vorm (Sucharitakul *et al.*, 2012). Dergelijke isomerisatie stappen zouden nodig kunnen zijn voor een optimale positionering van het substraat voor aanval door de flavine peroxide.

### NADH Binding En Flavine Mobiliteit

De kristalstructuur van 3HB6H geeft geen uitsluitel over de manier van binding van het NADH coenzym. Met substraat gebonden is er geen plaats voor de nicotinamide ring om de flavine te benaderen. Dit suggereert dat flavine mobiliteit, zoals waargenomen in andere flavine-afhankelijke hydroxylases (Monterisino *et al.*, 2011), een integraal onderdeel is van het katalytisch proces. Echter, met de huidige informatie kunnen andere conformatie verschuivingen niet worden uitgesloten.

Tot slot kan gesteld worden dat de resultaten van dit proefschrift een solide basis vormen voor verdere studies naar het werkingsmechanisme van 3HB6H en gerelateerde enzymen. De verkregen kennis heeft meer inzicht verschaft in de regioselectiviteit van flavine-afhankelijke hydroxylering en is een waardevolle toevoeging aan het flavine-afhankelijke monoxygenase repertoire.

## References

- Andersen, S.J., Quan, S., Gowan, B. and Dabbs, E.R., (1997) Monoxygenase-like sequence of a *Rhodococcus equi* gene conferring increased resistance to rifampin by inactivating this antibiotic. *Antimicrobial agents and chemotherapy*, 41(1), 218–221.
- Baron, R., Riley, C., Chenprakhon, P., et al., (2009) Multiple pathways guide oxygen diffusion into flavoenzyme active sites. *Proceedings of the National Academy of Sciences of the United States of America*, 106(26), 10603–10608.
- Brown, S.D. and Babbitt, P.C., (2012) Inference of functional properties from large-scale analysis of enzyme superfamilies. *Journal of Biological Chemistry*, 287(1), 35–42.
- Contreras, F.X., Ernst, A.M., Haberkant, P., et al., (2012) Molecular recognition of a single sphingolipid species by a protein's transmembrane domain. *Nature*, 481(7382), 525–529.
- Enroth, C., (2003) High-resolution structure of phenol hydroxylase and correction of sequence errors. *Acta crystallographica. Section D, Biological crystallography*, 59(Pt 9), 1597–1602.
- Entsch, B., Cole, L.J. and Ballou, D.P., (2005) Protein dynamics and electrostatics in the function of *p*-hydroxybenzoate hydroxylase. *Archives of Biochemistry and Biophysics*, 433(1), 297–311.
- Eppink, M.H.M., van Berkel, W.J.H. and Schreuder, H.A., (1997) Identification of a novel conserved sequence motif in flavoprotein hydroxylases with a putative dual function in FAD/NAD (P) H binding. *Protein Science*, 6(11), 2454–2458.
- Fraaije, M.W., Kamerbeek, N.M., van Berkel, W.J.H. and Janssen, D.B., (2002) Identification of a Baeyer-Villiger monoxygenase sequence motif. *FEBS Letters*, 518(1-3), 43–47.
- Furnham, N., Garavelli, J.S., Apweiler, R. and Thornton, J.M., (2009) Missing in action: enzyme functional annotations in

- biological databases. *Nature chemical biology*, 5(8), 521–525.
- Gerlt, J.A., Allen, K.N., Almo, S.C., et al.**, (2011) The Enzyme Function Initiative. *Biochemistry*, 50(46), 9950–9962.
- Greenhagen, B.T., Shi, K., Robinson, H., Gamage, S., Bera, A.K., Ladner, J.E. and Parsons, J.F.**, (2008) Crystal structure of the pyocyanin biosynthetic protein PhzS. *Biochemistry*, 47(19), 5281–5289.
- Hiramoto, T., Fujiwara, S., Hosokawa, K. and Yamaguchi, H.**, (2006) Crystal structure of 3-hydroxybenzoate hydroxylase from *Comamonas testosteroni* has a large tunnel for substrate and oxygen access to the active site. *Journal of Molecular Biology*, 364(5), 878–896.
- Hoshino, Y., Fujii, S., Shinonaga, H., Arai, K., Saito, F., Fukai, T., Satoh, H., Miyazaki, Y. and Ishikawa, J.**, (2010) Monooxygenation of rifampicin catalyzed by the *rox* gene product of *Nocardia farcinica*: structure elucidation, gene identification and role in drug resistance. *Journal of Antibiotics*, 63(1), 23–28.
- Kommoju, P.-R., Chen, Z.-W., Bruckner, R.C., Mathews, F.S. and Jorns, M.S.**, (2011) Probing oxygen activation sites in two flavoprotein oxidases using chloride as an oxygen surrogate. *Biochemistry*, 50(24), 5521–5534.
- Macheroux, P., Kappes, B. and Ealick, S.E.**, (2011) Flavogenomics—a genomic and structural view of flavin-dependent proteins. *FEBS Journal*, 278(15), 2625–2634.
- Mattevi, A.**, (1998) The PHBH fold: not only flavoenzymes. *Biophysical Chemistry*, 70(3), 217–222.
- McCulloch, K.M., Mukherjee, T., Begley, T.P. and Ealick, S.E.**, (2009) Structure of the PLP degradative enzyme 2-methyl-3-hydroxypyridine-5-carboxylic acid oxygenase from *Mesorhizobium loti* MAFF303099 and its mechanistic implications. *Biochemistry*, 48(19), 4139–4149.
- Meneely, K.M., Barr, E.W., Bollinger, J.M. and Lamb, A.L.**, (2009) Kinetic mechanism of ornithine hydroxylase (PvdA) from *Pseudomonas aeruginosa*: substrate triggering of O<sub>2</sub> addition but not flavin reduction. *Biochemistry*, 48(20), 4371–4376.
- Monterisino, S., Tischler, D., Gassner, G.T. and van Berkel, W.J.H.**, (2011) Catalytic and structural features of flavoprotein hydroxylases and epoxidases. *Advanced Synthesis & Catalysis*, 353(13), 2301–2319.
- Olucha, J. and Lamb, A.L.**, (2011) Mechanistic and structural studies of the N-hydroxylating flavoprotein monooxygenases. *Bioorganic Chemistry*, 39(5-6), 171–177.
- Riebel, A., Dudek, H.M., de Gonzalo, G., Stepniak, P., Rychlewski, L. and Fraaije, M.W.**, (2012) Expanding the set of rhodococcal Baeyer-Villiger monooxygenases by high-throughput cloning, expression and substrate screening. *Applied Microbiology and Biotechnology*.
- Ryan, K.S., Chakraborty, S., Howard-Jones, A.R., Walsh, C.T., Ballou, D.P. and Drennan, C.L.**, (2008) The FAD cofactor of RebC shifts to an IN conformation upon flavin reduction. *Biochemistry*, 47(51), 13506–13513.
- Schühle, K., Jahn, M., Ghisla, S. and Fuchs, G.**, (2001) Two similar gene clusters coding for enzymes of a new type of aerobic 2-aminobenzoate (anthranilate) metabolism in the bacterium *Azoarcus evansii*. *Journal of Bacteriology*, 183(18), 5268–5278.
- Sucharitakul, J., Wongnate, T., Monterisino, S., van Berkel, W.J.H. and Chaiyen, P.**, (2012) Reduction kinetics of 3-hydroxybenzoate 6-hydroxylase from *Rhodococcus jostii* RHA1. *Biochemistry*. dx.doi.org/10.1021/bi201823c
- Szolkowy, C., Eltis, L.D., Bruce, N.C. and Grogan, G.**, (2009) Insights into sequence-activity relationships amongst Baeyer-Villiger monooxygenases as revealed by the intragenomic complement of enzymes from *Rhodococcus jostii* RHA1. *ChemBioChem*, 10(7), 1208–1217.
- Treiber, N. and Schulz, G.E.**, (2008) Structure of 2,6-dihydroxypyridine 3-hydroxylase from a nicotine-degrading pathway. *Journal of Molecular Biology*, 379(1), 94–104.





## Acknowledgments

Done! It is time to look back and thank people for the nice journey. To start, I thank my supervisor and promotor Prof. Dr. Willem van Berkel. Thanks for giving me the possibility to work in your group and the freedom to investigate on those “yellow stuff.” I have learn a lot from you and I enjoyed all behind-the-scene stories you collected along your career.

The laboratory of Biochemistry provided me a nice working and social environment and I would like to thank Prof. Dr. Sacco de Vries for chairing such variety of scientists and all group leaders for the scientific challenges they bring forward. I am greatly indebted to Adrie, Willy, Cathy, Walter, Boudewijn, Sjef and Laura who handle all my bizarre questions, doubts, problems and ideas. Thanks also to all PhDs and Post-Docs in the Department for the nice laughs, but also for the empathy and support demonstrated during stressful moments. In particular to my wonderful paranymphs Christoph and Cristina. A special thanks to my Enzyme@work colleagues, former and present. I managed to daily increase the entropy of the lab and the office; it was nice to work together. Good luck to everybody for the future!

During my research I had the opportunity to work in collaboration with many people. Thank you all! The BIOMOX partners with whom I shared many (too many) progress meetings, especially to Evelien, Harini and Anette. Arjan and Esther for your patience and expertise for the never ending lipid story. Thanks to Jeerus Sucharitakul, Thanyaporn Wongnate and Prof. Pimchai Chaiyen for the nice job done on the other side of the world! A special thanks to my co-promotor Prof. Andrea Mattevi for hosting me in his lab. A deep thanks to Roberto Orru’ for the time and energy devote on this project, and to the Structural Biology group in Pavia for the nice time.

Every journey is made mostly by the traveling companion, and I was very lucky traveler! Hugs and kisses to my friends in Italy and in other corners of the world who have experienced with me this long distance friendship. To the *Corporatie van de Papegaai* for a lot of and beyond. Since is a secret society, names cannot be disclosed, some people actually do not know themselves they belong to it. To my *housemates*, *pandamates*, *tripmates*, *drinkingmates*, *dinnermates*, *concert* and *dancingmates*. Thank you all (pufpuf).

Eduardo, ha sido bonito y divertido, verdad? Ahora que estamos en modalidad 15 de junio vamos a preparar el siguiente paso, juntitos.

Un grazie speciale a Giusi e Enrica, per l’affetto, il supporto e la pazienza dimostrata.





## List of publications

Sucharitakul J, Wongnate T, **Montersino S**, van Berkel WJH and Chaiyen P (2012) Reduction kinetics of 3-hydroxybenzoate 6-hydroxylase from *Rhodococcus jostii* RHA1. *Biochemistry*, dx.doi.org/10.1021/bi201823c

**Montersino S** and van Berkel WJH (2012) Functional annotation and characterization of 3-hydroxybenzoate 6-hydroxylase from *Rhodococcus jostii* RHA1. *Biochim Biophys Acta* **1824**:433-42

**Montersino S**, Orru' R, Mattevi A, van Berkel WJH (2011) Structural basis of regioselective hydroxylation in 3-hydroxybenzoate 6-hydroxylases. In: *Flavins and Flavoprotein 2011: Proceedings 17th International Symposium*, Berkeley, US, 2011. (Miller S, Hille R, Palfey B, Eds), pp 291-296

van Berkel WJH, **Montersino S**, Tischler D, Kaschabek S, Schlömann M and Gassner GT (2011) Flavins on the move: flavoprotein hydroxylases and epoxidases. In: *Flavins and Flavoprotein 2011: Proceedings 17th International Symposium*, Berkeley, US, 2011. (Miller S, Hille R, Palfey B, Eds), pp 273-284

**Montersino S**, Tischler D, Gassner G, van Berkel WJH (2011). Catalytic and structural features on flavoprotein hydroxylases and epoxidases. *Adv Synth and Catal* **353**:2301-19

**Montersino S**, Golovleva LA, Schlömann M, van Berkel WJH. (2008) Another look at *p*-hydroxybenzoate hydroxylase. In: *Flavins and Flavoprotein 2008: Proceedings 16th International Symposium*, Jaca, Spain, 2008 (Medina M, Frago S, Gomez-Moreno C, Eds). Prensas Universitarias de Zaragoza, pp. 51-56.

**Montersino S**, Prieto A, Muñoz R, de Las Rivas B. (2008) Evaluation of exopolysaccharide production by *Leuconostoc mesenteroides* strains isolated from wine. *J Food Sci* **73**:196-9

## ***Curriculum vitae***

Stefania Montersino was born on the 29<sup>th</sup> of July 1982, in Alba, Italy. In 2001 she finished her high-school education (Liceo Scientifico Leonardo Cocito, Alba) and she started her studies at the Università degli Studi di Torino (Italy) with a BSc in Biomolecular Biotechnology and a MSc in Industrial Biotechnology.

In 2006 she spend ten months with a Erasmus fellowship at the Universidad Autonoma de Madrid (Spain) working also on her Msc thesis at the Microbiology group in the Instituto de Fermentaciones Industriales (IFI) of the National Spanish Council (CSIC).

In 2008 she joined the laboratory of Biochemistry at Wageningen University (The Netherlands) starting a PhD project under the supervision of Prof. Willem van Berkel. During her research Stefania took the opportunity to spend couple of months in the group of Prof. Andrea Mattevi at Università degli Studi di Pavia (Italy) performing experiments on protein crystallography. The positive findings obtained durign her PhD are presented in this thesis.

## Overview of the completed training activities

### Discipline Specific Activities

#### *Courses*

Food Enzymology, VLAG	2008
Understanding protein structures, EMBL Hinxton	2009
Training on crystallography, University of Pavia	2009

#### *Conferences and Meetings*

NWO - Protein study group	2008-2010
+ Lecture (2010)	
IBOS meetings	2008-2011
+ Lecture (2010)	
NVBVB fall symposium, Eindhoven	2008
16 <sup>th</sup> International Symposium on Flavins and Flavoproteins, Spain	2008
NWO - Organic chemistry study group	2009
EMBO conference: Catalytic mechanism by biological systems: at the interface between chemistry and biology, Hamburg	2010
5 <sup>th</sup> OxiZymes, Leipzig	2010
17 <sup>th</sup> International Symposium on Flavins and Flavoproteins, Berkeley	2011
CHAINS, Chemistry as innovating science, Utrecht	2011
+ Lecture (2011)	

#### **General courses**

VLAG PhD week	2008
Graphical artwork	2009
Academic writing II	2009
Scientific writing	2011

#### **Optional activities**

Biochemistry biweekly seminars	2008-2012
PhD retreat, Barcelona	2009

The research described in this thesis was financially supported by the Netherlands Organization for Scientific Research (NWO).

Financial support from Wageningen University for printing this thesis is gratefully acknowledged.

*Printed by Wöhrmann Print Service B.V. Zutphen, the Netherlands.*

*Cover design (freely inspired by Theo van Doesburg art work) and layout by Stefania Montersino.*